Scuola Superiore Meridionale
University of Naples Federico II

Scuola Superiore Meridionale

Doctoral Thesis
in Modeling and Engineering Risk and Complexity

Contracting Dynamics for Biologically Plausible Neural Networks and Optimization

Author:
Veronica Centorrino

Supervisors:
Prof. Francesco Bullo
Prof. Giovanni Russo

Submitted in fulfilment of the requirements for the degree of Doctor of Philosophy in Modeling and Engineering Risk and Complexity. Coordinator: Prof. Mario di Bernardo.

Modelling and Engineering Risk and Complexity

December 12, 2024

...alwayS

To my family.

Abstract

Our brain is perhaps one of the most striking examples of complex systems: about 10^{10} neurons, interconnected by approximately 10^{15} *recurrent* synaptic connections, capable of adapting and learning through *local synaptic rules*, continuously solving *optimization problems* like sparse representation. While artificial neural networks (ANN) were initially inspired by natural networks, nowadays they have significantly diverged from biological realism, driven by performance criteria. As a result, ANNs still exhibit errors and biases that are absent in natural networks and that cannot be explained and quantified a priori. This naturally raises important questions: What if we could design ANNs with today's performance, but that more closely mimic the way natural networks work? How can we obtain biologically plausible models and how can we guarantee their stability and robustness? What optimization problems do natural networks solve, and how can biologically plausible neural networks mimic these processes? Can we create a normative framework translating optimization problems into ANNs that are guaranteed to converge to equilibria representing optimal solutions of the initial optimization problems?

Motivated by these exciting open challenges, in this thesis we aim at laying the theoretical groundwork for the modeling and understanding of neural networks that align more closely with biological principles. We propose a normative framework that translates complex tasks, described as optimization problems, into biologically plausible neural networks that are guaranteed to converge to equilibria corresponding to the optimal solutions. Our models incorporate core principles of natural networks: the use of continuous-time dynamical systems for both neural and synaptic changes, recurrent connections, positivity of the system, and local learning rules. Specifically, for the neural dynamics we focus on two widely used recurrent neural network (RNN) models – the Hopfield neural network (HNN) and the firing rate neural network (FNN) – and model synaptic weight dynamics using continuous-time Hebbian learning rules. To ensure stability and robustness of our models, we leverage *contraction theory*, a robust computationally-friendly stability tool from control theory. This approach offers a significant advantage: with a single condition, it guarantees global exponential convergence, along with a number of highly ordered transient and asymptotic behaviors of contracting dynamics, which are advantageous for our objectives.

We begin our analysis by developing essential theoretical tools to analyze relevant neural dynamics, filling a gap in the literature by establishing conditions for strong and weak Euclidean contractivity of RNNs with locally Lipschitz activation functions.

Remarkably, our lower bound on the contraction rate is log-optimal for almost all symmetric weight matrices, making our results sharp – they are the best achievable within this framework. Additionally, we establish new algebraic results on matrix polytopes and symmetric matrix products, advancing both neural network stability and broader applications in matrix theory and optimization.

Building on these theoretical results, we propose a top-down normative framework for designing biologically plausible networks that solve sparse reconstructions and other optimization problems. This framework is based upon the theory of proximal operators for composite optimization and leads to continuous-time firing rate neural networks – the *firing rate competitive network* – that are therefore interpretable. We analyze the behavior of these dynamics, establishing a direct link between the network equilibria and the optimal solutions of sparse reconstruction problems. Under a standard assumption, we prove that the dynamics converge linear-exponentially (and thus globally) to the equilibrium. Importantly, we show that the positive variant of the firing rate competitive network preserves non-negativity in its state variables, aligning with biological principles and further underscoring the plausibility of the model.

In the second part, we explore the interaction between neural and synaptic dynamics by embedding Hebbian learning rules into the continuous-time RNN models of the first part. This results in the *coupled neural-synaptic networks:* RNNs with dynamic synaptic connections that closely mirror biological processes. We propose and analyze these systems, combining HNNs and FNNs with Hebbian learning rules. For these dynamics, we propose a low-dimensional formulation that captures synaptic sparsity of neural circuits. We establish sufficient conditions for the contractivity of each model by leveraging non-Euclidean contraction arguments. Additionally, we demonstrate biologically plausible forward invariance results and show that under suitable conditions, the models satisfy Dale's Principle – an empirical principle referring to the fact that a neuron has either only excitatory or only inhibitory synapses – further enhancing biological plausibility.

In the final part of the thesis, we explore the potential of a contractivity-based approach for optimization. We begin by translating canonical static optimization problems into continuous-time dynamical systems, establishing conditions for strong infinitesimal contractivity. For both static and time-varying optimization problems, we derive contractivity conditions and, in certain cases, demonstrate improved convergence rates. Our work includes two key results on equilibrium tracking in parameter-varying contracting dynamics, addressing both known and unknown rates of parameter change. Additionally, we extend our analysis to convex optimization problems with unique minimizers. We show that these problems lead to dynamics that are globally-weakly contracting in the state space and only locally-strongly contracting. For these dynamics, we present a detailed convergence analysis, showing that convergence is linear-exponential. This means that the distance between each solution and the equilibrium is upper-bounded by a function that first decreases linearly and then exponentially. We also provide input-to-state stability conditions for these dynamics, further strengthening the robustness and applicability of the approach.

We conclude by highlighting potential future directions and with an appendix with novel complementary results on the Euclidean contractivity of FNNs with dissipation.

Acknowledgements

> They say life is short, but it is long and it is lonely, so if you manage to find a group of people that will tolerate you, and elevate you, and one who will especially love you. Well, that is all it's about, that is what the fight is really for.
>
> *Emily Andras*

I would first like to deeply thank my advisors, Francesco Bullo and Giovanni Russo. Three years ago, I chose a project that seemed super interesting, proposed by two professors who struck me as not only brilliant scientists but also kind and enthusiastic people I wanted to work with and learn from. Three years later, I can say I hit the lottery with that choice. As a mathematician from Catania, I had no clue who Francesco Bullo was academically when I started, and it has been such a pleasure to discover it over these years. Francesco and Giovanni, thank you for welcoming me, for your time, kindness, immense patience, constant support, and encouragement, and for your priceless advices and guidance throughout these years. You have helped me grow both as a researcher and as a person. I will always be grateful to you and honored to have had you as mentors.
A special thanks also go to my collaborators, Sasha and Anand.

Francesco, and everyone in your lab – Sasha, Anand, Yohan, Abed, Francesco, Sean, Giulia, Kevin, Gilberto – thank you for making me feel welcome in your group from day one. I had an amazing and unforgettable time during my year at UCSB. I'll always cherish the stimulating conversations, the laughter, and even the bad pizzas and beers we shared. A special thanks to Margarita, Honey, and Ximena for welcoming me as a member of your family, and the football gang.

To Professor Mario Di Bernardo, thank you for being an incredible coordinator, always available, always listening, and ready to solve any problem. Thank you also to the MERC board members for the engaging discussions and constructive feedback. Thanks to my fellow PhD students, to Marco, Ale, Dimitri, Emanuela, the SPACE guys, and the brilliant researchers (all of the previous included!) I have crossed paths with at the Scuola Superiore Meridionale. A special shout-out to my yearmates: Giancarlo,

Domenico, Gianluca, Francesco, Ayman, and also Marcello and Dario. It has been a pleasure to share this journey with you. Last but not least, a special thank you to my Postddddddddoc, Davide, for all the coffees, laughs, and advices.

I am deeply thankful to Professor Florian Dörfler for welcoming me into his lab at ETH, to the Italians, and to everyone I met there. Those six weeks were an incredible experience, both professionally and personally, and I will always treasure them. Thank you also to Professor Giancarlo Ferrari Trecate and his group for their warm welcome and stimulating conversations during my visit.

To my thesis reviewers, Professors Emiliano Dall'Anese and Mihailo Jovanović, thank you for your time and for your kind, constructive comments.

Thank you to the soundtrack of my life, for giving the rhythm of this journey as well.

In my life, I have been incredibly lucky to meet amazing people everywhere I have been and I have lived and, as crazy as it can sound, even online.
To my family, my Nonna Maria – whose top shelf nonna-food has traveled the world with me –, the diamond of my heart, Filippo, my aunts Catena, Anna, Maria, my uncle Filippo, my cousins – Chiara, Ale, Daniele, Giuseppe (x2), Tony, Lety, Angelo, Graziana, Federica, Marina, Ludovica. My teammates, who are like a second family to me. The friends who have always be there, Valeria, Daniele, Marika and a long list of people. Thank you, for your constant support and because no matter where I go, I know you will always be there for me.
To my found family and Posse of Dipshits, whom I met during this PhD journey, you have been my best discovery. Our adventures, idioting, laughs, and calls have been essential for my mental health and sanity (assuming I have any left). A special shout-out to my favorite German, Isa, thank you for everything – I don't write the list but you know it.
To everyone mentioned above, thank you for your constant support and endless belief in me. It has meant more than I can ever express.

Last but not least, to my family: mom, dad, Peppe/Scema (aka il parassita del mio cuore), and Sofie (who will always be part of our family). Thank you for being my rock and believing in me more than I could ever believe in myself. Your love and support mean the world to me. I would be nothing without you.

I would love to end by thanking Her, my best friend. Sofie, I was lucky enough to grow up and spend 11 and a half years of my life with you. Unfortunately, someone decided you had to physically leave me at the beginning of this thesis journey... but let's skip over the shitty part of this story. The truth is, you never really left me. Thank you, My Love, cause you were, you are and you will always be the best part of me... alwayS.

Ringraziamenti

> They say life is short, but it is long and it is lonely, so if you manage to find a group of people that will tolerate you, and elevate you, and one who will especially love you. Well, that is all it's about, that is what the fight is really for.
>
> *Emily Andras*

Vorrei iniziare ringraziando principalmente i Professori Francesco Bullo e Giovanni Russo. Tre anni fa ho scelto un progetto che sembrava incredibilmente interessante, proposto da due professori che mi sono sembrati da subito non solo scienziati brillanti, ma anche persone gentili ed entusiaste con cui lavorare e da cui imparare. Tre anni dopo, posso dire di aver vinto alla lotteria con quella scelta. Venendo dall'Università di matematica a Catania, non avevo idea di chi fosse Francesco Bullo dal punto di vista accademico quando ho iniziato, ed è stato un vero piacere e onore scoprirlo nel corso di questi anni. Francesco e Giovanni, grazie per la vostra gentilezza, per il vostro tempo, la vostra immensa pazienza, il supporto e incoraggiamento costante, per i vostri inestimabili consigli e per la vostra guida. Mi avete aiutata a crescere sia come ricercatore che come persona. Sarò sempre grata e onorata di avervi avuto come mentori in questo percorso. Un ringraziamento speciale anche ai miei collaboratori Sasha e Anand.

Francesco, e tutti nel tuo laboratorio – Sasha, Anand, Yohan, Abed, Francesco, Sean, Giulia, Kevin, Gilberto – grazie per avermi fatta sentire benvenuta nel vostro gruppo fin dal primo giorno. Il mio anno a UCSB è stato straordinario e indimenticabile anche grazie a voi. Porterò sempre con me le conversazioni, le risate e persino le pessime pizze e birre che abbiamo condiviso. Un ringraziamento speciale a Margarita, Honey e Ximena per avermi accolta come parte della vostra famiglia, e al gruppo di calcio.

Al professore Mario Di Bernardo, grazie per essere un coordinatore eccezionale, sempre disponibile, pronto ad ascoltare e a risolvere qualsiasi problema. Grazie anche ai membri del consiglio MERC per le discussioni stimolanti e i feedback costruttivi. Ai miei compagni di dottorato, Marco, Ale, Dimitri, Emanuela, il gruppo SPACE, e tutti i ricercatori brillanti (i precedenti inclusi!) che ho avuto la fortuna di incontrare alla

Scuola Superiore Meridionale, grazie per aver reso questo percorso un pò più divertente. Un ringraziamento speciale ai miei compagni di corso: Giancarlo, Domenico, Gianluca, Francesco, Ayman, e anche Marcello e Dario. È stato un piacere condividere questa esperienza con voi. Infine, ma non per importanza, un ringraziamento speciale al mio Postddddddddoc personale, Davide, per tutti i caffè, le risate e i preziosi consigli.

Un grazie infinito al professore Florian Dörfler per avermi accolta nel suo laboratorio all'ETH, al gruppo degli italiani, e a tutti coloro che ho avuto la fortuna di incontrare lì. Quelle sei settimane sono state un'esperienza unica e incredibile, sia professionalmente che personalmente. Grazie anche al professore Giancarlo Ferrari Trecate e al suo gruppo per la disponibilità, l'accoglienza e le conversazioni stimolanti durante la mia visita.

Ai revisori della mia tesi, i professori Emiliano Dall'Anese and Mihailo Jovanović, grazie per il vostro tempo e per i vostri commenti gentili e costruttivi.

Grazie alla colonna sonora della mia vita, per avermi accompagnata anche in questo percorso. Nella mia vita sono stata incredibilmente fortunata a incontrare persone straordinarie ovunque sia stata e abbia vissuto e – lo so che suona da pazzi – anche online.
Alla mia famiglia, mia Nonna Maria – il cui super cibo-da-nonna ha viaggiato per il mondo con me – al diamante del mio cuore, Filippo, le mie zie Catena, Anna, Maria, a mio zio Filippo, i miei cugini – Chiara, Ale, Daniele, Giuseppe (x2), Tony, Lety, Angelo, Graziana, Marina, Ludovica e Federica. Alle mie compagne di squadra, che sono come una seconda famiglia per me, e ai miei amici di sempre Valeria, Daniele, Marika e tanti altri in questa lista. Grazie infinite per il vostro supporto costante e perché, ovunque io vada, so che ci sarete sempre per me.
Alla mia "found family and Posse of Dipshits", che ho incontrato durante questo percorso di dottorato, siete stata la mia scoperta più bella. Le nostre avventure, idiozie, risate e chiamate sono state essenziali per il mio benessere e la mia salute mentale (ammesso che ne abbia ancora una). Un ringraziamento speciale alla mia "favourite German", Isa, grazie di tutto – non scrivo tutta la lista, ma tu lo sai.
A tutti voi menzionati qui sopra, grazie per il continuo vostro sostegno e la vostra infinita fiducia in me. Hanno significato più di quanto possa mai esprimere.

Infine, ma di certo non per importanza, alla mia famiglia: mamma, papà, Peppe/Scema (alias il parassita del mio cuore), e Sofie (che sarà sempre parte della nostra famiglia). Grazie per essere la mia roccia e per credere in me più di quanto io possa mai fare. Il vostro amore e supporto significano il mondo per me. Non sarei nulla senza di voi.

Concludo ringraziando Lei, la mia migliore amica. Sofie, sono stata abbastanza fortunata da crescere e passare 11 anni e mezzo della mia vita con te. Purtroppo, qualcuno ha deciso che dovevi lasciarmi fisicamente all'inizio di questo percorso... ma sorvoliamo su questa parte della storia. La verità è che non mi hai mai davvero lasciata. Grazie, Amore Mio, perché sei stata, sei, e sarai sempre la parte migliore di me... alwayS.

Contents

1 Introduction

> Problems worthy of attack prove
> their worth by fighting back.
>
> *Paul Erdos*

This thesis proposes a normative framework for translating optimization problems into biologically plausible neural networks that are guaranteed to converge to equilibria corresponding to optimal solutions of the optimization problem. These neural networks are systems that more closely align with the principles governing natural neural networks. We aim to model and analyze such systems, using contraction theory – a robust computationally-friendly stability tool from control theory – to establish conditions ensuring their stability and robustness, and use these models to solve static and time-varying optimization problems.

Part of this thesis was conducted during research visits abroad. Specifically, from September 2022 to August 2023, I was at the University of California, Santa Barbara, working in Professor Francesco Bullo's lab at the Center for Control, Dynamical Systems, and Computation. Additionally, in May and June 2023, I was at the Automatic Control Laboratory at ETH Zürich, hosted by Professor Florian Dörfler.

1.1 Context of the Research Topic

Our brain is one of the most complex systems in nature: about 10^{10} neurons, interconnected by approximately 10^{15} recurrent synaptic connections [1]. These neurons are capable of adapting and learning through local synaptic rules [2], continuously solving complex optimization problems. A notable example is sparse representation [3], where biological neural networks efficiently process information using minimal resources.

Attempt to mimic the computations of natural neural networks is what originally inspired [4] artificial neural networks (ANNs). However, over time, most ANNs have diverged significantly from biological realism, driven by performance criteria. Today, the principles guiding ANNs are quite different from those governing biological networks. A clear example of this divergence is the backpropagation algorithm [5], the most commonly used learning algorithm in ANNs. Backpropagation is indeed recognized to

be biologically implausible [6, 7, 8, 9]. The key reason is that it violates the local nature of synaptic changes observed in biological neurons. To see this, consider a synaptic connection between a pre-synaptic neuron j and a post-synaptic neuron i, say it W_{ij}. In backpropagation, changes to W_{ij} depend not only on the activities of neurons i and j, but also on the activities of other neurons of the network. This non-locality contrasts with biological networks, where synaptic changes are local, that is changes to W_{ij} depend only on the activities of the pre- and the post-synaptic neuron.

Despite these differences, ANNs have achieved impressive results, even surpassing human performance in specific tasks, see, e.g., [10, 11]. However, ANNs still exhibit errors and biases that cannot be explained and quantified a-priori and that are absent in biological neurons [12]. For example, ANNs typically require extensive training with large datasets, may lack generalization ability, and can be unstable, with small changes in input leading to significant errors in output [13].

Given the success of ANNs, one might ask: why should we care about the differences between artificial and biological neural networks? The reason lies in what should be the broader goal of AI development. If the aim is to outperform humans on isolated tasks, the current trajectory of ANN development might suffice. However, if the aim is to create general-purpose artificial network that overcomes the actual limitations of ANN, understanding the algorithms governing biological neural networks becomes highly relevant. Quoting [14]: "Natural NNs must contain some "secret sauce" that artificial NNs lack. This is why we need to understand the algorithms implemented by natural NNs and go back to models that mimic the computations of such complex systems."

Motivated by these challenges, our research seeks to model and understand ANNs that more closely align with the principles governing natural networks. The moonshot objective is to develop *trustable neural networks*: robust systems with the ability, typical of human intelligence, to generalize, compose, and abstract knowledge from data.

While it is unrealistic to expect an exact replication of the complex dynamics in biological brains, we aim to develop models that respect some key biological constraints. Our approach does not attempt to reproduce all the intricate biological details. Instead, we focus on a few fundamental principles, including (i) positivity of the system, that is non-negative neuronal outputs [15, 16], and (ii) locality of the learning rules, that is synaptic weights are updated based on local learning rules [2].

Recent advances in neuroscience have provided valuable insights into how populations of neurons compute information. Research has increasingly shifted towards a dynamical systems perspective [17, 18, 19], where neural populations are seen as evolving systems that perform computations over time [20, 21]. In this framework, neural responses are treated as trajectories in high-dimensional state spaces, influenced by both the internal dynamics of the network and external inputs. Recurrent neural networks (RNNs), in particular, have proven useful as models for brain dynamics, as they allow for the study of high-dimensional, distributed, and time-varying neural activity. From a computational perspective, an important feature of RNNs is that they are modeled as nonlinear dynamical systems. This allows for the use of well-established techniques to analyze and understand the properties of those systems. For example, tools from control theory can be employed to ensure the *stability* and *robustness* of RNNs. Specifically,

the tool that we are gonna use throughout this thesis, is contraction theory. The main motivation for looking for contracting dynamics is that with just a single condition, global exponential convergence, along with a number of highly ordered transient and asymptotic behaviors of contracting dynamics, are guaranteed (we expand on why contraction theory is useful in this context in Section 1.3).

Understanding neural dynamics, however, is only one part of the puzzle. To build biologically plausible artificial systems, we must also consider how synaptic plasticity – changes in synaptic connections over time – is modeled. As emphasized in [22],

"Model neural networks, abstractions from neurobiology, are conceived in terms of two different kinds of variables. One class of variables represents the activity of the nerve cells, or 'units'. The other class of variables describes the synapses, or connections, between the nerve cells. A complete model of an adaptive neural system requires two sets of dynamical equations, one for each class of variables, to specify the evolution and behavior of the neural system (...)."

This insight suggests that continuous-time dynamical systems are essential not only for modeling neural dynamics but also for capturing synaptic changes (allowing for different time scales). Incorporating such synaptic dynamics is a key aspect of biologically plausible models, yet quite underexplored [22, 23, 24].

In this context, a normative approach to translate complex tasks, that mathematically can be described by optimization problems that model natural network mechanisms, into biologically plausible neural networks is still missing. The main advantage of such approach is that it provides a direct way to investigate the underlying principles of neural functioning – via the properties of the biologically plausible neural networks – while offering a mathematically tractable framework for understanding these mechanisms. At its core, this challenge can be seen as that to solve complex optimization problems using biologically plausible neural networks, which take the form of continuous-time dynamical systems. This process involves two key steps: (i) establishing the equivalence between the optimal solutions of the optimization problem and the equilibrium points of the network dynamics, and (ii) identifying conditions that guarantee stable convergence of these dynamics to their equilibria. Contraction theory will play a crucial role in ensuring both stability and convergence of the dynamics of our interest, as discussed in later chapters.

This area of research pushes the boundaries of our understanding of neural networks, bridging fields such as neuroscience, machine learning, optimization, control theory, and applied mathematics. In this thesis, we build on these ideas, by proposing a multidisciplinary approach that integrates concepts across diverse fields to lay the groundwork for how contractions theory can be used in the context of biologically plausible (stable) neural networks and optimization.

1.2 Key Research Questions

In the context of the scenario discussed in the previous section, the main objective of this thesis is to establish a normative framework to translate optimization problems into biologically plausible NNs that are guaranteed to converge to equilibria corresponding to the optimal solution to the starting problem. We aim to model and analyze such ANN systems, leverage contraction theory to establish conditions that ensure their stability and robustness, and use those dynamics to solve (static or time-varying) optimization problems. To achieve this, several key questions guide our research:

1. How can we obtain biologically plausible models and how can we guarantee stability and robustness of those dynamics?

2. What are the functional implications of these models? That is, what mechanisms (optimization problems) do natural neural networks solve, and how can biologically plausible neural networks mimic these processes?

3. Can we derive a normative framework to translate optimization problems into NNs that are guaranteed to converge to equilibria corresponding to the optimal solution to the corresponding problem?

4. Given a neural network in which both neural and synaptic change are ruled by continuous-time dynamics, can we establish conditions that guarantee the stability of these systems?

5. Can we effectively use contraction theory to study the stability and robustness of those systems?

6. Given the characteristics of contracting systems, can a contractivity-based approach be effectively applied to track solutions to time-varying optimization problems?

7. In many convex optimization problems, the associated dynamics are non-expansive. In such cases, under what conditions can we guarantee convergence? Additionally, what is the converge behavior for such dynamics?

These questions form the foundation of our research. In the following chapters, we address these questions through a rigorous theoretical and interdisciplinary approach that combines insights from computational neuroscience, control theory, monotone operator theory, and optimization. With our results, we aim to propose an alternative way to how model and analyze biologically plausible neural networks. At the same time, we aim to provide theoretical insights useful in broader contexts, such as the analysis of non-smooth neural networks, nonlinear dynamical systems, static and time-varying optimization – areas with a plethora of practical applications. The long-term objective of this project is to obtain *trustable neural networks*, i.e., robust neural networks having the ability typical of human intelligence to generalize and abstract knowledge from data. While there are many challenges ahead, our goal is to lay a possible groundwork for achieving this ambitious goal. Further discussions on potential future work are presented in Chapter 13.

1.3 Contraction Theory: What and Why?

Contraction theory is the central analytical tool used throughout this thesis to characterize stability and robustness of continuous-time dynamical models. While we refer to Chapter 4 for a comprehensive review of contraction theory, it is important to highlight the reasons why contracting dynamics are particularly well-suited for our analysis.

In *dynamical neuroscience*, biologically plausible continuous-time neural network models are widely studied to simplify and understand complex neural dynamics. These models must account for uncertainties such as unmodeled dynamics and delays. For instance, central pattern generators (CPGs) are biological neural circuits responsible for rhythmic behaviors like walking and swimming. To properly model CPGs in neural networks, one needs to ensure that, if a neural network is interconnected with a CPG, then all trajectories of the neural network converge to a unique stable limit cycle.

In *optimization* a growing body of work focuses on synthesizing continuous-time dynamical systems that converge to equilibria that are also optimal solutions of the corresponding optimization problem. Consequently, significant research effort has been dedicated to characterizing the stability and convergence rates of these systems, along with their robustness against uncertainty. In many applications, optimization algorithms must operate in real-time on time-varying problems, such as tracking a moving target or online learning. In these contexts, the dynamical system should converge to the unique optimal solution when the problem is time-invariant or to an explicitly computable neighborhood of the optimal solution trajectory when the problem is time-varying.

Remarkably, these challenges can be effectively addressed using contracting dynamics. Indeed, contracting systems exhibit highly ordered transient and asymptotic behaviors, which are advantageous in the above contexts. For example: (i) initial conditions are exponentially forgotten [25]; (ii) for time-invariant dynamics, there exists a unique globally exponential stable equilibrium [25]; (iii) contraction ensures entrainment to periodic inputs [26] and implies robustness properties such as input-to-state stability, also when there are delayed dynamics [27, 28]. Moreover, efficient numerical algorithms can be devised for numerical integration and fixed point computation of contracting systems [29]. For a more extensive list of these properties, we refer to Section 4.4.

1.4 Contributions of This Work

This section summarizes the main contributions of this thesis. Detailed statements and references for each contribution are provided in the corresponding chapters. In Chapters 2, 3, and 4 we introduce the main definitions, notations and review the main dynamical models and analytical tools needed for our analysis. With these, we give an answer to the research question number 1 in Section 1.2.

Next, in Chapter 5, we begin our analysis by developing the theoretical tools necessary to analyze the stability of the dynamics resulting when solving sparse reconstruction problems and other optimization problems. Specifically, we investigate stability conditions of two commonly used RNN models, i.e., the Hopfield neural network (HNN) and the firing rate neural network (FNN) by leveraging contraction theory. Initially, we

present several useful algebraic results on matrix polytopes and products of symmetric matrices. Then, we give sufficient conditions for strong and weak Euclidean contractivity of both models with symmetric weights and possibly non-smooth activation functions. The main contributions of this chapter, which includes results published in a paper that received the *2024 IEEE Control Systems Letters Outstanding Paper Award*, can be summarized as follows.

Contribution 1: We provide a set of sufficient conditions characterizing strong and weak infinitesimal contractivity of continuous-time HNNs and FNNs with symmetric weights and possibly non-smooth activation functions. This result is crucial for our analysis, enabling the use of common activation functions such as ReLU and soft-thresholding functions.

Contribution 2: We establish lower bounds on the contraction rates and prove that these bounds are log-optimal for almost all symmetric weight matrices. This implies that our results are sharp, in the sense that they are the best achievable within this framework.

Contribution 3: We present several general algebraic results on matrix polytopes, which are interesting per se. With these results, we: (i) determine a weighted Euclidean norm for matrix polytopes which is log-optimal for almost all synaptic matrices; (ii) give a lower bound on the spectral abscissa of matrix polytopes; (iii) provide optimal and log-optimal norms for the product of symmetric matrices.

In Chapters 6 and 7, we propose and analyze continuous-time FNNs, the *firing rate competitive networks*, to tackle sparse reconstruction problems. With the analysis in these chapters, we address the research questions 2 and 3 outlined in Section 1.2. The main contributions of these chapters are the following.

Contribution 4: We propose a top/down normative framework for a biologically plausible explanation of neural circuits solving sparse reconstruction and other optimization problems. This framework uses the recently studied proximal gradient dynamics, providing a means to transcribe a composite optimization problem into a continuous-time firing rate neural network, which is therefore interpretable.

Contribution 5: We propose and analyze the firing rate competitive network and the positive firing rate competitive network to tackle the sparse reconstruction and positive sparse reconstruction problems, respectively. We establish a result connecting the equilibria of these networks to the optimal solutions of sparse reconstruction problems. To the best of our knowledge, the positive firing rate competitive network is the first RNN designed to tackle positive sparse reconstruction problems.

Contribution 6: We characterize the convergence of the dynamics towards the equilibrium. With our main convergence result we prove that, under a standard assumption on the dictionary, our dynamics converge linear-exponentially to the equilibrium, in the sense that (in a suitably defined norm) the trajectory's distance from the equilibrium is initially upper bounded by a linear function and then convergence becomes exponential. This, in turn, implies that converge towards the equilibrium is global.

Contribution 7: We show that the positive firing rate competitive network is a positive system, i.e., if the system starts with non-negative initial conditions, its state variables remain non-negative. This is an important, biologically plausible property of the network, enabling to effectively model both excitatory and inhibitory synaptic connections in a biologically plausible way.

In Chapters 8 and 9, we propose the modeling and analysis of HNNs and FNNs with dynamic recurrent connections undergoing Hebbian learning rules. Through this analysis, we contribute to provide answers to the research questions 4 and 5 outlined in Section 1.2. The main contributions of these chapters are the following.

Contribution 8: We study a number of coupled neural-synaptic dynamical systems that combine Hopfield neural networks and firing rate neural networks for the neural dynamics and two different Hebbian learning rules for the synaptic dynamics. These models capture networks with both excitatory and inhibitory synapses governed by both Hebbian and anti-Hebbian learning rules.

Contribution 9: To capture synaptic sparsity of the neural circuits, we propose a low-dimensional formulation of our models.

Contribution 10: We give sufficient conditions for the contractivity of each coupled neural-synaptic model by leveraging non-Euclidean contraction arguments. Our sufficient conditions for contractivity and our lower bounds on the contraction rate are both based upon biologically meaningful quantities.

Contribution 11: For each coupled neural-synaptic model, we present a biologically inspired forward invariance result and show that, under suitable conditions, they satisfy Dale's principle. These results enhance the biological plausibility of our models.

In Chapters 10, 11, and 12, we explore the potential of a contractivity-based approach for optimization. With our results, we contribute to provide answers to the research questions 6 and 7 outlined in Section 1.2. Specifically, in Chapter 10, we review convex optimization theory and give natural transcriptions into contracting dynamics for canonical optimization problems. The main contributions of the chapter are the following.

Contribution 12: We give natural transcriptions into contracting dynamics for three canonical strongly convex optimization problems namely monotone inclusions, linear equality-constrained problems, and composite minimization problems. We also review the case of unconstrained optimization problem.

Contribution 13: For each problem we study, we prove the sharpest-known rates of contraction and provide explicit tracking error bounds between solution trajectories and minimizing trajectories.

In Chapter 11, we present a contraction-theoretic approach to continuous-time time-varying convex optimization. The main contributions of the chapter are the following.

Contribution 14: We prove a general theorem regarding parameter-dependent strongly infinitesimally contracting dynamics. Specifically, we show that the tracking error is asymptotically proportional to the rate of change of the parameter with a proportionality constant upper bounded by the Lipschitz constant in which the parameter appears divided by the square of the contraction rate of the dynamics.

Contribution 15: We propose an alternative dynamical system that augments contracting dynamics with a feedforward term. This augmentation ensures that the tracking error decays exponentially to zero.

Contribution 16: We provide explicit tracking error bounds between solution trajectories and minimizing trajectories for three canonical problems, namely monotone inclusions, linear equality-constrained problems, and composite minimization problems.

In Chapter 12, we investigate the convergence characteristics of dynamics that are globally weakly and locally strongly contracting. Such dynamics naturally arise in the context of convex (but not strongly convex) optimization problems with a unique minimizer. The main contributions of the chapter are the following.

Contribution 17: We analyze the convergence of globally-weakly and locally-strongly contracting dynamics, showing that this is linear-exponential, in the sense that the distance between each solution of the system and the equilibrium is upper bounded by a linear-exponential function, introduced in the corresponding chapter.

Contribution 18: Through a novel technical result, we characterize the evolution of certain dynamics with saturation in terms of the linear-exponential function.

Contribution 19: We characterize local input-to-state stability for input-dependent dynamics that are globally-weakly and locally-strongly contracting with respect to the same norm.

Finally, each chapter includes numerical examples to illustrate the effectiveness of our results.

1.5 Relevance to Risk and Complexity

When giving examples of complex systems, the human brain is almost always cited as a prime example. In fact, by definition, the brain embodies complexity: countless interconnected particles (neurons), interacting in a nonlinear way to produce a larger-scale collective outcome, and that are continually influenced by input signals. [30, 31]. This thesis builds on the starting idea of ANN to mimic the computations of the complex systems that are natural neural networks to lay the ground for a normative approach to translate complex tasks into stable and robust biologically plausible neural networks that are guaranteed to converge to equilibria, corresponding to optimal solutions of the original problem. The link to complexity is both direct and fundamental. Moreover, it is worth highlighting that this work is inherently interdisciplinary. To reach our goal we combine in new and unexplored ways insights from computational neuroscience, control theory, and optimization.

While the framework and results we propose are primarily theoretical, our findings hold significant promise for practical applications, particularly in managing risk and complexity in real-world systems that operate in dynamic, uncertain environments. Examples of such applications include time series forecasting, predictive modeling in smart cities, COVID-19 spread prediction, short-term load forecasting, tracking moving targets, estimating stochastic process paths, and online learning [32, 33, 34, 35]. Sparse representation – one of the key optimization problems we will focus on – and static and time-varying optimization problems are widely applicable in complex system scenarios. The biologically plausible neural networks we develop in this thesis, grounded in continuous-time dynamical systems and contraction theory, provide a potential framework for addressing the above problems. Additionally, the work on coupled neural-synaptic networks and time-varying optimization problems further strengthens the link between this research and the management of complex systems. Moreover, the modeling and analysis of locally-strongly and globally-weakly contracting systems provide valuable insights into complex systems that enjoy conservation or invariance properties, such as flow systems, traffic networks, and population dynamics [36].

In summary, the interdisciplinary framework we propose in this thesis has far-reaching implications for the design and analysis of biologically plausible neural networks capable of addressing complex and risk-related tasks. We believe that our findings lay a possible groundwork for future research that will lead to systems capable of enhancing the efficiency and reliability of applications operating in time-varying and risk-related environments.

1.6 Thesis Structure and Outline

The thesis is organized as follows. Detailed outlines are provided in each chapter.

Chapter 2 introduces definitions and notations used throughout the thesis together with needed mathematical preliminaries. Chapter 3 provides essential background on continuous-time dynamics governing both neural masses and synaptic weights. Chapter 4 reviews *contraction theory* for continuous-time dynamical systems. Next, the main contributions of this thesis are presented in three major parts.

Part I proposes a top-down normative framework for biologically plausible neural networks solving optimization problems. This part is made of three chapters. Chapter 5 establishes theoretical results related to the stability of continuous-time Hopfield and firing rate neural networks, providing a sharp characterization of their contractivity with respect to Euclidean norms. These results are essential for the analysis of our models. Next, in Chapters 6 and 7, we propose a top-down normative framework for biologically plausible neural networks that solve sparse reconstruction and other optimization problems. Specifically, in Chapters 6 the modeling of a novel family of continuous-time firing rate neural networks, called *firing rate competitive networks*, to address the sparse reconstruction problems is introduced. Chapter 7 then focuses on the analysis of the convergence behavior of the proposed models.

Part II explores embedding biologically plausible learning mechanisms within neural networks, specifically through Hebbian learning. This part is composed of two chapters.

Chapter 8 focuses on the modeling of coupled neural-synaptic dynamics. These models combine Hopfield neural networks and firing rate neural networks for the neural dynamics and two different Hebbian learning rules for the synaptic dynamics. Chapter 9 follows with the analysis of the dynamical properties and stability of these coupled systems.

Part III investigates the potential of a contractivity-based approach for convex optimization. This part is made of three chapters. In Chapter 10 we provide a transcription to continuous-time dynamical systems of canonical time-invariant optimization problems. For each of these dynamics, we give conditions under which these are strongly infinitesimally contracting. This is extended in Chapter 11, which explores time-varying optimization problems and gives results on equilibrium tracking for parameter-varying contracting systems. Finally, Chapter 12 extends the analysis to continuous-time dynamical systems that solve convex optimization problems with unique minimizers. As we will show, these dynamics are globally weakly contracting and locally strongly contracting. For these systems, we present a comprehensive analysis of their convergence behavior.

Chapter 13 summarizes the main findings and highlights potential future directions. The thesis concludes with Appendix A where additional novel complementary results on the Euclidean contractivity of firing rate neural networks with dissipation are presented.

2 Mathematical Preliminaries

This chapter introduces the main notations, acronyms, and mathematical tools we use throughout the thesis to obtain our results. The chapter is organized as follows. We start in Section 2.1 by introducing the general notation we use throughout the manuscript. Next, in Section 2.2, we give the main definitions and properties of maps necessary for our analysis. In Sections 2.3 and 2.4, we review the properties of logarithmic norms and one-sided Lipschitz conditions. Following this, we recall the concept of composite norms in Section 2.5 and some useful concepts of graph theory in Section 2.6. We conclude the chapter with a primer on proximal operator in Section 2.7.

2.1 Notation

We adopt standard notation throughout the thesis. Unless explicitly stated otherwise, we use the definitions and notations listed here.

General notation:

- $\mathbb{R} := (-\infty, +\infty)$ is the set of real numbers,
- $\overline{\mathbb{R}} := [-\infty, +\infty]$ is the set of extended real numbers,
- $\mathbb{R}^n$ is the set of n-dimensional real numbers,
- $\mathbb{R}_{\geq 0} := [0, +\infty)$ is the set of non-negative real numbers,
- $\mathbf{S}^n$ is the set of real symmetric $n \times n$ matrices,
- $\mathbb{1}_n \in \mathbb{R}^n$ is the all-ones vector of size n,
- $\mathbb{0}_n \in \mathbb{R}^n$ is the all-zeros vector of size n,
- I_n is the $n \times n$ identity matrix,
- $\mathbb{0}_{n,m}$ is the $n \times m$ zero matrix,
- $A^\top$ denotes the transpose of a vector/matrix A,

- $[x] \in \mathbb{R}^{n\times n}$ is the diagonal matrix with diagonal entries equal to the vector $x \in \mathbb{R}^n$,
- "$\circ$" denotes the Hadamard product.

Acronyms:

- LMI := Linear Matrix Inequality,
- SVD := Singular Value Decomposition,
- ReLU := Rectified Linear Units,
- ANN := Artificial Neural Network,
- RNN := Recurrent Neural Network,
- FNN := Firing rate Neural Network,
- HNN := Hopfield Neural Network,
- FCN := Firing rate Competitive Network,
- PFCN := Positive Firing rate Competitive Network,
- LCA := Locally Competitive Algorithm,
- RIP := Restricted Isometry Property,
- GW-LS-C := Globally-Weakly and Locally-Strongly Contracting.

Elements of matrix theory: Vector inequalities of the form $x \leq (\geq)\ y$ are entrywise. We let $A \in \mathbb{R}^{n\times m}$ denote a $n \times m$ matrix with real entries a_{ij}, $i \in \{1, \dots n\}, j \in \{1, \dots, m\}$. Given $A \in \mathbb{R}^{n\times n}$ we denote by

- $\mathrm{rank}(A)$ its rank,
- $\mathrm{spec}(A) := \{\lambda \mid \lambda \text{ eigenvalue of } A\}$ its spectrum,
- $\alpha(A) := \max\{\mathrm{Re}(\lambda) \mid \lambda \text{ eigenvalue of } A\}$ its spectral abscissa, where $\mathrm{Re}(\lambda)$ denotes the real part of λ,
- $\lambda_{\max}(A)$, $\lambda_{\min}(A)$ the maximum and minimum eigenvalue of A, respectively.

Given $A \in \mathbf{S}^n$, we say that A is positive definite (semi-positive definite) and we write $A \succ 0$ (resp. $\succeq 0$) if $x^\top Ax > 0$ (resp. ≥ 0) for all $x \in \mathbb{R}^n$ (resp. for all $x \in \mathbb{R}^n \setminus \{\mathbb{0}_n\}$). Given $A, B \in \mathbf{S}^n$, we write $A \preceq B$ (resp. $A \prec B$) if $B - A$ is positive semidefinite (resp. definite). A triple (U_A, Σ_A, V_A) denote the *singular value decomposition* (SVD) of $A \in \mathbb{R}^{m\times n}$, that is $A = U_A\Sigma_A V_A^\top$, where

- $U_A = [u_1^A, \dots, u_m^A] \in \mathbb{R}^{m\times m}$ is orthonormal, with the eigenvectors of $AA^\top$ as columns,

- $V_A = [v_1^A, \dots, v_n^A] \in \mathbb{R}^{n\times n}$ is orthonormal, with the eigenvectors of $A^\top A$ as columns,
- for positive diagonal matrix $\Sigma_A^r \in \mathbb{R}^{r\times r}$, $r \leq \min\{m, n\}$,

$$\Sigma_A = \begin{bmatrix} \Sigma_A^r & \mathbb{0}_{r,n-r} \\ \mathbb{0}_{m-r,r} & \mathbb{0}_{n-r,n-r} \end{bmatrix} \in \mathbb{R}^{m\times n},$$

  where $\Sigma_A^r = [\sigma_A] := [\sqrt{\lambda_A}]$, with $\lambda_A \in \mathbb{R}^r$ being the positive eigenvalues of $AA^\top$ and $A^\top A$.

When $m = n$, $U_A = V_A$, $\Sigma_A = \Lambda_A := [\lambda_A]$, and we denote by (U_A, Λ_A) the SVD of A.

Next, we recall the definition of two important types of matrices commonly used in the study of the stability of continuous-time dynamical systems: Hurwitz matrices and Metzler matrices. In our analysis, we will run into Hurwitz matrices several times when analyzing stability of the dynamical systems of our interest. Metzler matrices will play a significant role in the stability analysis of coupled neural-synaptic systems in Chapter 9.

Definition 2.1 (Hurwitz and Metzler matrices)**.** *A matrix $A \in \mathbb{R}^{n\times n}$ is*

1. Hurwitz *if $\alpha(A) < 0$,*
2. Metzler *if $a_{ij} \geq 0$ for all $i \neq j$, $i, j \in \{1, \dots, n\}$.*

Norms: We let $\|\cdot\|$ denote both a norm on $\mathbb{R}^n$ and its corresponding induced matrix norm on $\mathbb{R}^{n\times n}$. For a given $p \in [1, +\infty]$ and an invertible matrix R, the *weighted vector norm* and *weighted matrix norm* are, respectively, defined by

$$\|x\|_{p,R} = \|Rx\|_p \quad \text{and} \quad \|A\|_{p,R} = \|RAR^{-1}\|_p, \quad \text{for all } x \in \mathbb{R}^n, A \in \mathbb{R}^{n\times n}.$$

Given $x \in \mathbb{R}^n$ and $r > 0$, we let $B_p(x, r) := \{z \in \mathbb{R}^n \mid \|z - x\|_p \leq r\}$ be the *ball of radius r centered at x* computed with respect to the norm p. Given two vector norms $\|\cdot\|_\alpha$ and $\|\cdot\|_\beta$ on $\mathbb{R}^n$ there exist positive *equivalence coefficients* $k_\alpha^\beta > 0$ and $k_\beta^\alpha > 0$ such that

$$\|x\|_\alpha \leq k_\alpha^\beta \|x\|_\beta, \quad \|x\|_\beta \leq k_\beta^\alpha \|x\|_\alpha, \quad \text{for all } x \in \mathbb{R}^n. \tag{2.1}$$

We recall the concept of *equivalence ratio between two norms*. This is used in Chapters 7 and 12 for analyzing the convergence behavior of non-expansive dynamics with a locally exponentially stable equilibrium.

Definition 2.2 (Equivalence ratio between two norms)**.** *Given two norms $\|\cdot\|_\alpha$ and $\|\cdot\|_\beta$, let k_α^β and k_β^α be the minimal coefficients satisfying inequalities (2.1). The* equivalence ratio between $\|\cdot\|_\alpha$ and $\|\cdot\|_\beta$ *is $k_{\alpha,\beta} := k_\alpha^\beta k_\beta^\alpha$.*

Functions: Finally, we give a list of useful functions used throughout the manuscript. Given $d > 0$ and a set $\mathcal{C}$, we denote by

- $\lceil\,\rceil\colon \mathbb{R} \to \mathbb{Z}$ the *ceiling function*, defined by $\lceil x \rceil = \min\{y \in \mathbb{Z} \mid x \leq y\}$,
- $\operatorname{sign}\colon \mathbb{R} \to \{-1, 0, 1\}$ the *sign function*, defined by $\operatorname{sign}(x) := -1$ if $x < 0$, $\operatorname{sign}(x) := 0$ if $x = 0$, and $\operatorname{sign}(x) := 1$ if $x > 0$,
- $\operatorname{soft}_d\colon \mathbb{R} \to \mathbb{R}$ the *soft thresholding function*, defined by $\operatorname{soft}_d = 0$ if $|x| \leq d$, and $\operatorname{soft}_d = x - d\operatorname{sign}(x)$ if $|x| > d$,
- $\operatorname{sat}_d\colon \mathbb{R} \to [-d, d]$ the *saturation function*, defined by $\operatorname{sat}_d(x) = x$ if $|x| \leq d$, $\operatorname{sat}_d(x) = d$ if $x > d$, and $\operatorname{sat}_d(x) = -d$ if $x < -d$,
- $\iota_{\mathcal{C}}\colon \mathbb{R}^n \to [0, +\infty]$ the *zero-infinity indicator function on* $\mathcal{C}$, defined by $\iota_{\mathcal{C}}(x) = 0$ if $x \in \mathcal{C}$ and $\iota_{\mathcal{C}}(x) = +\infty$ otherwise,
- $\mathbf{1}_{\mathcal{C}}\colon \mathbb{R} \to \{0, 1\}$ the *indicator function on* $\mathcal{C}$, defined by $\mathbf{1}_{\mathcal{C}}(x) = 1$ if $x \in \mathcal{C}$ and $\mathbf{1}_{\mathcal{C}}(x) = 0$ otherwise,
- $\operatorname{ReLU}\colon \mathbb{R} \to \mathbb{R}_{\geq 0}$ the *Rectified Linear Units*, defined by $\operatorname{ReLU}(x) = \max\{0, x\}$,
- $\operatorname{ReLU}_d\colon \mathbb{R} \to [d, +\infty[$ the *shifted Rectified Linear Units*, defined by $\operatorname{ReLU}_d(x) = \max\{0, x - d\}$.

2.2 Operators

We review the main definitions and properties of maps used in this thesis. We begin with the following standard definition.

Definition 2.3 (Lipschitz map)**.** *Given two normed spaces $(\mathcal{X}, \|\cdot\|_{\mathcal{X}})$, $(\mathcal{Y}, \|\cdot\|_{\mathcal{Y}})$, a map $T\colon \mathcal{X} \to \mathcal{Y}$ is* Lipschitz *from $(\mathcal{X}, \|\cdot\|_{\mathcal{X}})$ to $(\mathcal{Y}, \|\cdot\|_{\mathcal{Y}})$ with constant $L \geq 0$ if*

$$\|T(x_1) - T(x_2)\|_{\mathcal{Y}} \leq L\|x_1 - x_2\|_{\mathcal{X}}, \text{ for all } x_1, x_2 \in \mathcal{X}.$$

If $\mathcal{Y} = \mathcal{X}$ and $\|\cdot\|_{\mathcal{X}} = \|\cdot\|_{\mathcal{Y}}$, we say that T is Lipschitz on $(\mathcal{X}, \|\cdot\|_{\mathcal{X}})$ with constant $L \geq 0$. Additionally, we omit to specify the vector space in which the map is Lipschitz if this is clear from the context or is simply $(\mathbb{R}^n, \|\cdot\|_{\mathbb{R}^n})$. We let $\operatorname{Lip}(T)$ be the minimum *Lipschitz constant* of a map T. If T is a multi-variable function we write $\operatorname{Lip}_{(\cdot)}(T)$ to specify the variable with respect to which we are computing the Lipschitz constant.

Definition 2.4 (Upper-right Dini derivative)**.** *The* upper-right Dini derivative *of a function $f\colon \mathbb{R} \to \mathbb{R}$ at t is defined by*

$$D^+ f(t) := \limsup_{h \to 0^+} \frac{f(t+h) - f(t)}{h}.$$

We recall the following theorem [37, 38] for locally Lipschitz function. With this result, in Section 12.5, we characterize local input-to-state stability of non-expansive dynamical systems with a locally exponentially stable equilibrium.

Theorem 2.1 (Mean value theorem for locally Lipschitz function)**.** *Let $\mathcal{C} \subseteq \mathbb{R}^n$ be an open and convex set, and $f : \mathcal{C} \to \mathbb{R}^m$ be a locally Lipschitz map. Then, for almost every $x, y \in \mathcal{C}$ it holds*

$$f(x) - f(y) = \left(\int_0^1 Df(y + s(x - y))ds \right) (x - y),$$

where the integral of a matrix is to be understood component-wise.

2.3 Logarithmic Norm

In this section, we review the properties of *logarithmic norm*, also known as *matrix measure*. The concept of logarithmic norms was introduced in 1958 separately by Dahlquist [39] and Lozinskij [40] as a tool to study the growth of ODE's solutions and the error growth in discretization methods for their approximate solution. For continuous-time dynamical systems, logarithmic norms have become a fundamental tool for defining infinitesimal contractivity and inferring various properties of dynamical systems.

We begin with the following.

Definition 2.5 (Logarithmic norm)**.** *Given a norm $\|\cdot\|$ and a matrix $A \in \mathbb{R}^{n\times n}$, the* logarithmic norm (log-norm) *of A, $\mu(A)$, is defined by*

$$\mu(A) = \lim_{h\to 0^+} \frac{\|I_n + hA\| - 1}{h}. \tag{2.2}$$

Remark 2.1.

- *The existence of the limit in (2.2) is established based on the convexity of the norm function.*
- *The name* logarithmic norm *is justified by the following reason. Consider the dynamics $\dot{x} = Ax$. By applying Coppel's upper bound [41] [42, Th. 2.3] we get*

  $$\frac{d}{dx} \log \|x\| \leq \mu(A),$$

  i.e., the maximal growth rate of the logarithm of the norm of x is bounded by $\mu(A)$.
- *The log-norm of a matrix A can be interpreted as the directional derivative of the matrix norm in the direction of A and evaluated at the point I_n.*

□

Given a weighted matrix norm $\|\cdot\|_{p,R}$, with $p \in [1, +\infty]$ and R invertible matrix, the corresponding *weighted log-norm* is defined as

$$\mu_{p,R}(A) = \mu_p(RAR^{-1}).$$

It is worth highlighting that the log-norm of a matrix can be negative, which is a key difference from matrix norms. This property makes the log-norm a useful tool for studying the stability of continuous-time dynamical systems. Table 2.1 provides explicit formulas for computing the log-norms corresponding to some of the most commonly used norms, along with the corresponding vector norms and induced matrix norms.

Vector Norm	**Induced matrix norm**	**Logarithmic norm**
$\|x\|_1 = \sum_{i=1}^{n} \|x_i\|$	$\|A\|_1 = \max_{j\in\{1,\dots,n\}} \sum_{i=1}^{n} \|a_{ij}\|$	$\mu_1(A) = \max_{j\in\{1,\dots,n\}} \Big(a_{jj} + \sum_{i=1,i\neq j}^{n} \|a_{ij}\|\Big)$
$\|x\|_2^2 = \sum_{i=1}^{n} x_i^2$	$\|A\|_2^2 = \lambda_{\max}(A^\top A)$	$\mu_2(A) = \lambda_{\max}\Big(\frac{A^\top + A}{2}\Big)$
$\|x\|_\infty = \max_{i\in\{1,\dots,n\}} \|x_i\|$	$\|A\|_\infty = \max_{i\in\{1,\dots,n\}} \sum_{j=1}^{n} \|a_{ij}\|$	$\mu_\infty(A) = \max_{i\in\{1,\dots,n\}} \Big(a_{ii} + \sum_{j=1,i\neq j}^{n} \|a_{ij}\|\Big)$

Table 2.1: Vector norms, induced matrix norms, and corresponding log-norms, for $x \in \mathbb{R}^n$ and $A \in \mathbb{R}^{n\times n}$.

Next, we give some of the main properties of the log-norms used throughout the manuscript.

Proposition 2.2 (Properties of the log-norm)**.** *Given A, $B \in \mathbb{R}^{n\times n}$, the following properties hold*

(i) positive homogeneity: $\mu(cA) = |c|\mu(\text{sign}(c)A), \quad \forall c \in \mathbb{R},$

(ii) subadditivity: $\mu(A + B) \leq \mu(A) + \mu(B),$

(iii) translation: $\mu(A + cI_n) = \mu(A) + c, \quad \forall c \in \mathbb{R},$

(iv) product: $\max\{-\mu(A), -\mu(-A)\}\|x\| \leq \|Ax\|, \quad \forall x \in \mathbb{R}^n,$

(v) norm of difference: $|\mu(A) - \mu(B)| \leq \|A - B\|,$

(vi) norm spectrum: $\forall \lambda \in \text{spec}(A).$ $-\|A\| \leq -\mu(-A) \leq \text{Re}(\lambda) \leq \alpha(A) \leq \mu(A) \leq \|A\|,$

The norm spectrum property shows that the log-norm of a matrix A is an upper bound on the spectral abscissa of A. This is fundamental for analyzing the stability of continuous-time dynamical systems. As a consequence, it is interesting to understand the gap between the spectral abscissa and the log-norm of a matrix. To this purpose, we recall the following definition of logarithmic optimality of norms. We extend this definition in Chapter 5 to matrix polytopes.

Definition 2.6 (Logarithmic optimality of norms)**.** *Given a matrix $A \in \mathbb{R}^{n\times n}$ with spectral abscissa $\alpha(A)$ and a scalar $\varepsilon > 0$, the norm $\|\cdot\|$ with associated log-norm μ is*

1. *logarithmically optimal for A if $\mu(A) = \alpha(A)$,*
2. *logarithmically ε-optimal for A if $\alpha(A) \leq \mu(A) \leq \alpha(A) + \varepsilon$.*

Finally, we recall a result on Metzler matrices [43] (see also [44]) that we use in Chapter 8 to analyze contractivity of the coupled neural-synaptic models.

Lemma 2.3 (Optimal diagonally-weighted norms for Metzler matrices)**.** *Consider a Metzler matrix $M \in \mathbb{R}^{n\times n}$. For any $p \in [1,\infty]$, and $\delta > 0$, define $\eta_{M,p,\delta} \in \mathbb{R}^n_{\geq 0}$ by*

$$\eta_\delta = \left(\frac{l_1^{1/p}}{r_1^{1/q}}, \dots, \frac{l_n^{1/p}}{r_n^{1/q}} \right),$$

where $q \in [1,\infty]$ is the conjugate index of p, while l and $r \in \mathbb{R}^n_{\geq 0}$ are the left and right dominant eigenvectors of $M + \delta \mathbb{1}_n \mathbb{1}_n^\top$. Then for each $\varepsilon > 0$ there exists $\delta > 0$ such that

1. *the norm $\|\cdot\|_{p,[\eta_\delta]}$ is ε-logarithmically optimal for M, that is*

$$\alpha(M) \leq \mu_{p,[\eta_\delta]}(M) \leq \alpha(M) + \varepsilon,$$

2. *if M is irreducible, then $\|\cdot\|_{p,[\eta_0]}$ is logarithmically optimal for M, that is*

$$\alpha(M) = \mu_{p,[\eta_0]}(M).$$

2.4 One-sided Lipschitz Conditions

In this section, we review the concept of one-sided Lipschitz conditions, which serve as a useful tool for characterizing the contractivity of continuous-time dynamical systems. To do so, we first introduce the notion of weak pairing.

Definition 2.7 (Weak pairing)**.** *A weak pairing $[\![\cdot,\cdot]\!]$ on $\mathbb{R}^n$ is a map $[\![\cdot,\cdot]\!] : \mathbb{R}^n \times \mathbb{R}^n \to \mathbb{R}$ satisfying*

- sub-additivity of first argument: $[\![x+z,y]\!] \leq [\![x,y]\!] + [\![z,y]\!]$, *for all* $x,y,z \in \mathbb{R}^n$,
- curve norm derivative formula: $\|y(t)\| D^+\|y(t)\| = [\![\dot{y}(t), y(t)]\!]$, *for every differentiable curve* $y\colon]a,b[\to \mathbb{R}^n$ *and for almost every* $t \in]a,b]$,
- Cauchy-Schwartz inequality: $|[\![x,y]\!]| \leq \|x\|\|y\|$, *for all* $x,y \in \mathbb{R}^n$,
- Lumer's equality: $\mu(A) = \sup_{z\in\mathbb{R}^n, z\neq \mathbb{0}_n} \dfrac{[\![Az,z]\!]}{[\![z,z]\!]}$, *for every* $A \in \mathbb{R}^{n\times n}$.

For every norm $\|\cdot\|$ on $\mathbb{R}^n$, there exists a (possibly not unique) compatible weak pairing $[\![\cdot,\cdot]\!]$ such that $\|x\|^2 = [\![x,x]\!]$, for every $x \in \mathbb{R}^n$. We give the following.

Definition 2.8 (One-sided Lipschitz constant)**.** *Given a convex set $C \subseteq \mathbb{R}^n$, a norm with compatible weak pairing, and a continuous map $f\colon C \to \mathbb{R}^n$, the* minimal one-sided Lipschitz constant of f*, denoted by* $\mathrm{osL}(f)$*, is defined by*

$$\mathsf{osLip}(f) := \sup_{x,y\in C, x\neq y} \frac{[\![f(x)-f(y), x-y]\!]}{\|x-y\|^2} \in \mathbb{R}.$$

For a continuously differentiable map $f\colon C \to \mathbb{R}^n$, where $C \subseteq \mathbb{R}^n$ is convex, the log-norm of the Jacobian matrix of f, denoted by $Df(x)$, satisfies the following property

$$\mathrm{osL}(f) = \sup_{x\in C} \mu(Df(x)).$$

Given $f\colon \mathbb{R}_{\geq 0} \times C \to \mathbb{R}^n$, where $C \subseteq \mathbb{R}^n$ is open and connected, we denote by $\mathrm{osL}(f_t)$ the *one-sided Lipschitz constant* of $f_t := f(t,\cdot)$. Note that the Cauchy-Schwarz inequality for weak pairings implies $\mathrm{osL}(f_t) \leq \mathsf{Lip}\,(f_t)$.

Given an invertible matrix Q, a scalar $p \in [0,+\infty]$, and a map f, we write $\mathsf{osLip}_{p,Q}(f)$ to specify that the one-sided Lipschitz constant of f is computed with respect to a Q-weighted ℓ_p norm. For example, for the Q-weighted Euclidean norm we have

$$\mathrm{osL}_{2,Q^{1/2}}(f_t) = \sup_{x,y\in C, x\neq y} \frac{(x-y)^\top Q(f(x)-f(y))}{\|x-y\|^2_{2,Q^{1/2}}}.$$

2.5 Composite Norms

In this section, we review the concept of composite norms, originally studied in [45] (see also [46]). Composite norms provide a framework for studying systems with interconnected components by combining different norms in a structured manner. This approach is particularly useful when dealing with systems where multiple subsystems interact, such as the coupled neural-synaptic systems we study in Chapter 9. Specifically, we use composite norms for analyzing the overall stability and contractivity properties of these interconnected dynamical systems.

Consider r positive integers $n_1, \ldots, n_r$, such that $\sum_{i=1}^r n_i = n$, and

- r *local norms* $\|\cdot\|_i$ defined on $\mathbb{R}^{n_i}$ with induced log-norms $\mu_i(\cdot)$,
- an *aggregating norm* $\|\cdot\|_{\mathrm{agg}}$ on $\mathbb{R}^r$ with induced log-norm $\mu_{\mathrm{agg}}(\cdot)$.

The *composite norm* $\|\cdot\|_{\mathrm{cmpst}}$ on $\mathbb{R}^n$ is defined as

$$\|x\|_{\mathrm{cmpst}} = \left\| \begin{bmatrix} x_1 \\ \vdots \\ x_r \end{bmatrix} \right\|_{\mathrm{cmpst}} = \left\| \begin{bmatrix} \|x_1\|_1 \\ \vdots \\ \|x_r\|_r \end{bmatrix} \right\|_{\mathrm{agg}}.$$

We denote by $\mu_{\mathrm{cmpst}}(\cdot)$ the log-norm induced by $\|\cdot\|_{\mathrm{cmpst}}$. Next, consider a block matrix $A \in \mathbb{R}^{n\times n}$ with blocks $A_{ij} \in \mathbb{R}^{n_i \times n_j}$, $i,j \in \{1,\ldots,r\}$. The *aggregate majorant* $|A|_{\mathrm{agg}}$

and *aggregate Metzler majorant* $|A|_{\mathrm{M}}$ in $\mathbb{R}^{r\times r}$ are defined by

$$\big(|A|_{\mathrm{agg}}\big)_{ij} := \|A_{ij}\|_{ij}, \quad (|A|_{\mathrm{M}})_{ij} := \begin{cases} \mu_i(A_{ii}), & \text{if } j = i, \\ \|A_{ij}\|_{ij}, & \text{if } j \neq i, \end{cases}$$

where $\|A_{ij}\|_{ij} = \max\{\|A_{ij}y_j\|_i \mid y_j \in \mathbb{R}^{n_j} \text{ s.t. } \|y_j\|_j = 1\}$. Finally, we report results that can be found, under different technical statements, in [45, 28] with the upper bound for the log-norm introduced in [46].

Theorem 2.4. *For any set of local norms $\|\cdot\|_i$, $i \in \{1,\dots,r\}$, consider a monotonic aggregating norm $\|\cdot\|_{\mathrm{agg}}$ over a decomposition of $\mathbb{R}^n$ and a matrix $A \in \mathbb{R}^{n\times n}$. Then:*

$$\begin{aligned} \max_{i\in\{1,\dots,r\}} \|A_{ii}\|_i \leq \|A\|_{\mathrm{cmpst}} \leq \||A|_{\mathrm{agg}}\|_{\mathrm{agg}}, \\ \max_{i\in\{1,\dots,r\}} \mu_i(A_{ii}) \leq \mu_{\mathrm{cmpst}}(A) \leq \mu_{\mathrm{agg}}(|A|_{\mathrm{M}}). \end{aligned} \tag{2.3}$$

2.6 Out-Incidence and In-Incidence Matrices

In this section, we review some concepts from graph theory used in Chapter 8 to derive low-dimensional reformulations of the coupled neural-synaptic models.

Let G be a weighted directed graph with n nodes and m edges, and let $V = \{1,\dots,n\}$ and $E = \{1,\dots,m\}$ be the set of nodes and edges of G, respectively. We write $e = (i,j)$, $i,j \in V$, when we want to emphasize the nodes associated with the edge e, and we refer to i as the *tail* and to j as the *head* of e. According to the context, with a little abuse of notation, we let e denote both an ordered pair (i,j) as well as an element of E. We let $\{a_e\}_{e\in E}$ be the set of weights for the edges of G.

The *adjacency matrix* $A \in \mathbb{R}^{n\times n}$ is defined as follows: for each edge $e = (i,j) \in E$, the entry (i,j) of A is equal to the weight a_e of the edge (i,j), and all other entries of A are equal to zero. The *weight matrix* $\mathcal{A} \in \mathbb{R}^{m\times m}$ is the diagonal matrix of edge weights, that is $\mathcal{A} := [\{a_e\}_{e\in E}]$.

Definition 2.9 (Topological in-degree and out-degree)**.** *Given a weighted directed graph G and a vertex $i \in V$, the* topological in-degree *and* out-degree *of i are the number of in-neighbors and out-neighbors of i, respectively. We define* maximum topological in-degree *and* maximum topological out-degree*, the highest topological in-degree and out-degree among all vertices in G, respectively.*

Next, we introduce the key tools we use in Section 8.4 to derive low-dimensional reformulations for the coupled neural-synaptic models.

Definition 2.10 (Out-incidence and in-incidence matrices)**.** *Given a weighted directed graph G, for any node $i \in V$ and edge $e \in E$, the* out-incidence matrix $B_{\mathrm{out}} \in \{0,1\}^{n\times m}$

and in-incidence matrix $B_{\text{in}} \in \{0,1\}^{n\times m}$ *are respectively defined by*

$$(B_{\text{out}})_{ie} = \begin{cases} 1 & \text{if node } i \text{ is the head of edge } e, \\ 0 & \text{otherwise}, \end{cases} \tag{2.4}$$

$$(B_{\text{in}})_{ie} = \begin{cases} 1 & \text{if node } i \text{ is the tail of edge } e, \\ 0 & \text{otherwise}. \end{cases} \tag{2.5}$$

Note that, by construction, the matrices B_{out} and B_{in} have unit row sums, thus $B_{\text{out}}^\top$ and $B_{\text{in}}^\top$ have unit column sums. The following result can be found in [47, Ex. 9.4].

Proposition 2.5. *Consider the adjacency matrix $A \in \mathbb{R}^{n\times n}$, the weight matrix $\mathcal{A} \in \mathbb{R}^{m\times m}$, the out-incidence matrix $B_{\text{out}} \in \{0,1\}^{n\times m}$, and the in-incidence matrix$B_{\text{in}} \in \{0,1\}^{n\times m}$. Then:*

1. *for each $x \in \mathbb{R}^n$ and $e \in E$ of the form $e = (i, j)$,*

$$(B_{\text{out}}^\top x)_e = x_j, \text{ and } (B_{\text{in}}^\top x)_e = x_i. \tag{2.6}$$

2. *the following identity holds*

$$A = B_{\text{in}} \mathcal{A} B_{\text{out}}^\top. \tag{2.7}$$

3. *$\|B_{\text{out}}^\top\|_\infty = \|B_{\text{in}}^\top\|_\infty = 1$, $\|B_{\text{out}}\|_\infty$ and $\|B_{\text{in}}\|_\infty$ are the maximum topological out-degree and maximum topological in-degree of G, respectively.*

Finally, we give a representative example to clarify the graph theoretic concepts introduced in this section.

Example 2.1. *Consider the directed graph G in Figure 2.1. The set of nodes and edges of G, are, respectively, $V = \{1,\dots,4\}$ and $E = \{e_1,\dots,e_5\}$. Specifically, we have $e_1 = (4,1)$, $e_2 = (1,2)$, $e_3 = (4,2)$, $e_4 = (1,3)$, $e_5 = (3,4)$.*

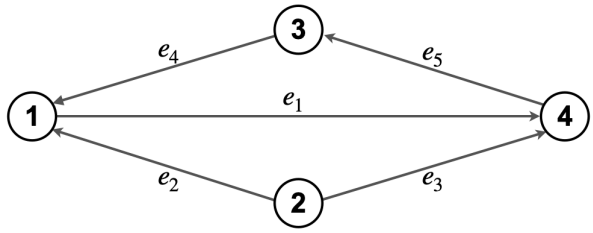

Figure 2.1: Directed graph G with nodes i, $i \in \{1,\dots,4\}$, and edges, e_j, $j \in \{1,\dots,5\}$.

The out- and in-incidence matrices for G are:

$$B_{\text{in}} = \begin{bmatrix} 0 & 1 & 0 & 1 & 0 \\ 0 & 0 & 0 & 0 & 0 \\ 0 & 0 & 0 & 0 & 1 \\ 1 & 0 & 1 & 0 & 0 \end{bmatrix}, \; B_{\text{out}} = \begin{bmatrix} 1 & 0 & 0 & 0 & 0 \\ 0 & 1 & 1 & 0 & 0 \\ 0 & 0 & 0 & 1 & 0 \\ 0 & 0 & 0 & 0 & 1 \end{bmatrix}.$$

2.7 A Primer on Proximal Operators

We provide a brief overview of proximal operators and outline the key properties relevant to our analysis. The proximal operator of a convex function extends the concept of a projection operator onto a convex set, offering a powerful tool for dealing with non-smooth optimization problems. This concept has gained increasing significance in various fields including signal processing and optimization [48, 49]. In our analysis, proximal operators play a crucial role in Chapter 6 for transcribing a composite optimization problem into an interpretable continuous-time RNN. Additionally, this operator is instrumental in Chapters 10 and 11 to design continuous-time dynamical systems solving the monotone inclusion problem in both static and time-varying scenarios.

We start by giving several preliminary concepts. Given a function $g\colon \mathbb{R}^n \to \overline{\mathbb{R}}$, the *epigraph* of g is the set $\operatorname{epi}(g) = \{(x, y) \in \mathbb{R}^{n+1} \mid g(x) \leq y\}$.

Definition 2.11 (Convex, proper, and closed function)**.** *A function $g\colon \mathbb{R}^n \to \overline{\mathbb{R}}$ is*

- convex *if* $\operatorname{epi}(g)$ *is a convex set,*
- proper *if its value is never $-\infty$ and there exists at least one $x \in \mathbb{R}^n$ such that $g(x) < \infty$,*
- closed *if it is proper and* $\operatorname{epi}(g)$ *is a closed set.*

Next, we define the proximal operator of a function g, which is a map that takes a vector $x \in \mathbb{R}^n$ and maps it into a subset of $\mathbb{R}^n$, which can be either empty, contain a single element, or be a set with multiple vectors.

Definition 2.12 (Proximal Operator)**.** *The* proximal operator *of a function $g\colon \mathbb{R}^n \to \overline{\mathbb{R}}$ with parameter $\gamma > 0$, $\operatorname{prox}_{\gamma g}\colon \mathbb{R}^n \to \mathbb{R}^n$, is defined by*

$$\operatorname{prox}_{\gamma g}(x) = \operatorname*{arg\,min}_{z \in \mathbb{R}^n} g(z) + \frac{1}{2\gamma}\|x - z\|_2^2, \qquad \forall x \in \mathbb{R}^n. \tag{2.8}$$

Of particular interest for our analysis is the case when $\operatorname{prox}_{\gamma g}$ is a singleton. The next Theorem [49, Th. 6.3] provides conditions under which $\operatorname{prox}_{\gamma g}$ exists and is unique.

Theorem 2.6 (Existence and uniqueness)**.** *Let $g\colon \mathbb{R}^n \to \overline{\mathbb{R}}$ be a convex, closed, and proper function. Then $\operatorname{prox}_{\gamma g}(x)$ is a singleton for all $x \in \mathbb{R}^n$.*

The above result shows that for any convex, closed, and proper function g, the proximal operator $\operatorname{prox}_{\gamma g}(x)$ exists and is unique for all $x \in \mathbb{R}^n$. Next, we recall key a result in the calculus of proximal mappings [49, Section 6.3]. This result is instrumental in our interpretation of certain dynamics as recurrent neural networks in Chapter 6. Specifically, this property enables us to view in our context the proximal operator as the activation function of an RNN.

Lemma 2.7 (Prox of separable functions)**.** *Let $g\colon \mathbb{R}^n \to \mathbb{R}$ be a convex, closed, proper, and separable function, that is $g(x) = \sum_{i=1}^n g_i(x_i)$, with $g_i\colon \mathbb{R} \to \mathbb{R}$ being convex, closed, and proper functions. Then*

$$(\operatorname{prox}_{\gamma g}(x))_i = \operatorname{prox}_{\gamma g_i}(x_i), \quad i \in \{1, \dots, n\}.$$

Remark 2.2. *Given a convex set $\mathcal{C}$, the proximal operator of the zero-infinity indicator function on $\mathcal{C}$ is the Euclidean projection onto $\mathcal{C}$, that is* $\operatorname{prox}_{\gamma\iota_{\mathcal{C}}}(x) = \mathbb{P}_{\mathcal{C}}(x) := \arg\min_{z\in\mathcal{C}} \|x - z\|_2 \in \mathcal{C}$. □

Finally, we introduce the Moreau envelope associated with the proximal operator of a function g.

Definition 2.13. *The* Moreau envelope *of a function $g\colon \mathbb{R}^n \to \overline{\mathbb{R}}$ with parameter $\gamma > 0$, $M_{\gamma g}\colon \mathbb{R}^n \to \overline{\mathbb{R}}$, is defined by*

$$M_{\gamma g}(x) = g(\operatorname{prox}_{\gamma g}(x)) + \frac{1}{2\gamma}\|x - \operatorname{prox}_{\gamma g}(x)\|_2^2. \tag{2.9}$$

The Moreau envelope of a function g is essentially a smoothed or regularized form of the function. An important property of the Moreau envelope is that it is always continuously differentiable, even when g is not, and its gradient is given by

$$\nabla M_{\gamma g}(x) = \frac{1}{\gamma}(x - \operatorname{prox}_{\gamma g}(x)). \tag{2.10}$$

The gradient of the Moreau envelope is Lipschitz on $(\mathbb{R}^n, \|\cdot\|_2)$ with constant $1/\gamma$.

Example 2.2. *Let $g(x) = \|x\|_1$. Note that g is separable, thus satisfies Lemma 2.7. We have that*

- *the proximal operator of g is the soft-thresholding function, that is*

$$\operatorname{prox}_{\gamma g}(x) = \operatorname{soft}_{\gamma}(x),$$

- *the associated Moreau envelope of g is the Huber function, i.e.,*

$$M_{\gamma g}(x_i) = \begin{cases} \frac{1}{2\gamma}x_i^2 & \text{if } |x_i| \le \gamma, \\ \gamma\left(|x_i| - \frac{1}{2}\gamma\right), & \text{if } |x_i| > \gamma, \end{cases}$$

- *the gradient of the Moreau envelope is the saturation function*

$$\nabla M_{\gamma g}(x_i) = \operatorname{sign}(x_i)\min\left(\frac{|x_i|}{\gamma}, 1\right).$$

2.7.1 Proximal Gradient Method

The proximal gradient method generalizes standard gradient descent to certain classes of non-smooth optimization problems. Based on the use of proximal operators, *proximal gradient method* (see, e.g., [50]) can be devised to iteratively solve a class of composite (possibly non-smooth) convex problems of the form

$$\min_{x\in\mathbb{R}^n} f(x) + g(x), \tag{2.11}$$

where $f\colon \mathbb{R}^n \to \mathbb{R}$, $g\colon \mathbb{R}^n \to \overline{\mathbb{R}}$ are convex, proper and closed functions, and f is differentiable. At its core, the proximal gradient method updates the estimate of the solution of the optimization problem by computing the proximal operator of αg, where $\alpha > 0$ is a step size, evaluated at the difference between the current estimate and the gradient of αf computed at the current estimate. That is,

$$x^{k+1} := \operatorname{prox}_{\alpha^k g}\big(x^k - \alpha^k \nabla f(x^k)\big).$$

Remark 2.3. *When $g = 0$, the proximal gradient method simplifies to standard gradient descent. When g is the indicator function of a convex set, the proximal gradient method simplifies to projected gradient descent.* □

Notably, this method has been recently extended and generalized to a continuous-time framework [51, 52, 53], resulting in solving a continuous-time FNN. In this case, the iteration becomes the *continuous-time proximal gradient dynamics*

$$\dot{x} = -x + \operatorname{prox}_{\gamma g}\big(x - \gamma \nabla f(x)\big), \tag{2.12}$$

with $\gamma > 0$. The above dynamics are central to developing a normative framework for biologically plausible neural networks solving sparse reconstruction problems in Chapter 6. Additionally, these dynamics are useful for the design of contracting continuous-time dynamical systems solving non-smooth and convex composite optimization problems, as we show in Chapters 10 and 11.

2.8 Summary

In this chapter, we introduced the main symbols and notations we will use throughout the thesis and provided a self-contained review of the key concepts and theories that underpin our results, providing the details useful for our developments. Specifically, we listed the main functions we will use in this thesis. Then, we reviewed the concept of logarithmic norm. This is an important tool for analyzing the stability of continuous-time dynamical systems, as it provides an upper bound on the spectral abscissa of a matrix. Next, we recalled the concept of one-sided Lipschitz conditions, which, together with logarithmic norms, we use throughout the thesis to characterize the contractivity of possibly non-smooth continuous-time dynamical systems. We then discussed composite norms, a useful tool for analyzing interconnected systems. Following this, we presented key concepts from graph theory that, as we will see in Chapter 9, allow us to derive low-dimensional reformulations of the interconnected neural-synaptic models we propose. This low-dimensional formulation allows to capture synaptic sparsity of the neural circuits. Finally, we provided a review of proximal operators. In the following chapters, the continuous-time proximal gradient dynamics, in particular, play a key role in designing contracting continuous-time dynamical systems solving non-smooth and convex composite optimization problems, including the sparse reconstruction problem.

3 Neural and Synaptic Dynamics

In this chapter, we provide backgrounds on the continuous-time dynamical rules governing both neural masses and synaptic weights, which are central to our analysis. Specifically, for the neural dynamics, we focus on two widely used continuous-time RNN models: the Hopfield neural network (HNN) and the firing rate neural network (FNN). In Chapter 5, we analyze the stability of these dynamics, providing novel stability conditions for non-smooth activation function, allowing the use of the more commonly used ones. Additionally, we run into FNNs in Chapters 6 and 7, where we propose a top/down normative framework for a biologically plausible explanation of neural circuits solving sparse reconstruction problems and other optimization problems. These neural dynamics are also at the basis of the coupled neural-synaptic problems we propose and analyze in Part II. There, we assume the synaptic weight dynamics evolve according to continuous-time Hebbian learning rules.

3.1 Introduction

Artificial neural networks, inspired by biological neural systems, are typically conceptualized through two distinct sets of variables: one representing the activity of neurons and the other describing the synapses (or connections) between them. Understanding and modeling these two aspects is crucial in both computational neuroscience and machine learning, as they form the basis of how networks process information and learn.

Recurrent neural networks naturally emerge when modeling neural dynamics due to both anatomical and functional properties of the brain [54, 20]. A large fraction of the output from cortical regions loops back to the area of origin, making recurrent connections a fundamental feature of cortical organization [55]. Furthermore, RNNs can generate rich intrinsic activity patterns, reminiscent of ongoing activity observed in the brain [56]. From a computational perspective, RNNs are particularly powerful because feedback loops enable the modeling of temporal dependencies, making these networks well-suited for tasks involving sequential data or time-series predictions. Another important feature of RNNs is that they are modeled as nonlinear dynamical systems. This allows to apply tools from dynamical systems theory to study key properties like stability, attractor

dynamics, and convergence, as we will explore in the following chapters.

Synaptic plasticity refers to changes in the strength of connections between neurons over time. This process is at the basis of learning and memory in biological systems. One of the most widely accepted theories of synaptic plasticity is *Hebbian learning* [2], often captured by the phrase *"neurons that fire together, wire together"*. Hebbian learning is a form of unsupervised learning and provides a biologically plausible mechanism for how networks adapt based on experience. Over the years, this rule has inspired various learning algorithms in artificial neural networks, with the goal of developing biologically plausible models of learning.

The chapter is organized as follows. In Section 3.2, we provide a concise literature review on RNNs and Hebbian learning. Then, in Section 3.3, we introduce the continuous-time dynamical rules governing the neural masses of the RNN models we are interested in: the Hopfield neural network and the firing rate neural network. Finally, in Section 3.4 we review Hebbian learning rules and the mathematical formulation we use in our analysis.

3.2 Overview

Wilson and Cowan pioneered the study of RNN in a biological context work by describing the average firing rates of groups of neurons through differential equations, thus modeling the dynamics of neural populations [57]. This model laid the foundation for modern RNN frameworks, which have since become instrumental in analyzing neural circuit behaviors through rate-based equations.

Two common models of RNNs are the *firing rate neural network* (FNN) [54] and *Hopfield neural network* (HNN) [58]. The key difference between these models lies in the order in which the activation function is applied. For certain synaptic weight matrices and initial conditions, the two models can be shown to be mathematically equivalent via a transformation of coordinates and input states [59]. However, this transformation is state-dependent, particularly when the synaptic matrix is rank deficient. Additionally, the transformation of solutions from HNNs to FNNs requires that the initial condition of the input depends on the initial condition of the state. RNNs have been demonstrated to be suitable in applications requiring the learning of sequential tasks. For example, they have been successfully used in time series forecasting [60] and pattern generation [61]. Over the years, Hopfield neural networks, originally designed to model associative memory systems, have found applications in optimization and machine learning tasks [62, 63, 64, 65].

One of the central mechanisms underlying learning in both biological and artificial systems is synaptic plasticity—the process by which synaptic connections between neurons are strengthened or weakened based on neural activity. This principle is often captured through Hebbian learning rules, first introduced by Donald Hebb in his seminal work, *"The Organization of Behavior"* [2]. Hebbian learning rules have since played a crucial role in modeling and understanding neural learning dynamics and have been extensively studied within the framework of unsupervised feedforward neural networks. For instance, Hebbian learning rules have been used in training a neuron to extract the

first principal component of its inputs [66]. In [67] it is shown that a layer of simple Hebbian units connected by modifiable anti-Hebbian feedback connections can learn to code a set of patterns so that statistical dependency between the representation elements is reduced, while information is preserved. Several mathematical formulations of Hebbian learning are presented in [68]. In [69] is presented a mathematical analysis of the effects of Hebbian learning in random recurrent neural networks. In the context of Hopfield neural networks with adapting synapses undergoing Hebbian rules, we recall [22, 24, 70]. Additionally, Hopfield neural networks with a coupled Hebbian learning rule have been shown to be able to learn the underlying geometry of a given set of inputs [23]. Along these lines, recently, [8] proposed an unsupervised biologically plausible learning rule that allows the network to achieve good performance on the MNIST and CIFAR datasets. Finally, Hebbian learning has been generalized to a variety of computational paradigms, including sparse coding [71] and similarity matching [72, 73, 74, 15, 14, 16].

3.3 Neural Dynamics: Hopfield Neural Network and Firing Rate Neural Network

In this section, we introduce the dynamical rules governing the neural masses. Specifically, we are interested in two widely used continuous-time RNN models: the Hopfield neural network and the firing rate neural network.

Hopfield neural network: the continuous-time HNN follows the dynamics of the form

$$\tau_{\mathrm{H}}\dot{x} = -x + W\Phi(x) + u_{\mathrm{H}}, \tag{3.1}$$

where

- $x \in \mathbb{R}^n$ is the neural activation vector,
- $\tau_{\mathrm{H}} > 0$ is the timescale of the network,
- $W \in \mathbb{R}^{n\times n}$ is the synaptic matrix, with $W_{ij} \in \mathbb{R}$ being the synaptic weight from a pre-synaptic neuron j to a post-synaptic neuron i,
- $\Phi\colon \mathbb{R}^n \to \mathbb{R}^n$ is a nonlinear and diagonal activation function, that is, for $x \in \mathbb{R}^n$, $(\Phi(x))_i = \phi(x_i)$, where $\phi\colon \mathbb{R} \to \mathbb{R}$,
- $u_{\mathrm{H}} \in \mathbb{R}^n$ represents external stimuli, which may be time-dependent.

Firing rate neural network: the dynamics of the FNN are given by

$$\tau_{\mathrm{F}}\dot{\nu} = -\nu + \Phi(W\nu + u_{\mathrm{F}}) \tag{3.2}$$

where, similar to (3.1),

- $\nu \in \mathbb{R}^n$ is the neural activation vector,
- $\tau_{\mathrm{F}} > 0$ is the timescale of the network,
- $W \in \mathbb{R}^{n\times n}$ is the synaptic matrix, with $W_{ij} \in \mathbb{R}$ being the synaptic weight from a pre-synaptic neuron j to a post-synaptic neuron i,
- $\Phi\colon \mathbb{R}^n \to \mathbb{R}^n$ is a nonlinear and diagonal activation function,
- $u_{\mathrm{F}} \in \mathbb{R}^n$ represents the external stimuli, which may be time-dependent.

Remark 3.1.

(i) We term the RNN (3.2) *as* firing rate neural network *because when the activation function is non-negative, the positive orthant is forward-invariant and the state ν is interpreted as a firing rate. In contrast, in* (3.1)*, the state x can be either positive or negative, and thus x is interpreted as a membrane potential.*

(ii) The HNN (3.1) *has the same form as the original Hopfield model [58] with the key difference that the synaptic matrix is not assumed symmetric if not explicitly stated. Despite the absence of the symmetry assumption, with a slight abuse of terminology, we also term the Hopfield-like neural network* (3.1) *as Hopfield neural network. This terminology is consistent with the terminology used in, e.g., [75, 76, 23].*

□

An important characteristic of the HNN in equation (3.1) is that it can be implemented as an analog electronic circuit (see, e.g., [77, Section 13.5]). To the best of our knowledge, there is no such implementation for the FNN in equation (3.2).

The HNN (3.1) and FNN (3.2) are known to be mathematical equivalent through suitably defined state and input transformations. [59]. However, the input transformation is state-dependent when the synaptic matrix is rank deficient (as in the sparse reconstruction problem we analyze in Part I) and, counter-intuitively, the transformation of solutions from HNN to FNN requires that the initial condition of the input depends on the initial condition of the state. Moreover, the FNN might hold an advantage over the HNN in terms of biological plausibility in the following sense. When the activation function is non-negative, the positive orthant is forward-invariant, i.e., the state remains non-negative from non-negative initial conditions and is thus interpreted as a vector of firing rates. Therefore, even if the HNN state can be interpreted as a vector of membrane potentials, it is more natural to interpret negative (resp. positive) synaptic connections as inhibitory (resp. excitatory) in the FNN rather than the HNN.

A complete understanding of the correspondence between (3.1) and (3.2) remains an ongoing area of research. In [78] we take a step further in the analysis of this correspondence.

3.4 Synaptic Dynamics: Hebbian Learning

Biological synaptic plasticity is believed to be a fundamental process underlying human learning and memory. One of the most widely accepted theories of synaptic plasticity is *Hebbian learning*, introduced by Donald Hebb in 1949 [2]. Hebb proposed that learning is based on the correlated activity of connected neurons. Specifically, in a famous passage of [2], he stated the following postulate:

> "When an axon of cell A is near enough to excite cell B and repeatedly or persistently takes part in firing it, some growth process or metabolic change takes place in one or both cells such that A's efficiency, as one of the cells firing B, is increased."

In essence, Hebb's rule suggests that synapses are strengthened or stabilized when there is a correlation between pre- and post-synaptic neurons. Hebb formulated his principle on purely theoretical grounds, therefore the postulate does not have a single mathematical formulation. Instead, Hebbian learning can be seen as a *family* of learning rules that share two key characteristics derived from Hebb's law: (i) the learning rule must be *local*, meaning that only the activities of the connected neurons A and B matter, without any influence from any other neurons C that might make a connection onto A or B, and (ii) *cooperativity*, meaning that both pre-synaptic neuron A and post-synaptic neuron B must be active to induce a weight increase. Locality is one of the key properties that a learning rule must possess to be considered *biologically plausible* [16]. As discussed in Section 1.1, the absence of this property is one of the primary reasons why backpropagation is considered biologically implausible.

Mathematical Formulation

A rigorous mathematical description of Hebbian learning, along with the key properties that make it significant for implementation in artificial neural networks (ANNs), is given in [79]. Here, we review these properties and their formulations, following the approach presented in [79]. For further details, we refer the reader to the original paper. To this purpose, we focus on a single synapse with efficacy w_{ij}, which transmits signals from a pre-synaptic neuron ν_j to a post-synaptic neuron ν_i. The first two properties, *locality* and *cooperativity*, are direct consequences of Hebb's postulate.

- **Locality:** the learning rule for the synapse w_{ij} should depend only on the activity of j and i and not on that of any other neurons. Mathematically, this can be expressed as:

$$\frac{d}{dt}w_{ij} = F(w_{ij}, \nu_i, \nu_j), \tag{3.3}$$

  where F is a function that should be chosen according to the additional properties we want the dynamics to satisfy.

- **Cooperativity:** pre- and post-synaptic neurons have to be active simultaneously to induce a weight increase. Given a parameter c, mathematically, the simplest

choice for the function F in (3.3) is

$$\frac{d}{dt}w_{ij} = c\nu_i\nu_j. \tag{3.4}$$

Equation (3.4) represents the simpler and more direct implementation of Hebb's postulate, but from this simple formulation, one can see that it leads to unrealistic behavior, as the weights diverge. To have a more realistic system, additional properties must be considered:

- **Synaptic depression:** To avoid divergence, synaptic weights should be able to decrease (or increase). Given $c_{\mathrm{d}} > 0$, this, for example, can be modeled by adding a weight decay to equation (3.4), obtaining

$$\frac{d}{dt}w_{ij} = c\nu_i\nu_j - c_{\mathrm{d}}w_{ij}. \tag{3.5}$$

- **Boundedness:** In realistic systems, synaptic weights should remain bounded.

- **Competition:** If some synaptic weights grow, they should do so at the expense of others, ensuring a competitive balance. Given $c > 0$, a well-known rule that satisfies this property is Oja's rule [66] given by

$$\frac{d}{dt}w_{ij} = c\nu_i\nu_j - c\nu_i^2 w_{ij}. \tag{3.6}$$

The above mathematical formulations play a central role in Part II, where we theoretically explore the embedding of biologically plausible learning mechanisms – and Hebbian learning one is the most widely accepted of such mechanisms – into neural networks. Specifically, we introduce and analyze there coupled neural-synaptic dynamics that combine HNNs and FNNs with two different Hebbian learning rules for the synaptic dynamics. The first rule satisfies the biological properties of locality, cooperativity, synaptic depression, and boundedness; the second rule – which we refer to as Oja's like learning rule – fulfills, in addition, a competitiveness property.

3.5 Summary

This chapter presented a self-contained review of the continuous-time dynamical rules governing neural masses and synaptic weights central to our analysis. Specifically, in Section 3.3 we introduced the continuous-time dynamical rules governing the neural dynamics. Then, in Section 3.4 we reviewed Hebbian learning rules and the mathematical formulation used in our analysis. The rationale behind choosing these dynamics is supported by both theoretical and experimental evidence, as discussed in the introduction (Section 3.1) and overview (Section 3.2) sections. These dynamics play a key role in Parts I and II, where we propose a normative framework for translating optimization problems into biologically plausible neural networks and a possible way to embed learning within this framework.

4 Contraction Theory for Dynamical Systems

Contraction theory is the main analytical tool we use throughout the thesis for studying the convergence, stability, and robustness properties of the dynamics of our interest. In this chapter, we review basic results of contraction theory for continuous-time dynamical systems. The treatment presented is based on the monograph [42]. We refer to the monograph and the original papers referenced in this chapter for further details.

4.1 Introduction

Contraction theory is a powerful mathematical framework for the analysis and understanding of the stability and convergence behavior of dynamical systems. Traditionally, stability properties are defined in terms of convergence to an invariant set, such as an equilibrium or a periodic orbit, combined with a Lyapunov stability requirement that trajectories starting near the attractor remain close to it for all future times. However, these methods typically require prior knowledge of the system's attractors, which can make them challenging to apply in complex scenarios where such information is not readily available. In contrast, rather than focusing on specific attractors, contraction theory focuses on the distance between trajectories, requiring that any two trajectories (exponentially and without overshoot) converge towards each other. In general, contraction theory can be viewed as a unified and coherent framework that aims to combine results from Lyapunov stability theory, incremental stability, fixed point theorems, monotone systems theory, and the geometry of Banach and Riemann spaces.

The importance of contraction theory extends beyond its theoretical elegance and lies in its practical effectiveness. In fact, contraction theory has been successfully applied in various fields, including, e.g., network synchronization [80], learning-based control [81], and convex optimization [53].

The chapter is organized as follows. In Section 4.2, we provide a brief literature review on contraction theory. Then, in Section 4.3, we review some basic concepts and results on continuous-time dynamical systems that we use throughout the manuscript to prove our results. Finally, Section 4.4 presents the definition and main properties of contracting dynamics.

4.2 Overview

The study of contraction theory started with the seminal work of Stefan Banach in 1922 [82]. The groundwork for understanding contraction properties in dynamical systems through the use of logarithmic norms was laid by Lewis [83], Demidovič [84], and Krasovskiĭ [85]. A historical review is given by Pavlov et al. [86].

Contraction theory applied to control problems began with the seminal work of Lohmiller and Slotine [25], who introduced an approach based on differential conditions for contraction using the Euclidean norm. This work marked a pivotal shift in the analysis of nonlinear systems, opening new avenues for research and application. Since then, contraction analysis has been extensively studied and numerous generalizations have been proposed. These include partial contraction [87], contraction of stochastic differential equations [88, 89], contraction on Riemannian and Finsler manifolds [90, 91], weak and semi-contraction [36], contraction in systems with different time scales [92], and k-contraction [93].

The application of contraction theory has also expanded beyond smooth dynamical systems. For instance, the framework has been extended to piecewise smooth dynamical systems [80], and more recently to locally Lipschitz functions [38].

The classic approach to contraction theory is with respect to the Euclidean norm, using linear matrix inequality (LMI) tools to design optimal weight matrices. However, recent works have shown that stability can be studied more systematically and efficiently using non-Euclidean norms (e.g., ℓ_1, ℓ_∞, and polyhedral norms), particularly in large classes of network systems. Examples include biological transcriptional systems [26], coupled oscillators [46], chemical reaction networks [94], Hopfield neural networks [95, 38], biologically plausible models [96, 70], and traffic networks [97, 98].

Beyond these results, contractivity has proven effective in other application domains, including modern control design on multiple time scales [99] and online feedback optimization [100]. An implicit model that uses contraction theory to allow for a convex parametrization of stable models is presented in [101]. Contraction-theoretic tools have also been applied to machine learning and ANNs. For example, in [28] contraction-based conditions are given to characterize disturbance rejection properties of HNNs with delays. Euclidean contractivity is analyzed in the context of RNN with dynamic synapses [24] and in [102], where a number of contractivity conditions are proposed. Additionally, contractivity has been shown to enhance the robustness of neural ordinary differential equations [103] and implicit neural networks [104, 27] against adversarial perturbations.

Contraction dynamics have also been effectively employed to solve optimization problems [105, 53, 106]. The asymptotic behavior of weakly contracting dynamics has been characterized in various contexts, including monotone systems [98] and primal-dynamics with locally stable equilibria [36], as well as in non-expansive functions with a locally exponentially stable equilibrium [107, 106].

For a more comprehensive understanding of contraction theory, notable surveys, and reviews include [108, 109, 80, 81, 110, 111], along with the recent monograph by Bullo [42].

4.3 Nonlinear Dynamical Systems: Basic Concepts

In this section, we introduce key notations and basic concepts for nonlinear continuous-time dynamical systems, which will be referenced throughout this manuscript.

Specifically, we consider dynamical systems of the form

$$\dot{x} = f(t, x), \tag{4.1}$$

where $f\colon \mathbb{R}_{\geq 0} \times C \to \mathbb{R}^n$, is a smooth nonlinear function and $C \subseteq \mathbb{R}^n$ is a forward invariant (see the above definition) set for the dynamics. We let $t \mapsto \phi_t\big(x(0)\big)$ denote the *flow map* at time t of (4.1) starting from initial condition $x(0) := x_0$. We denote by $Df(t, x) := \partial f(t, x)/\partial x$ the *Jacobian* matrix of f with respect to x. If f is a multi-variable function, we write $D_{(\cdot)}f$ to specify the variable with respect to which we are computing the partial derivative. Whenever it is clear from the context, we omit specifying the dependence of functions on time t.

We now recall some standard definitions useful for our analysis.

Definition 4.1 (Forward Invariant set)**.** *A set $\mathcal{A} \subseteq \mathbb{R}^n$ is said to be* forward invariant *for system (4.1) if the trajectories of every solution of (4.1) starting from any point of $x(0) \in \mathcal{A}$ remains in $\mathcal{A}$ for all $t \geq 0$, that is*

$$x_0 \in \mathcal{A} \quad \Longrightarrow \quad \phi_t\big(x_0\big) \in \mathcal{A} \quad \forall t \geq 0.$$

Definition 4.2 (Attractive set)**.** *A set $\mathcal{A} \subseteq \mathbb{R}^n$ is said to be* attractive *for system (4.1) if the trajectories of every solution of (4.1) starting from any point of $\mathbb{R}^n$ asymptotically converge to the set $\mathcal{A}$, that is for any initial condition $x_0 \in \mathbb{R}^n$ there exists a time $t_0 > 0$ such that*

$$\phi_t\big(x_0\big) \in \mathcal{A} \quad \forall t \geq t_0.$$

Next, we recall the following result from [112, pp. 102-103] that we will use several times to prove our statements.

Theorem 4.1 (Comparison Lemma)**.** *Let $f\colon \mathbb{R}_{\geq 0} \times C \subset \mathbb{R} \to \mathbb{R}$ be continuous in t and locally Lipschitz in x, for all $t \geq 0$ and $x \in C$. Consider the scalar differential equation*

$$\dot{x} = f(t, x), \quad x(t_0) = x_0,$$

and let $[t_0, T)$ (T could be infinity) be the maximal interval of existence of the solution $x(t)$. Suppose that $x(t) \in C$, for all $t \in [t_0, T)$. Let $v(t)$ be a continuous function whose Dini derivative satisfies the differential inequality

$$D^+v(t) \leq f(t, v(t)), \quad v(t_0) \leq x_0,$$

with $v(t) \in C$, for all $t \in [t_0, T)$. Then $v(t) \leq x(t)$ for all $t \in [t_0, T)$.

Finally, we recall Nagumo's Theorem [113] for the positive orthant. We refer to [42, Exercise 3.13] for more details. We use this result to prove that the positive orthant is forward invariant for a given dynamical system. This, in turn, implies that the dynamical systems is positive, which, as we argue in Section 1.1, is a key property for biologically plausible dynamical models.

Theorem 4.2 (Nagumo's Theorem for the positive orthant)**.** *The positive orthant $\mathbb{R}^n_{\geq 0}$ is forward invariant for a vector field f if and only if*

$$f_i(x) \geq 0 \quad \forall x \in \mathbb{R}^n_{\geq 0} \text{ such that } x_i = 0. \tag{4.2}$$

4.4 Contraction Theory

In this section, we review the main properties of continuous-time contracting dynamical systems. Throughout this manuscript we follow the approach in [109, 42], characterizing contractivity through the log-norm of the Jacobian of the system. Specifically, we focus on continuous-time dynamical systems whose Jacobians have log-norms uniformly upper-bounded by a negative constant either everywhere or almost everywhere in the state space, depending on the differentiability properties of the system under consideration.

We begin with the following:

Definition 4.3 (Contracting systems [42])**.** *Let $\|\cdot\|$ be a norm on $\mathbb{R}^n$ with compatible weak pairing and with associated log-norm μ. Given a function $f\colon \mathbb{R}_{\geq 0} \times C \to \mathbb{R}^n$, with $C \subseteq \mathbb{R}^n$ f-invariant, open and convex, and a constant $c > 0$ ($c = 0$) referred as* contraction rate*, f is strongly (weakly) infinitesimally contracting on C if*

$$\mathsf{osLip}(f_t) \leq -c, \text{ for all } t \in \mathbb{R}_{\geq 0},$$

or, equivalently for differentiable vector fields, if

$$\mu(Df(t,x)) \leq -c, \text{ for all } x \in C \text{ and } t \in \mathbb{R}_{\geq 0}. \tag{4.3}$$

Of particular interest is the case of non-smooth map f, as such functions appear in several frameworks. For example, in neural network models, non-smooth activation functions such as ReLU and saturation functions are prevalent. Indeed, as we will see, these models naturally arise when using contracting dynamics for solving convex optimization problems. The next result [38, Theorem 16] allows using condition (4.3) for locally Lipschitz function, for which, by Rademacher's theorem, the Jacobian $Df(t,x)$ exists almost everywhere in C.

Theorem 4.3 (osLip and log-norm equivalence for locally Lipschitz functions)**.** *Given a norm $\|\cdot\|$ on $\mathbb{R}^n$ with compatible weak pairing and with associated log-norm μ, consider a function $f\colon \mathbb{R}_{\geq 0} \times C \to \mathbb{R}^n$ locally Lipschitz on $C \subset \mathbb{R}^n$ open and convex set. Then for every $c \in \mathbb{R}$ the following statements are equivalent:*

1. $\mathsf{osLip}(f_t) \leq c$*, for all* $t \in \mathbb{R}_{\geq 0}$*,*
2. $\mu(Df(t,x)) \leq c$*, for almost every* $x \in C$*, and* $t \in \mathbb{R}_{\geq 0}$*.*

It is evident from the definition that contractivity is a metric property and depends on the specific metric used. A system may be contracting with respect to one metric but not with respect to another. We show this statement in the following simple example of a linear dynamical system.

Example 4.1. *Consider the system*

$$\begin{bmatrix}\dot{x}\\ \dot{y}\end{bmatrix} = A\begin{bmatrix}x\\ y\end{bmatrix} := \begin{bmatrix}-0.1 & 1\\ -1 & -0.1\end{bmatrix}\begin{bmatrix}x\\ y\end{bmatrix}. \tag{4.4}$$

We have

$$\mu_2(A) = \lambda_{\max}\Big(\frac{A^\top + A}{2}\Big) = \lambda_{\max}\Big(\begin{bmatrix}-0.1 & 0\\ 0 & -0.1\end{bmatrix}\Big) = -0.1 < 0,$$

and

$$\mu_1(A) = \max_{j\in\{1,\dots,n\}}\Big(a_{jj} + \sum_{i=1, i\neq j}^{n} |a_{ij}|\Big) = \max\{-1.1, 0.9\} = 0.9 > 0.$$

Therefore system (4.4) is 0.1*-strongly contracting with respect to the norm* $\|\cdot\|_2$*, but it is not strongly contracting with respect to the norm* $\|\cdot\|_1$*.*

One of the benefits of contraction theory is that it enables the study of the convergence behavior of the flow map with a single condition. Specifically, if f is contracting, for any two trajectories $x(\cdot)$ and $y(\cdot)$ of (4.1) rooted from $x_0, y_0 \in C$ it holds

$$\|\phi_t(x_0) - \phi_t(y_0)\| \leq \mathrm{e}^{-ct}\|x_0 - y_0\|, \qquad \text{for all } t \geq 0,$$

i.e., the distance between the two trajectories rooted in C shrinks exponentially with rate c if f is c-strongly infinitesimally contracting, and never increases if f is weakly infinitesimally contracting.

Properties of Strongly Infinitesimally Contracting Dynamics

Strongly infinitesimally contracting dynamical systems exhibit highly ordered transient and asymptotic behavior, making them particularly advantageous for analyzing and controlling dynamical systems. Namely,

1. initial conditions are forgotten exponentially quickly,
2. the distance between any two trajectories is monotonically decreasing,
3. time-invariant dynamics admit a unique globally exponential stable equilibrium (see Figure 4.1). Additionally, two natural Lyapunov functions are automatically available: the distance from the equilibrium and norm of the vector field itself,
4. time-varying and periodic vector fields admit a unique periodic orbit, which is globally exponentially stable,
5. contracting dynamics enjoy highly robust behavior including:
    - incremental input-to-state stability,
    - finite input-state gain,

- contraction margin to unmodeled dynamics, and
- input-to-state stability in the presence of delayed dynamics.

6. contraction theory is a modular framework: under proper conditions, the interconnection of contracting dynamical systems is contracting, with an explicit estimate of the contraction rate available (see Section 4.4.1 for more details).

Additionally, contracting dynamical systems admit systematic procedures for the computation of their equilibria. We recall the following result that shows that, for a given time-invariant contracting dynamical system, the forward Euler integration of the dynamics with a proper step size guarantees that this discrete-time iteration is also a contraction.

Theorem 4.4 (Contractivity of Euler discretization)**.** *Given a norm $\|\cdot\|$ induced by an inner product $\langle\cdot,\cdot\rangle$, consider a Lipschitz map $f\colon \mathbb{R}^n \to \mathbb{R}^n$. The following statements are equivalent*

1. *the dynamical system $\dot{x} = f(x)$ is strongly infinitesimally contracting with respect to the norm $\|\cdot\|$,*
2. *for $\alpha \in]0, 2c/L^2[$ the* explicit Euler integration algorithm *$x_{k+1} = x_k + \alpha f(x_k) = (\mathsf{Id} + \alpha f)(x_k)$ is strongly contracting with respect to the norm $\|\cdot\|$.*

Proof. Let $f\colon \mathbb{R}^n \to \mathbb{R}^n$ be Lipschitz with constant L, and $[\![\cdot,\cdot]\!]$ be the weak pairing associated to the norm $\|\cdot\|$. First we prove that statement 1 implies statement 2.

Assume $\dot{x} = f(x)$ is strongly infinitesimally contracting with respect to the norm $\|\cdot\|$ with rate $c > 0$, that is, by using the one-sided Lipschitz condition,

$$[\![f(x) - f(y), (x - y)]\!] = \langle f(x) - f(y), (x - y)\rangle \leq -c\|x - y\|^2, \quad \forall x, y \in \mathbb{R}^n,$$

where in the first equality we used the fact that if a norm is induced by an inner product, then the weak pairing coincides with the inner product. To prove statement 2 we show that there exists a constant $d < 1$ such that $\|x_{k+1} - y_{k+1}\| \leq d\|x_k - y_k\|$, for all x_k, and $y_k \in \mathbb{R}^n$. We compute

$$\begin{aligned}
\|x_{k+1} - y_{k+1}\|^2 :&= \|x_k + \alpha f(x_k) - y_k - \alpha f(y_k)\|^2 \\
&= \|x_k - y_k + \alpha\big(f(x_k) - f(y_k)\big)\|^2 \\
&= \|x_k - y_k\|^2 + 2\alpha\langle f(x_k) - f(y_k), x_k - y_k\rangle + \alpha^2\|f(x_k) - f(y_k)\|^2 \\
&\leq \|x_k - y_k\|^2 - 2\alpha c\|x_k - y_k\|^2 + \alpha^2 L^2\|x_k - y_k\|^2 \\
&= \big(1 - 2\alpha c + \alpha^2 L^2\big)\|x_k - y_k\|^2
\end{aligned}$$

where in the last inequality we used the contractivity and Lipschitzness of the map f. The statement then follows by noticing that $1 - 2\alpha c + \alpha^2 L^2 < 1$ if and only if $\alpha \in]0, 2c/L^2[$.

Viceversa, assume that statement 2 holds, that is $\mathsf{Lip}\,(\mathsf{Id} + \alpha f) < 1$ for $\alpha \in]0, 2c/L^2[$. To prove statement 1 we show that $\mathrm{osL}\,(f) < 0$. We have

$$\mathrm{osL}\,(\mathsf{Id} + \alpha f) = 1 + \mathrm{osL}\,(\alpha f) = 1 + \alpha\,\mathrm{osL}\,(f).$$

On the other hand, it always holds $\operatorname{osL}(\mathsf{Id} + \alpha f) \leq \mathsf{Lip}(\mathsf{Id} + \alpha f)$ and, by assumption, $\mathsf{Lip}(\mathsf{Id} + \alpha f) < 1$. These inequalities imply

$$1 + \alpha \operatorname{osL}(f) < 1 \iff \operatorname{osL}(f) < 0.$$

This concludes the proof. □

The optimal choice of step size depends on the norm. For more details and guidance on the step-size selection, we refer to [114] for the Euclidean case, and to [115] for the non-Euclidean case.

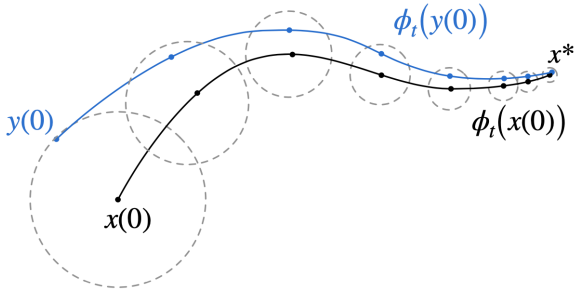

Figure 4.1: Strongly infinitesimally contracting systems: the distance between any two trajectories converges exponentially to the unique equilibrium point $x^\star$. The figure illustrates contractivity with respect to the Euclidean norm. Given two initial conditions x_0, and y_0, the trajectory of $y(t)$ remains inside the ball centered at $x(t)$ with radius e^{-ct} and both trajectories converge exponentially to $x^\star$. Image reused with permission from [42].

Properties of Weakly Infinitesimally Contracting Dynamics

The properties listed in the previous section do not generally extend to weakly infinitesimally contracting (or non-expansive) systems, where the distance between trajectories is non-increasing. These systems are, e.g., systems that exhibit conservation or invariance properties and that, therefore, cannot be strongly infinitesimally contracting since the system trajectories cannot fully forget initial conditions. Nevertheless, these systems still enjoy numerous useful properties, such as the so-called dichotomy property [36]. This property states that a weakly infinitesimally contracting system on C has either:

- no equilibrium point in C, and every trajectory starting in C is unbounded (see Figure 4.2.a),
- at least one equilibrium, and every trajectory starting in C is bounded (see Figure 4.2.b).

Moreover, if there exists an equilibrium point that is locally asymptotically stable, then it is also globally asymptotically stable. We rigorously prove this result and provide a detailed

characterization of the convergence behavior for systems that are weakly contracting over the entire state space and have a locally asymptotically stable equilibrium point.

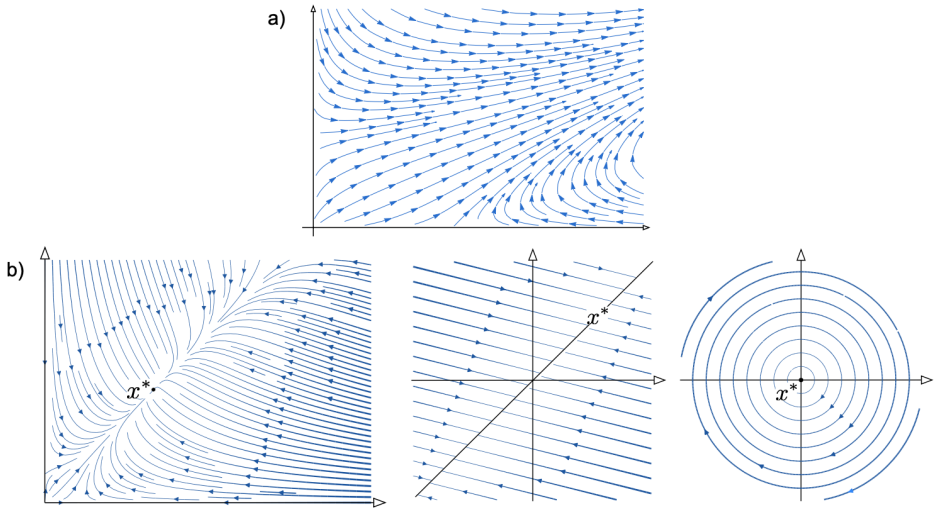

Figure 4.2: Illustration of the dichotomy property of weakly contracting systems: a) the system has no equilibrium and every trajectory is unbounded or b) there exists at least one equilibrium and every trajectory is bounded. Images reused with permission from [42].

4.4.1 Interconnected Systems

In this section, we briefly review the theory of contracting interconnected systems. This is crucial for analyzing the stability of complex systems, and we use it in Chapter 9 to establish the contractivity of coupled neural-synaptic dynamics.

Given r positive integers $n_1, \dots, n_r$ such that $n_1 + \cdots + n_r = n$, consider the decomposition $\mathbb{R}^n = \mathbb{R}^{n_1} \times \cdots \times \mathbb{R}^{n_r}$, a local norm $\|\cdot\|_i$ on $\mathbb{R}^{n_i}$, for each $i \in \{1, \dots, r\}$, with associated log-norm $\mu_i(\cdot)$. Now, consider the *interconnection of r dynamical systems* given by

$$\dot{x}_i = f_i(t, x_i, x_{-i}), \quad \forall i \in \{1, \dots, r\}, \tag{4.5}$$

where $x_i \in \mathbb{R}^{n_i}$, and $x_{-i} \in \mathbb{R}^{n-n_i}$ denotes the vector x without the component x_i. We recall the following result [45, 46], which provides conditions under which interconnected systems are contracting.

Theorem 4.5 (Contractivity of interconnected system)**.** *Consider the interconnected system in (4.5). For each $i \in \{1, \dots, r\}$, assume that*

(1) *(contractivity-at-each-node) at fixed x_{-i} and t, the map $x_i \to f_i(t, x_i, x_{-i})$ is strongly infinitesimally contracting with rate c_i with respect to $\|\cdot\|_i$.*
(2) *(Lipschitz interconnections) at fixed x_i and t, each function $x_{-i} \to f_i(t, x_i, x_{-i})$ is Lipschitz with Lipschitz constant $\gamma_{ij} \in \mathbb{R}_{\geq 0}$, $i \neq j$.*

Define the gain matrix

$$\Gamma = \begin{bmatrix} -c_1 & \dots & \gamma_{1r} \\ \vdots & \dots & \vdots \\ \gamma_{r1} & \dots & -c_r \end{bmatrix} \in \mathbb{R}^{r \times r}. \tag{4.6}$$

If the gain matrix Γ *is Hurwitz, then the interconnected system is strongly infinitesimally contracting with respect to a composite norm* $\|\cdot\|$ *generated by logarithmic optimal norm for* Γ*, with rate* $|\alpha(\Gamma) + \varepsilon|$.

Let $Df(x)$ denote the Jacobian of the interconnected system (4.5) and note that the gain matrix Γ is an aggregate Metzler majorant of (4.5). By applying inequality (2.3) and the monotonicity property of the log-norm, we have

$$\sup_x \mu_{\text{cmpst}}(Df(x)) \leq \mu_{\text{agg}}(\sup_x |Df(x)|_{\text{M}}) = \mu_{\text{agg}}(\Gamma).$$

Then a logarithmic optimal norm for Γ in Theorem 4.5 can be selected by applying Lemma 2.3.

4.5 Summary

In this chapter, we provided a self-contained review of contraction theory for nonlinear continuous-time dynamical systems. This is the main theoretical framework we use to analyze the stability and robustness of the dynamics we study. We began by introducing the basic concepts of dynamical systems needed for our analysis. Then, we dive into the analysis of contracting systems. After formally defining contracting dynamics, we outlined the key properties that make contraction theory a powerful analytical tool, as discussed in Section 1.3. In the following chapters, we give conditions that ensure contractivity in our models, explicitly stating the norm and contractivity rate for each case. Moreover, in Part III we show the effectiveness of contracting dynamics in analyzing static and time-varying convex optimization problems.

Part I

A Normative Framework for Biologically Plausible Neural Networks

I.1 Introduction

Recurrent neural networks are a class of computational models used for explaining neurobiological phenomena and for solving machine learning problems. In RNNs, the neurons' activity is influenced not only by the current stimulus but also by the current state of the network. This feedback property makes RNNs particularly suited for computations that unfold over time, such as tasks involving sequential data or time-series predictions.

RNNs have been successfully applied to many domains, including solving optimization problems. Typically, in this framework, researchers define the dynamics and then demonstrate that these dynamics effectively solve the problem at hand. However, this approach often lacks a clear biological interpretability.

Research questions: As a result, key questions arise:

- What are the *functional implications* of RNN models? That is, what mechanisms (optimization problems) do natural neural networks solve, and how can biologically inspired neural networks mimic these processes?
- How do the dynamics of such networks emerge when solving optimization problems, and how can we use these dynamics to tackle these problems effectively?

I.2 A Normative Framework for Biologically Plausible Neural Networks

In this part, to address the above questions, we propose a top/down, normative framework for a biologically plausible explanation of neural networks solving sparse reconstruction and other optimization problems. By *normative framework*, we refer to an approach that starting with an optimization problem that models natural network mechanisms, derives an artificial neural network that provides a theoretical understanding of the computation principles of the circuit. This approach has the advantage of directly investigating the underlying principles of neural functioning, while also providing a mathematically tractable framework for understanding the network.

It is widely believed that a key function of both biological and artificial neural networks is to extract information from large amounts of data and there are empirical and theoretical evidences that support the use of sparse representations in neural systems. Motivated by this, we focus on sparse reconstruction problems, which are ubiquitous in a wide range of domains including compressed sensing, image processing, and machine learning. These problems entail approximating a given stimulus as a combination of a sparse set of neurons and a dictionary and can be formalized as a regularized least squares problem. At its core, our approach can be viewed as the task of solving optimization problems through the use of continuous-time RNNs. This process essentially consists of two key steps:

1. establishing the equivalence between the optimal solutions of the optimization problem and the equilibrium points of the network dynamics,

2. identifying conditions that guarantee stable convergence of these dynamics to their equilibria.

A fundamental aspect of this analysis, and a crucial property for any complex system, is the stability of the system of interest. Among the tools for characterizing the stability of a dynamical system, we adopt a control-theory perspective leveraging contraction theory – a robust method that ensures more than simple stability, as discussed in Chapter 4.

In this framework, we identified a gap in the literature regarding the contractivity analysis of RNNs: contractivity conditions for some of the most common activation functions and systems – including RNNs designed for solving sparse reconstruction problems – were missing. This gap motivated us to develop the theoretical tools necessary to analyze the stability of the dynamics resulting when solving sparse reconstruction problems and others. Specifically, in Chapter 5, we conduct a comprehensive sharp Euclidean contractivity analysis of continuous-time Hopfield and firing rate neural networks with symmetric weights. The assumption of symmetric weights is motivated by the wide range of optimization problems whose solutions can be encoded via the equilibrium points of neural networks with symmetric synaptic matrices. We provide several examples of these throughout the thesis. Remarkably our main results give logarithmically optimal contractivity bounds for almost all symmetric synaptic matrices and for RNNs with locally Lipschitz activation functions. Our analysis focuses on HNN and FNN, but is built upon two useful classes of matrix polytopes which includes the Jacobian of the HNN and FNN, but does not exclude the application of our results to other dynamical systems whose Jacobian belongs to one of the matrix polytopes defined in Section 5.3.

We continue our analysis by proposing a top-down normative framework for biologically plausible neural networks that solve sparse reconstruction and other optimization problems. To streamline the analysis, we divide our results into two chapters: Chapter 6 presents the modeling of our dynamics, while Chapter 7 focuses on the analysis of the convergence behavior. Specifically, in Chapter 6 we introduce a novel family of continuous-time FNNs, called *firing rate competitive networks* (FCN), to address the sparse reconstruction problems, by leveraging tools from monotone operator theory. This general theory explains how to transcribe a composite optimization problem into a continuous-time firing rate neural network, which is therefore interpretable. Because real neurons produce non-negative outputs in response to non-negative stimuli (e.g., visual input), we are particularly interested in solving the positive sparse reconstruction problem, where solutions are constrained to be non-negative. This leads to the introduction of the positive firing rate competitive network (PFCN), which is the first RNN, to our knowledge, designed to tackle positive sparse reconstruction problems.

Next, we proceed to the analysis of the proposed model. Our key findings can be informally summarized as follows:

Informal statement (Summary of the main results in Chapters 6 and 7)**.** *The equilibria of FCN are the optimal solutions to sparse reconstruction problems, and vice-versa. Furthermore, the trajectories of the FCN are bounded. Additionally, if the dictionary satisfies a standard assumption (that is the restricted isometry property), then:*

1. *the FCN converges to* an *equilibrium point that is also* the *optimal solution of the*

corresponding sparse reconstruction problem;

2. *the convergence is linear-exponential, in the sense that the trajectory's distance from the equilibrium point initially decays at worst linearly, and then, after a transient, exponentially.*

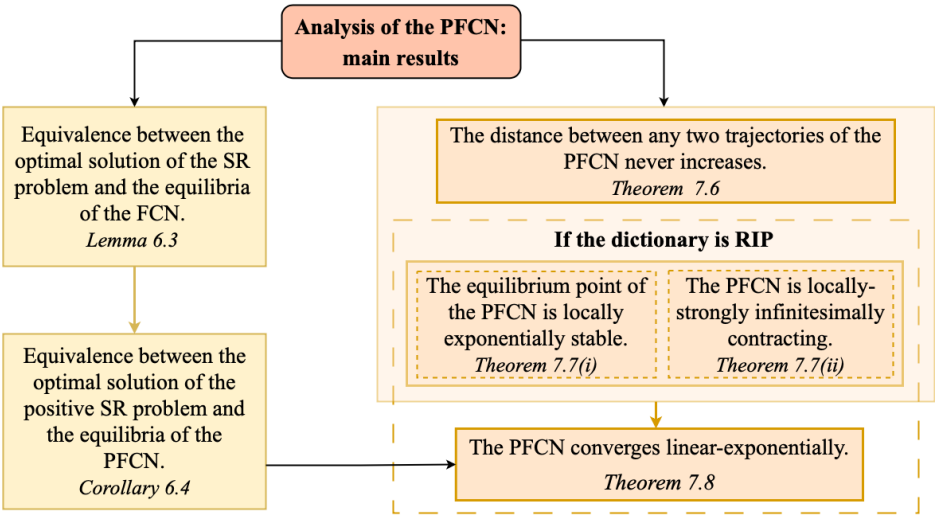

Figure 4.3: Schematic diagram summarizing the main results of Chapters 6 and 7 and their assumptions. To streamline the presentation, we focus on the PFCN in the diagram. With Theorem 7.8 we show that the PFCN exhibits linear-exponential convergence towards the optimal solution of the positive sparse reconstruction problem. The result follows from: (i) establishing a link between the optimal solution of the optimization problem and the equilibria of the PFCN; and (ii) characterizing the contractivity of the PFCN.

The assumptions, the results, and their links towards building the claims in the informal statement are also summarized in Figure 4.3 for the PFCN. Specifically, in Chapter 6 we show that the equilibria of both the FCN and PFCN are the optimal solutions of the sparse reconstruction problem and the positive sparse reconstruction problem, respectively (Lemma 6.3 and Corollary 6.4). Then, in Chapter 7 we focus on the convergence behavior of our dynamics, focusing on the PFCN to streamline the presentation. We demonstrate that the distance between any two trajectories of the PFCN never increases (Theorem 7.6). Moreover, we show that if the dictionary satisfies a standard assumption, then the equilibrium point for the PFCN is not only locally exponentially stable but it is also strongly contracting in a neighborhood of the equilibrium (Theorem 7.7). These results then lead to Theorem 7.8, where we show that the PFCN (6.9) has a linear-exponential convergence behavior. That is, the distance between any trajectory of the PFCN and its equilibrium is upper bounded, up to some *linear-exponential crossing time*, say t_{cross}, by a decreasing linear function. Then, for all

$t > t_{\text{cross}}$, the distance is upper bounded by a decreasing exponential function.

The analysis of the FCN and PFCN dynamics naturally leads to the study of the convergence of *globally-weakly and locally-strongly contracting systems*. These are dynamics that are weakly infinitesimally contracting on $\mathbb{R}^n$ and strongly infinitesimally contracting on a subset of $\mathbb{R}^n$. While in this part we provide a preliminary result on the convergence behavior of this class of dynamics instrumental for the analysis of our FCN models, we formalize and extend the study of such systems, which naturally arise in the context of convex (but not strongly convex) optimization problems with a unique minimizer, in Chapter 12.

I.3 Overview

Historically, understanding how neural systems represent sensory input has been a central challenge in neuroscience. The evidence that many sensory neural systems employ sparse reconstruction traces back to the pioneering work by Hubel and Wiesel, where it is shown that the responses of simple-cells in the mammalian visual cortex (V1) can be described as a linear filtering of the visual input [116]. This insight was further expanded upon by Barlow, who hypothesized that sensory neurons aim to encode an accurate representation of the external world using the fewest active neurons possible [117]. Subsequently, Field showed that simple cells in V1 efficiently encode natural images using only a sparse fraction of active units [118]. Then, Olshausen and Field proposed that biological vision systems encode sensory input data and showed that a neural network trained to reconstruct natural images with sparse activity constraints develops units with properties similar to those found in V1 [3]. These ideas have since gained substantial support from studies on different animal species and the human brain [119].

From a mathematical perspective, the sparse reconstruction problem can be formulated as a composite minimization problem given by a least squares optimization problem regularized with a sparsity-inducing penalty function. While traditional optimization methods rely on discrete algorithms, recently an increasing number of continuous-time recurrent neural networks have been used to solve optimization problems. Essentially, these RNNs are continuous-time dynamical systems converging to an equilibrium that is also the optimizer of the problem. Consequently, much research effort has been devoted to characterizing the stability of those systems and their convergence rates [120, 121, 63, 122, 78, 53]. A particularly notable RNN designed to tackle the sparse reconstruction problem is the Locally Competitive Algorithm (LCA) introduced by Rozell et al. [64]. This network is a continuous-time Hopfield-like neural network [58] in equation (3.1). Following [64], several results were established to analyze the properties of the LCA. Specifically, in [123] it is proven that, provided that the fixed point of the LCA is unique then, for a certain class of activation functions, the LCA globally asymptotically converges. Then, in [124] it is shown that the fixed points of the LCA coincide with the solutions of the sparse reconstruction problem. Using a Lyapunov approach, under certain conditions on the activation function and on the solutions of the systems, it is also shown that the LCA converges to a single fixed point with exponential rate of convergence. In [125] a technique using the Łojasiewicz inequality is used to prove

convergence of both the output and state variables of the LCA. Various sparsity-based probabilistic inference problems are shown to be implemented via the LCA in [126]. [127], [128], [129] focus on analyzing the LCA for the sparse reconstruction problem with ℓ_1 sparsity-inducing penalty function. Specifically, the convergence rate is analyzed in [127]. In [129] it is rigorously shown how the LCA can recover a time-varying signal from streaming compressed measurements. Additionally, physiology experiments in [128] demonstrate that numerous response properties of non-classical receptive field (nCRF) can be reproduced using a model having the LCA as neural dynamics with an additional non-negativity constraint enforced on the output to represent the instantaneous spike rate of neurons within the population.

In a broader context, RNNs have been used both for explaining neurobiological phenomena and as a tool for solving machine learning problems [130, 131, 44, 132, 102, 133]. While multistability is a key feature of the original Hopfield model [58] (with multiple equilibria interpreted as *memories*), significant interest has grown over the years in establishing conditions that ensure convergence to a unique equilibrium point [75, 44, 76, 134]. The use of continuous-time RNNs to solve optimization problems and research on stability conditions for these RNNs has gained considerable interest in a wide range of fields, see, e.g., [122, 124, 125, 135]. For example, sufficient conditions for the stability of HNNs are given in [134] based on the use of Lyapunov diagonally stable matrices. A recent comprehensive survey is [122]. A powerful tool to simultaneously establish stability and robustness of RNNs is contraction theory (which precludes multistability). Among recent works studying contractivity of RNNs we recall [101, 103, 24, 38, 102].

5 Euclidean Contractivity of Neural Networks with Symmetric Weights

To deepen the understanding of the correspondence between the Hopfield neural network in equation (3.1) and the firing rate neural network in equation (3.2), and to derive results applicable to the study of biologically plausible neural networks addressing the sparse reconstruction problem, this chapter provides a comprehensive sharp characterization of the contractivity of HNNs and FNNs with respect to Euclidean norms. Notably, we address the case of weak contractivity, which makes our results applicable to systems that exhibit conservation or invariance properties. Moreover, we handle weakly increasing and locally Lipschitz activation functions, allowing us to consider commonly used activation functions such as the ReLU and soft-thresholding functions.

The results presented in this chapter appeared in:

- **V. Centorrino**, A. Gokhale, A. Davydov, G. Russo, and F. Bullo. "Euclidean Contractivity of Neural Networks with Symmetric Weights". *IEEE Control Systems Letters*, 7:1724-1729, 2023. doi: 10.1109/LCSYS.2023.3278250. Recipient of the *2024 IEEE Control Systems Letters Outstanding Paper Award*.

Additionally, these results were presented at:

- **V. Centorrino**, A. Davydov, A. Gokhale, G. Russo, and F. Bullo. "Euclidean Contractivity of Neural Networks with Symmetric Weights", *62nd IEEE Conference on Decision and Control*, Singapore, December 2023. Presented in the invited session "Contraction Theory for Analysis, Synchronization, and Regulation I".

5.1 Introduction

Continuous-time recurrent neural networks are dynamical models that have been extensively studied in various fields, including computational neuroscience, machine learning, and optimization. Recent research efforts have been directed to establish the contractivity properties of continuous-time RNNs. Motivated by optimization [62, 63] and neuroscientific applications [64], [54, Chapter 17], this work specifically targets the analysis of symmetric synaptic interactions. Indeed, as we will see in later chapters, continuous-time RNNs used to solve optimization problems often involve symmetric synaptic interactions.

While a comprehensive contractivity analysis with respect to non-Euclidean ℓ_1 and ℓ_∞ norms was recently presented in [38], the corresponding analysis with respect to Euclidean norms was not complete yet. In this chapter, we bridge this gap, following a recent breakthrough in this direction that was obtained in [102]. Specifically, we focus on two common models of RNNs: the *firing rate neural network* and the *Hopfield neural network*, both introduced in Chapter 3. As previously discussed, for certain synaptic matrices and initial conditions, FNN and HNN can be shown to be equivalent through an appropriate change of coordinates and input transformation [59]. However, the understanding of this partial correspondence is not complete and, as we show below, their contractivity properties are similar but not entirely equivalent. Finally, to demonstrate the practical application of our contractivity analysis, we propose a firing rate neural network to solve certain quadratic optimization problems. This analysis sets the stage for further exploration of contracting dynamical systems in the context of solving optimization problems, which is the focus of Part III.

The chapter is organized as follows. Section 5.2 presents the initial setup for the chapter, outlining the assumptions and notations needed for the analysis. In Section 5.3, we introduce the matrix polytopes relevant to our analysis and extend the concept of logarithmic optimal norm for a matrix, given in Definition 2.6, to matrix polytopes. We then give two general algebraic results: a lower bound on the spectral abscissa of matrix polytopes and a result concerning products of symmetric matrices. These findings are then used to prove the main result of the section, that is the explicit weighted ℓ_2 norm for the matrix polytopes which is log-optimal for almost all synaptic matrices. Building on this result, we establish a set of sufficient conditions characterizing strong and weak infinitesimal contractivity of FNNs and HNNs, in Section 5.4.1. Finally, in Section 5.5, we propose an FNN solving quadratic optimization problems with box constraints and apply our results to ensure global exponential convergence of the proposed dynamics, along with all the other properties of contracting systems.

5.1.1 Contributions

The main contributions of this chapter are a set of comprehensive, sharp sufficient conditions that characterize both strong and weak infinitesimal contractivity of FNNs and HNNs with symmetric weights and possibly non-smooth activation functions. Here, by *comprehensive* we mean that we provide the specific norms with respect to which the models are contracting, as well as explicit lower bounds on the contraction rates. Remarkably, we demonstrate that these lower bounds are log-optimal in almost all symmetric weight matrices, making our results sharp – they are the best achievable within this framework.

These theoretical findings are fundamental for the analysis in the next chapters of this thesis and, in general, for the analysis of continuous-time RNNs. Indeed, with these results, we address a significant gap in the existing literature by establishing conditions for the Euclidean contractivity of RNNs with locally Lipschitz activation functions, which, to the best of our knowledge, were missing. Our findings not only characterize the contractivity properties of HNNs and FNNs with symmetric weights but also extend to a broader family of matrix polytopes. Additionally, we also address the weak contractivity case, thereby extending the applicability of our results to systems with conservation or invariance properties, as well as to RNNs designed to solve specific convex optimization problems, which we explore in subsequent chapters. To derive our main results, we extend the concept of logarithmic optimal norms for matrices, recalled in Definition 2.6, to matrix polytopes. Our approach leverages several general algebraic results, which are interesting *per se* and constitute a contribution in their own right. With these algebraic results, we: (i) determine a weighted ℓ_2 norm for matrix polytopes which is log-optimal for almost all synaptic matrices; (ii) give a lower bound on the spectral abscissa of matrix polytopes; (iii) provide optimal and log-optimal norms for the product of symmetric matrices.

Finally, we apply our sufficient contractivity conditions to propose an FNN that solves certain quadratic optimization problems with box constraints. This application sets the stage for further exploration of contracting FNNs for solving optimization problems, which is the focus of the next chapters.

5.2 Set-up

Motivated by optimization [62, 63] and neuroscientific applications [64], [54, Chapter 17], we work under the following assumption on the weight matrices.

Assumption 5.1 (Symmetric synaptic weights)**.** *The synaptic matrix $W \in \mathbb{R}^{n\times n}$ is symmetric.*

We remark that Assumption 5.1 is valid in optimization applications, as the solutions to a wide range of optimization problems can be encoded via the equilibrium points of neural networks with symmetric synaptic weights. An example of this is provided in Section 5.5, along with several other examples throughout this thesis.

Under Assumption 5.1, the eigenvalues of W are real, $\alpha(W) = \lambda_{\max}(W)$ and it holds the inequality $W \preceq \alpha(W) I_n$. We let the pair (U_W, Λ_W) denote the SVD of W (see Section 2.1 for a review of SVD).

We start by defining a function that plays a crucial role in determining the contractivity weight matrices. Given $\lambda_{\mathrm{m}} > 0$, we define the map $\theta_{\lambda_{\mathrm{m}}} :]-\infty, \lambda_{\mathrm{m}}] \to [2\lambda_{\mathrm{m}}, +\infty[$ by

$$\theta_{\lambda_{\mathrm{m}}}(z) := 2\lambda_{\mathrm{m}}\big(1 + \sqrt{1 - z/\lambda_{\mathrm{m}}}\big), \quad \forall z \in]-\infty, \lambda_{\mathrm{m}}]. \tag{5.1}$$

We illustrate $\theta_{\lambda_{\mathrm{m}}}(\cdot)$ in Figure 5.1. For our derivations, it is useful to introduce the shorthand notation $\theta_{\lambda_{\mathrm{m}}}(\Lambda_W) := [(\theta_{\lambda_{\mathrm{m}}}(\lambda_1), \dots, \theta_{\lambda_{\mathrm{m}}}(\lambda_n))]$, where $(\lambda_1, \dots, \lambda_n)$ is the vector of eigenvalues of W. Additionally, we introduce the matrix $Q_{\mathrm{F},\lambda_{\mathrm{m}}} \in \mathbb{R}^{n \times n}$ defined as

$$Q_{\mathrm{F},\lambda_{\mathrm{m}}} := U_W \theta_{\lambda_{\mathrm{m}}}(\Lambda) U_W^\top \succ 0, \tag{5.2}$$

and, when W is invertible, the matrix $Q_{\mathrm{H},\lambda_{\mathrm{m}}} \in \mathbb{R}^{n \times n}$ defined as

$$Q_{\mathrm{H},\lambda_{\mathrm{m}}} := Q_{\mathrm{F},\lambda_{\mathrm{m}}} W^{-1} = U_W \theta_{\lambda_{\mathrm{m}}}(\Lambda_W) \Lambda_W^{-1} U_W^\top \succ 0. \tag{5.3}$$

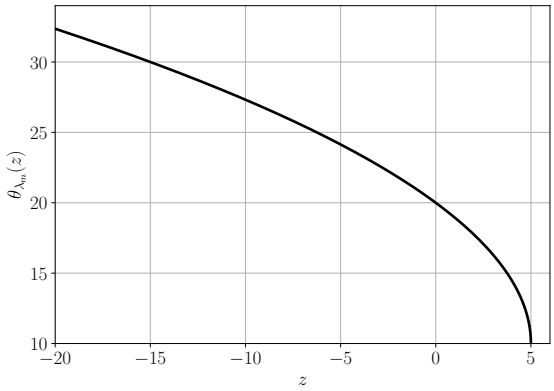

Figure 5.1: Plot of the function $\theta_{\lambda_{\mathrm{m}}}(\cdot)$ in equation (5.1) with $\lambda_{\mathrm{m}} = 5$.

Remark 5.1. *The matrix $Q_{\mathrm{H},\lambda_{\mathrm{m}}}$ defined in (5.3) can be written as $Q_{\mathrm{H},\lambda_{\mathrm{m}}} = U_W g_{\lambda_{\mathrm{m}}}(\Lambda_W) U_W^\top$, where we use the notation $g_{\lambda_{\mathrm{m}}}(\Lambda_W) := [g_{\lambda_{\mathrm{m}}}(\lambda_1), \dots, g_{\lambda_{\mathrm{m}}}(\lambda_n)]$, with $g_{\lambda_{\mathrm{m}}}(\cdot)$ defined by*

$$g_{\lambda_{\mathrm{m}}}(z) := 2b \frac{1 + \sqrt{1 - z/\lambda_{\mathrm{m}}}}{z}, \quad \forall z \in]-\infty, b] \setminus \{0\}.$$

□

Our first result, instrumental in proving the main result of this chapter, is on upper-bounded symmetric matrices.

Lemma 5.1 (Splitting upper-bounded symmetric matrices)**.** *Consider a symmetric matrix W (Assumption 5.1). Assume $W \preceq \lambda_{\mathrm{m}} I_n$, for some $\lambda_{\mathrm{m}} > 0$ and let $\theta_{\lambda_{\mathrm{m}}}(\cdot)$ and $Q_{\mathrm{F},\lambda_{\mathrm{m}}}$ be defined in equations (5.1) and (5.2), respectively. Then,*

$$W = Q_{\mathrm{F},\lambda_{\mathrm{m}}} - \frac{1}{4\lambda_{\mathrm{m}}} Q_{\mathrm{F},\lambda_{\mathrm{m}}}^2. \tag{5.4}$$

Proof. By definition of the function $\theta_{\lambda_{\mathrm{m}}}(\cdot)$, for all $\lambda_i \leq \lambda_{\mathrm{m}}$, $i \in \{1, \ldots, n\}$, it holds

$$\lambda_i = \theta_{\lambda_{\mathrm{m}}}(\lambda_i) - \frac{1}{4\lambda_{\mathrm{m}}} \theta_{\lambda_{\mathrm{m}}}(\lambda_i)^2. \tag{5.5}$$

In fact, we have

$$\begin{aligned}
\theta_{\lambda_{\mathrm{m}}}(\lambda_i) - \frac{1}{4\lambda_{\mathrm{m}}} \theta_{\lambda_{\mathrm{m}}}(\lambda_i)^2 &= 2\lambda_{\mathrm{m}} \left(1 + \sqrt{1 - \frac{\lambda_i}{\lambda_{\mathrm{m}}}}\right) - \frac{1}{4\lambda_{\mathrm{m}}} 4\lambda_{\mathrm{m}}^2 \left(1 + \sqrt{1 - \frac{\lambda_i}{\lambda_{\mathrm{m}}}}\right)^2 \\
&= 2\lambda_{\mathrm{m}} \left(1 + \sqrt{1 - \frac{\lambda_i}{\lambda_{\mathrm{m}}}}\right) - \lambda_{\mathrm{m}} \left(2 + 2\sqrt{1 - \frac{\lambda_i}{\lambda_{\mathrm{m}}}} - \frac{\lambda_i}{\lambda_{\mathrm{m}}}\right) \\
&= \lambda_{\mathrm{m}} \left(2 + 2\sqrt{1 - \frac{\lambda_i}{\lambda_{\mathrm{m}}}} - 2 + \frac{\lambda_i}{\lambda_{\mathrm{m}}} - 2\sqrt{1 - \frac{\lambda_i}{\lambda_{\mathrm{m}}}}\right) \\
&= \lambda_i.
\end{aligned}$$

Equation (5.5) implies $\Lambda_W = \theta_{\lambda_{\mathrm{m}}}(\Lambda_W) - \frac{1}{4\lambda_{\mathrm{m}}} \theta_{\lambda_{\mathrm{m}}}(\Lambda_W)^2$. Equality (5.4) follows by multiplying by U_W and $U_W^\top$ to the left and to the right. □

5.3 Main Results

This section presents the main results of the chapter. Namely, we give algebraic results on weighted Euclidean norms of certain matrix polytopes. These polytopes naturally arise in the analysis of the contractivity properties of HNNs and FNNs.

First, in the following definition, we extend the concept of logarithmic optimal norm for a matrix, given in Definition 2.6, to matrix polytopes.

Definition 5.1 (Log-optimal and log-ε-optimal norms for matrix polytopes)**.** *Given $A_1, \ldots, A_m \in \mathbb{R}^{n \times n}$, consider the polytope*

$$\mathcal{P} = \left\{ \sum_{j=1}^{m} \beta_j A_j \;\middle|\; \beta_j \geq 0, \sum_{j=1}^{m} \beta_j = 1 \right\}$$

and a scalar $\varepsilon > 0$. We say that the norm $\|\cdot\|$ is

(i) logarithmically optimal (log-optimal) for $\mathcal{P}$ *if*

$$\max_{A \in \mathcal{P}} \alpha(A) = \max_{j \in \{1,\ldots,m\}} \mu(A_j),$$

(ii) logarithmically ε-optimal (log-ε-optimal) for $\mathcal{P}$ *if*

$$\max_{A\in\mathcal{P}} \alpha(A) \leq \max_{j\in\{1,\dots,m\}} \mu(A_j) \leq \max_{A\in\mathcal{P}} \alpha(A) + \varepsilon.$$

We are specifically interested in the matrix polytopes $\mathcal{P}_{\mathrm{F}} := \{[d]W \mid d \in [0,1]^n\}$ and $\mathcal{P}_{\mathrm{H}} := \{W[d] \mid d \in [0,1]^n\}$. Namely, in Theorem 5.4 we give algebraic results on the Euclidean log-norm of matrices in $\mathcal{P}_{\mathrm{F}}$ and $\mathcal{P}_{\mathrm{H}}$.

Remark 5.2. *It is always possible to rewrite $\mathcal{P}_{\mathrm{F}}$ and $\mathcal{P}_{\mathrm{H}}$ in the form of Definition 5.1. In fact, let $A_1, \dots, A_{2^n} \in \mathbb{R}^{n\times n}$ be the 2^n vertices defined by $A_j = [v_j]W$ where $v_j \in \{0,1\}^n$ is the binary vector with entries either 0 or 1 (note that there are 2^n such binary vectors). Then the set $\{\sum_{j=1}^{2^n} \beta_j A_j \mid \beta_j \geq 0, \sum_{j=1}^{2^n} \beta_j = 1\}$ is exactly the set $\mathcal{P}_F := \{[d]W \mid d \in [0,1]^n\}$. To prove this, note that the vertices of the convex set $[0,1]^n$ are the 2^n vectors v_j. Therefore, given $d \in [0,1]^n$ there exist $\beta_j \geq 0$, $j = 1, \dots, 2^n$, with $\sum_{j=1}^{2^n} \beta_j = 1$ such that $[d] = \sum_{j=1}^{2^n} \beta_j [v_j]$. Thus,*

$$\begin{aligned}\mathcal{P}_F := \{[d]W \mid d \in [0,1]^n\} &= \Big\{ \sum_{j=1}^{2^n} \beta_j [v_j]W \;\Big|\; \beta_j \geq 0, \sum_{j=1}^{2^n} \beta_j = 1, v_j \in \{0,1\}^n \Big\} \\ &= \Big\{ \sum_{j=1}^{2^n} \beta_j A_j \;\Big|\; \beta_j \geq 0, \sum_{j=1}^{2^n} \beta_j = 1 \Big\}.\end{aligned}$$

The same reasoning holds for $\mathcal{P}_{\mathrm{H}}$. □

Before stating the main result of this section, we provide some technical lemmas necessary for the proof. First, we give a technical result for the spectral abscissa of matrix polytopes.

Lemma 5.2 (Lower bound on spectral abscissa of polytope of matrices)**.** *For any matrix $W \in \mathbb{R}^{n\times n}$, we have*

$$\max_{d\in[0,1]^n} \alpha([d]W) \geq \max\{0, \alpha(W)\}, \tag{5.6}$$

$$\max_{d\in[0,1]^n} \alpha(W[d]) \geq \max\{0, \alpha(W)\}. \tag{5.7}$$

Proof. First, note that the spectral abscissa is a continuous function and that the set $\mathcal{P}_{\mathrm{F}}$ is compact, hence the maximum is well-defined. To prove (5.6) we compute:

$$\begin{aligned}\max_{d\in[0,1]^n} \alpha([d]W) &\geq \max\{\, \alpha([d]W)|_{d=\mathbb{0}_n}, \alpha([d]W)|_{d=\mathbb{1}_n} \,\} \\ &= \max\{\, 0, \alpha(W) \,\}.\end{aligned}$$

The same calculation applies to prove inequality (5.7). □

Next, we give the following algebraic result for products of symmetric matrices.

Lemma 5.3 (Optimal norms for products of symmetric matrices)**.** *Let $A_1 = SQ \in \mathbb{R}^{n\times n}$ and $A_2 = QS \in \mathbb{R}^{n\times n}$, where S, $Q \in \mathbf{S}^n$, with $Q \succ 0$. Then, for each $i \in \{1, 2\}$,*

(i) $\operatorname{spec}(A_i)$ *is real and has the same number of negative, zero, and positive eigenvalues as S;*

(ii) the norm $\|\cdot\|_{2,Q^{1/2}}$ is optimal for the matrix A_i, i.e., $\|A_i\|_{2,Q^{1/2}} = \rho(A_i)$;

(iii) the norm $\|\cdot\|_{2,Q^{1/2}}$ is log-optimal for A_i, i.e., $\mu_{2,Q^{1/2}}(A_i) = \alpha(A_i)$.

Proof. Let $i = 1$. A_1 is similar to $Q^{1/2}SQ^{1/2} \in \mathbf{S}^n$, hence $\operatorname{spec}(A_1)$ is real. Statement (i) then follows from Sylvester's law of inertia, noting that $Q^{1/2}SQ^{1/2}$ is congruent to S. Regarding statement (ii), we compute

$$\begin{aligned}\|A_1\|^2_{2,Q^{1/2}} &= \lambda_{\max}(Q^{-1}A_1^\top QA_1) = \lambda_{\max}(Q^{-1}(QS)Q(SQ))\\ &= \lambda_{\max}((SQ)^2) = \rho(SQ)^2,\end{aligned}$$

where the last equality follows from the fact that $(SQ)^2$ has the same eigenvectors as SQ and real eigenvalues equal to the square of the real eigenvalues of SQ. Finally, to prove statement (iii) we compute

$$\begin{aligned}\mu_{2,Q^{1/2}}(A_1) &= \lambda_{\max}\Big(\frac{QA_1Q^{-1} + A_1^\top}{2}\Big) = \lambda_{\max}\Big(\frac{Q(SQ)Q^{-1} + QS}{2}\Big)\\ &= \lambda_{\max}(QS) = \lambda_{\max}(QSQQ^{-1})\\ &= \lambda_{\max}(QA_1Q^{-1}) = \lambda_{\max}(A_1) = \alpha(A_1).\end{aligned}$$

This concludes the proof of item (ii). The proof for $i = 2$ is a straightforward adaptation. □

We now give the main result of this section. To enhance clarity we prove its parts case by case. Statements (i) and (ii) in Theorem 5.4, are based upon and extend the treatment in [102, Theorem 2] – see Remark 5.3 for more details.

Theorem 5.4 (Euclidean log-norm of matrix polytopes)**.** *Given a symmetric synaptic matrix W (Assumption 5.1), the following statements holds:*

(i) if $\alpha(W) > 0$, then $\|\cdot\|_{2,Q_{\mathrm{F},\alpha(W)}}$, with $Q_{\mathrm{F},\alpha(W)} \in \mathbb{R}^{n\times n}$ defined in (5.2), is log-optimal for $\mathcal{P}_{\mathrm{F}}$, i.e.,

$$\max_{d\in[0,1]^n} \mu_{2,Q_{\mathrm{F},\alpha(W)}}([d]W) = \max_{d\in[0,1]^n} \alpha([d]W) = \alpha(W).$$

In addition, if W is invertible, then $\|\cdot\|_{2,Q_{\mathrm{H},\alpha(W)}}$, with $Q_{\mathrm{H},\alpha(W)} \in \mathbb{R}^{n\times n}$ defined in (5.3), is log-optimal for $\mathcal{P}_{\mathrm{H}}$, i.e.,

$$\max_{d\in[0,1]^n} \mu_{2,Q_{\mathrm{H},\alpha(W)}}(W[d]) = \max_{d\in[0,1]^n} \alpha(W[d]) = \alpha(W),$$

(ii) *if $\alpha(W) = 0$, then for each $\varepsilon > 0$ the norm $\|\cdot\|_{2,Q_{\mathrm{F},\varepsilon}}$, with $Q_{\mathrm{F},\varepsilon} \in \mathbb{R}^{n\times n}$ defined in (5.2), is log ε-optimal for $\mathcal{P}_{\mathrm{F}}$, i.e.,*

$$\max_{d\in[0,1]^n} \mu_{2,Q_{\mathrm{F},\varepsilon}}([d]W) \le \max_{d\in[0,1]^n} \alpha([d]W) + \varepsilon = \varepsilon,$$

(iii) *if $\alpha(W) < 0$, then $\|\cdot\|_{2,(-W)^{1/2}}$ is log-optimal for $\mathcal{P}_{\mathrm{F}}$ and $\mathcal{P}_{\mathrm{H}}$, i.e.,*

$$\max_{d\in[0,1]^n} \mu_{2,(-W)^{1/2}}([d]W) = \max_{d\in[0,1]^n} \alpha([d]W) = 0,$$
$$\max_{d\in[0,1]^n} \mu_{2,(-W)^{1/2}}(W[d]) = \max_{d\in[0,1]^n} \alpha(W[d]) = 0.$$

Proof of statement (i). First, we prove that $\|\cdot\|_{2,Q_{\mathrm{F},\alpha(W)}}$ is log-optimal for $\mathcal{P}_{\mathrm{F}}$ and it holds $\max_{d\in[0,1]^n} \alpha([d]W) = \alpha(W)$. For this purpose, define

$$P := \frac{1}{4\alpha(W)} Q_{\mathrm{F},\alpha(W)}^2 \succ 0.$$

Lemma 5.1 implies $W = Q_{\mathrm{F},\alpha(W)} - P$. Next, pick $d \in \mathbb{R}^n$ satisfying $\mathbb{0}_n < d \le \mathbb{1}_n$, so that $[d]$ is diagonal and invertible. Then

$$\begin{aligned} & 2\alpha(W)P - \frac{1}{2}Q_{\mathrm{F},\alpha(W)}^2 \succeq 0 \qquad (5.8)\\ \implies & 2\alpha(W)P - \frac{1}{2}Q_{\mathrm{F},\alpha(W)}[d]Q_{\mathrm{F},\alpha(W)} \succeq 0\\ \iff & 2\alpha(W)P - Q_{\mathrm{F},\alpha(W)}[d]P(2P[d]P)^{-1}P[d]Q_{\mathrm{F},\alpha(W)} \succeq 0. \end{aligned}$$

Since $P[d]P \succ 0$, we can apply the Schur complement to this LMI to conclude that

$$y^\top \begin{bmatrix} 2\alpha(W)P & -Q_{\mathrm{F},\alpha(W)}[d]P \\ -P[d]Q_{\mathrm{F},\alpha(W)} & 2P[d]P \end{bmatrix} y \ge 0, \quad \forall y \in \mathbb{R}^{2n}. \qquad (5.9)$$

Setting $y = (y_1, y_1)$ for arbitrary $y_1 \in \mathbb{R}^n$, the inequality (5.9) implies

$$\begin{aligned} & 2\alpha(W)P - Q_{\mathrm{F},\alpha(W)}[d]P - P[d]Q_{\mathrm{F},\alpha(W)} + 2P[d]P \succeq 0\\ \iff & Q_{\mathrm{F},\alpha(W)}[d]P + P[d]Q_{\mathrm{F},\alpha(W)} - 2P[d]P \preceq 2\alpha(W)P\\ \overset{W=Q_{\mathrm{F},\alpha(W)}-P}{\iff} & W[d]P + P[d]W \preceq 2\alpha(W)P\\ \iff & Q_{\mathrm{F},\alpha(W)}^2[d]W + W[d]Q_{\mathrm{F},\alpha(W)}^2 \preceq 2\alpha(W)Q_{\mathrm{F},\alpha(W)}^2. \qquad (5.10) \end{aligned}$$

In summary, we have established that the weak LMI (5.8) (independent of d) implies the weak LMI (5.10) for all $0 < d \le \mathbb{1}_n$. Here, by weak LMI, we mean to state that the linear matrix inequality is not strict. It is known [136, Theorem 6.3.5] that the eigenvalues of a symmetric matrix are continuous functions of the matrix entries. Therefore, the LMI (5.10) holds also for $\mathbb{0}_n \le d \le \mathbb{1}_n$. Finally, note that the LMI (5.10) is equivalent to the condition $\mu_{2,Q_{\mathrm{F},\alpha(W)}}([d]W) \le \alpha(W)$ for all $d \in [0,1]^n$, therefore

$$\max_{d\in[0,1]^n} \mu_{2,Q_{\mathrm{F},\alpha(W)}}([d]W) \le \alpha(W).$$

Moreover, the norm spectrum property of log-norm (vi) implies that for every log-norm μ and every matrix A it holds $\alpha(A) \leq \mu(A)$. Specifically in our case:

$$\max_{d\in[0,1]^n} \alpha([d]W) \leq \max_{d\in[0,1]^n} \mu_{2,Q_{\mathrm{F},\alpha(W)}}([d]W).$$

The proof then follows from (5.6), after noticing that under the assumptions of statement (i) it holds $\max\{0, \alpha(W)\} = \alpha(W)$.

Next, assume that W is invertible. We need to prove that $\|\cdot\|_{2,Q_{\mathrm{H},\alpha(W)}}$ is log-optimal for $\mathcal{P}_{\mathrm{H}}$ and that it holds $\max_{d\in[0,1]^n} \alpha(W[d]) = \alpha(W)$. Note that for two invertible matrices $Q_1, Q_2 \in \mathbb{R}^{n\times n}$, it holds

$$\mu_{p,Q_1Q_2}(A) = \mu_{p,Q_1}(Q_2AQ_2^{-1}). \tag{5.11}$$

We have

$$\begin{aligned}\max_{d\in[0,1]^n} \mu_{2,Q_{\mathrm{H},\alpha(W)}}(W[d]) &= \max_{d\in[0,1]^n} \mu_{2,Q_{\mathrm{F},\alpha(W)}W^{-1}}(W[d]) \\ &\overset{(5.11)}{=} \max_{d\in[0,1]^n} \mu_{2,Q_{\mathrm{F},\alpha(W)}}([d]W) = \alpha(W),\end{aligned}$$

where the last equality follows from the log-optimality of $\|\cdot\|_{2,Q_{\mathrm{F},\alpha(W)}}$ for $\mathcal{P}_{\mathrm{F}}$. The proof again follows from (5.6). □

Proof of statement (ii). The proof follows the same reasoning as that of statement (i) by considering $\varepsilon > 0$ instead of $\alpha(W)$. Hence, we omit it here for brevity. □

Proof of statement (iii). Pick $d \in \mathbb{R}^n$ satisfying $\mathbb{0}_n \leq d \leq \mathbb{1}_n$ and consider the matrices $[d]W$ and $W[d]$. Lemma 5.3 with $S := [-d]$ and $Q := -W \succ 0$, implies that the spectrum of the product matrices $[d]W = [-d](-W)$ and $W[d] = (-W)[-d]$ is real and has the same number of negative, zero, positive eigenvalues as $[-d]$. Therefore,

$$\mu_{2,(-W)^{1/2}}([d]W) = \alpha([d]W) \begin{cases} < 0 & \text{if } d > \mathbb{0}_n, \\ \leq 0 & \text{otherwise,} \end{cases}$$

$$\mu_{2,(-W)^{1/2}}(W[d]) = \alpha(W[d]) \begin{cases} < 0 & \text{if } d > \mathbb{0}_n, \\ \leq 0 & \text{otherwise.} \end{cases}$$

Maximizing over $d \in [0,1]^n$ we get statement (iii). □

It is worth elaborating on the previous results, as it is key for obtaining sufficient conditions for the strong infinitesimal contractivity of the FNNs and HNNs with symmetric weights with respect to weighted Euclidean norms. Given a symmetric matrix W, Theorem 5.4 provides weighted Euclidean log-optimal log-norms for matrix polytopes in $\mathcal{P}_{\mathrm{F}}$ and $\mathcal{P}_{\mathrm{H}}$. Moreover, it applies also to polytopes that arise when studying contractivity of the FNNs and HNNs, that are polytopes of the form $aI_n + [d]W$ and $aI_n + W[d]$, for all $a \in \mathbb{R}$, where $d \in [0,1]^n$. This last statement follows from the log-norm translation property (iii). The log-optimality of the proposed log-norms is key to obtain sharp results in our contractivity analysis for some cases.

5.4 Contractivity of Recurrent Neural Networks

Consider the neural network dynamics for the FNN in equation (3.2) and for the HNN in equation (3.1). Using the results in Section 5.3, we now derive sufficient conditions for the strong infinitesimal contractivity of the FNN and the HNN with symmetric weights with respect to weighted Euclidean norms.

We make the following assumption on the activation functions.

Assumption 5.2 (Slope restricted activation function)**.** *The activation function* $\phi\colon \mathbb{R} \to \mathbb{R}$ *is Lipschitz and slope restricted in* $[0, 1]$*, i.e.,*

$$0 \leq \frac{\phi(x) - \phi(y)}{x - y} \leq 1, \text{ for all } x, y \in \mathbb{R}, x \neq y.$$

Assumption 5.2 ensures that $\phi'(x) \in [0, 1]$ for almost all $x \in \mathbb{R}$. Many common activation functions including ReLU, and sigmoid, satisfy Assumption 5.2, possibly after rescaling. In fact, Assumption 5.2 can be relaxed for larger classes of coupling by restricting the slope to $[0, \bar{d}]$, where $\bar{d} > 0$. By defining $[d] := D\Phi/\bar{d}$ and $W := \bar{d}W$ our following results still hold for this general case, with $\alpha(W)$ replaced by $\alpha(\bar{d} \cdot W) = \bar{d} \cdot \alpha(W)$. We assume $\bar{d} = 1$ to simplify the notation.

Remark 5.3. *Our results for strong infinitesimal contractivity of the FNN and HNN with symmetric weights are based on and generalize [102, Theorem 2]. Specifically, in the next sections, we (i) provide the explicit expression of the matrix weights for which the models are contracting. The matrices we find are different for the two dynamics, highlighting the importance of choosing the appropriate model based on the properties being studied; (ii) address the weak contractivity case, making our results applicable for, e.g., systems that enjoy conservation or invariance properties; (iii) handle weakly increasing and (iv) locally Lipschitz activation functions, which allows our framework to encompass common activation functions such as the rectified linear unit (ReLU) and soft thresholding functions.* □

5.4.1 Contractivity of Firing Rate Neural Networks

We now provide an upper bound on the ℓ_2 one-sided Lipschitz constant and sufficient conditions for the Euclidean contractivity of the FNN with symmetric weights.

Theorem 5.5 (Euclidean one-sided Lipschitz constant of the FNN)**.** *Consider the FNN* (3.2) *with symmetric synaptic matrix (Assumption 5.1), Lipschitz and slope restricted in* $[0, 1]$ *activation function (Assumption 5.2),*

(i) if $\alpha(W) > 0$*, then*

$$\mathsf{osLip}_{2, Q_{\mathrm{F}, \alpha(W)}}(f_{\mathrm{F}}) \leq -1 + \alpha(W),$$

with $Q_{\mathrm{F}, \alpha(W)} \in \mathbb{R}^{n \times n}$ *defined in* (5.2)*;*

(ii) if $\alpha(W) = 0$*, then*

$$\mathsf{osLip}_{2,Q_{\mathrm{F},\varepsilon}}(f_{\mathrm{F}}) \leq -1 + \varepsilon,$$

with $Q_{\mathrm{F},\varepsilon} \in \mathbb{R}^{n\times n}$ *defined in* (5.2)*;*

(iii) if $\alpha(W) < 0$*, then*

$$\mathsf{osLip}_{2,(-W)^{1/2}}(f_{\mathrm{F}}) \leq -1.$$

Proof. Regarding statement (i) note that for almost all $\nu \in \mathbb{R}^n$ we have

$$\begin{aligned}\mu_{2,Q_{\mathrm{F},\alpha(W)}}(Df_{\mathrm{F}}(\nu)) &= \mu_{2,Q_{\mathrm{F},\alpha(W)}}(-I_n + D\Phi(W\nu + u)W)\\ &\leq \max_{d\in[0,1]^n} \mu_{2,Q_{\mathrm{F},\alpha(W)}}(-I_n + [d]W) = -1 + \alpha(W),\end{aligned}$$

where the last equality follows by the log-norm translation property (iii) and statement (i) in Theorem 5.4. The proof follows by applying Theorem 4.3. Statements (ii) and (iii) can be proved similarly, using statements (ii) and (iii) in Theorem 5.4. □

The next result shows that, under further assumptions on the synaptic matrix and the activation function, some inequalities in Theorem 5.5 are tight.

Lemma 5.6 (Sharp Euclidean one-sided Lipschitz constant of the FNN)**.** *Given the FNN* (3.2) *with symmetric (Assumption 5.1) and invertible synaptic matrix* W*, Lipschitz and slope restricted in* $[0,1]$ *(Assumption 5.2) activation function* ϕ *satisfying the equalities* $\inf_{x\in\mathbb{R}} \phi'(x) = 0$ *and* $\sup_{x\in\mathbb{R}} \phi'(x) = 1$*,*

(i) if $\alpha(W) > 0$*, then*

$$\mathsf{osLip}_{2,Q_{\mathrm{F},\alpha(W)}}(f_{\mathrm{F}}) = -1 + \alpha(W),$$

with $Q_{\mathrm{F},\alpha(W)} \in \mathbb{R}^{n\times n}$ *defined in* (5.2)*;*

(ii) if $\alpha(W) < 0$*, then*

$$\mathsf{osLip}_{2,(-W)^{1/2}}(f_{\mathrm{F}}) = -1.$$

Proof. The proof of both statements follows by applying Theorem 5.5 and noticing that under the above assumptions for any log-norm μ it holds the reverse inequality

$$\mu(Df_{\mathrm{F}}(\nu)) \geq -1 + \alpha(W), \quad \forall \nu \in \mathbb{R}^n. \tag{5.12}$$

To prove (5.12), let $h\colon \mathbb{R}\setminus\Omega_\phi \to [0,1]$ be the function defined by $h(\nu) = \phi'(\nu)$ where Ω_ϕ is the measure zero set of points in $\mathbb{R}$ where ϕ is not differentiable. It is well-known that for any closed and bounded set $S \subset \mathbb{R}$, $S \supseteq \{\inf(S), \sup(S)\}$. Then, since h is bounded, the closure of $\mathrm{Im}(h)$ satisfies

$$\overline{\mathrm{Im}(h)} \supseteq \left\{ \inf_{\nu\in\mathbb{R}\setminus\Omega_\phi} \phi'(\nu), \sup_{\nu\in\mathbb{R}\setminus\Omega_\phi} \phi'(\nu) \right\} = \{0,1\}. \tag{5.13}$$

Letting Ω_Φ be the measure zero points in $\mathbb{R}^n$ where Φ is not differentiable, we compute

$$\begin{aligned}
\sup_{\nu\in\mathbb{R}^n\setminus\Omega_\Phi} \mu(D\Phi(W\nu+u)W) &= \sup_{\nu\in\mathbb{R}^n\setminus\Omega_\Phi} \mu(D\Phi(\nu)W) && (5.14)\\
&= \sup\{\mu([d]W) \mid d_i \in \mathrm{Im}(h), \forall i\}\\
&= \max\{\mu([d]W) \mid d_i \in \overline{\mathrm{Im}(h)}, \forall i\}\\
&\geq \max_{d\in\{0,1\}^n} \mu([d]W) && (5.15)\\
&= \max_{d\in[0,1]^n} \mu([d]W). && (5.16)
\end{aligned}$$

We justify the above (in)equalities as follows. Equality (5.14) holds because W is invertible. Inequality (5.15) holds because of the condition (5.13). Finally, equality (5.16) follows because μ is a convex function of its argument and the maximum value of a convex function over a polytope occurs at one of its vertices.

In particular, for the respective choice of norm in statements (i) and (ii), the result is proved in view of Theorem 5.4 and the translation property for log-norms (iii). □

The following is an immediate consequence of Theorem 5.5.

Corollary 5.7 (Euclidean contractivity of the FNN)**.** *Under the same assumptions and notations as in Theorem 5.5,*

(i) if $\alpha(W) = 1$, then the FNN is weakly infinitesimally contracting with respect to $\|\cdot\|_{2,Q_{\mathrm{F},\alpha(W)}}$,

(ii) if $0 < \alpha(W) < 1$, then the FNN is strongly infinitesimally contracting with rate $1-\alpha(W) > 0$ with respect to $\|\cdot\|_{2,Q_{\mathrm{F},\alpha(W)}}$,

(iii) if $\alpha(W) = 0$, then for any $0 < \varepsilon < 1$ the FNN is strongly infinitesimally contracting with rate $1-\varepsilon > 0$ with respect to $\|\cdot\|_{2,Q_{\mathrm{F},\varepsilon}}$,

(iv) if $\alpha(W) < 0$, then the FNN is strongly infinitesimally contracting with rate 1 with respect to $\|\cdot\|_{2,(-W)^{1/2}}$.

5.4.2 Contractivity of Hopfield Neural Networks

We first provide an upper bound on the Euclidean one-sided Lipschitz constant and sufficient conditions for the ℓ_2 contractivity of HNNs with non-singular symmetric synaptic matrix. Then, we give sufficient conditions for the ℓ_2 contractivity with singular symmetric synapses, as the two scenarios require a distinct mathematical approach.

Theorem 5.8 (Euclidean one-sided Lipschitz constant of the HNN with non-singular symmetric weights)**.** *Consider the HNN (3.1) satisfying Assumptions 5.1 and 5.2 with non-singular weight matrix W,*

(i) if $\alpha(W) > 0$, then

$$\mathsf{osLip}_{2,Q_{\mathrm{H},\alpha(W)}}(f_{\mathrm{H}}) \leq -1 + \alpha(W),$$

with $Q_{\mathrm{H},\alpha(W)} \in \mathbb{R}^{n\times n}$ defined in (5.3),

(ii) if $\alpha(W) < 0$*, then*

$$\mathsf{osLip}_{2,(-W)^{1/2}}(f_{\mathrm{H}}) \leq -1.$$

Proof. Regarding statement (i), note that for almost all $x \in \mathbb{R}^n$ we have

$$\begin{aligned}\mu_{2,Q_{\mathrm{H},\alpha(W)}}(Df_{\mathrm{H}}(x)) &= \mu_{2,Q_{\mathrm{H},\alpha(W)}}(-I_n + WD\Phi(x)) \\ &\leq \max_{d\in[0,1]^n} \mu_{2,Q_{\mathrm{H},\alpha(W)}}(-I_n + W[d]) = -1 + \alpha(W),\end{aligned}$$

where the last equality follows by the log-norm translation property (iii) and statement (i) in Theorem 5.4. The proof then follows by applying Theorem 4.3. statement (ii) can be proved similarly, using statement (iii) in Theorem 5.4. □

Remark 5.4. *Following the same reasoning as in Lemma 5.6, under the same assumptions of Theorem 5.8, if the activation function satisfies* $\inf_{x\in\mathbb{R}} \phi'(x) = 0$*, and* $\sup_{x\in\mathbb{R}} \phi'(x) = 1$*, then the inequalities in Theorem 5.8 are tight.* □

Corollary 5.9 (Euclidean contractivity of the HNN with non-singular symmetric weights)**.** *Under the same assumptions and notations as in Theorem 5.8,*

(i) if $\alpha(W) = 1$*, then the HNN is weakly infinitesimally contracting with respect to* $\|\cdot\|_{2,Q_{\mathrm{H},\alpha(W)}}$*,*

(ii) if $0 < \alpha(W) < 1$*, then the HNN is strongly infinitesimally contracting with rate* $1 - \alpha(W) > 0$ *with respect to* $\|\cdot\|_{2,Q_{\mathrm{H},\alpha(W)}}$*,*

(iii) if $\alpha(W) < 0$*, then the HNN is strongly infinitesimally contracting with rate* 1 *with respect to* $\|\cdot\|_{2,(-W)^{1/2}}$*.*

Finally, we give sufficient infinitesimal contractivity conditions of the HNN with singular symmetric synapses.

Theorem 5.10 (Contractivity of the HNN with singular symmetric weights)**.** *Consider the HNN (3.1) satisfying Assumptions 5.1 and 5.2 with* W *having kernel* $\mathcal{K} \neq \{\mathbb{0}_n\}$*, and such that* $\alpha(W) < 1$*. Then, for each* $\varepsilon \in]0, 1 - \alpha(W)[$ *the HNN is strongly infinitesimally contracting with rate* $|1 - \alpha(W) - \varepsilon|$*.*

Proof. Let r be the number of non-zero eigenvalues of $W \in \mathbb{R}^{n\times n}$. For simplicity of notation, we here drop the subscript W in the SVD decomposition of W, denoting it simply as (U, Λ). Without loss of generality, we reorder the elements in $\lambda \in \mathbb{R}^n$ and $U \in \mathbb{R}^{n\times n}$, so that $\lambda = (\lambda_1, \ldots, \lambda_r, 0, \ldots, 0)$ and $U = [u_1, \ldots, u_r, u_{r+1}, \ldots, u_n]$, where $u_i \in \mathbb{R}^n$ is the eigenvector of $\lambda_i \in \mathbb{R}$.

Next, let $\mathcal{K}^* := \mathsf{span}\{\, u_1, \ldots, u_r \,\}$, $n_{\|} := \dim(\mathcal{K}^*)$, $\mathcal{K} := \mathsf{span}\{\, u_{r+1}, \ldots, u_n \,\}$, $n_{\perp} := \dim(\mathcal{K})$, and define $U_{\|} := [u_1, \ldots, u_r] \in \mathbb{R}^{n\times n_{\|}}$, $U_{\perp} := [u_{r+1}, \ldots, u_n] \in \mathbb{R}^{n\times n_{\perp}}$, so that $U = [U_{\|} \quad U_{\perp}]$.

We have $\mathbb{R}^n = \{\, x \in \mathbb{R}^n \mid x \in \mathcal{K}^* \,\} \oplus \{\, x \in \mathbb{R}^n \mid x \in \mathcal{K} \,\}$. Therefore, given $x \in \mathbb{R}^n$ we can always define $x_{\|} = U_{\|}^\top x \in \mathcal{K}^*$ and $x_{\perp} = U_{\perp}^\top x \in \mathcal{K}$. We note that $U^\top U = I_n$ implies $U_{\|}^\top U_{\|} = I_{n_{\|}}$, $U_{\perp}^\top U_{\perp} = I_{n_{\perp}}$, $U_{\perp}^\top U_{\|} = \mathbb{0}_{n_{\perp}\times n_{\|}}$, and

$U_\parallel^\top U_\perp = \mathbb{0}_{n_\parallel \times n_\perp}$. Additionally, we define $\theta_\parallel := [(\theta_{\alpha(W)}(\lambda_1), \dots, \theta_{\alpha(W)}(\lambda_r))]$ and $\theta_\perp := [(\theta_{\alpha(W)}(\lambda_{r+1}), \dots, \theta_{\alpha(W)}(\lambda_n))]$. Also,

$$
\begin{aligned}
W &= \begin{bmatrix} U_\parallel & U_\perp \end{bmatrix} \begin{bmatrix} \Lambda_\parallel & 0_{n_\parallel \times n_\perp} \\ 0_{n_\perp \times n_\parallel} & 0_{n_\perp \times n_\perp} \end{bmatrix} \begin{bmatrix} U_\parallel^\top \\ U_\perp^\top \end{bmatrix} = U_\parallel \Lambda_\parallel U_\parallel^\top, \\
Q_{\mathrm{F},\alpha(W)} &= U \theta_{\alpha(W)}(\Lambda) U^\top = \begin{bmatrix} U_\parallel & U_\perp \end{bmatrix} \begin{bmatrix} \theta_\parallel & 0_{n_\parallel \times n_\perp} \\ 0_{n_\perp \times n_\parallel} & \theta_\perp \end{bmatrix} \begin{bmatrix} U_\parallel^\top \\ U_\perp^\top \end{bmatrix} \\
&= U_\parallel \theta_\parallel U_\parallel^\top + U_\perp \theta_\perp U_\perp^\top.
\end{aligned}
$$

Moreover, we have

$$
\max_{d \in [0,1]^n} \mu_{2,\theta_\parallel}(-I_{n_\parallel} + U_\parallel^\top [d] U_\parallel \Lambda_\parallel) \leq -1 + \alpha(W). \tag{5.17}
$$

In fact, from Corollary 5.7 we know:

$$
\begin{aligned}
& 2\alpha(W) Q_{\mathrm{F},\alpha(W)} + Q_{\mathrm{F},\alpha(W)}[d] W + W[d] Q_{\mathrm{F},\alpha(W)} \preceq 0 \\
\iff\ & 2\alpha(W)(U_\parallel \theta_\parallel^2 U_\parallel^\top + U_\perp \theta_\perp^2 U_\perp^\top) \\
& \quad + (U_\parallel \theta_\parallel^2 U_\parallel^\top + U_\perp \theta_\perp^2 U_\perp^\top)[d] U_\parallel \Lambda_\parallel U_\parallel^\top \\
& \quad + U_\parallel \Lambda_\parallel U_\parallel^\top [d] (U_\parallel \theta_\parallel^2 U_\parallel^\top + U_\perp \theta_\perp^2 U_\perp^\top) \preceq 0.
\end{aligned}
$$

By multiplying by $U_\parallel^\top$ and $U_\parallel$ to the left and to the right, respectively, we get

$$
2\alpha(W)\theta_\parallel^2 + \theta_\parallel^2 U_\parallel^\top [d] U_\parallel \Lambda_\parallel + \Lambda_\parallel U_\parallel^\top [d] U_\parallel \theta_\parallel^2 \preceq 0. \tag{5.18}
$$

Thus, $\mu_{2,\theta_\parallel}(-I_{n_\parallel} + U_\parallel^\top [d] U_\parallel \Lambda_\parallel) \leq -1 + \alpha(W)$. Next, by multiplying (3.1) by $U_\perp^\top$ and $U_\parallel^\top$ we obtain the interconnected system:

$$
\begin{cases}
U_\perp^\top \dot{x} = -U_\perp^\top x + U_\perp^\top W \Phi(x) + U_\perp^\top u, \\
U_\parallel^\top \dot{x} = -U_\parallel^\top x + U_\parallel^\top W \Phi(Wx) + U_\parallel^\top u,
\end{cases}
$$

thus,

$$
\begin{cases}
\dot{x}^\perp = -x^\perp + u^\perp := f_{\mathrm{H}}^\perp(x^\perp, u^\perp), & (5.19) \\
\dot{x}^\parallel = -x^\parallel + \Lambda_\parallel U_\parallel^\top \Phi(x) + u^\parallel := f_{\mathrm{H}}^\parallel(x, u^\parallel). & (5.20)
\end{cases}
$$

Equation (5.19) is always contracting with respect to any norm in the subspace $\mathcal{K}$ with $\mathsf{osLip}(f_{\mathrm{H}}^\perp) = -1$, being $\mu(Df_{\mathrm{H}}^\perp) = \mu(-I_{n_\perp}) = -1$. For system (5.20) we define $Q_{\mathrm{H},\alpha(W)} := Q_{\mathrm{F},\alpha(W)} W^\dagger = U \theta_{\alpha(W)} \Lambda^\dagger U^\top$, where $W^\dagger = U \Lambda^\dagger U^\top$ is the *Moore-Penrose pseudoinverse* of W, with $\Lambda^\dagger$ defined as

$$
\Lambda^\dagger = \begin{bmatrix} \Lambda_\parallel^{-1} & 0_{n_\parallel \times n_\perp} \\ 0_{n_\perp \times n_\parallel} & 0_{n_\perp \times n_\perp} \end{bmatrix}.
$$

Next, we note that the matrix $Q_{\mathrm{H}\|} := U_\|^\top Q_{\mathrm{F},\alpha(W)} W^\dagger U_\| = \theta_\| \Lambda_\|^{-1}$ and that it holds $Df_{\mathrm{H}}^\| = -I_{n_\|} + \Lambda_\| U_\|^\top [d] U_\|$. Thus, we have

$$\begin{aligned}
\mathsf{osLip}_{2,Q_{\mathrm{H}\|}}(f_{\mathrm{H}}^\|) &\leq \max_{d\in[0,1]^n} \mu_{2,Q_{\mathrm{H}\|}}(Df_{\mathrm{H}}^\|) \leq \max_{d\in[0,1]^n} \mu_{2,\theta_\|\Lambda_\|^{-1}}(-I_{n_\|} + \Lambda_\| U_\|^\top [d] U_\|) \\
&\overset{(5.11)}{=} \max_{d\in[0,1]^n} \mu_{2,\theta_\|}(-I_{n_\|} + U_\|^\top [d] U_\| \Lambda_\|) \\
&\overset{(5.17)}{\leq} -1 + \alpha(W).
\end{aligned}$$

Thus system (5.20) is strongly infinitesimally contracting in $\mathcal{K}^*$ with respect to $\|\cdot\|_{Q_{\mathrm{H}\|}}$ with rate $1-\alpha(W)$.

Finally, we note that at fixed $x_\|$ and t, the map $x_\perp \to f_\|$ is Lipschitz with constant $L_{\|\perp} := \alpha(W)$. In fact, $\forall x_\perp^1, x_\perp^2 \in \mathcal{K}$, we get

$$\begin{aligned}
\|f_\|(x_\|, x_\perp^1) - f_\|(x_\|, x_\perp^2)\| &= \|-x_\| + W\Phi(x_\perp^1 + x_\|) + u + x_\| - W\Phi(x_\perp^2 + x_\|) - u\| \\
&= \|W(\Phi(x_\perp^1 + x_\|) - \Phi(x_\perp^2 + x_\|))\| \\
&\leq \alpha(W)\|\Phi(x_\perp^1 + x_\|) - \Phi(x_\perp^2 + x_\|)\| \leq \alpha(W)\|x_\perp^1 - x_\perp^2\|.
\end{aligned}$$

We can now construct the gain matrix (4.6)

$$\Gamma = \begin{bmatrix} -1 & 0 \\ \alpha(W) & -1 + \alpha(W) \end{bmatrix} \in \mathbb{R}^{2\times 2}. \tag{5.21}$$

The eigenvalues of Γ are $\lambda_1 = -1, \lambda_2 = -1 + \alpha(W)$. The fact that $\mathcal{K} \neq \{\mathbb{0}_n\}$ implies $\alpha(W) \geq 0$. In turn, since by assumptions $\alpha(W) < 1$, we have $\lambda_2 \in [-1, 0[$. Thus Γ is Hurwitz and $\alpha(\Gamma) = -1 + \alpha(W)$. By applying Theorem 4.5, for each $\varepsilon \in]0, 1 - \alpha(W)[$ we have that the HNN is strongly infinitesimally contracting with rate $|\alpha(\Gamma) + \varepsilon|$. This concludes the proof. □

Remark 5.5. *If $W = 0$, then the FNN (3.2) and the HNN (3.1) are contracting with rate 1. As a consequence of Corollaries 5.7, 5.9 and Theorem 5.10, when coupling is added to the networks, they remain (strongly) contracting as long as $\alpha(W) < 1$. Note that the entries of W are allowed to be large, so as the activation function and this allows to have different types of coupling as long as the matrix $I_n - W$ is Hurwitz.* □

5.5 Using Euclidean Contractivity to Solve Quadratic Optimization Problems

To demonstrate the practical application of the previous results, we now apply them to propose a firing rate neural network solving certain quadratic optimization problems with box constraints. Leveraging Corollary 5.7, we ensure global exponential convergence of our dynamic, along with all the other properties of contracting systems. We focus on the use of contracting dynamical systems to solve optimization problems in Part III.

Given $A = A^\top \succ 0$, an input $u \in \mathbb{R}^n$, and $a \leq b \in \mathbb{R}^n$ the *quadratic optimization problem with box constraints* is

$$\min_{y \in \mathbb{R}^n} \Big(J_{A,u}(y) := \frac{1}{2} y^\top A y - u^\top y \Big), \quad \text{s.t. } a \leq y \leq b. \tag{5.22}$$

Note that $J_{A,u}(\cdot)$ is strongly convex and the constraints are convex, thus (5.22) admits a unique global optimal solution.

We propose the following FNN model to solve (5.22). Given a single-layered neural network of n neurons, the state $\nu \in \mathbb{R}^n$ evolves according to

$$\dot{\nu} = -\nu + \operatorname{sat}_{a,b}\big((I_n - A)\nu + u\big), \tag{5.23}$$

with output $y = \nu$. The activation function $\operatorname{sat}_{a,b}(\cdot) \colon \mathbb{R}^n \to [a, b] := [a_1, b_1] \times \cdots \times [a_n, b_n]$, illustrated in Figure 5.2, is defined as $(\operatorname{sat}_{a,b}(z))_i = \operatorname{sat}_{a_i,b_i}(z_i)$, where $\operatorname{sat}_{a_i,b_i}(\cdot) \colon \mathbb{R} \to [a_i, b_i]$ is

$$\operatorname{sat}_{a_i,b_i}(z_i) = \begin{cases} a_i & \text{if } z_i \leq a_i, \\ z_i & \text{if } a_i < z_i < b_i, \\ b_i & \text{if } z_i \geq b_i. \end{cases}$$

To simplify the notation, whenever it is clear from the context, we use the same symbol for both the scalar and vector forms of the saturation function.

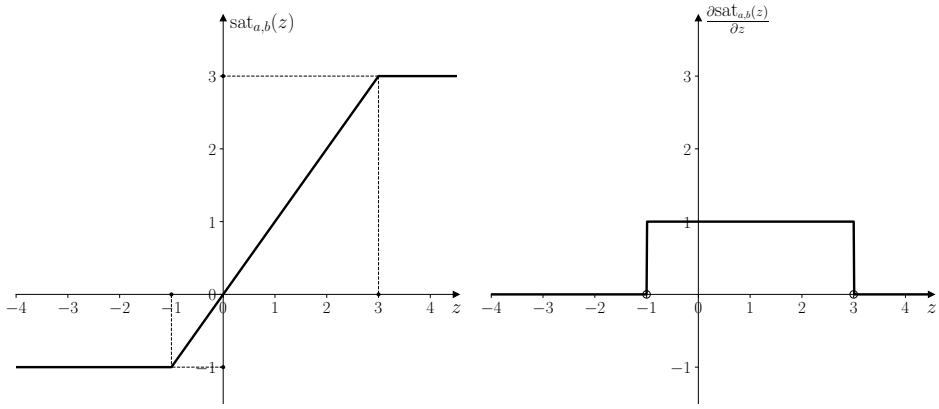

Figure 5.2: Saturation function $\operatorname{sat}_{a,b}(\cdot)$ for $a = -1$ and $b = 3$ (left panel) and its derivative (right panel). As shown, the saturation function is slope restricted in $[0, 1]$.

Remark 5.6. *The function* $\operatorname{sat}_{a_i,b_i}(\cdot)$ *satisfies Assumption 5.2 (see Figure 5.2). Almost everywhere, its partial derivative is* $\partial \operatorname{sat}_{a,b}(\cdot) \colon \mathbb{R} \setminus \{a, b\} \to \{0, 1\}$ *defined by*

$$\frac{\partial \operatorname{sat}_{a,b}(z)}{\partial z} = \begin{cases} 0 & \text{if } z \notin]a, b[, \\ 1 & \text{if } z \in]a, b[. \end{cases}$$

□

Next, we use Corollary 5.7 to give sufficient conditions for the strong infinitesimal contractivity of (5.23). Then, we show that the equilibrium of the FNN (5.23) is the optimal solution of the optimization problem (5.22).

Lemma 5.11 (Strong infinitesimal contractivity)**.** *Let $A = A^\top \succ 0$ in (5.23). The FNN (5.23) is strongly infinitesimally contracting with rate $c > 0$ with respect to the norm $\|\cdot\|_{2,P}$, where*

(i) if $\lambda_{\min}(A) < 1$, then $c = \lambda_{\min}(A)$ and $P = Q_{\mathrm{F},1-\lambda_{\min}(A)}$, with $Q_{\mathrm{F},1-\lambda_{\min}(A)}$ defined in (5.2);

(ii) if $\lambda_{\min}(A) = 1$, then for any $0 < \varepsilon < 1$, $c = 1 - \varepsilon > 0$ and $P = Q_{\mathrm{F},\varepsilon}$, with $Q_{\mathrm{F},\varepsilon}$ defined in (5.2);

(iii) if $\lambda_{\min}(A) > 1$, then $c = 1$ and $P = (A - I_n)^{1/2}$.

Proof. The thesis follows by applying Corollary 5.7 noticing that $A \succ 0$ implies $W = I_n - A \prec I_n$, thus $\alpha(W) = 1 - \lambda_{\min}(A) < 1$, and $\mathrm{sat}_{\mu,\nu}(\cdot)$ satisfies Assumption 5.2. □

A consequence of Lemma 5.11 is that the FNN (5.23) admits a unique equilibrium point. Next, we prove that this equilibrium point is the optimal solution of (5.22).

Lemma 5.12. *The vector $\nu^\star \in \mathbb{R}^n$ is the global minimum for the quadratic optimization point (5.22) if and only if $\nu^\star$ is the equilibrium point of the FNN (5.23).*

Proof. Let $\nu^\star \in \mathbb{R}^n$ be a global minimum for (5.22), thus $\nu^\star \in [a, b]$. Then it follows from the KKT conditions that, for all $i \in \{1, \dots, n\}$,

$$\frac{\partial J_{A,u}}{\partial x_i}(\nu^\star) = (A\nu^\star)_i - u_i \begin{cases} \geq 0 & \text{if } \nu_i^\star = a_i, \\ = 0 & \text{if } a_i < \nu_i^\star < b_i, \\ \leq 0 & \text{if } \nu_i^\star = b_i. \end{cases} \tag{5.24}$$

Note that $\nu^\star$ is an equilibrium of (5.23) if, for all $i \in \{1, \dots, n\}$, we have

$$-\nu_i^\star + \mathrm{sat}_{a_i,b_i}\left(\nu_i^\star - (A\nu^\star)_i + u_i\right) = 0. \tag{5.25}$$

If $\nu_i^\star = a_i$, let $z^\star := (A\nu^\star)_i|_{\nu_i^\star = a_i} - u_i$. By definition of $\mathrm{sat}_{a_i,b_i}(\cdot)$ it holds $-a_i + \mathrm{sat}_{a_i,b_i}(a_i - z^\star) \geq 0$. Moreover, from the KKT conditions (5.24), and being $\mathrm{sat}_{a_i,b_i}(\cdot)$ monotonically non-decreasing, we get the reverse inequality. Thus $\nu_i^\star = a_i$ verifies (5.25). Similarly it can be proved that (5.25) holds for $a_i < \nu_i^\star < b_i$, and $\nu_i^\star = b_i$.

Vice versa, let $\nu^\star \in \mathbb{R}^n$ be an equilibrium of (5.22), i.e., (5.25) holds. If $\nu_i^\star \leq a_i$, then (5.25) implies $\nu_i^\star = \mathrm{sat}_{a_i,b_i}(a_i - z^\star)$. By definition of $\mathrm{sat}_{a_i,b_i}(\cdot)$ we get $\nu_i^\star \in [a_i, b_i]$, thus $\nu_i^\star = a_i$, and $a_i - z^\star \leq a_i$, which implies $z^\star \geq 0$. Similarly, if $a_i < \nu_i^\star < b_i$, then $z^\star = 0$, while if $\nu_i^\star \geq b_i$, then $\nu_i^\star = b_i$ and $z^\star \leq 0$. This ends the proof since we have shown that the KKT conditions (5.24) hold for all i. □

5.5.1 Numerical Example

We validate the effectiveness of the FNN (5.23) in solving the quadratic optimization problem with box constraints (5.22) via a simple numerical example.

Consider problem (5.22) with $A = \begin{pmatrix} 4 & -1 \\ -1 & 2 \end{pmatrix}$, $u = \begin{pmatrix} 1 \\ 0 \end{pmatrix}$, $a = -1$, and $b = 5$, that is the following quadratic optimization problem with box constraints

$$\begin{aligned} \min_{y \in \mathbb{R}^2} \quad & 2y_1^2 - y_1 y_2 + y_2^2 - y_1, \\ \text{s.t.} \quad & -1 \leq y_1 \leq 5, -1 \leq y_2 \leq 5. \end{aligned} \tag{5.26}$$

Solving (5.26) in Python using the function minimize we obtain the vector $y^\star = (0.28, 0.14)$. The corresponding FNN for problem (5.26) reads

$$\begin{aligned} \dot{\nu}_1 &= -\nu_1 + \mathrm{sat}_{-1,5}\big((I_2 - A)\nu + 1\big), \\ \dot{\nu}_2 &= -\nu_2 + \mathrm{sat}_{-1,5}\big((I_2 - A)\nu\big). \end{aligned} \tag{5.27}$$

We simulate the dynamics (5.27) over the time interval $t \in [0, 5]$ with a forward Euler discretization with step-size $\Delta t = 0.01$ from 100 randomly generated initial conditions. We plot the trajectories of the variables ν_1 and ν_2 along with the optimal values $y^\star$ in Figure 5.3. We empirically observe how the trajectories of the dynamics converge to the optimal values $y^\star$ of the quadratic optimization problem with box constraints (5.26) from any initial conditions.

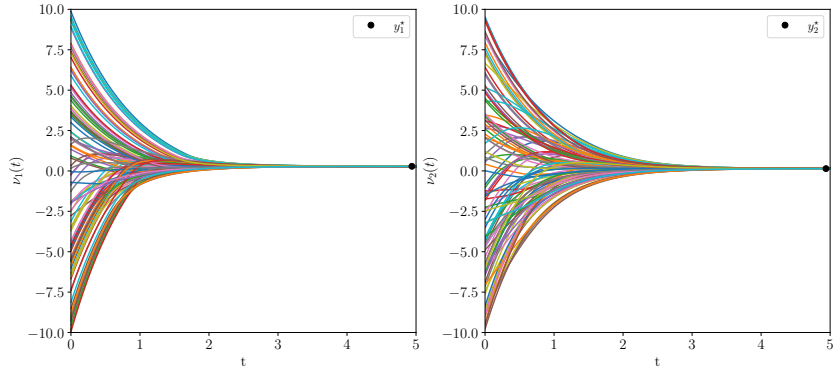

Figure 5.3: Trajectories of the FNN dynamics (5.27) solving the quadratic optimization problem with box constraints (5.26). The left panel shows the evolution of the variables $\nu_1(t)$ from 100 randomly chosen initial conditions as solid curves and the optimal values $y_1^\star$ as dot. The right panel shows the evolution of the variables $\nu_2(t)$ from 100 randomly chosen initial conditions as solid curves and the optimal values $y_2^\star$ as dot.

5.6 Summary

In this chapter, we provided sharp conditions for strong and weak Euclidean contractivity of HNNs and FNNs with symmetric weights and potentially non-smooth activation functions, together with a number of general algebraic results of independent interest.

We began our analysis by extending the concept of logarithmic optimal norm for a matrix to matrix polytopes in Definition 5.1. Building on this, in Theorem 5.4, we gave algebraic results on the Euclidean log-norm of matrix polytopes which includes the Jacobian of HNNs and FNNs. With these results, which are fundamental for the contractivity analysis, we proposed norms that are log-optimal for almost all matrices. Next, leveraging these algebraic results, we analyzed the contractivity of FNNs and HNNs. This was built upon Theorems 5.5 and 5.8, where upper bounds on the ℓ_2 one-sided Lipschitz constant of the FNN and of the HNN (with non-singular symmetric weights) are given. We then analyzed the contractivity of HNNs with non-singular symmetric synaptic matrix separately, as this scenario required a distinct mathematical approach. For each case, we provided a complete contractivity analysis, specifying the norms with respect to which the models are contracting, as well as lower bounds on the contraction rates. Notably, we considered networks with (possibly) non-smooth activation functions, enabling the use of common activation functions such as ReLU and soft thresholding functions. These results are instrumental for the analysis in the following chapter, where, by studying biologically plausible RNNs for solving convex optimization problems like sparse representation, we will run into FNNs with locally Lipschitz activation function.

Finally, to demonstrate the application-oriented implications of our contractivity results, we proposed an FNN to solve quadratic optimization problems with box constraints. This example opens the door to the use of contracting FNNs for solving convex optimization problems, which is the focus of the next chapters of this Part I and of Part III.

6 From Optimization Problems to Biologically Plausible Neural Networks: Modeling

In this chapter, we propose a top-down normative framework for a biologically plausible explanation of neural circuits solving sparse reconstruction and other optimization problems. To do so, we leverage tools from monotone operator theory [48, 50] and, specifically, the recently studied *proximal gradient dynamics* [52, 53]. This general theory explains how to transcribe a composite optimization problem into a continuous-time firing rate neural network, which is therefore interpretable.

The results in this chapter appeared in:

- **V. Centorrino**, A. Gokhale, A. Davydov, G. Russo, and F. Bullo. "Positive Competitive Networks for Sparse Reconstruction". *Neural Computation*, May, 36 (6): 1163–1197, 2024. doi: 10.1162/neco_a_01657.

Additionally, part of these results were presented at:

- **V. Centorrino**, A. Gokhale, A. Davydov, G. Russo, and F. Bullo. "Contractivity of Symmetric Neural Networks for Non-negative Sparse Approximation". *CCS/Italy23 Conference*, Naples, October 9-11, 2023. Website: https://italy.cssociety.org/index.php/2023/05/23/ccs-italy-conference-2023/,
- Workshop "Mathematics for Artificial Intelligence and Machine Learning". "Biologically Plausible Neural Networks for Sparse Reconstruction: a Normative Framework", Oral Talk, Milan, January 17-19, 2024. https://dec.unibocconi.eu/mathematics-artificial-intelligence-and-machine-learning.

6.1 Introduction

Sparse reconstruction or sparse approximation problems are ubiquitous in a wide range of domains, including neuroscience, signal processing, compressed sensing, and machine learning [137, 138, 139, 140]. These problems involve approximating a given input stimulus from a dictionary, using a set of sparse (active) units/neurons. Over the past years, an increasing body of theoretical and experimental evidence [116, 117, 118, 141, 3, 119] has supported the use of sparse representations in neural systems. Formally, sparse reconstruction problems can be formulated as a composite minimization problem[1], specifically, a least squares optimization problem regularized with a sparsity-inducing penalty function. Among the methods for solving optimization problems, we focus on the use of continuous-time recurrent neural networks.

In this context, we propose (and characterize the behavior of) a novel family of continuous-time firing rate neural networks that we show tackle sparse reconstruction problems. Given their biological relevance, we are particularly interested in sparse reconstruction problems with non-negativity constraints, and, to solve these problems, we propose the *positive firing rate competitive network*. This is an FNN whose state variables have the desirable, biologically plausible property of remaining non-negative.

The chapter is organized as follows. In Section 6.2, we provide an overview of the sparse reconstruction problems. Then, in Section 6.3, we propose the firing rate competitive networks to solve the sparse reconstruction problems and present its specific formulation for the ℓ_1 sparsity-inducing cost function with and without non-negative constraint. Our primary focus is on the latter due to its biological plausibility. Finally, in Section 6.4 we demonstrate the equivalence between the equilibria of the firing rate competitive networks and the optimal solutions of the sparse reconstruction problems.

6.1.1 Contributions

In this chapter, we present a top/down normative framework to translate composite optimization problems into continuous-time firing rate neural networks. This framework is based upon the theory of proximal operators for composite optimization and leads to continuous-time FNNs that are therefore interpretable. Starting from the sparse representation problem, a task that has both theoretical and empirical evidence supporting its use in the human brain, we propose a normative approach for designing biologically plausible neural networks, such as FNNs. Specifically, we introduce a family of continuous-time FNNs, called *firing rate competitive networks*, to address sparse reconstruction problems. Within this framework, we provide explicit formulations for two common cases: the sparse reconstruction problem with the ℓ_1-norm regularization and its variant with non-negative constraints, the positive sparse reconstruction problem.

Motivated by the fact that biological neurons produce non-negative outputs, we are specifically interested in the dynamics solving the positive sparse reconstruction problem.

[1] A composite minimization problem refers to an optimization task that involves minimizing a function composed of the sum of a differentiable and a non-differentiable component, typically combining a smooth loss function with a non-smooth regularization term.

We call this dynamics the *positive firing rate competitive network*. A significant property of this network, as we demonstrate, is its nature as a positive system: starting from non-negative initial conditions, its state variables remain non-negative.

Finally, we formally demonstrate the equivalence between the equilibria of the proposed networks and the optimal solutions of the sparse reconstruction problems.

6.2 The Sparse Reconstruction Problems

Given a m-dimensional input $u \in \mathbb{R}^m$ (e.g., a m-pixel image), the *sparse reconstruction* problem consists in reconstructing u with a linear combination of a sparse vector $y \in \mathbb{R}^n$ and a *dictionary* $D \in \mathbb{R}^{m \times n}$ composed of n (unit-norm) vectors $D_i \in \mathbb{R}^m$ (see Figure 6.1.b). Following [3], *sparse reconstruction problems* can be formulated as the following composite minimization problem

$$\min_{y \in \mathbb{R}^n} \Big(E(y) := \frac{1}{2} \big\| u - Dy \big\|_2^2 + \lambda S(y) \Big), \tag{6.1}$$

where $\lambda \geq 0$ is a scalar parameter that controls the trade-off between accurate reconstruction error (the first term) and sparsity (the second term). Indeed, in (6.1) $S \colon \mathbb{R}^n \to \mathbb{R}$ is a non-linear cost function that induces sparsity. We make use of the following standard assumption on the sparsity-inducing cost function S.

Assumption 6.1 (Sparsity-inducing cost function)**.** *The function S is convex, closed, proper, and separable across the indices, i.e., $S(y) = \sum_{i=1}^n s(y_i)$, for all $y \in \mathbb{R}^n$, where $s \colon \mathbb{R} \to \mathbb{R}$ is a convex, closed, and proper scalar function.*

Using the definitions of the Euclidean norm we can write the cost function in (6.1) as

$$E(y) = \frac{1}{2}(u^\top u - 2u^\top Dy + y^\top D^\top Dy) + \lambda S(y).$$

The matrix $D^\top D \in \mathbb{R}^{n \times n}$ is known as *Gramian matrix* of D.

Remark 6.1. *When S is convex and $\operatorname{rank}(D) = n$, the objective function $E(y)$ is strongly convex, therefore (6.1) admits a unique solution. While, when $\operatorname{rank}(D) < n$, $E(y)$ is not strongly convex, leading to possibly multiple solutions.* □

Sparse reconstruction problems focus on the underdetermined case, i.e., when $n \gg m$ (Note that, when $n > m$ we have $\operatorname{rank}(D) < n$).

A common choice of the sparsity inducing cost function S is the ℓ_1 norm, resulting in the following formulation of (6.1), known as *basis pursuit denoising* or *LASSO*:

$$\min_{y \in \mathbb{R}^n} \Big(E_{\mathrm{L}}(y) := \frac{1}{2} \big\| u - Dy \big\|_2^2 + \lambda \|y\|_1 \Big). \tag{6.2}$$

For problem (6.2), accurate reconstruction of u is possible under the condition that u is sparse enough and the dictionary satisfies the following:

Definition 6.1 (k-sparse vector)**.** *Let $k < n$ be natural numbers. A vector $x \in \mathbb{R}^n$ is* k-sparse *if it has at most k non-zero entries.*

Definition 6.2 (RIP condition [142])**.** *Let $k < n$ be natural numbers. A matrix $D \in \mathbb{R}^{n\times m}$ satisfies the* restricted isometry property (RIP) *of order k if there exist a constant $\delta \in [0, 1)$, such that for all k-sparse $x \in \mathbb{R}^n$ we have*

$$(1-\delta)\|x\|_2^2 \leq \|Dx\|_2^2 \leq (1+\delta)\|x\|_2^2. \tag{6.3}$$

The order-k restricted isometry constant δ_k *is the smallest δ such that (6.3) holds.*

We are particularly interested in the minimization problem (6.2) with non-negative constraints, which we term *positive sparse reconstruction problem*. The goal of this constrained minimization problem is to reconstruct an input u using a linear combination of a non-negative and sparse vector $y \in \mathbb{R}^n_{\geq 0}$ and a unit-norm *dictionary* $D \in \mathbb{R}^{m\times n}$. Formally, the positive sparse reconstruction problem can be stated as follows:

$$\begin{aligned} &\min_{y\in\mathbb{R}^n} \frac{1}{2}\big\|u - Dy\big\|_2^2 + \lambda\|y\|_1, \\ &\text{s.t. } y \in \mathbb{R}^n_{\geq 0}. \end{aligned} \tag{6.4}$$

The minimization problem (6.4) can equivalently be written as the unconstrained optimization problem

$$\min_{y\in\mathbb{R}^n} \frac{1}{2}\big\|u - Dy\big\|_2^2 + \lambda\|y\|_1 + \iota_{\mathbb{R}^n_{\geq 0}}(y). \tag{6.5}$$

We note that problem (6.5) can be formally written as problem (6.1) when the sparsity inducing cost in (6.1) is

$$S_1(y) := \|y\|_1 + \frac{1}{\lambda}\iota_{\mathbb{R}^n_{\geq 0}}(y) = \sum_{i=1}^{n}\big(y_i + \frac{1}{\lambda}\iota_{\mathbb{R}_{\geq 0}}(y_i)\big),$$

where we used the fact that y must belong to $\mathbb{R}^n_{\geq 0}$. Also, for our derivations, it is useful to introduce the scalar function $s_1(y_i) := y_i + \frac{1}{\lambda}\iota_{\mathbb{R}_{\geq 0}}(y_i)$.

6.3 Firing Rate Neural Networks for Solving Sparse Reconstruction Problems

The sparse reconstruction problems introduced in Section 6.2 naturally arise in the context of visual information processing. For example, as illustrated in Figure 6.1.a for mammalians, the visual sensory input data $u \in \mathbb{R}^m$ is encoded by the receptive fields of simple cells in V1 using only a small fraction of active (sparse) neurons. Formally (see Figure 6.1.b), the input signal u is reconstructed through a linear combination of an overcomplete matrix $D \in \mathbb{R}^{m\times n}$ and a sparse vector $y \in \mathbb{R}^n$. The FCN and PFCN introduced in this thesis to tackle the sparse reconstruction and positive sparse reconstruction problems are schematically illustrated in Figure 6.1.c. Namely, each

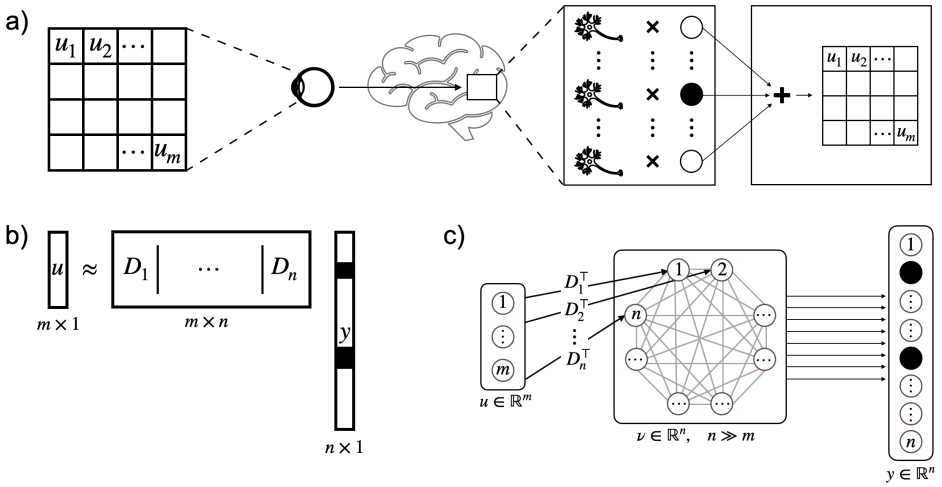

Figure 6.1: The visual sensory input data $u \in \mathbb{R}^m$ is encoded by the receptive fields of simple cells in the mammalian visual cortex (V1) using only a small fraction of active (sparse) neurons. Formally, b) the input u is reconstructed by a linear combination of an overcomplete ($n \gg m$) set of features $D_i \in \mathbb{R}^n$ and sparse neurons $y \in \mathbb{R}^n$. c) Block scheme of the proposed (positive) firing rate competitive network. The hidden node ν_i receives as stimulus the similarity score between the input signal $u \in \mathbb{R}^m$ and the dictionary element $D_i \in \mathbb{R}^n$ and collectively all hidden neurons give as output a sparse (non-negative) vector $y = \nu \in \mathbb{R}^n$.

hidden node, or neuron in what follows, ν_i receives as stimulus the similarity score between the input signal $u \in \mathbb{R}^m$ and the dictionary element $D_i \in \mathbb{R}^n$ and, collectively, all the hidden neurons give as output a sparse (non-negative) vector $y = \nu \in \mathbb{R}^n$.

To transcribe the sparse reconstruction problem in (6.1) into an interpretable continuous-time firing rate neural network, we leverage the theory of *proximal operators* (see Section 2.7 for a self-contained primer on proximal operators). We start by noticing that the sparse reconstruction problem (6.1) is a special instance of the composite minimization problem of the form (2.11) with $f(x) := \frac{1}{2}\|u - Dy\|_2^2$ and $g(x) := \lambda S(y)$. Therefore, to tackle problem (6.1) we introduce the following special instance of proximal gradient dynamics, that we denote the *firing rate competitive network* (FCN):

$$\dot{\nu}(t) = -\nu(t) + \mathrm{prox}_{\lambda S}\big((I_n - D^\top D)\nu(t) + D^\top u(t)\big), \tag{6.6}$$

with output $y(t) = \nu(t)$. This dynamics is schematically illustrated in Figure 6.1.c. In (6.6), the term $D^\top u(t)$ is the input to the FCN and it captures the similarity between the input signal and the dictionary elements, while the term $\big(I_n - D^\top D\big)\nu(t)$ models the recurrent interactions between the neurons. These interactions implement competition between nodes to represent the stimulus. Additionally, we note that in (6.6) the particular form of the activation function is linked to the sparsity-inducing term in (6.1), λS, via the proximal operator. To be precise, the activation function is the proximal operator of

λS computed at the point $\nu - \nabla\big(\frac{1}{2}\|u - D\nu\|_2^2\big) = \nu - D^\top D\nu + D^\top u$.

The dynamics given in (6.6) are quite general, as they encompass a broad class of sparse reconstruction problems. Next, we provide specific formulas for how these dynamics read in two common problems: the ℓ_1 sparse reconstruction problem in (6.2) and the positive sparse reconstruction problem in (6.5).

6.3.1 LASSO Problem

For the LASSO problem (6.2), the sparsity-inducing cost function is $S(\nu) = \|\nu\|_1$. This function is convex, separable and $s(\nu_i) = |\nu_i|$, for all $\nu_i \in \mathbb{R}$, thus satisfying Assumption 6.1. Moreover, it is well known (see, e.g., [50]) that for any $\nu \in \mathbb{R}^n$, the proximal operator of $\lambda\|\nu\|_1$ is $\mathrm{prox}_{\lambda\|\nu\|_1} = \mathrm{soft}_\lambda\big(\nu\big)$. We illustrate the activation function soft_λ in Figure 6.2 for a given value of the parameter λ. Now and throughout the rest of the chapter, we adopt a slight abuse of notation by using the same symbol to represent both the scalar and vector form of the activation function. The corresponding FCN (6.6) for the LASSO problem (6.2) is therefore:

$$\dot{\nu}(t) = -\nu(t) + \mathrm{soft}_\lambda\big((I_n - D^\top D)\nu(t) + D^\top u(t)\big). \tag{6.7}$$

Remarkably, the dynamics (6.7) is the firing rate version of the LCA designed for tackling the LASSO problem (6.2), which is a continuous-time Hopfield-like neural network of the form [64]:

$$\dot{\nu}(t) = -\nu(t) + \big(I_n - D^\top D\big)\mathrm{soft}_\lambda(\nu(t)) + D^\top u(t), \tag{6.8}$$

with output $y(t) = \mathrm{soft}_\lambda(\nu(t))$.

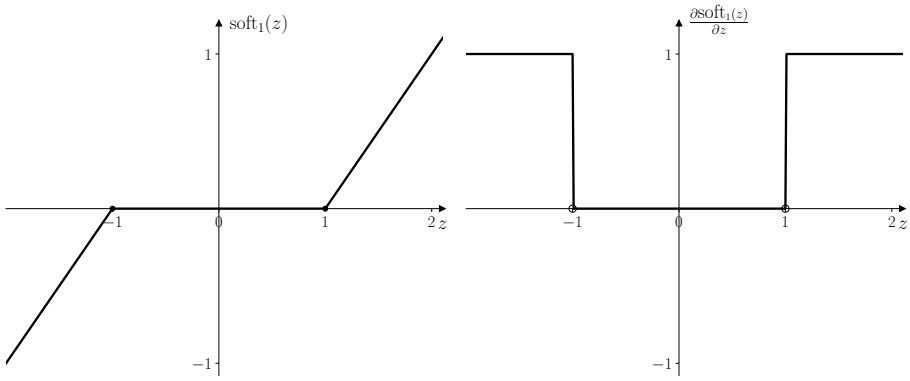

Figure 6.2: Soft thresholding function $\mathrm{soft}_\lambda(\cdot)$ with $\lambda = 1$ (left panel) and its derivative (right panel). As shown, the soft thresholding function is slope restricted in $[0, 1]$.

6.3.2 Positive Sparse Reconstruction Problem

Next, we define the FCN that solves the positive sparse reconstruction problem (6.5). For this purpose, we need to determine the proximal operator of the sparsity-inducing term $\lambda S_1(\nu) = \sum_{i=1}^n \big(\lambda \nu_i + \iota_{\mathbb{R}_{\geq 0}}(\nu_i)\big)$. The next result shows that this operator is the *(shifted) ReLU function*.

Lemma 6.1 (Proximal operator of λS in the positive sparse reconstruction problem)**.** *Consider $\lambda > 0$ and a function $S_1 \colon \mathbb{R}^n \to \mathbb{R}$ defined by $S_1(y) = \|y\|_1 + \frac{1}{\lambda}\iota_{\mathbb{R}^n_{\geq 0}}(y)$, $\forall y \in \mathbb{R}^n$. Then*

$$\operatorname{prox}_{\lambda S_1}(y) = \operatorname{ReLU}(y - \lambda \mathbb{1}_n).$$

Proof. We start by noticing that λS_1 is separable across indices and, for any $y_i \in \mathbb{R}$, we have $\lambda s_1(y_i) = \lambda y_i + \iota_{\mathbb{R}_{\geq 0}}(y_i)$. Hence, Lemma 2.7 implies that the computation of the proximal operator of λS_1 reduces to computing scalar proximals of $\lambda s_1(y_i)$. This can be done as follows:

$$\begin{aligned}\operatorname{prox}_{\lambda s_1}(y_i) &= \operatorname*{arg\,min}_{z \in \mathbb{R}} \frac{1}{2}(y_i - z)^2 + \lambda z + \iota_{\mathbb{R}_{\geq 0}}(z) \\ &= \begin{cases} 0 & \text{if } y_i \leq \lambda \\ y_i - \lambda & \text{if } y_i > \lambda \end{cases} := \operatorname{ReLU}(y_i - \lambda).\end{aligned}$$

This proves the statement. □

Lemma 6.1 implies that the FCN (6.6) that solves the positive sparse reconstruction problem (6.5) is

$$\dot{\nu}(t) = -\nu(t) + \operatorname{ReLU}\left((I_n - D^\top D)\nu(t) + D^\top u(t) - \lambda \mathbb{1}_n\right) := f_{\text{PFCN}}(\nu), \qquad (6.9)$$

with output $y(t) = \nu(t)$. We illustrate the activation function $\operatorname{ReLU}_\lambda$ in Figure 6.3 for a given value of the parameter λ. We call the dynamics (6.9) *positive firing rate competitive network* (PFCN). In the next lemma we show a key property of the PFCN, that it is the fact that this is a *positive system*, i.e., given a non-negative initial state, the state variables are always non-negative. In order words, the positive orthant $\mathbb{R}^n_{\geq 0}$ is forward invariant.

Lemma 6.2 (On the positiveness of the PFCN)**.** *The PFCN (6.9) is a positive system.*

Proof. To prove the statement we use Nagumo's Theorem 4.2 to prove that the positive orthant $\mathbb{R}^n_{\geq 0}$ is forward invariant for f_{PFCN}. To this purpose, let us consider the PFCN written in components

$$\dot{\nu}_i = -\nu_i + \operatorname{ReLU}\left(-\sum_{j=1, j\neq i}^n D_i^\top D_j \nu_j(t) + D_i^\top u(t) - \lambda\right) = f_{\text{PFCN,i}}(\nu), \quad i \in \{1, \dots, n\}.$$

Then, for all $\nu \in \mathbb{R}^n_{\geq 0}$ such that $\nu_i = 0$ we have

$$f_{\text{PFCN,i}}(\nu) = \operatorname{ReLU}\left(-\sum_{j=1, j\neq i}^n D_i^\top D_j \nu_j(t) + D_i^\top u(t) - \lambda\right) \geq 0,$$

for each i. This concludes the proof. □

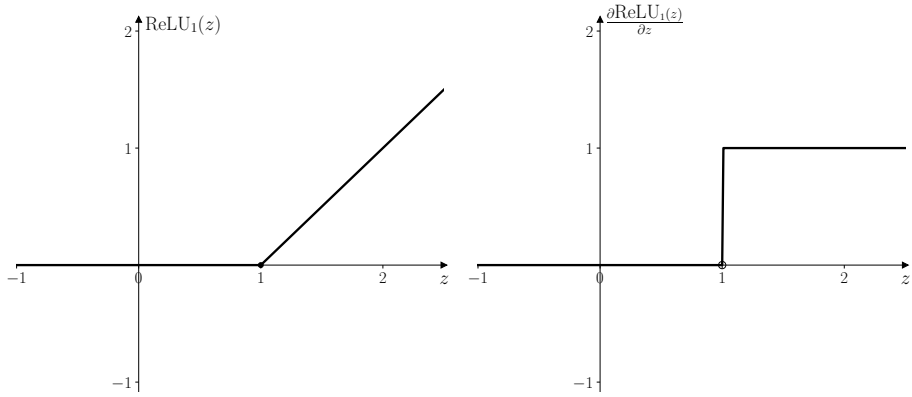

Figure 6.3: Shifted ReLU function, $\text{ReLU}_\lambda(\cdot)$, with $\lambda = 1$ (left panel) and its derivative (right panel). As shown, the ReLU function is slope restricted in $[0, 1]$.

To the best of our knowledge, the PFCN is the first continuos-time RNN designed to tackle the positive sparse reconstruction problem. The positiveness of the PFCN is a desirable property that can be useful to effectively model both excitatory and inhibitory synaptic connections. In fact, in the PFCN the nature of excitatory and inhibitory recurrent interactions, described by the term $-\sum_{j\neq i, j=1}^{n} D_i^\top D_j \nu_j$, only depends on the sign of the weights. Specifically, the recurrent interaction between two nodes, say them i and j, is inhibitory if $-\sum_{j\neq i, j=1}^{n} D_i^\top D_j < 0$, and excitatory if $-\sum_{j\neq i, j=1}^{n} D_i^\top D_j > 0$.

Finally, for later use, we note that the Jacobian of f_{PFCN} exists almost everywhere by Rademacher's theorem, and now and throughout the rest of the thesis we denote by $\Omega_f \subset \mathbb{R}^n$ the measure zero set of points where the function f_{PFCN} is not differentiable.

6.4 Relating the FCN and PFCN with Sparse Reconstruction Problems

We conclude the chapter by demonstrating that the firing rate competitive networks effectively solve the sparse reconstruction problems. Specifically, we establish that a given vector is the optimal solution to the problem (6.1) if and only if it is also an equilibrium of the FCN (6.6)

Lemma 6.3 (Linking the optimal solutions of the sparse reconstruction problem and the equilibria of the FCN)**.** *The vector $x^* \in \mathbb{R}^n$ is an optimal solution of the sparse reconstruction problem* (6.1) *if and only if it is an equilibrium point of the FCN* (6.6)*.*

Proof. The necessary and sufficient condition for $x^\star \in \mathbb{R}^n$ to be a solution of problem (6.1) is

$$\mathbb{0}_n \in \partial E(x^\star) = D^\top D x^\star - D^\top u + \lambda \partial S(x^\star) := \mathsf{G}(x^\star) + \lambda \partial S(x^\star),$$

where we have introduced the function $\mathsf{G} : \mathbb{R}^n \to \mathbb{R}^n$ defined as $\mathsf{G}(x) = D^\top Dx - D^\top u$. Note that G is a linear function of x, thus it is Lipschitz, and $\mathsf{G}(x) = \nabla\big(\frac{1}{2}\|u - Dx\|_2^2\big)$. That is, G is the gradient (with respect to x) of a convex function, and thus it is monotone. Moreover, by Assumption 6.1, the function S is convex, closed, and proper, and therefore, so it is λS. Then, by applying the result in [53, Proposition 4] (picking $\gamma = 1$, $\mathsf{F} = \mathsf{G}$, and $g = \lambda S$ in such proposition), we have that $\mathbb{0}_n \in \big(\mathsf{G} + \partial\lambda S\big)(x^\star)$ if and only if $x^\star$ is an equilibrium of $\dot{x} = -x + \operatorname{prox}_{\lambda S}\big(x - \mathsf{G}(x)\big) = -x + \operatorname{prox}_{\lambda S}\big((I_n - D^\top D)x + D^\top u\big)$. This concludes the proof. □

The next result relates the optimal solutions of (6.5) with the equilibria of the PFCN (6.9).

Corollary 6.4 (Linking the optimal solutions of the positive sparse reconstruction problem and the equilibria of the PFCN)**.** *The vector $x^* \in \mathbb{R}^n$ is an optimal solution of the positive sparse reconstruction problem* (6.5) *if and only if it is an equilibrium point of the PFCN* (6.9).

Proof. The proof, which follows the arguments used to prove Lemma 6.3, is omitted for brevity. □

6.5 Summary

In this chapter, we addressed several key research questions posed in Section 1.2. Specifically, we understood that one of the functional implications of the FNN in equation 3.2 is dimensionality reduction, being sparse representation a mechanism believed to occur in V1, and demonstrate how it can be modeled by continuous-time FNNs. To this end, we proposed a top-down normative framework that translates composite optimization problems into interpretable continuous-time firing rate neural networks. First, we considered the sparse reconstruction problem in equation (6.1) and transcribed this optimization problem into a continuous-time firing rate neural network. This framework is based upon the theory of proximal operators for composite optimization and leads to FNNs that are therefore interpretable. The key idea behind our analysis relies on the fact that the sparse reconstruction problem (6.1) is a special instance of a composite minimization problem that is the sum of a smooth loss term, which captures the reconstruction error, and a non-smooth regularization term, $S(\cdot)$, which promotes sparsity. As we demonstrated, the resulting FNN is therefore dependent on the specific form of the function $S(\cdot)$. We gave specific formulas for two common cases: the sparse reconstruction problem with the ℓ_1-norm regularization, leading to the soft-thresholding activation function, and its variant with non-negative constraints, resulting in the ReLU activation. The positive sparse reconstruction problem is particularly relevant, as it aligns with the non-negative output characteristics of biological neurons. We called to the resulting dynamics *positive firing rate competitive network* (PFCN). Crucial for the PFCN is the fact that this is a positive system (see Lemma 6.2). This, in turn, can be useful to effectively model both excitatory and inhibitory synaptic connections in a biologically plausible way. To the

best of our knowledge, the PFCN is the first RNN designed to tackle the positive sparse reconstruction problem.

Finally, we established (Lemma 6.3 and Corollary 6.4) the equivalence between the optimal solutions of the sparse reconstruction and positive sparse reconstruction problems to the equilibria of the FCN and PFCN, respectively. In the next chapter, we complete this analysis by identifying conditions that guarantee stable convergence of the FCN (and the PFCN) to their equilibria, which corresponds to the optimal solutions of the sparse reconstruction (and positive sparse reconstruction) problems.

7 From Optimization Problems to Biologically Plausible Neural Networks: Analysis

Chapter 6 laid the groundwork for a biologically plausible framework for neural circuits solving sparse reconstruction problems, focusing on the modeling of these dynamics through continuous-time firing rate neural networks. Specifically, we introduced the *firing rate competitive network* and the *positive firing rate competitive network*, which are designed to solve sparse reconstruction problems, including those with non-negativity constraints. In this chapter, we advance this framework by providing a comprehensive analysis of these networks, focusing on their convergence properties and stability.

The results in this chapter appeared in the same paper and were presented at the same conferences as those in Chapter 6.

7.1 Introduction

In the previous chapter, we introduced biologically plausible neural networks solving optimization problems and established the equivalence between the equilibria of the proposed FNN models and the solutions of sparse reconstruction problems (see Section 6.4). This foundational result demonstrated that the steady states of both the FCN and PFCN correspond to the minimizers of their respective optimization problems, and vice versa. The next crucial step in our analysis is to understand and characterize the convergence behavior of these networks. This step is essential not only to confirm that the networks will eventually converge to solutions to the optimization problems but also to provide insights into the stability and rate of convergence of the dynamics.

As a consequence, building upon the theoretical foundation established in the previous chapter, we now present a detailed analysis of the dynamic behavior and convergence properties of the proposed networks. Specifically, we aim to rigorously establish the conditions under which these networks converge to their respective equilibria.

The chapter is organized as follows. In Section 7.3, we begin by analyzing the convergence behavior of globally-weakly and locally-strongly contracting systems, showing

that this is linear-exponential. We also provide an algebraic result of the ℓ_2 log-norm of upper triangular block matrices. In Section 7.4 we analyze the convergence behavior of the FCN. Specifically, we first prove that the PFCN is weakly infinitesimally contracting in the entire state space. Then, under a standard assumption on the dictionary, we show that the PFCN is locally-strongly contracting and apply the results in Section 7.3 to show that the PFCN converges linear-exponentially to the equilibrium. Finally, in Section 7.5, we illustrate the effectiveness of our approach via a numerical example.

7.1.1 Contributions

In the previous chapter, we presented a normative way for designing biologically plausible neural networks that solve sparse reconstruction problems. These networks are the firing rate competitive network and, for the specific case with non-negative constraints, the positive firing rate competitive network. In this chapter, we complete the analysis by giving conditions that guarantee stable convergence of our proposed dynamics to their equilibria, which correspond to the minimizers of the original optimization problems.

Our analysis for the FCN and PFCN dynamics naturally leads to the study of the convergence behavior of *globally-weakly and locally-strongly contracting systems*. These are dynamics that are weakly infinitesimally contracting on $\mathbb{R}^n$ and strongly infinitesimally contracting on a subset of $\mathbb{R}^n$. For this class of dynamics, we show that convergence is *linear-exponential*, in the sense that (in a suitably defined norm) the trajectory's distance from the equilibrium is initially upper bounded by a linear function, and then convergence becomes exponential. An immediate and key implication of this result is that convergence towards the equilibrium is *global*. We also provide a useful technical result on the Euclidean logarithm norm of upper triangular block matrices.

Building upon these results, we analyze the convergence behavior of the FCN and PFCN. Specifically, after characterizing the local stability and contractivity of these dynamics, with our main convergence result we prove that, under a standard assumption on the dictionary, the FCN and PFCN converge linear-exponentially to the equilibrium. We also give explicit expressions for the average linear decay rate and the time at which exponential convergence begins. Finally, we illustrate the effectiveness of our results via numerical experiments. The code to replicate our numerical examples is available at `https://tinyurl.com/PFCN-for-Sparse-Reconstruction`.

7.2 Set-up

Given their central role in this chapter, we begin by reviewing the dynamics of the firing rate competitive network and its positive variant introduced in the previous chapter.

For a m-dimensional input $u \in \mathbb{R}^m$ (e.g., a m-pixel image), a *dictionary* $D \in \mathbb{R}^{m\times n}$ composed of n (unit-norm) vectors $D_i \in \mathbb{R}^m$, consider the *sparse reconstruction problems*

$$\min_{y\in\mathbb{R}^n}\Big(E(y) := \frac{1}{2}\big\|u - Dy\big\|_2^2 + \lambda S(y)\Big), \tag{7.1}$$

where $\lambda \geq 0$ is a scalar parameter that controls the trade-off between accurate reconstruction error and sparsity, and $S\colon \mathbb{R}^n \to \mathbb{R}$ is a non-linear cost function that induces sparsity. We assume that the sparsity-inducing cost function S satisfies Assumption 6.1.

To tackle problem (7.1), we introduced in Chapter 6 the following biologically plausible neural network, the FCN:

$$\dot{\nu}(t) = -\nu(t) + \operatorname{prox}_{\lambda S}\big((I_n - D^\top D)\nu(t) + D^\top u(t)\big), \tag{7.2}$$

with output $y(t) = \nu(t)$.

While the dynamics in (7.2) are quite general, as they encompass a broad class of sparse reconstruction problems, we also provided specific formulas for two common problems: the ℓ_1 sparse reconstruction problem and its non-negative variant. Specifically, when S is the ℓ_1 norm, problem (7.1) is known as *basis pursuit denoising* or *LASSO*:

$$\min_{y\in\mathbb{R}^n}\Big(E_{\mathrm{L}}(y) := \frac{1}{2}\big\|u - Dy\big\|_2^2 + \lambda\|y\|_1\Big). \tag{7.3}$$

The corresponding FCN (7.2) is

$$\dot{\nu}(t) = -\nu(t) + \operatorname{soft}_\lambda\big((I_n - D^\top D)\nu(t) + D^\top u(t)\big). \tag{7.4}$$

For biological plausibility, we are particularly the non-negative variant of the above optimization problem, the positive sparse reconstruction problem, that can be written as the following unconstrained optimization problem

$$\min_{y\in\mathbb{R}^n} \frac{1}{2}\big\|u - Dy\big\|_2^2 + \lambda\|y\|_1 + \iota_{\mathbb{R}^n_{\geq 0}}(y). \tag{7.5}$$

The corresponding FCN (7.2), termed as positive firing rate competitive network, is:

$$\dot{\nu}(t) = -\nu(t) + \operatorname{ReLU}\big((I_n - D^\top D)\nu(t) + D^\top u(t) - \lambda\mathbb{1}_n\big) := f_{\mathrm{PFCN}}(\nu), \tag{7.6}$$

with output $y(t) = \nu(t)$. A key property of the PFCN is the fact that this is a positive system (see Lemma 6.2).

7.3 Methods

In this section, we present a convergence result for a class of dynamical systems, from which the convergence of the firing rate competitive networks introduced in Chapter 6 follows. Specifically, we consider nonlinear systems of the form (4.1) that are globally-weakly contracting and locally-strongly contracting (possibly, in different norms). Through our analysis, we characterize their convergence behavior, showing that this is linear-exponential, in the sense that the trajectory's distance from the equilibrium is initially upper bounded by a linear function, and then convergence becomes exponential. This analysis will be formalized, sharpened, and extended in Chapter 12, as this class of systems is of significant interest due to their occurrence in various scenarios.

We begin our analysis by giving a general algebraic result on the inclusion relationship between balls computed with respect to different norms.

Lemma 7.1 (Inclusion between balls computed with respect to different norms)**.** *Given two norms $\|\cdot\|_\alpha$ and $\|\cdot\|_\beta$ on $\mathbb{R}^n$ and a point $x^\star \in \mathbb{R}^n$, for all $r > 0$, it holds that*

$$B_\beta\big(x^\star, r/k_\alpha^\beta\big) \subseteq B_\alpha\big(x^\star, r\big) \subseteq B_\beta\big(x^\star, rk_\beta^\alpha\big), \tag{7.7}$$

where k_α^β and k_β^α are the minimal equivalence coefficients given in (2.1).

Proof. We start by proving the inequality $B_\alpha\big(x^\star, r\big) \subseteq B_\beta\big(x^\star, rk_\beta^\alpha\big)$. By definition of ball of radius r, for any $x \in B_\alpha\big(x^\star, r\big)$, we know that $\|x - x^\star\|_\alpha \leq r$. Also, we have

$$\frac{1}{k_\beta^\alpha}\|x - x^\star\|_\beta \leq \frac{1}{k_\beta^\alpha}k_\beta^\alpha\|x - x^\star\|_\alpha \leq \|x - x^\star\|_\alpha \leq r.$$

Therefore $\|x - x^\star\|_\beta \leq rk_\beta^\alpha$, so that $x \in B_\beta\big(x^\star, rk_\beta^\alpha\big)$.

The inequality $B_\beta\big(x^\star, r/k_\alpha^\beta\big) \subseteq B_\alpha\big(x^\star, r\big)$ follows directly from the above inequality and from the fact that $k_\alpha^\beta k_\beta^\alpha \geq 1$. Specifically, we have:

$$\|x - x^\star\|_\alpha \leq k_\alpha^\beta\|x - x^\star\|_\beta \leq k_\alpha^\beta rk_\beta^\alpha \leq r.$$

□

We are now ready to state the main result of this section, which characterizes the convergence of globally-weakly and locally-strongly contracting dynamics.

Theorem 7.2 (Finite decay in finite time of globally-weakly and locally-strongly contracting systems)**.** *Let $\|\cdot\|_{\mathrm{L}}$ and $\|\cdot\|_{\mathrm{G}}$ be two norms on $\mathbb{R}^n$. Consider a dynamical system (4.1) with $f\colon \mathbb{R}_{\geq 0} \times \mathbb{R}^n \to \mathbb{R}^n$ being a locally Lipschitz map satisfying the following assumptions*

- *(A1) f is weakly infinitesimally contracting on $\mathbb{R}^n$ with respect to $\|\cdot\|_{\mathrm{G}}$;*
- *(A2) f is c_{exp}-strongly infinitesimally contracting on a forward-invariant set $\mathcal{S}$ with respect to $\|\cdot\|_{\mathrm{L}}$;*
- *(A3) $x^\star \in \mathcal{S}$ is an equilibrium point, i.e., $f(t, x^\star) = \mathbb{0}_n$, for all $t \geq 0$.*

Also, let $B_{\mathrm{G}}\big(x^\star, r\big) \subset \mathcal{S}$ be the largest closed ball centered at $x^\star$ with radius $r > 0$ with respect to $\|\cdot\|_{\mathrm{G}}$. Then, for each trajectory $x(t)$ starting from $x(0) \notin \mathcal{S}$ and for any contraction factor $0 < \rho < 1$, the distance along the trajectory decreases at worst linearly with an average linear decay rate

$$c_{\mathrm{lin}} = \frac{(1-\rho)r}{t_\rho}, \tag{7.8}$$

up to at most the linear-exponential crossing time

$$t_{\mathrm{cross}} = \left\lceil \frac{\|x(0) - x^\star\|_{\mathrm{G}} - r}{(1-\rho)r} \right\rceil t_\rho, \tag{7.9}$$

when the trajectory enters $B_{\mathrm{G}}\big(x^\star, r\big)$.

Proof. Consider a trajectory $x(t)$ of the dynamical system in equation (4.1) starting from initial condition $x(0) \notin \mathcal{S}$ and define the *intermediate point* $x_{\text{tmp}} = x^\star + r\frac{x(0)-x^\star}{\|x(0)-x^\star\|_{\text{G}}}$, as in Figure 7.1. Note that x_{tmp} is a point on the boundary of $B_{\text{G}}(x^\star, r)$, since $\|x_{\text{tmp}} - x^\star\|_{\text{G}} = r$. Moreover, the points $x^\star$, x_{tmp}, and $x(0)$ lie on the same line segment, thus

$$\|x(0) - x^\star\|_{\text{G}} = \|x(0) - x_{\text{tmp}}\|_{\text{G}} + \|x_{\text{tmp}} - x^\star\|_{\text{G}}. \tag{7.10}$$

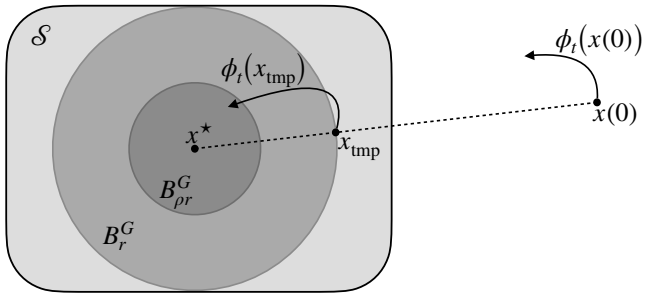

Figure 7.1: Illustration of the set up for the proof of Theorem 7.2 with $\|\cdot\|_{\text{G}} = \|\cdot\|_2$. Given the equilibrium point $x^\star \in \mathcal{S}$, with $\mathcal{S}$ forward invariant set, we consider a trajectory $\phi_t(x(0))$ of (4.1) starting from $x(0) \notin \mathcal{S}$ and define the *intermediate point* $x_{\text{tmp}} \in B_{\text{G}}(x^\star, r)$. After a time t_ρ the trajectory starting at x_{tmp} (which may exit $B_{\text{G}}(x^\star, r)$) must enter $B_{\text{G}}(x^\star, \rho r)$, for $0 < \rho < 1$. Image reused with permission from [42].

Using the triangle inequality, we get

$$\|\phi_t(x(0)) - x^\star\|_{\text{G}} \leq \|\phi_t(x(0)) - \phi_t(x_{\text{tmp}})\|_{\text{G}} + \|\phi_t(x_{\text{tmp}}) - x^\star\|_{\text{G}}.$$

By Assumption (A1) and equality (7.10), we know that $\|\phi_t(x(0)) - \phi_t(x_{\text{tmp}})\|_{\text{G}} \leq \|x(0) - x_{\text{tmp}}\|_{\text{G}} = \|x(0) - x^\star\|_{\text{G}} - r$, thus

$$\|\phi_t(x(0)) - x^\star\|_{\text{G}} \leq \|x(0) - x^\star\|_{\text{G}} - r + \|\phi_t(x_{\text{tmp}}) - x^\star\|_{\text{G}}.$$

Next, we upper bound the term $\|\phi_t(x_{\text{tmp}}) - x^\star\|_{\text{G}}$. We note that, because each trajectory originating in $B_{\text{G}}(x^\star, r)$ remains in $\mathcal{S}$, the time required for each trajectory starting in $B_{\text{G}}(x^\star, r)$, to be inside $B_{\text{G}}(x^\star, \rho r)$ for the c-strongly contracting map f is

$$t_\rho = \frac{\ln(k_{\text{L,G}}\rho^{-1})}{c_{\text{exp}}}.$$

This follows by noticing that

$$\begin{aligned} x(0) \in B_{\text{G}}(x^\star, r) &\overset{\text{(7.7), 2}^{\text{nd}}\text{ inequality}}{\Longrightarrow} x(0) \in B_{\text{L}}(x^\star, r k_{\text{L}}^{\text{G}}), \\ x(t_\rho) \in B_{\text{G}}(x^\star, \rho r) &\overset{\text{(7.7), 1}^{\text{st}}\text{ inequality}}{\Longleftarrow} x(t_\rho) \in B_{\text{L}}(x^\star, \rho r / k_{\text{G}}^{\text{L}}). \end{aligned}$$

Thus, the time required for a trajectory starting in $B_{\mathrm{G}}(x^\star, r)$ to be inside $B_{\mathrm{G}}(x^\star, \rho r)$ is upper bounded by the time required for the trajectory to go from $B_{\mathrm{L}}(x^\star, r k_{\mathrm{L}}^{\mathrm{G}})$ to $B_{\mathrm{L}}(x^\star, \rho r / k_{\mathrm{G}}^{\mathrm{L}})$. In these balls, Assumption (A2) implies $\|x(t) - x^\star\|_{\mathrm{L}} \leq \mathrm{e}^{-c_{\exp} t} \|x(0) - x^\star\|_{\mathrm{L}}$ and so t_ρ is determined by the equality $\mathrm{e}^{-c_{\exp} t_\rho} r k_{\mathrm{L}}^{\mathrm{G}} = \rho r / k_{\mathrm{G}}^{\mathrm{L}}$.

Therefore, at time t_ρ, we know $\phi_{t_\rho}(x_{\mathrm{tmp}}) \in B_{\mathrm{G}}(x^\star, \rho r)$ and we have

$$\|\phi_{t_\rho}(x(0)) - x^\star\|_{\mathrm{G}} \leq \|x(0) - x^\star\|_{\mathrm{G}} - r + \rho r = \|x(0) - x^\star\|_{\mathrm{G}} - (1-\rho) r.$$

By iterating the above argument, it follows that after each interval of duration t_ρ, the distance $\|x(t) - x^\star\|_{\mathrm{G}}$ has decreased by an amount $(1-\rho)r$ for each $x(t)$. Therefore the average linear decay satisfies

$$c_{\mathrm{lin}} := \frac{\text{variation in distance to } x^\star}{\text{variation in time}} = \frac{(1-\rho) r}{t_\rho} = c_{\exp} r \frac{1-\rho}{\ln(k_{\mathrm{L,G}} \rho^{-1})}. \tag{7.11}$$

Hence, after at most a linear-exponential crossing time $t_{\mathrm{cross}} := \left\lceil \frac{\|x(0) - x^\star\|_{\mathrm{G}} - r}{(1-\rho) r} \right\rceil t_\rho$, the trajectory will be inside $B_{\mathrm{G}}(x^\star, r) \subset \mathcal{S}$. This concludes the proof. □

Remark 7.1. *Assumptions (A2) and (A3) of Theorem 7.2 imply that for any $x(0) \in \mathcal{S}$, the distance $\|x(t) - x^\star\|_{\mathrm{L}}$ decreases exponentially with time with rate $c_{\exp}$. Specifically, for all $t \geq 0$ it holds that*

$$\|x(t) - x^\star\|_{\mathrm{L}} \leq \mathrm{e}^{-c_{\exp} t} \|x(0) - x^\star\|_{\mathrm{L}}. \tag{7.12}$$

□

The next result, which establishes the linear-exponential convergence of dynamical systems of the form system (4.1), follows from Theorem 7.2.

Corollary 7.3 (Linear-exponential decay of globally-weakly and locally-strongly contracting systems)**.** *Under the same assumptions and notations as in Theorem 7.2, for each $x(0) \notin \mathcal{S}$ and for any contraction factor $0 < \rho < 1$, the distance $\|x(t) - x^\star\|_{\mathrm{G}}$ decreases linear-exponentially with time, in the sense that:*

$$\|x(t) - x^\star\|_{\mathrm{G}} \leq \begin{cases} \|x(0) - x^\star\|_{\mathrm{G}} + (1-\rho) r - c_{\mathrm{lin}} t, & \text{if } t \leq t_{\mathrm{cross}}, \\ k_{\mathrm{L,G}}\, r\, \mathrm{e}^{-c_{\exp}(t - t_{\mathrm{cross}})} & \text{if } t > t_{\mathrm{cross}}. \end{cases} \tag{7.13}$$

Proof. The result follows directly from Theorem 7.2. Indeed, given a trajectory $x(t)$ of (4.1) starting from $x(0) \notin \mathcal{S}$, for all $t \leq t_{\mathrm{cross}}$, from Theorem 7.2 we know that the distance $\|x(t) - x^\star\|_{\mathrm{G}}$ decreases linearly by an amount $(1-\rho)r$ with an average linear decay rate $c_{\mathrm{lin}} = (1-\rho) r / t_\rho$ towards $B_{\mathrm{G}}(x^\star, r) \subset \mathcal{S}$, which implies the upper bound

$$\|x(t) - x^\star\|_{\mathrm{G}} \leq \|x(0) - x^\star\|_{\mathrm{G}} + (1-\rho) r - c_{\mathrm{lin}} t.$$

Next, for all $t > t_{\mathrm{cross}}$ the trajectory $x(t)$ is inside $B_{\mathrm{G}}(x^\star, r)$ and Assumption (A2), i.e., $c_{\exp}$-strongly infinitesimally contractivity on $\mathcal{S}$, implies the bound

$$\|\phi_t(x(0)) - x^\star\|_{\mathrm{L}} \leq \|x(0) - x^\star\|_{\mathrm{L}}\, \mathrm{e}^{-c_{\exp}(t - t_{\mathrm{cross}})}, \quad \forall t > t_{\mathrm{cross}}.$$

Applying the equivalence of norms to the above inequality we have

$$\|\phi_t\big(x(0)\big) - x^\star\|_{\mathrm{G}} \leq k_{\mathrm{L,G}}\, \|x(0) - x^\star\|_{\mathrm{G}}\, \mathrm{e}^{-c_{\exp}(t - t_{\mathrm{cross}})}, \quad \forall t > t_{\mathrm{cross}}.$$

Therefore, for all $t > t_{\mathrm{cross}}$ we have

$$\|x(t) - x^\star\|_{\mathrm{G}} := \|\phi_t\big(x(0)\big) - x^\star\|_{\mathrm{G}} \leq k_{\mathrm{L,G}}\, r\, \mathrm{e}^{-c_{\exp}(t - t_{\mathrm{cross}})}.$$

This concludes the proof. □

7.3.1 The ℓ_2 Logarithmic Norm of Upper Triangular Block Matrices

We present an algebraic result on the ℓ_2 log-norm of upper triangular block matrices. This result is inspired by [42, E2.28] and is instrumental for determining the rate and norm with respect to which the PFCN exhibits strong infinitesimal contractivity. We also refer to [26] for a result on the log-norm of these triangular matrices using non-Euclidean norms.

Lemma 7.4 (The ℓ_2 logarithmic norm of upper triangular block matrices)**.** *Consider the block matrix*

$$A = \begin{bmatrix} A_{11} & A_{12} \\ 0 & A_{22} \end{bmatrix} \in \mathbb{R}^{(n+m)\times(n+m)}.$$

For all $\varepsilon > 0$ and for $P_\varepsilon = \begin{bmatrix} \varepsilon P_1 & 0 \\ 0 & \varepsilon^{-1} P_2 \end{bmatrix}$ with $P_1 = P_1^\top \succ 0$ and $P_2 = P_2^\top \succ 0$, we have

$$\mu_{2,P_\varepsilon^{1/2}}(A) \leq \max\left\{\mu_{2,P_1^{1/2}}(A_{11}), \mu_{2,P_2^{1/2}}(A_{22})\right\} + \varepsilon \|P_1^{1/2} A_{12} P_2^{-1/2}\|_2. \tag{7.14}$$

Proof. We compute

$$\begin{aligned}
\mu_{2,P_\varepsilon^{1/2}}(A) &= \mu_2\left(\begin{bmatrix} P_1^{1/2} A_{11} P_1^{-1/2} & \varepsilon P_1^{1/2} A_{12} P_2^{-1/2} \\ 0 & P_2^{1/2} A_{22} P_2^{-1/2} \end{bmatrix}\right) \\
&= \mu_2\left(\begin{bmatrix} P_1^{1/2} A_{11} P_1^{-1/2} & 0 \\ 0 & P_2^{1/2} A_{22} P_2^{-1/2} \end{bmatrix} + \begin{bmatrix} 0 & \varepsilon P_1^{1/2} A_{12} P_2^{-1/2} \\ 0 & 0 \end{bmatrix}\right) \\
&\leq \mu_2\left(\begin{bmatrix} P_1^{1/2} A_{11} P_1^{-1/2} & 0 \\ 0 & P_2^{1/2} A_{22} P_2^{-1/2} \end{bmatrix}\right) + \varepsilon \left\| \begin{bmatrix} 0 & P_1^{1/2} A_{12} P_2^{-1/2} \\ 0 & 0 \end{bmatrix} \right\|_2
\end{aligned}$$

where the last inequality follows by applying the log-norm translation property (iii) and the norm spectrum inequality (vi), $\mu(B) \leq \|B\|$, for all matrix B. From the LMI characterization of the ℓ_2 logarithmic norm, we obtain

$$\mu_2\left(\begin{bmatrix} P_1^{1/2} A_{11} P_1^{-1/2} & 0 \\ 0 & P_2^{1/2} A_{22} P_2^{-1/2} \end{bmatrix}\right) = \max\left\{\mu_{2,P_1^{1/2}}(A_{11}), \mu_{2,P_2^{1/2}}(A_{22})\right\}.$$

The claim then follows by noting that

$$\left\| \begin{bmatrix} 0 & P_1^{1/2} A_{12} P_2^{-1/2} \\ 0 & 0 \end{bmatrix} \right\|_2 = \|P_1^{1/2} A_{12} P_2^{-1/2}\|_2.$$

□

Next, we give a specific result for a particular case of the matrix A, where we can explicitly determine the matrices P_1 and P_2. This specific matrix form is of significant interest because, as we will see, the Jacobian of the PFCN computed at the equilibrium exhibits this structure.

Corollary 7.5. *Consider the block matrix*

$$B = \begin{bmatrix} -B_{11} & B_{12} \\ 0 & -I_m \end{bmatrix} \in \mathbb{R}^{(n+m)\times(n+m)},$$

with $B_{11} = B_{11}^\top \succ 0$ *satisfying* $\lambda_{\min}(B_{11}) \geq l$, *with* $l \in]0, 1]$. *Then, for all* $\varepsilon > 0$ *and for* $Q_\varepsilon = \begin{bmatrix} \varepsilon I_n & 0 \\ 0 & \varepsilon^{-1} I_m \end{bmatrix}$, *we have*

$$\mu_{2,Q_\varepsilon}(B) \leq -\big(l - \varepsilon^2 \|B_{12}\|_2\big). \tag{7.15}$$

Proof. By applying Lemma 7.4 to the block matrix B, for all $\varepsilon > 0$ we obtain

$$\begin{aligned} \mu_{2,Q_\varepsilon}(B) &\leq \max\big\{\mu_{2,I_n}(-B_{11}), \mu_{2,I_m}(-I_m)\big\} + \varepsilon^2 \|I_n B_{12} I_m\|_2 \\ &\leq \max\big\{-l, -1\big\} + \varepsilon^2 \|B_{12}\|_2 = -l + \varepsilon^2 \|B_{12}\|_2. \end{aligned}$$

This concludes the proof. □

Remark 7.2. *The result in Corollary 7.5 implies that:*

(i) if $\|B_{12}\|_2 = 0$, *then* $\mu_{2,Q_\varepsilon}(B) < 0$ *for all* $\varepsilon > 0$,

(ii) if $\|B_{12}\|_2 \neq 0$, *then* $\mu_{2,Q_\varepsilon}(B) < 0$, *for all* $\varepsilon \in]0, \sqrt{l/\|B_{12}\|_2}[$.

□

7.4 Analysis of the Firing Rate Competitive Networks

In this section, we investigate the key properties of the models introduced in Chapter 6. To streamline the presentation and due to its biological relevance, our primary focus is on the analysis of the PFCN. However, the results presented here are not limited to this specific model, but can be extended to any FCN (7.2), whose proximal operator is Lipschitz and slope restricted in $[0, 1]$. For example, our convergence analysis can be applied to the firing rate version of the LCA tackling problem (7.3), i.e., the dynamics (7.4), given that the operator soft_λ is Lipschitz and slope restricted in $[0, 1]$.

7.4.1 Convergence Analysis

We now present our convergence analysis for the PFCN in equation (7.6). We start with the following.

Definition 7.1 (Active and inactive neuron)**.** *Consider the PFCN* (7.4)*. Given a neural state* $\nu^\star \in \mathbb{R}^n$*, an input* $u \in \mathbb{R}^m$*, and a parameter* $\lambda > 0$*, the* i*-th neuron is* active *if* $\mathrm{ReLU}\big(((I_n - D^\top D)\nu^\star + D^\top u - \lambda \mathbb{1}_n)_i\big) \neq 0$*,* inactive *if* $\mathrm{ReLU}\big(((I_n - D^\top D)\nu^\star + D^\top u - \lambda \mathbb{1}_n)_i\big) = 0$*.*

Remark 7.3.

(i) The definition of active *and* inactive *neuron/node in our model aligns with the definitions provided in [124] for the LCA. Specifically, as in [124], for an equilibrium point* $\nu^\star \in \mathbb{R}^n$*, the activation function in our model is also composed of two operational regions. Namely: (i) one region characterized by having* $(I_n - D^\top D)\nu^\star + D^\top u - \lambda \mathbb{1}_n$ *below zero, in which case the output* y *is zero, as the system is at the equilibrium* $\nu^\star = \mathrm{ReLU}\big((I_n - D^\top D)\nu^\star + D^\top u - \lambda \mathbb{1}_n\big)$*. (ii) one region characterized by having* $(I_n - D^\top D)\nu^\star + D^\top u - \lambda \mathbb{1}_n$ *above zero, in which case* y *is strictly increasing with the state* ν*.*

(ii) For the FCN, the ReLU *in Definition 7.1 is replaced by* $\mathrm{prox}_{\lambda S}$*.*

□

We now show that the distance between any two trajectories of the PFCN never increases (see Figure 4.3). We do so by proving that the PFCN is weakly infinitesimally contracting.

Theorem 7.6 (Global weak contractivity of the PFCN)**.** *The PFCN* (7.4) *is weakly infinitesimally contracting on* $\mathbb{R}^n$ *with respect to the weighted norm* $\|\cdot\|_{2,Q}$*.*[1]

Proof. First, we note that the activation function ReLU is Lipschitz with constant 1 and slope restricted in $[0, 1]$. Moreover, $\alpha\big(W\big) = \alpha\big(I_n - D^\top D\big) = 1$, being $D^\top D \succeq 0$. The result then follows by applying Corollary 5.7 in Chapter 5. □

Essentially, with the above results we established that the trajectories of the PFCN are bounded. Next, we further characterize the stability of the equilibria of the PFCN when the dictionary is RIP. We prove that the equilibrium is not only locally exponentially stable but also locally-strongly contracting in a suitably defined norm (see Figure 4.3).

Theorem 7.7 (Local exponential stability and local strong contractivity of the PFCN)**.** *Let* $\nu^\star \in \mathbb{R}^n_{\geq 0} \setminus \Omega_f$ *be an equilibrium point of the PFCN* (7.4) *having* n_a *active neurons. If the dictionary* D *is* RIP *of order* n_a *and parameter* $\delta \in [0, 1[$*, then*

(i) $\nu^\star$ *is locally exponentially stable,*

[1] the explicit expression of $Q \in \mathbb{R}^{n\times n}$ is given in (5.2) in Chapter 5.

(ii) the PFCN (7.4) is strongly infinitesimally contracting with rate $c_{\text{exp}} > 0$ with respect to the norm $\|\cdot\|_{2,S_\varepsilon}$ in a neighborhood of $\nu^\star$.

Proof. To prove statement (i), we show that $Df_{\text{PFCN}}(\nu^\star)$ is a Hurwitz matrix, i.e., $\alpha(Df_{\text{PFCN}}(\nu^\star)) < 0$. We start noticing that

$$Df_{\text{PFCN}}(\nu^\star) = -I_n + [d]\big(I_n - D^\top D\big), \tag{7.16}$$

where $[d] = \big[\partial \operatorname{ReLU}\big((I_n - D^\top D)\nu^\star + D^\top u - \lambda \mathbb{1}_n\big)\big]$ is a diagonal matrix having diagonal entries equal to 0 or 1. We let n_{a} and n_{ia} be the number of active and inactive neurons of $\nu^\star$, respectively, and rearrange the ordering of the elements in $\nu^\star$ such that $\nu^\star = [\nu^\star_{\text{a}}, \quad \nu^\star_{\text{ia}}]^\top$, where, $\nu^\star_{\text{a}} \in \mathbb{R}^{n_{\text{a}}}$ and $\nu^\star_{\text{ia}} \in \mathbb{R}^{n_{\text{ia}}}$, so that

$$[d] = \begin{bmatrix} I_{n_{\text{a}}} & 0 \\ 0 & 0 \end{bmatrix}. \tag{7.17}$$

Further, we also decompose $D^\top D$ into

$$D^\top D = \begin{bmatrix} D_{\text{a}}^\top D_{\text{a}} & D_{\text{a}}^\top D_{\text{ia}} \\ D_{\text{ia}}^\top D_{\text{a}} & D_{\text{ia}}^\top D_{\text{ia}} \end{bmatrix}, \tag{7.18}$$

where $D_{\text{a}}^\top D_{\text{a}} \in \mathbb{R}^{n_{\text{a}} \times n_{\text{a}}}$, $D_{\text{a}}^\top D_{\text{ia}} \in \mathbb{R}^{n_{\text{a}} \times n_{\text{ia}}}$, $D_{\text{ia}}^\top D_{\text{a}} \in \mathbb{R}^{n_{\text{ia}} \times n_{\text{a}}}$, $D_{\text{ia}}^\top D_{\text{ia}} \in \mathbb{R}^{n_{\text{ia}} \times n_{\text{ia}}}$. The fact that D is RIP of order n_{a} implies that

$$\|D_{\text{a}}^\top \nu_{\text{a}}\|_2^2 = x_a^\top D_{\text{a}}^\top D_{\text{a}} \nu_a = \begin{bmatrix} \nu_a \\ \mathbb{0}_{n_{\text{ia}}} \end{bmatrix}^\top \begin{bmatrix} D_{\text{a}}^\top D_{\text{a}} & D_{\text{a}}^\top D_{\text{ia}} \\ D_{\text{ia}}^\top D_{\text{a}} & D_{\text{ia}}^\top D_{\text{ia}} \end{bmatrix} \begin{bmatrix} \nu_{\text{a}} \\ \mathbb{0}_{n_{\text{ia}}} \end{bmatrix} \geq (1-\delta)\|\nu_{\text{a}}\|_2^2 > 0.$$

Therefore, $D_{\text{a}}^\top D_{\text{a}}$ is positive definite, and its smallest eigenvalue is bounded below by $1 - \delta$. Moreover, $Df_{\text{PFCN}}(\nu^\star)$ can be written as

$$Df_{\text{PFCN}}(\nu^\star) = \begin{bmatrix} -D_{\text{a}}^\top D_{\text{a}} & -D_{\text{a}}^\top D_{\text{ia}} \\ 0 & -I_{n_{\text{ia}}} \end{bmatrix}, \tag{7.19}$$

that is a block upper triangular matrix with Hurwitz diagonal block matrices, and $\alpha\big(Df_{\text{PFCN}}(\nu^\star)\big) = \delta - 1 < 0$. Thus $Df_{\text{PFCN}}(\nu^\star)$ is Hurwitz. This concludes the proof of the statement.

Next, to prove statement (ii) we note that $\lambda_{\min}\big(D_{\text{a}}^\top D_{\text{a}}\big) \geq 1 - \delta$. By applying Corollary 7.5 to the matrix $Df_{\text{PFCN}}(\nu^\star)$, we have

$$\mu_{2,S_\varepsilon}(Df_{\text{PFCN}}(\nu^\star)) \leq -c_{\text{exp}} < 0,$$

with the explicit expression of c_{exp} and S_ε given in (7.24). Let $\mathcal{K}$ be the region of differentiable points in a neighborhood of $\nu^\star$. Then, by the continuity property of the log-norm, there exists a neighborhood of $\nu^\star$,

$$B_{S_\varepsilon}\big(\nu^\star, q\big) := \{z \in \mathbb{R}^n \mid \|z - \nu^\star\|_{2,S_\varepsilon} \leq q\}, \text{ with } q := \sup\{z > 0 \mid B_{S_\varepsilon}\big(\nu^\star, z\big) \subset \mathcal{K}\}, \tag{7.20}$$

where $Df_{\text{PFCN}}(\nu)$ exists and $\mu_{2,S_\varepsilon}(Df_{\text{PFCN}}(\nu)) \leq -c_{\text{exp}}$, for all $\nu \in B_{S_\varepsilon}\big(\nu^\star, q\big)$. This concludes the proof. □

Symbol	Meaning	Ref.
Q	Weight matrix with respect to the PFCN is globally-weakly contracting	Eq. (5.2)
$\|\cdot\|_{2,Q}$	Euclidean weighted norm with respect to the PFCN is globally-weakly contracting	Th. 7.6
S_ε	Weight matrix with respect to the PFCN is locally-strongly contracting	Eq. (7.24)
$\|\cdot\|_{2,S_\varepsilon}$	Euclidean weighted norm with respect to the PFCN is locally-strongly contracting	Th. 7.7
$k_{S_\varepsilon,Q}$	Equivalence ratio between $\|\cdot\|_{2,S_\varepsilon}$ and $\|\cdot\|_{2,Q}$	Def. 2.2
q	Radius of the ball where the system is strongly infinitesimally contracting	Eq. (7.20)
$B_{S_\varepsilon}(q)$	Ball of radius q centered at $\nu^\star$ computed with respect to $\|\cdot\|_{2,S_\varepsilon}$	Eq. (7.20)
r	Radius of the largest ball $B_Q(r)$ contained in $B_{S_\varepsilon}(q)$	Th. 7.8
$B_Q(r)$	Ball of radius r centered at $\nu^\star$ computed with respect to $\|\cdot\|_{2,Q}$	Th. 7.8
c_{exp}	Exponential decay rate	Eq. (7.24)
c_{lin}	Average linear decay rate	Eq. (7.22)
t_{cross}	Linear-exponential crossing time	Eq. (7.23)
ρ	Contraction factor, $0 < \rho < 1$	Th. 7.8

Table 7.1: Symbols used in Theorem 7.8.

Remark 7.4. *To improve readability, in the statement of Theorem 7.7 we do not provide the explicit expression for c_{exp} and S_ε. These are instead given in Remark 7.5. For the same reason, we do not report in the statement of Theorem 7.7 the neighborhood in which the PFCN is strongly infinitesimally contracting. However, as apparent from the proof, the neighborhood is $B_{S_\varepsilon}(\nu^\star, q)$, which is defined in (7.20).* □

With the next result, we prove that the PFCN converges linear-exponentially to $\nu^\star$ (see Figure 7.2 for an illustration of this behavior). We summarize the key symbols used in the next theorem in Table 7.1.

Theorem 7.8 (Linear-exponential stability of the PFCN)**.** *Consider the PFCN (7.4) satisfying the same assumptions and with the same notations of Theorems 7.6 and 7.7. Let $B_{S_\varepsilon}(\nu^\star, q)$ be the ball around $\nu^\star$ where the system is strongly infinitesimally contracting. Then, for each trajectory $\nu(t)$ starting from $\nu(0) \notin B_{S_\varepsilon}(\nu^\star, q)$ and for any $0 < \rho < 1$, the distance $\|\nu(t) - \nu^\star\|_{2,Q}$ decreases* linear-exponentially*, in the sense that:*

$$\|\nu(t) - \nu^\star\|_{2,Q} \leq \begin{cases} \|\nu(0) - \nu^\star\|_{2,Q} + (1-\rho)r - c_{\text{lin}} t & \text{if } t \leq t_{\text{cross}}, \\ k_{S_\varepsilon,Q}\, r\, \mathrm{e}^{-c_{\text{exp}}(t - t_{\text{cross}})} & \text{if } t > t_{\text{cross}}, \end{cases} \tag{7.21}$$

where $r > 0$ is the radius of the largest ball $B_Q(\nu^\star, r)$ centered at $\nu^\star$ such that

$B_Q(\nu^\star, r) \subset B_{S_\varepsilon}(\nu^\star, q)$ *and where*

$$c_{\text{lin}} = \frac{c_{\text{exp}}(1-\rho)r}{\ln(k_{S_\varepsilon,Q}\rho^{-1})}, \tag{7.22}$$

$$t_{\text{cross}} = \left\lceil \frac{\|\nu(0)-\nu^\star\|_{2,Q} - r}{(1-\rho)r} \right\rceil \frac{\ln(k_{S_\varepsilon,Q}\rho^{-1})}{c_{\text{exp}}}, \tag{7.23}$$

are the average linear decay rate *and the* linear-exponential crossing time*, respectively.*

Proof. We begin by noting that, under the assumptions of the theorem we have that (i) Theorem 7.6 implies that the PFCN is weakly infinitesimally contracting on $\mathbb{R}^n$ with respect to $\|\cdot\|_{2,Q}$; (ii) Theorem 7.7 implies that the PFCN is c_ε-strongly infinitesimally contracting on $B_{S_\varepsilon}(\nu^\star, q)$ with respect to $\|\cdot\|_{2,S_\varepsilon}$. Hence, the statement follows from Corollary 7.3 with $\mathcal{S} = B_{S_\varepsilon}(\nu^\star, q)$, $\|\cdot\|_{\text{G}} = \|\cdot\|_{2,Q}$ and $\|\cdot\|_{\text{L}} = \|\cdot\|_{2,S_\varepsilon}$. □

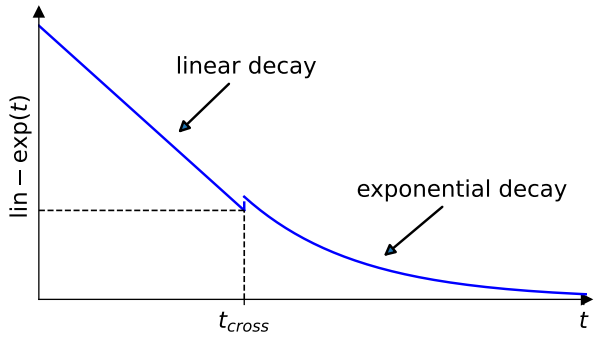

Figure 7.2: Schematic representation of the linear-exponential convergence behavior exhibited by the PFCN. The distance of the trajectory from the equilibrium point is upper bounded by a function that decreases linearly with time until t_{cross} and then exponentially for all $t > t_{\text{cross}}$. While the solution of the PFCN is continuous, a bounded jump in the upper bound we obtain might occur at time t_{cross}.

Remark 7.5 (Expression of S_ε and c_{exp} in Theorem 7.7)**.** *Corollary 7.5 enables the computation of the rate and the norm with respect to which the PFCN is strongly infinitesimally contracting, as stated in Theorem 7.7. In fact, the Jacobian of* f_{PFCN} *computed at the equilibrium, given by equation (7.19), is in the form of the matrix* B *in Corollary 7.5 with* $n = n_{\text{a}}$, $m = n_{\text{ia}}$, $B_{11} := D_{\text{a}}^\top D_{\text{a}} \succ 0$, $l = 1-\delta \in]0,1]$, *and* $B_{12} := -D_{\text{a}}^\top D_{\text{ia}}$. *Therefore the PFCN is strongly infinitesimally contracting with respect to the norm* $\|\cdot\|_{2,S_\varepsilon}$ *with rate* c_{exp}*, where*

$$\begin{aligned} &\textit{(i) if } \|D_{\text{a}}^\top D_{\text{ia}}\|_2 = 0, \textit{ then } S_\varepsilon := Q_\varepsilon, c_{\text{exp}} = 1-\delta, \forall \varepsilon > 0, \\ &\textit{(ii) if } \|D_{\text{a}}^\top D_{\text{ia}}\|_2 \neq 0, \textit{ then } S_\varepsilon := Q_\varepsilon, c_{\text{exp}} = 1-\delta-\varepsilon^2\|D_{\text{a}}^\top D_{\text{ia}}\|_2, \\ &\qquad\qquad \forall \varepsilon \in \left]0, \sqrt{(1-\delta)/\|D_{\text{a}}^\top D_{\text{ia}}\|_2}\right[. \end{aligned} \tag{7.24}$$

□

It is important to highlight the significance and practical implication of Theorems 7.6, 7.7 and 7.8. First, a key aspect to emphasize is the fact that convergence is *global*: the PFCN converges towards the equilibrium point $\nu^\star$ from any initial condition. Moreover, global linear-exponential convergence is a stronger result than global asymptotic convergence, since with the bound in (7.21) we provide an explicit estimate of the time required to reach a neighborhood of the equilibrium. Next, the role of the RIP assumption to obtain this result deserves some comments. From Theorem 7.6, we know that the trajectories of the PFCN are bounded, meaning that the distance between any two trajectories never increases over time. However, boundedness alone is not enough to guarantee global convergence. For this, we need more "structure" on the problem. The RIP assumption provides this structure, ensuring (Theorem 7.7) the existence of a locally stable equilibrium point $\nu^\star$. This, in turn, ensures a number of highly ordered transient and asymptotic behaviors, characteristic of contracting dynamics.

7.5 Simulations

We now illustrate the effectiveness of the PFCN in solving the positive SR problem (7.3) via a numerical example[2]. This example, built upon the one in [124], serves two key purposes: first, to validate the ability of the PFCN to solve the positive SR problem while respecting the non-negativity bounds of its state variables; and second, to illustrate the global convergence behavior of the PFCN.

To this aim, we consider a $n = 512$ dimensional sparse signal $y_0 \in \mathbb{R}^n_{\geq 0}$, with $n_\text{a} = 5$ randomly selected non-zero entries. The amplitude of these non-zero entries is obtained by drawing from a normal Gaussian distribution and then taking the absolute values. As in [124] the dictionary $D \in \mathbb{R}^{m\times n}$ is built as a union of the canonical basis and a sinusoidal basis (each basis is normalized so that the dictionary columns have unit norms). Also, we set: (i) the measurements $u \in \mathbb{R}^m$, with $m = 256$, to be $u = Dy_0 + \eta$, where η is a Gaussian random noise with standard deviation $\sigma = 0.0062$; (ii) $\lambda = 0.025$.

Given this set-up, we simulated both the PFCN (7.4) and, for comparison, the LCA (6.8). Simulations were performed with Python using the ODE solver *solve_ivp*. In all the numerical experiments, the simulation time was $t \in [0, 15]$, and initial conditions were set to 0, except for 20 randomly selected neurons (initial conditions were kept constant across the simulations). The time evolution of the state variables for both the PFCN and LCA is shown in Figure 7.3. Both panels illustrate that both the PFCN and the LCA converge to an equilibrium that is close to y_0 (although it can not be exactly y_0 because of the measurement noise). Also, the figure clearly shows, in accordance with Lemma 6.2, that the trajectories of the PFCN are always non-negative. Instead, the trajectories of the LCA nodes exhibit also negative values over time.

To illustrate the global convergence behavior of the PFCN (7.4), we performed an additional set of simulations, this time with the PFCN starting from 20 randomly

[2]The code to replicate all the simulations in this section is available at the GitHub https://tinyurl.com/PFCN-for-Sparse-Reconstruction.

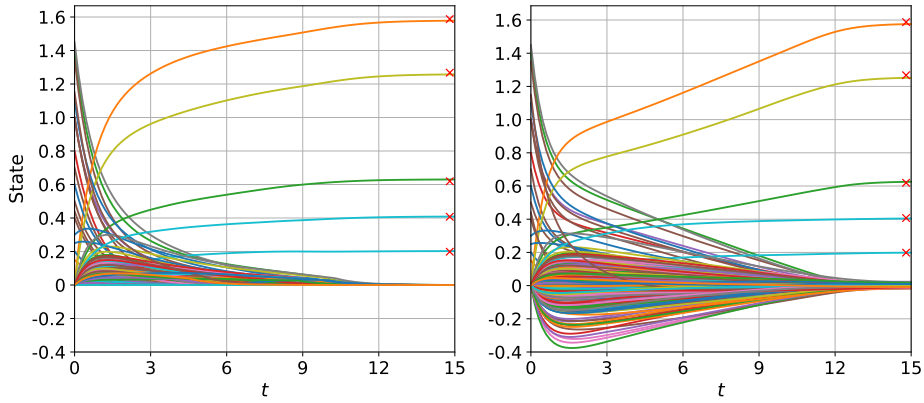

Figure 7.3: Time evolution of the state/neuron variables of the proposed PFCN (7.4) (leftward panel) and of the LCA (6.8) (rightward panel) networks. The cross symbols are the non-zero elements of the sparse vector y_0. Both the PFCN and the LCA converge to an equilibrium that is close to y_0. Note that, in accordance with Lemma 6.2, the state variables of the PFCN never become negative.

generated initial conditions. Then, we randomly selected two neurons from the active and inactive sets and recorded their evolution. The result of this process is shown in Figure 7.4, which reports a projection of the phase plane defined by these nodes. Figure 7.4 shows that the trajectories of the selected nodes converge to the equilibrium point from any of the chosen initial conditions. Specifically, in accordance with our results, the trajectories of the active neurons converge to positive values, while the trajectories of the inactive nodes converge to the origin.

Finally, we performed an additional, exploratory, numerical study to investigate what happens when the activation function of the LCA is the shifted ReLU. Even though the assumptions in [124] on the activation function exclude the use of the ReLU for the LCA, we decided to simulate this scenario to investigate if the LCA dynamics would become positive if the ReLU was used as activation function. Hence, for our last numerical study, we considered the following LCA dynamics:

$$\dot{\nu}(t) = -\nu(t) + \left(I_n + D^\top D\right) \mathrm{ReLU}\big(\nu(t) - \lambda \mathbb{1}_n\big) + D^\top u(t), \tag{7.25}$$

with output $y(t) = \mathrm{ReLU}\big(\nu(t) - \lambda \mathbb{1}_n\big)$. In Figure 7.5 the time evolution of the state variables of the LCA (7.25) is shown. As apparent from the figure, even using the ReLU as activation function, the trajectories of the LCA states still exhibit negative values over time.

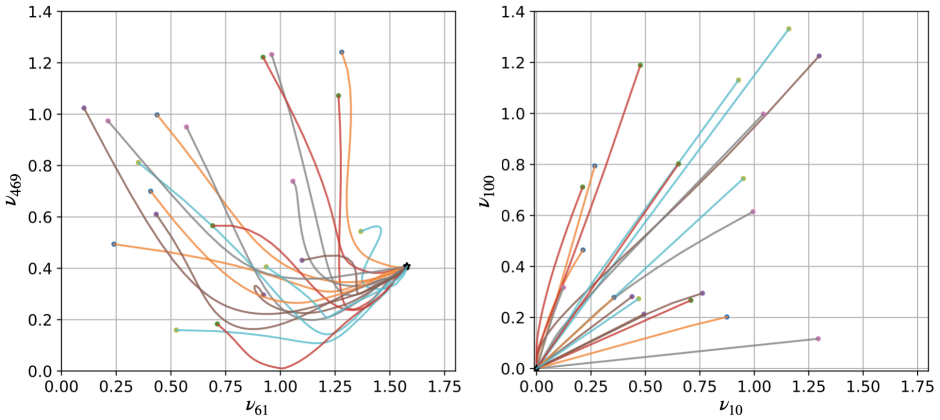

Figure 7.4: Trajectories of two randomly chosen nodes of the PFCN (7.4) from the active (leftward panel) and inactive (rightward panel) set in the planes defined by these two nodes, respectively. In the panels, the evolution is shown from 20 randomly chosen initial conditions. In accordance with our results, the trajectories of the active neurons converge to positive values, while the trajectories of the inactive nodes converge to the origin.

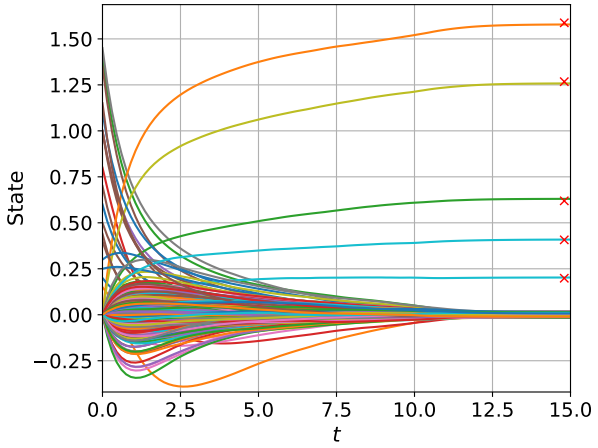

Figure 7.5: Time evolution of the state variables of the LCA (7.25) with ReLU as activation function. The cross symbols are the non-zero elements of y_0. The LCA converges to an equilibrium close to y_0. Even using the ReLU as activation function, the trajectories of the LCA states still exhibit negative values over time.

7.6 Summary

In this chapter, we completed the analysis we began in Chapter 6 for a biologically plausible framework for neural networks solving sparse reconstruction problems, by giving a comprehensive convergence analysis of the proposed network dynamics. For simplicity of presentation, we provided an explicit analysis only for the PFCN and gave rigorous conditions to extend this analysis to the FCN. Specifically, we showed that (i) the PFCN (7.4) is weakly contracting on $\mathbb{R}^n$ (Theorem 7.6); (ii) if the dictionary is RIP, then the equilibrium point of the PFCN is locally exponentially stable and, as a consequence, in a suitably defined norm, it is also strongly contracting in a neighborhood of the equilibrium (Theorem 7.7). These results lead to the main result of the chapter, i.e., Theorem 7.8, which establishes the global linear-exponential convergence of the PFCN.

To derive our key findings, we also devised a number of instrumental results, interesting *per se*, providing: (i) algebraic results on the log-norm of triangular matrices; (ii) convergence analysis for a broader class of non-linear dynamics (globally-weakly and locally-strongly contracting systems) that naturally arise from the study of the FCN and PFCN. Finally, we illustrated the effectiveness of our results via numerical experiments.

The findings in the Methods section 7.3 open the way for an exciting research direction, which we investigate further in Chapter 12: the study of *globally-weakly contracting and locally-strongly contracting* systems. As we will show, this class of systems naturally arises in the context of convex (but not strongly convex) optimization problems with a unique minimizer, making them relevant to a wide array of applications.

Part II

Towards Embedding Learning

II.1 Introduction

Driven by the massive availability of data in many applications and the increase in computing power, the leading paradigm to train artificial neural networks has become that of feeding them with data, using backpropagation to learn the network weights. This approach has achieved impressive results, spanning from computer vision to natural language processing. However, despite their initial biological inspiration and performance achievements, these systems differ from human intelligence in several ways. As already discussed in Section 1.1, the backpropagation algorithm is not biologically plausible and this might explain the poor ability, typical of human intelligence, of certain deep networks to generalize, compose, and abstract knowledge from data. In this context, it has been recently shown that models trained via backpropagation can be extremely *fragile*, in the sense that even small changes in the input can produce large changes in the output.

This gap between artificial learning networks and biological learning drives the exploration of more biologically plausible neural networks, particularly RNNs with synapses undergoing Hebbian learning rules. Hebbian learning, based on the principle *"neurons that fire together wire together"*, mimics the plasticity observed in synaptic connections in the brain.

Research questions: In the above context, several questions naturally arise:

- How can we design RNNs that incorporate biologically plausible learning rules, such as Hebbian learning?
- What conditions ensure that these networks exhibit stable, robust behavior?
- How can these biologically plausible RNNs be analyzed and controlled to guarantee convergence and reliable performance?

II.2 Towards Embedding Learning

In this part, to address the above questions, inspired by [22], we propose embedding nonlinear Hebbian learning rules into the continuous-time RNN models analyzed in Part I, allowing for dynamic synaptic weight updates that mirror biological processes more closely. We name these systems *coupled neural-synaptic networks*. Our goal is to characterize the behavior of these systems and provide conditions that ensure their stability and robustness. To streamline the analysis we divide our results into two chapters: Chapter 8 focuses on the modeling of these networks, while Chapter 9 explores their dynamic behavior and stability properties.

Specifically, in Chapter 8 we introduce the coupled neural-synaptic dynamics. These models combine HNNs and FNNs for the neural dynamics and two different Hebbian learning rules for the synaptic dynamics. The first rule fulfills the biological properties of locality, cooperativity, synaptic depression, and boundedness; the second rule fulfills, in addition, a competitiveness property (see Chapter 3.4 for further details on these

principles). To capture and reflect the synaptic sparsity of biological neural circuits, we propose a low-dimensional formulation for our coupled neural-synaptic models.

Next, in Chapter 9 we turn to the analysis of the dynamical properties of the proposed models. First, we show that the solutions to the coupled neural-synaptic systems are bounded, reflecting the biological reality that neurons eventually saturate in response to high input levels, and synaptic weights do not grow indefinitely. Then, we provide sufficient conditions to guarantee contractivity of each model. We recall that, by ensuring contractivity, global exponential convergence and other useful robustness properties are guaranteed. Finally, we show that, under suitable conditions, our coupled neural-synaptic models satisfy *Dale's law* [143]. This is an empirical principle referring to the fact that a neuron has the same type of effect, inhibitory or excitatory, on all its neighbor neurons.

II.3 Overview

Over the last few years, there has been a growing interest in the study of biologically plausible learning rules to train neural networks and in finding connections between these rules and backpropagation [144, 9]. For example, HNNs coupled with a Hebbian learning rule have been shown to be able to learn the underlying geometry of a given set of inputs [23]. Recently, an unsupervised biologically plausible learning rule has been proposed and it has been demonstrated how this rule allows the network to achieve good performance on the MNIST and CIFAR [8] datasets; also, in [14] it has been shown that neural networks equipped with both Hebbian and anti-Hebbian learning rules can perform a broad range of unsupervised learning tasks.

When studying RNN models a key problem is that of guaranteeing stability and robustness; see, e.g., [135, 122]. Over the years, significant interest has grown in establishing conditions that ensure convergence of RNNs to a unique equilibrium point [75, 44, 76, 134]. As already emphasized multiple times, contraction theory (which precludes multistability) is a useful tool for studying stability and robustness. An implicit model that uses contraction analysis to allow for a convex parametrization of stable models is presented in [101], while in [28] contraction-based conditions are given to characterize disturbance rejection properties of HNNs with delays. Contraction theory is also used in [102] to find conditions under which assemblies of RNNs are stable. Recently, non-Euclidean contractivity of RNNs has been studied in [38]. In the context of networks with adapting synapses undergoing Hebbian rules we recall [22], where stability of the combined neural and synaptic dynamics is shown via Lyapunov analysis, and [24], where Euclidean contraction theory is used to study the stability of RNNs with linear coupling between the different nodes and with dynamic synapses undergoing a correlation-based Hebbian learning rule.

8 Coupled Neural-Synaptic Networks: Modeling

This chapter focuses on the modeling and analysis of coupled neural-synaptic networks that combine recurrent neural networks with dynamical recurrent connections undergoing Hebbian learning rules. The aim is to model neural circuits that not only learn from input data but also adapt their synaptic strengths in a way that mirrors learning processes observed in biological systems. For these models, we also propose a low-dimensional formulation to capture the synaptic sparsity of the neural circuits.

The results presented in this chapter appeared in:

- **V. Centorrino**, F. Bullo, and G. Russo. "Modeling and Contractivity of Neural-Synaptic networks with Hebbian learning". *Automatica*, 164:111636, 2024. doi: 10.1016/j.automatica.2024.111636,
- **V. Centorrino**, F. Bullo, G. Russo. "Contraction Analysis of Hopfield Neural Networks with Hebbian Learning". *2022 IEEE 61st Conference on Decision and Control*, Cancun, Mexico, pp. 622-627, 2022. doi: 10.1109/CDC51059.2022.9993009. Presented in the invited session "Brain Dynamics and Control".

8.1 Introduction

Driven by the massive availability of data and the increase in computing power, the leading paradigm to train *deep* neural networks has become that of feeding them with data, using backpropagation to learn the network weights. This approach has achieved impressive results, spanning from computer vision to natural language processing [6] and to the end-to-end control of complex video games [145]. Nevertheless, as discussed in Section 1.1, despite their initial biological inspiration and performance achievements, these systems differ from human intelligence in several ways [12]. Today, the principles guiding artificial neural networks are quite different from those governing biological networks. A clear example of this divergence is the backpropagation algorithm itself, which is indeed well-known to be biologically implausible [6, 7, 8, 9] and this might explain [12] the poor ability, typical of human intelligence, of certain artificial networks to generalize, compose and abstract knowledge from data.

Motivated by these observations, this chapter aims to model and understand ANNs that more closely align with the principles governing natural neural networks. As highlighted in [22] a complete model of biologically plausible neural networks requires two sets of continuous-time dynamical systems, one for the activity of the neurons and one describing synaptic changes. As a consequence, this chapter presents the modeling and analysis of biologically plausible recurrent neural networks with dynamical recurrent connections. Specifically, following the motivations in Chapter 3, for the neural dynamics we focus here on two widely used continuous-time RNN models: the Hopfield neural network and the firing rate neural network. As for the synaptic weight dynamics, we use continuous-time Hebbian learning rules.

The chapter is organized as follows. In Section 8.2 we introduce the dynamical rules governing the neural masses and synaptic weights. Namely, Hopfield neural networks and firing rate neural networks for modeling the neural dynamics, and Hebbian Learning rules for synaptic dynamics. Then, in Section 8.3, we present the coupled neural-synaptic dynamics we are interested in. These systems combine HNN and FNN (for the neural dynamics) and two different Hebbian learning rules (for the synaptic dynamics). Finally, in Section 8.4 we propose a low dimensional formulation for the neural-synaptic models introduced in Section 8.3.

8.1.1 Contributions

This chapter presents the modeling of biologically plausible coupled neural-synaptic systems: recurrent neural networks with dynamic recurrent connections. Specifically, we study a number of neural-synaptic systems that combine HNN and FNN (for the neural dynamics) and two different Hebbian learning rules (for the synaptic dynamics). The first rule, simply termed Hebbian learning rule, fulfills the biological properties of locality, cooperativity, synaptic depression, and boundedness; the second rule (Oja-like learning rule) fulfills, in addition, a competitiveness property. We refer to the resulting models as Hopfield-Hebbian, firing-rate-Hebbian, Hopfield-Oja, and firing-rate-Oja networks. The models capture networks with both excitatory and inhibitory synapses governed by both Hebbian and anti-Hebbian learning rules. We note that our Hopfield-Hebbian model generalizes the ones analyzed in [22, 24] by relaxing the assumptions of these papers on the sign of the coefficients of the Hebbian rule and on the linearity of the coupling between neurons. Additionally, to capture synaptic sparsity, which is a defining feature of many biological neural networks, we propose a low-dimensional formulation of these models, relying on out-incidence and in-incidence matrices.

8.2 Set-up

We begin by introducing the dynamical rules governing the neural masses and synaptic weights. Then, we present the coupled neural-synaptic dynamical systems we analyze.

8.2.1 Neural Dynamics

As discussed in Chapter 3, for the dynamical rules governing the neural masses we are interested in two widely used continuous-time RNN models: the Hopfield neural network (8.1) and firing rate neural network (8.3). We briefly recall these dynamics here for completeness and also introduce slight modifications in the notation to streamline our analysis.

Hopfield Neural Network

For each neural mass i, we denote its mean membrane potential at time t by $x_i(t) \in \mathbb{R}$ and assume it evolves according to the following continuous-time HNN:

$$\dot{x}_i(t) = -c_{\mathrm{n}} x_i(t) + \sum_{j=1}^{n} W_{ij}(t)\phi(x_j(t)) + u_i(t). \tag{8.1}$$

The first term on the right-hand side of (8.1) models the intrinsic dynamics of neuron i, where c_{n} is its decay rate. The second term models the coupling of neuron i with the other neurons. Specifically, $W_{ij} : \mathbb{R}_{\geq 0} \to \mathbb{R}$ denotes the effective time-dependent synaptic weight of the signal transmitted from a pre-synaptic neuron j to a post-synaptic neuron i, and $\phi : \mathbb{R} \to \mathbb{R}$ is the activation function. Finally, $u_i : \mathbb{R}_{\geq 0} \to \mathbb{R}$ is a time-dependent external stimulus to neuron i.

In vector form the dynamics (8.1) reads:

$$\dot{x}(t) = -c_{\mathrm{n}} x(t) + W(t)\Phi(x(t)) + u(t), \tag{8.2}$$

where $x \in \mathbb{R}^n$, $\Phi \colon \mathbb{R}^n \to \mathbb{R}^n$ is a nonlinear and diagonal activation function, i.e., $(\Phi(x))_i = \phi(x_i)$, $W \in \mathbb{R}^{n \times n}$ is the synaptic matrix, and $u \in \mathbb{R}^n$ are the external neural stimuli.

Firing rate Neural Network

For each neural mass i, we denote its firing rate at time t by $\nu_i(t) \in \mathbb{R}$ and we assume it evolves according to the following continuous-time FNN:

$$\dot{\nu}_i(t) = -c_{\mathrm{n}} \nu_i(t) + \phi\left(\sum_{j=1}^{n} W_{ij}(t)\nu_j(t) + u_i(t) \right), \tag{8.3}$$

where, as in (8.1), the decay rate is c_{n}, the synaptic weight is $W_{ij} : \mathbb{R}_{\geq 0} \to \mathbb{R}$, the external stimulus is $u_i : \mathbb{R}_{\geq 0} \to \mathbb{R}$, and the activation function is $\phi : \mathbb{R} \to \mathbb{R}$. The vector

form of the dynamics (8.3) is:

$$\dot{\nu}(t) = -c_{\mathrm{n}}\nu(t) + \Phi\big(W(t)\nu(t) + u(t)\big), \tag{8.4}$$

where $\nu \in \mathbb{R}^n$, $\Phi\colon \mathbb{R}^n \to \mathbb{R}^n$ is a nonlinear and diagonal activation function, $W \in \mathbb{R}^{n\times n}$ is the synaptic matrix, and $u \in \mathbb{R}^n$ are the external neural stimuli.

Remark 8.1. *The activation functions in* (8.1) *and* (8.3) *can be different, but they have the same properties. Therefore, to streamline our derivation, we are using the same symbol for both activation functions.* □

8.2.2 Synaptic Dynamics

For modeling the synaptic dynamics, as discussed in Chapter 3, we consider continuous-time Hebbian learning rules. Following Hebb's postulate [2], the synaptic weight between two neurons, say i and j, should increase if both neurons are simultaneously active. Our models capture this aspect and are based upon the framework presented in [79], where a number of formulations of Hebbian learning are reviewed (see Section 3.4 for more details). The first synaptic rule we consider is modeled via a dynamic of the form:

$$\dot{W}_{ij}(t) = H_{ij}\phi(y_i(t))\phi(y_j(t)) - c_{\mathrm{s}}W_{ij}(t) + \bar{U}_{ij}(t), \tag{8.5}$$

where y_i can be either the membrane potential or the firing rate (from now on we use y_i when referring to both state variables). As described next, the dynamics (8.5) satisfies the properties of locality, cooperativity, and synaptic depression, which are biologically-inspired requirements for any model aiming to capture Hebbian synaptic plasticity, [79]. Specifically,

- *Cooperativity Property:* the first term on the right-hand side of (8.5) describes the cooperation between pre- and post-synaptic activity: in the absence of external stimuli, both the pre- and post-synaptic neurons must be active to induce a synaptic weight increase or decrease. The coefficient $H_{ij} \in \mathbb{R}$ is defined so that a non-zero entry corresponds to an existing synaptic connection and a corresponding evolution of the synaptic weight. Specifically, H_{ij} describes the topology of the network (and this is constant over time), while $W_{ij}(t)$ describes the time-varying evolution of the corresponding synaptic weight.

- *Synaptic Depression Property:* the second term on the right-hand side of (8.5) is a decay factor ($c_{\mathrm{s}} > 0$) that prevents the weights from diverging.

- *Locality Property:* the rule modeled in (8.5) is local, in the sense that changes in W_{ij} only depend on the activities of neurons j and i.

Finally, the third term on the right-hand side of (8.5), $\bar{U}_{ij} : \mathbb{R}_{\geq 0} \to \mathbb{R}$, is a time-dependent external stimulus, e.g., it can represent some exogenous phenomena.

In compact form, the dynamics (8.5) reads

$$\dot{W}(t) = H\Phi(y(t))\Phi(y(t)) - c_{\mathrm{s}}W_{ij}(t) + \bar{U}(t), \tag{8.6}$$

where $W \in \mathbb{R}^{n\times n}$ is the synaptic matrix, $y \in \mathbb{R}^n$ is the neural variable, $\Phi : \mathbb{R}^n \to \mathbb{R}^n_{\geq 0}$ is the term by term application of the activation function ϕ, i.e., $\Phi(x)_i = \phi(x_i)$, $\bar{U} \in \mathbb{R}^{n\times n}$ are the external synaptic stimuli.

For our derivations, it is useful to define:

$$h_{\max} := \max_{i,j\in\{1,\dots,n\}} |H_{ij}| \,. \tag{8.7}$$

Moreover, following [79], we give the following

Definition 8.1 (Hebbian and anti-Hebbian learning rules)**.** *We call a Hebbian learning rule with* $H_{ij} > 0$ Hebbian learning*, and a rule with* $H_{ij} < 0$ anti-Hebbian learning.

The second model for Hebbian learning we consider also fulfills a

- *competivity property:* feature implying that if some synaptic weights grow, they do so at the expense of others.

To capture this feature, we consider the following Oja's like learning rule [66]:

$$\dot{W}_{ij} = H_{ij}\phi(y_i)\phi(y_j) - \big(c_{\mathrm{s}} + c_{\mathrm{o}}\phi^2(y_i)\big)W_{ij} + \bar{U}_{ij}, \tag{8.8}$$

with $c_{\mathrm{o}} > 0$. We observe that if $c_{\mathrm{o}} = 0$, the dynamics (8.8) reduces to (8.5).

Remark 8.2. *When* y_i *is the membrane potential and there are no external stimuli, equations* (8.5) *and* (8.8) *become the ones found in [79]. When* y_i *is the firing rate, through the activation function we are introducing a non-linearity. We emphasize that to streamline our derivations we are using the same notation for the activation functions across the models since they verify the same properties. However the activation function in* (8.1)*,* (8.3)*,* (8.5)*, and* (8.8) *can be different.* □

8.3 Coupled Neural-Synaptic Dynamics

Consider an RNN of n neurons with dynamic synapses and fixed topology of interactions. That is, the coefficients of $H = (H_{ij})_{i,j} \in \mathbb{R}^{n\times n}$ describing the Hebbian and anti-Hebbian learning connections are constant. We make no assumptions on the relative timescales of synaptic and neural activity. We now present the models that are the subject of our study. These models are obtained by combining the neural and synaptic dynamics introduced in Section 8.2. See Figure 8.1 for an illustration of a coupled neural-synaptic model.

Hopfield-Hebbian Model

The coupled *Hopfield-Hebbian model* is obtained by combining the HNN (8.1), and the Hebbian learning rule (8.5), with initial neural and synaptic conditions $x_i(0) \in \mathbb{R}$ and $W_{ij}(0) \in \mathbb{R}$, respectively. For our analysis, it is useful to write this system in vector form:

$$\begin{cases} \dot{x} = -c_{\mathrm{n}}x + W\Phi(x) + u, \\ \dot{W} = H \circ \Phi(x)\Phi(x)^\top - c_{\mathrm{s}}W + \bar{U}, \end{cases} \tag{8.9}$$

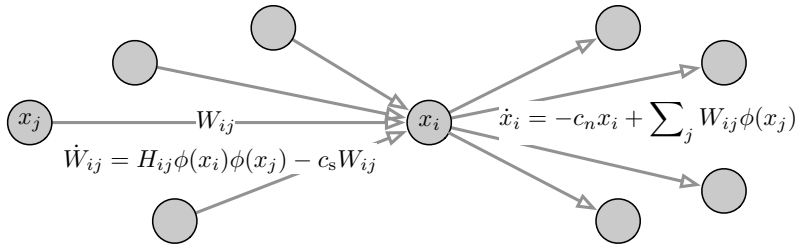

Figure 8.1: Example of a coupled neural-synaptic (Hopfield-Hebbian) model (without external stimuli, for simplicity) describing the dynamical evolution of both neural activity x_i and synaptic weights W_{ij}.

with initial neural and synaptic conditions $x(0) := x_0 \in \mathbb{R}^n$ and $W(0) := W_0 \in \mathbb{R}^{n\times n}$, respectively.

Firing-rate-Hebbian Model

The coupled *firing-rate-Hebbian model* is obtained by combining the FNN (8.3), and the Hebbian learning rule (8.5), with initial neural and synaptic conditions $\nu_i(0) \in \mathbb{R}$ and $W_{ij}(0) \in \mathbb{R}$, respectively. In vector form, the system is:

$$\begin{cases} \dot{\nu} = -c_n \nu + \Phi\big(W\nu + u\big), \\ \dot{W} = H \circ \Phi(\nu)\Phi(\nu)^\top - c_s W + \bar{U}, \end{cases} \tag{8.10}$$

with initial neural and synaptic conditions $\nu(0) := \nu_0 \in \mathbb{R}^n$, and W_0, respectively. In system (8.10), $\nu \in \mathbb{R}^n$ is the vector of the firing rates, while for notational convenience the other terms are defined consistently with (8.9).

Hopfield-Oja Model

The coupled *Hopfield-Oja model* is obtained by combining the HNN (8.1), and the Oja's like synaptic plasticity rule (8.8), with initial neural and synaptic conditions $x_i(0)$ and $W_{ij}(0)$, respectively. Using the same notation as for the dynamics in (8.9) we write this system in vector form as

$$\begin{cases} \dot{x} = -c_n x + W\Phi(x) + u, \\ \dot{W} = H \circ \Phi(x)\Phi(x)^\top - \big(c_s I_n + c_o[\Phi(x)][\Phi(x)]\big)W + \bar{U}, \end{cases} \tag{8.11}$$

with initial neural and synaptic conditions x_0 and W_0, respectively.

Firing-rate-Oja Model

The coupled *firing-rate-Oja model* is obtained by combining the FNN (8.3), and the Oja's like synaptic plasticity model (8.8), with initial neural and synaptic conditions $\nu_i(0)$ and $W_{ij}(0)$, respectively. Using the same notation as in (8.10) we write this system in vector form as

$$\begin{cases} \dot{\nu} = -c_{\mathrm{n}}\nu + \Phi\big(W\nu + u\big), \\ \dot{W} = H \circ \Phi(\nu)\Phi(\nu)^{\top} - \big(c_{\mathrm{s}} I_n + c_{\mathrm{o}}[\Phi(\nu)][\Phi(\nu)]\big)W + \bar{U}, \end{cases} \tag{8.12}$$

with initial neural and synaptic conditions ν_0 and W_0, respectively.

8.4 Low Dimensional Reformulations

The neural-synaptic models introduced in Section 8.3 consist of $n \times n^2$ variables – n neurons and n^2 synaptic connections. However, in biological systems, synaptic connectivity is sparse compared to the number of neurons [1, 24]. To see this, just think about the C. Elegans, one of the simplest organisms with a nervous system and the first multicellular organism to have a completed mapped connectome. C. Elegans has a system that contains 302 neurons but only about 7,000 synapses [146], so it is pretty sparse.

To effectively exploit this sparsity, we now propose low-dimensional reformulations of the models introduced in Section 8.3. These reformulations, which leverage the out-incidence and in-incidence matrices reviewed in Section 2.6, are used in the next chapter to give biologically-inspired forward invariance results and to obtain sufficient conditions for non-Euclidean contractivity of the models.

Let m be the number of synaptic connections in the neural-synaptic dynamics introduced in Section 8.3. To obtain the reduced formulation, we pick the m nonzero elements of H, say H_{ij}, and the corresponding elements of W and $\bar{U}$, say W_{ij} and $\bar{U}_{ij}$. We then vectorize these elements in $h \in \mathbb{R}^m$, $w \in \mathbb{R}^m$ and $\bar{u} \in \mathbb{R}^m$, respectively. We stress that, in our notation, W_{ij} is the synaptic weight of the signal transmitted from a pre-synaptic neuron j to a post-synaptic neuron i. These connections define a graph, whose $n \times n$ adjacency matrix has the weight W_{ij} as the element at position (i, j). By applying the identity (2.7), we can write the synaptic weight matrix W as $W = B_{\mathrm{in}}[w]B_{\mathrm{out}}^{\top}$, where B_{out} and B_{in} are defined as in (2.4) and (2.5). Moreover, from (2.6) for each edge (i.e., synaptic connection) of the form $e = (i, j)$, we get $\big(B_{\mathrm{out}}^{\top}\Phi(y)\big)_e = \phi(y_j)$, and $\big(B_{\mathrm{in}}^{\top}\Phi(y)\big)_e = \phi(y_i)$. Substituting the above identities into the full dimensional coupled neural-synaptic models introduced in Section 8.3, we obtain the corresponding low dimensional reformulations. It is worth remarking that, in each case, we obtain a system with $n \times m$ variables, with $m \ll n^2$, instead of a system with $n \times n^2$ variables. Specifically, these reformulations yield the following systems.

Hopfield-Hebbian Model Reformulation

$$\begin{cases} \dot{x} = -c_{\text{n}} x + B_{\text{in}}[w] B_{\text{out}}^{\top} \Phi(x) + u, \\ \dot{w} = h \circ B_{\text{out}}^{\top} \Phi(x) \circ B_{\text{in}}^{\top} \Phi(x) - c_{\text{s}} w + \bar{u}, \end{cases} \tag{8.13}$$

with $x(0) := x_0 \in \mathbb{R}^n$ and $w(0) := w_0 \in \mathbb{R}^m$. The components of w_0 are the m elements of W_0 having non zero H_{ij}'s.

Firing-rate-Hebbian Model Reformulation

$$\begin{cases} \dot{\nu} = -c_{\text{n}} \nu + \Phi\big(B_{\text{in}}[w] B_{\text{out}}^{\top} \nu + u\big), \\ \dot{w} = h \circ B_{\text{out}}^{\top} \Phi(\nu) \circ B_{\text{in}}^{\top} \Phi(\nu) - c_{\text{s}} w + \bar{u}, \end{cases} \tag{8.14}$$

with $\nu(0) := \nu_0 \in \mathbb{R}^n$ and $w_0 \in \mathbb{R}^m$ defined consistently with the initial conditions in (8.13).

Hopfield-Oja Model Reformulation

$$\begin{cases} \dot{x} = -\, c_{\text{n}} x + B_{\text{in}}[w] B_{\text{out}}^{\top} \Phi(x) + u, \\ \dot{w} = h \circ B_{\text{out}}^{\top} \Phi(x) \circ B_{\text{in}}^{\top} \Phi(x) - \big(c_{\text{s}} I_m + c_{\text{o}} [B_{\text{in}}^{\top} \Phi(x)][B_{\text{in}}^{\top} \Phi(x)]\big) w + \bar{u}, \end{cases} \tag{8.15}$$

with $x_0 \in \mathbb{R}^n$ and $w_0 \in \mathbb{R}^m$ defined consistently with the initial conditions in (8.13).

Firing-rate-Oja Model Reformulation

$$\begin{cases} \dot{\nu} = -c_{\text{n}} \nu + \Phi\big(B_{\text{in}}[w] B_{\text{out}}^{\top} \nu + u\big), \\ \dot{w} = h \circ B_{\text{out}}^{\top} \Phi(\nu) \circ B_{\text{in}}^{\top} \Phi(\nu) - \big(c_{\text{s}} I_m + c_{\text{o}} [B_{\text{in}}^{\top} \Phi(\nu)][B_{\text{in}}^{\top} \Phi(\nu)]\big) w + \bar{u}, \end{cases} \tag{8.16}$$

with $\nu_0 \in \mathbb{R}^n$ and $w_0 \in \mathbb{R}^m$ defined consistently with the initial conditions in (8.14).

8.5 Summary

Motivated by the aim to model and study ANNs that more closely align with the principles governing natural neural networks, in this chapter we introduced biologically plausible recurrent neural networks with dynamical recurrent connections. Specifically, we presented the modeling of four coupled neural-synaptic models: the Hopfield-Hebbian model, the firing-rate-Hebbian model, the Hopfield-Oja model, and the firing-rate-Oja model. We considered networks with both excitatory and inhibitory synapses governed by both Hebbian and anti-Hebbian rules. To reflect the inherent synaptic sparsity found in neural circuits, in Section 8.4 we proposed a low dimensional modeling formulation of each model that allowed us to go from a system with $n \times n^2$ variables–n neurons and n^2 synaptic connections–to a system with $n \times m$ variables, where $m \ll n^2$ is the number of non zero elements of the synaptic connection matrix H. In the next chapter, we analyze the dynamical properties of these coupled neural-synaptic models, focusing on their stability and convergence behaviors.

9 Coupled Neural-Synaptic Networks: Analysis

In Chapter 8 we introduced a number of coupled neural-synaptic models, combining biologically plausible recurrent neural networks with dynamical recurrent connections undergoing Hebbian learning rules. In this chapter, we shift our focus to a rigorous analysis of the dynamical behavior of these models. Building on the framework presented in the previous chapter, we now aim to deepen our understanding of the properties of such networks. Specifically, we aim to explore and establish conditions for the stability, robustness, and convergence properties of our coupled neural-synaptic dynamics.

The results in this chapter appeared in the same paper and were presented at the same conferences as those in Chapter 8.

9.1 Introduction

Understanding the dynamical behavior of coupled neural-synaptic networks is important for advancing both biological and artificial systems. Indeed, the analysis of such networks is not only crucial for understanding the underlying mechanisms of learning in biological systems but also for designing ANNs capable of more accurately mimicking natural processes. In this context, Chapter 8 laid the groundwork by introducing models that capture the complex interplay between neurons and synapses. Namely, we presented a number of coupled neural-synaptic models that combine HNN and FNN for the neural dynamics and two different Hebbian learning rules for the synaptic dynamics.

Building upon this framework, we now take a step forward by analyzing the dynamical properties of these models to derive conditions under which the networks exhibit desirable dynamical properties. The goal is to take a first step in the understanding of ANNs that more closely align with the principles governing natural neural networks, to ensure that not only these networks can learn and adapt efficiently but also to guarantee that they do so in a stable and robust manner, mirroring the resilience of biological neural systems. By leveraging tools from contraction theory and other mathematical frameworks, we provide rigorous conditions that guarantee the stability and robustness of our coupled neural-synaptic networks, together with other biologically-inspired forward invariance results.

The chapter is organized as follows. Section 9.2 presents the initial setup for the chapter, outlining the assumptions and notations needed for the analysis. In Section 9.3 we show bounded evolutions of the solutions of the proposed coupled neural-synaptic models. Then, in Section 9.4 we analyze the stability of those systems, by giving sufficient strong infinitesimal contractivity conditions. The contractivity tests we propose are based on biologically meaningful quantities, such as the neural and the synaptic decay rate, the maximum out-degree, the maximum synaptic strength. In Section 9.5, we analyze invariance properties of the synaptic dynamics. Specifically, we show that these dynamics satisfy Dale's principle and analyze the case of symmetric synaptic matrices. Finally, in Section 9.6, we validate the effectiveness of our approach via a numerical example.

9.1.1 Contributions

In this chapter, we establish several key results that advance the understanding of the dynamical properties of the coupled neural-synaptic networks introduced in Chapter 8.

First, we provide biologically-inspired forward invariance results for the coupled neural-synaptic dynamics. Specifically, we show that the solutions of these models are bounded, aligning with the biological observation that neurons eventually saturate with high input values and that synaptic weights are inherently bounded. We also show that, under suitable conditions, our models satisfy Dale's principle – an empirical principle [143] referring to the fact that an individual neuron has either only excitatory or only inhibitory synapses. We then focus on the stability and robustness analysis of the coupled neural-synaptic models. We do so by providing sufficient conditions for the contractivity of each coupled model and leveraging non-Euclidean contraction arguments. Remarkably, our sufficient conditions for contractivity and our lower bounds on the contraction rate are both based upon biologically meaningful quantities, i.e., neural and synaptic decay rate, maximum in-degree, and maximum synaptic strength.

Finally, we complement our theoretical results with numerical simulations on a biologically-inspired network [146]. We leverage this network to illustrate the effectiveness of our conditions and use the numerical results as a motivation to outline possible avenues for future research.

9.2 Set-up

Starting from the low-dimensional reformulations of the coupled neural-synaptic models introduced in Section 8.4 of the previous chapter, we now analyze several dynamical properties of those systems. To conduct this analysis, in this chapter, we work under the following assumptions.

Assumption . *For every neuron i we assume that the activation function satisfies*

(9.A1) $0 \leq \phi(y_i) \leq \phi_{\max} := \max_{i\in\{1,\dots,n\}} \sup_t \phi(y_i(t))$,

(9.A2) $0 \leq \phi'(y_i) \leq 1$.

Moreover, for every i and j, we assume that the external stimuli are such that

(9.A3) $|u_i(t)| \leq u_{\max} := \max_{i\in\{1,\dots,n\}} \sup_t u_i(t)$,

(9.A4) $\left|\bar{U}_{ij}(t)\right| \leq \bar{u}_{\max} := \max_{i,j\in\{1,\dots,n\}} \sup_t \bar{U}_{ij}(t)$.

Remark 9.1.

(i) The assumptions on bounded activation function and external stimuli are used to prove forward invariance results for the coupled neural-synaptic dynamics. While all the assumptions are used for the contraction analysis, as we will show, for the results on the firing-rate-Hebbian and firing-rate-Oja models, Assumption (9.A3) is not needed.

(ii) For each result of this chapter, except for Dale's principle, we can relax Assumption (9.A1) by letting $\phi_{\min} := \min_{i\in\{1,\dots,n\}} \sup_t \phi(y_i(t)) \leq \phi(y_i) \leq \phi_{\max} := \max_{i\in\{1,\dots,n\}} \sup_t \phi(y_i(t))$. We assume $\phi_{\min} = 0$ for simplicity of notations.

(iii) The assumptions are not restrictive in practice. Indeed, widely used activation functions (e.g., sigmoid – see Figure 9.1 for an illustration) satisfy, possibly after rescaling, Assumptions (9.A1) and (9.A2). It is also physically plausible that the external stimuli are bounded.

□

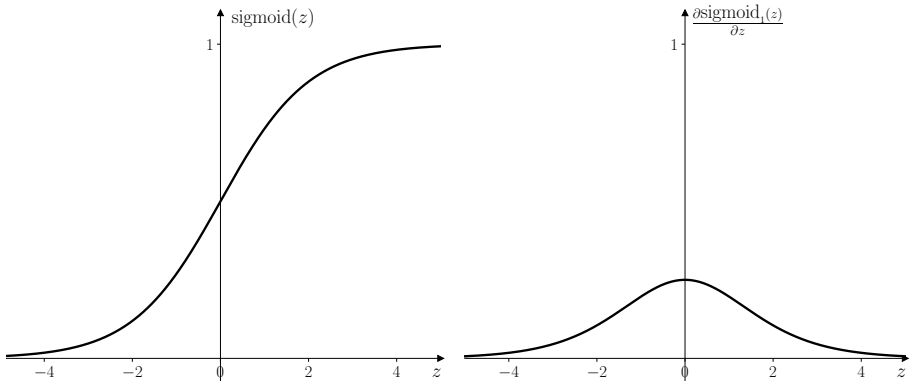

Figure 9.1: Sigmoid function $\text{sigmoid}(z) = \frac{1}{1+e^{-z}}$ (left panel) and its derivative (right panel). As shown, the sigmoid function is slope restricted in $[0, 1]$.

Additionally, we define the following quantities:

- $d_{\max} := \|B_{\text{in}}\|_\infty$ is the maximum topological in-degree of the network.
- $x_{\max} := (u_{\max} + d_{\max}\phi_{\max}w_{\max})/c_{\text{n}}$ is the maximum membrane potential,
- $\nu_{\max} := \phi_{\max}/c_{\text{n}}$ is the maximum firing rate,
- $w_{\max} := (h_{\max}\phi_{\max}^2 + \bar{u}_{\max})/c_{\text{s}}$ is the maximum synaptic weight value.

These quantities are used throughout our analysis to derive conditions for stability, forward invariance, and contractivity of the neural-synaptic models under consideration.

9.3 Dynamical Property of the Models: Bounded Evolution

All biological neurons eventually saturate for high input values and the synaptic weights remain bounded. Inspired by these properties, we now investigate whether the solutions of the coupled neural-synaptic models introduced in Section 8.4 are bounded. To state our results, we define the following sets:

$$\begin{aligned}\mathcal{X} &:= \{x \in \mathbb{R}^n \mid |x_i| \leq x_{\max},\ i \in \{1,\dots,n\}\},\\ \mathcal{V} &:= \{\nu \in \mathbb{R}^n \mid |\nu_i| \leq \nu_{\max},\ i \in \{1,\dots,n\}\},\\ \mathcal{W} &:= \{W \in \mathbb{R}^{n\times n} \mid |W_{ij}| \leq w_{\max},\ i,j \in \{1,\dots,n\}\}.\end{aligned}$$

With the next result, we show that the solutions of the Hopfield-Hebbian model have bounded evolutions when Assumptions (9.A1), (9.A3), and (9.A4) hold.

Lemma 9.1 (Bounded evolutions Hopfield-Hebbian)**.** *Consider model the coupled Hopfield-Hebbian system* (8.13) *and let Assumptions* (9.A1)*,* (9.A3)*, and* (9.A4) *hold. Then, the set $\mathcal{X} \times \mathcal{W}$ is forward invariant and attractive, in the sense that, for every neuron $i \in \{1,\dots,n\}$, and every edge $e \in \{1,\dots,m\}$, the following inequalities hold*

$$|x_i(t)| \leq \big(|x_i(0)| - x_{\max}\big)\mathrm{e}^{-c_{\text{n}}t} + x_{\max}, \qquad t \geq 0, \tag{9.1}$$

$$|w_e(t)| \leq \big(|w_e(0)| - w_{\max}\big)\mathrm{e}^{-c_{\text{s}}t} + w_{\max}, \qquad t \geq 0. \tag{9.2}$$

Proof. Let $(\overline{x}^\top, \overline{w}^\top)^\top$ be a solution of (8.13) having initial conditions $(\overline{x}_0^\top, \overline{w}_0^\top)^\top \in \mathcal{X} \times \mathcal{W}$. Considering the synaptic dynamics in (8.13) written in component, for each edge e we have $\dot{\overline{w}}_e(t) = h_e\big(B_{\text{out}}^\top\Phi(x)\big)_e\big(B_{\text{in}}^\top\Phi(x)\big)_e - c_{\text{s}}\overline{w}_e(t) + \bar{u}_e$, for all $t \geq 0$. Assumptions (9.A1) and (9.A4) and the fact that the matrices $B_{\text{out}}^\top$ and $B_{\text{in}}^\top$ are unit column sum, imply the upper bound

$$\dot{\overline{w}}_e(t) \leq h_{\max}\phi_{\max}^2 - c_s\overline{w}_e(t) + \bar{u}_{\max}. \tag{9.3}$$

Next, let $v(t) := |\overline{w}_e(t)|$, for all $t \geq 0$.From inequality (9.3) we get

$$\begin{aligned}
D^+ |\overline{w}_e(t)| &= \limsup_{k\to 0^+} \frac{1}{k}\big(|\overline{w}_e(t+k)| - |\overline{w}_e(t)|\big) \\
&\leq \limsup_{k\to 0^+} \frac{\big|\overline{w}_e(t) + k\big(h_{\max}\phi^2_{\max} - c_{\mathrm{s}}\overline{w}_e(t) + \bar{u}_{\max}\big)\big| - |\overline{w}_e(t)|}{k} \\
&\leq \limsup_{k\to 0^+} \frac{\|I_m - kc_{\mathrm{s}}I_m\| - 1}{k} |\overline{w}_e(t)| + h_{\max}\phi^2_{\max} + \bar{u}_{\max} \\
&= \mu(-c_{\mathrm{s}}I_m)\, |\overline{w}_e(t)| + h_{\max}\phi^2_{\max} + \bar{u}_{\max} = -c_{\mathrm{s}}\, |\overline{w}_e(t)| + h_{\max}\phi^2_{\max} + \bar{u}_{\max}.
\end{aligned}$$

Therefore $D^+ |\overline{w}_e(t)| \leq -c_{\mathrm{s}} |\overline{w}_e(t)| + h_{\max}\phi^2_{\max} + \bar{u}_{\max}$, for all $t \geq 0$. Next, consider the function $u : \mathbb{R}_{\geq 0} \to \mathbb{R}$ and define the differential equation

$$\dot{u}(t) = g(u,t) := -c_{\mathrm{s}}u(t) + h_{\max}\phi^2_{\max} + \bar{u}_{\max}, \quad u(0) = |\overline{w}_e(0)|\,.$$

Its solution is $u(t) = (|\overline{w}_e(0)| - w_{\max})\mathrm{e}^{-c_{\mathrm{s}}t} + w_{\max}$, where $w_{\max} := \big(h_{\max}\phi^2_{\max} + \bar{u}_{\max}\big)/c_{\mathrm{s}}$. Applying the comparison Lemma 4.1 we have $v(t) \leq u(t)$, for all $t \geq 0$, i.e.,

$$|\overline{w}_e(t)| \leq \big(|\overline{w}_e(0)| - w_{\max}\big)\mathrm{e}^{-c_{\mathrm{s}}t} + w_{\max}. \tag{9.4}$$

Being $\overline{w}_e(0) \in \mathcal{W}$ we get $|\overline{w}_e(t)| \leq w_{\max}$, hence $\overline{w}_e(t) \in \mathcal{W}$, for all $t \geq 0$ and edges e. Moreover, considering the neural dynamics in (8.13) written in component, for each i we have $\dot{\overline{x}}_i = -c_{\mathrm{n}}\overline{x}_i + (B_{\mathrm{in}}[w]B^{\top}_{\mathrm{out}}\Phi(\overline{x}))_i + u_i$. By Assumption (9.A1), Definition (8.7) and having proved that $\overline{w}_e(t) \in \mathcal{W}$, for all $t \geq 0$ and $e \in \{1,\dots,m\}$, it holds

$$\dot{\overline{x}}_i(t) \leq u_{\max} + d_{\max}\phi_{\max}w_{\max} - c_{\mathrm{n}}\overline{x}_i(t).$$

Hence, following steps similar to those we used to bound the synaptic dynamics, we have

$$|\overline{x}_i(t)| \leq \big(|\overline{x}_i(0)| - x_{\max}\big)\mathrm{e}^{-c_{\mathrm{n}}t} + x_{\max}, \tag{9.5}$$

where $x_{\max} := (u_{\max} + d_{\max}\phi_{\max}w_{\max})/c_{\mathrm{n}}$. Being $\overline{x}_i(0) \in \mathcal{X}$ we get $|\overline{x}_i(t)| \leq x_{\max}$. This implies that $\overline{x}_i(t) \in \mathcal{X}$, for all $t \geq 0$ and for all i. Thus the trajectories of any solution $(\overline{x}^{\top}, \overline{w}^{\top})^{\top}$ of the coupled Hopfield-Hebbian system (8.13) having initial conditions in the set $\mathcal{X} \times \mathcal{W}$ remain in this set, which therefore is forward invariant.

Finally, to prove that the set is also attractive, we observe that as $t \to +\infty$ conditions (9.4) and (9.5) are verified for all initial conditions $(x_0^{\top}, w_0^{\top})^{\top}$, not only for those starting in $\mathcal{X} \times \mathcal{W}$. Thus, inequalities (9.1) and (9.2) hold and according to Definition 4.2, the set $\mathcal{X} \times \mathcal{W}$ is attractive. □

Next, we consider the coupled firing-rate-Hebbian model and show that it exhibits bounded evolution of the solutions if Assumptions (9.A1) and (9.A4) hold.

Lemma 9.2 (Bounded evolutions firing-rate-Hebbian)**.** *Consider the coupled firing-rate-Hebbian system* (8.14) *and let Assumptions* (9.A1)*, and* (9.A4) *hold. Then, the set* $\mathcal{V} \times \mathcal{W}$ *is forward invariant and attractive, in the sense that, for every neuron* $i \in \{1,\dots,n\}$*, and every edge* $e \in \{1,\dots,m\}$*, the following inequalities hold*

$$|\nu_i(t)| \leq \big(|\nu_i(0)| - \nu_{\max}\big)\mathrm{e}^{-c_{\mathrm{n}}t} + \nu_{\max}, \qquad t \geq 0, \tag{9.6}$$

$$|w_e(t)| \leq \big(|w_e(0)| - w_{\max}\big)\mathrm{e}^{-c_{\mathrm{s}}t} + w_{\max}, \qquad t \geq 0. \tag{9.7}$$

Proof. The proof, which follows similar steps to the one given for Lemma 9.1, is omitted here for brevity. □

Then, we give the following result for the bounded evolution of the solutions of the Hopfield-Oja model.

Lemma 9.3 (Bounded evolutions Hopfield-Oja)**.** *Consider the coupled Hopfield-Oja system* (8.15) *and let Assumptions* (9.A1)*,* (9.A3) *and* (9.A4) *hold. Then, the set* $\mathcal{X} \times \mathcal{W}$ *is forward invariant and attractive in the sense that, for every neuron* $i \in \{1, \dots, n\}$*, and every edge* $e \in \{1, \dots, m\}$*, inequalities* (9.1) *and* (9.2) *hold.*

Proof. The proof, which follows a reasoning similar to the proof of Lemma 9.1, is obtained once the following upper bound for $D^+ |\overline{w}_e(t)|$ is established

$$D^+ |\overline{w}_e(t)| \leq \mu\big(-c_s I_m - c_o[B_{in}^\top \Phi(x)][B_{in}^\top \Phi(x)]\big) |\overline{w}_e(t)| + h_{max}\phi_{max}^2 + \bar{u}_{max}.$$

Applying the translation property of the log-norm (iii) and noticing that the inequality $-\mu\big(c_o[B_{in}^\top \Phi(x)][B_{in}^\top \Phi(x)]\big) \leq 0$ hold, we get $D^+ |\overline{w}_e(t)| \leq h_{max}\phi_{max}^2 + \bar{u}_{max} - c_s |\overline{w}_e(t)|$, for all $t \geq 0$. The desired results then follow. □

Finally, we show that coupled firing-rate-Oja model exhibits bounded evolution of the solutions if Assumptions (9.A1) and (9.A4) hold.

Lemma 9.4 (Bounded evolutions firing-rate-Oja)**.** *Consider coupled firing-rate-Oja system* (8.16) *and let Assumptions* (9.A1)*, and* (9.A4) *hold. Then, the set* $\mathcal{V} \times \mathcal{W}$ *is forward invariant and attractive, in the sense that, for every neuron* $i \in \{1, \dots, n\}$*, and every edge* $e \in \{1, \dots, m\}$*, inequalities* (9.6) *and* (9.7) *hold.*

Proof. The proof, which follows similar steps to the one given for Lemma 9.3, is omitted here for brevity. □

Remark 9.2. *Lemmas 9.1, 9.2, 9.3, 9.4 ensure that the synaptic rule of each of our models fulfills the boundedness property. This is a desirable property for realistic neural network models, see e.g. [79].* □

9.4 Showing Contractivity of the Models

We now investigate the contractivity of the coupled neural-synaptic models introduced in Section 8.4. Specifically, we give sufficient conditions for strong infinitesimal contractivity by leveraging suitably-defined composite norms (see Section 2.5 for more details). For each model, we propose a contractivity test based on biologically meaningful quantities, such as the neural and the synaptic decay rate, the maximum out-degree, and the maximum synaptic strength. Our first result in this section presents a sufficient condition for the contractivity of the coupled Hopfield-Hebbian model.

Theorem 9.5 (Strong infinitesimal contractivity of the Hopfield-Hebbian model)**.** *Consider the coupled Hopfield-Hebbian model* (8.13) *and let Assumptions* (9.A1) – (9.A4) *hold. Further, assume that:*

$$c_{\mathrm{n}} c_{\mathrm{s}} > 3 d_{\max} h_{\max} \phi_{\max}^2 + d_{\max} \bar{u}_{\max}. \tag{9.8}$$

Then, the dynamics (8.13) *is strongly infinitesimally contracting on* $\mathcal{X} \times \mathcal{W}$ *with respect to the norm* $\| \, [\|x\|_\infty, \|W\|_\infty] \, \|_{p,[\eta]}$*, for any* $p \in [1, \infty]$ *and where* η *is some positive vector. Moreover, the contraction rate is at least*

$$\lambda_{\mathrm{HH}} = -\frac{\tilde{c}_{\mathrm{HH}} + g_{\mathrm{h}} - \sqrt{(\tilde{c}_{\mathrm{HH}} + g_{\mathrm{h}})^2 - 4 g_{\mathrm{h}} c_{\mathrm{s}}^2}}{2 c_{\mathrm{s}}}, \tag{9.9}$$

where $b_{\max} := d_{\max} h_{\max} \phi_{\max}^2$, $\tilde{c}_{\mathrm{HH}} := c_{\mathrm{s}}^2 + 2 b_{\max}$ *, and* $g_{\mathrm{h}} := c_{\mathrm{n}} c_{\mathrm{s}} - 3 b_{\max} - d_{\max} \bar{u}_{\max}$.

Proof. Let us consider the low dimensional formulation of the coupled Hopfield-Hebbian model (8.13) satisfying Assumptions (9.A1) – (9.A4). Its Jacobian is

$$J(x, w) := \left[\begin{array}{c|c} J_{\mathrm{nn}} & J_{\mathrm{ns}} \\ \hline J_{\mathrm{sn}} & J_{\mathrm{ss}} \end{array}\right],$$

where, defining $f_{\mathrm{n}} := -c_{\mathrm{n}} x + B_{\mathrm{in}}[w] B_{\mathrm{out}}^\top \Phi(x) + u$, and $f_{\mathrm{s}} := h \circ B_{\mathrm{out}}^\top \Phi(x) \circ B_{\mathrm{in}}^\top \Phi(x) - c_{\mathrm{s}} w + \bar{u}$, we have

$$\begin{aligned}
J_{\mathrm{nn}} &= \frac{\partial f_{\mathrm{n}}}{\partial x} = -c_{\mathrm{n}} I_n + B_{\mathrm{in}}[w] B_{\mathrm{out}}^\top [\Phi'(x)], \\
J_{\mathrm{ns}} &= \frac{\partial f_{\mathrm{n}}}{\partial w} = \frac{\partial \big(B_{\mathrm{in}}[B_{\mathrm{out}}^\top \Phi(x)] w \big)}{\partial w} = B_{\mathrm{in}}[B_{\mathrm{out}}^\top \Phi(x)], \\
J_{\mathrm{sn}} &= \frac{\partial f_{\mathrm{s}}}{\partial x} = [h] \big([B_{\mathrm{out}}^\top \Phi(x)] B_{\mathrm{in}}^\top + [B_{\mathrm{in}}^\top \Phi(x)] B_{\mathrm{out}}^\top \big) [\Phi'(x)], \\
J_{\mathrm{ss}} &= \frac{\partial f_{\mathrm{s}}}{\partial w} = -c_{\mathrm{s}} I_m.
\end{aligned}$$

We consider the infinity norm both on $\mathbb{R}^n$ and $\mathbb{R}^m$ and we define the aggregate Metzler majorant of the matrix $J(x, w)$:

$$|J(x, w)|_{\mathrm{M}} = \left[\begin{array}{cc} \mu_\infty(J_{\mathrm{nn}}) & \|J_{\mathrm{ns}}\|_\infty \\ \|J_{\mathrm{sn}}\|_\infty & \mu_\infty(J_{\mathrm{ss}}) \end{array}\right]. \tag{9.10}$$

For any $p \in [1, \infty]$ and for $\eta > 0$ as in Lemma 2.3 we consider the aggregation norm $\| \cdot \|_{\mathrm{agg}} = \| \cdot \|_{p,[\eta]}$. Then Theorem 2.4 implies

$$\mu_{\mathrm{cmpst}}(J(x, W)) \leq \mu_{p,[\eta]}(|J(x, w)|_{\mathrm{M}}).$$

From Proposition 2.5 we know $\|B_{\mathrm{in}}^\top\|_\infty = \|B_{\mathrm{out}}^\top\|_\infty = 1$. Also, being $\|[\Phi'(x)]\|_\infty \leq 1$, $\|\Phi(x)\|_\infty = \phi_{\max}$ and $|W_{ij}| \leq (h_{\max} \phi_{\max}^2 + \bar{u}_{\max})/c_{\mathrm{s}}$, for all $i, j \in \{1, \dots, n\}$, we

bound:

$$
\begin{aligned}
\|J_{\text{ns}}\|_\infty &\le \|B_{\text{in}}\|_\infty \|[B_{\text{out}}^\top \Phi(x)]\|_\infty \le d_{\max}\phi_{\max},\\
\|J_{\text{sn}}\|_\infty &\le \|[h]\|_\infty \|[B_{\text{out}}^\top \Phi(x)]B_{\text{in}}^\top + [B_{\text{in}}^\top \Phi(x)]B_{\text{out}}^\top\|_\infty \le 2h_{\max}\phi_{\max},\\
\mu_\infty(J_{\text{nn}}) &= -c_{\text{n}} + \mu_\infty\big(B_{\text{in}}[w]B_{\text{out}}^\top[\Phi'(x)]\big) \le -c_{\text{n}} + \|B_{\text{in}}[w]B_{\text{out}}^\top[\Phi'(x)]\|_\infty\\
&\le d_{\max}\big(h_{\max}\phi_{\max}^2 + \bar{u}_{\max}\big)/c_{\text{s}} - c_{\text{n}},\\
\mu_\infty(J_{\text{ss}}) &= -c_{\text{s}}.
\end{aligned}
$$

Hence $|J(x,w)|_{\text{M}} \le \begin{bmatrix} \dfrac{d_{\max}\big(h_{\max}\phi_{\max}^2 + \bar{u}_{\max}\big)}{c_{\text{s}}} - c_{\text{n}} & d_{\max}\phi_{\max} \\ 2h_{\max}\phi_{\max} & -c_{\text{s}} \end{bmatrix} := \tilde{J}_{\text{M-HH}}$.

Applying the monotonicity property of the log-norm of a Metzler matrix, and being $\tilde{J}_{\text{M-HH}}$ an irreducible Metzler matrix, from Lemma 2.3 we get

$$\mu_{p,[\eta]}(|J(x,w)|_{\text{M}}) \le \mu_{p,[\eta]}(\tilde{J}_{\text{M-HH}}) = \alpha(\tilde{J}_{\text{M-HH}}).$$

Finally, the last step is to find conditions for which $\tilde{J}_{\text{M-HH}}$, and thus $|J(x,w)|_{\text{M}}$, is Hurwitz. In our case, being $\tilde{J}_{\text{M-HH}}$ a 2×2 matrix this happens if and only if

$$\det(\tilde{J}_{\text{M-HH}}) = c_{\text{n}}c_{\text{s}} - 3d_{\max}h_{\max}\phi_{\max}^2 - d_{\max}\bar{u}_{\max} > 0, \tag{9.11}$$

and $\operatorname{tr}(\tilde{J}_{\text{M-HH}}) = d_{\max}(h_{\max}\phi_{\max}^2 + \bar{u}_{\max})/c_{\text{s}} - c_{\text{n}} - c_{\text{s}} < 0$, i.e.,

$$c_{\text{n}}c_{\text{s}} > -c_{\text{s}}^2 + d_{\max}(h_{\max}\phi_{\max}^2 + \bar{u}_{\max}). \tag{9.12}$$

Now, since condition (9.11) implies (9.12), $\tilde{J}_{\text{M-HH}}$ is Hurwitz if and only if condition (9.11), that is condition (9.8), holds. Next, we determine the spectral abscissa of $\tilde{J}_{\text{M-HH}}$. Note that the eigenvalues of $\tilde{J}_{\text{M-HH}}$ are the zero of the characteristic polynomial

$$p(\lambda) = \lambda^2 - \operatorname{tr}(\tilde{J}_{\text{M-HH}})\lambda + \det(\tilde{J}_{\text{M-HH}}),$$

where $b_{\max} := d_{\max}h_{\max}\phi_{\max}^2$, $\operatorname{tr}(\tilde{J}_{\text{M-HH}}) = (b_{\max} + \bar{u}_{\max}d_{\max})/c_{\text{s}} - c_{\text{s}} - c_{\text{n}}$, and $\det(\tilde{J}_{\text{M-HH}}) = c_{\text{n}}c_{\text{s}} - 3b_{\max} - \bar{u}_{\max}d_{\max}$. Defining $\tilde{c}_{\text{HH}} := c_{\text{s}}^2 + 2b_{\max}$, and $g_{\text{h}} := c_{\text{n}}c_{\text{s}} - 3b_{\max} - d_{\max}\bar{u}_{\max}$, we write $p(\lambda) = \lambda^2 + \left(\dfrac{\tilde{c}_{\text{HH}} + g_{\text{h}}}{c_{\text{s}}}\right)\lambda + g_{\text{h}}$. We have $p(\lambda) = 0$ if and only if

$$
\begin{aligned}
\lambda_1 &= -\frac{\tilde{c}_{\text{HH}} + g_{\text{h}} - \sqrt{(\tilde{c}_{\text{HH}} + g_{\text{h}})^2 - 4g_{\text{h}}c_{\text{s}}^2}}{2c_{\text{s}}},\\
\lambda_2 &= -\frac{\tilde{c}_{\text{HH}} + g_{\text{h}} + \sqrt{(\tilde{c}_{\text{HH}} + g_{\text{h}})^2 - 4g_{\text{h}}c_{\text{s}}^2}}{2c_{\text{s}}}.
\end{aligned}
$$

We observe that the delta of the polonium $p(\lambda)$ is

$$\Delta = \frac{(c_{\text{s}}^2 + g_{\text{h}} + 2b_{\max})^2 - 4g_{\text{h}}c_{\text{s}}^2}{c_{\text{s}}^2} = \frac{(g_{\text{h}} - c_{\text{s}}^2)^2 + 4b_{\max}(b_{\max} + c_{\text{s}}^2 + g_{\text{h}})}{c_{\text{s}}^2}.$$

Assuming condition (9.8) (which implies that $g_{\text{h}} > 0$) and being $b_{\max}$ and c_{s} non negative, we have $\Delta > 0$, so that $\lambda_2 < \lambda_1 = \alpha(\tilde{J}_{\text{M-HH}}) := \lambda_{\text{HH}}$.

Hence, if (9.8) is satisfied, then, from the definition of contracting systems 4.3, we have that the coupled neural synaptic dynamics (8.13) is strongly infinitesimally contracting and its contraction rate is at least λ_{HH}. This completes the proof. □

With the next result, we give a sufficient condition for the contractivity of the firing-rate-Hebbian model.

Theorem 9.6 (Strong infinitesimal contractivity of the firing-rate-Hebbian model)**.** *Consider the coupled firing-rate-Hebbian system* (8.14) *and let Assumptions* (9.*A*1), (9.*A*2) *and* (9.*A*4) *hold. Further, assume that:*

$$c_{\text{n}} c_{\text{s}} > d_{\max} h_{\max} \phi_{\max}^2 \left(1 + \frac{2}{c_{\text{n}}}\right) + d_{\max} \bar{u}_{\max}. \tag{9.13}$$

Then, the dynamics (8.14) *is strongly infinitesimally contracting on* $\mathcal{V} \times \mathcal{W}$ *with respect to the norm* $\| \, [\|\nu\|_\infty, \|W\|_\infty] \, \|_{p,[\eta]}$*, for any* $p \in [1, \infty]$ *and where* η *is some positive vector. Moreover, the contraction rate is at least*

$$\lambda_{\text{FH}} = -\frac{\tilde{c}_{\text{FH}} + g_{\text{f}} - \sqrt{(\tilde{c}_{\text{FH}} + g_{\text{f}})^2 - 4 g_{\text{f}} c_{\text{s}}^2}}{2 c_{\text{s}}}, \tag{9.14}$$

where $g_{\text{f}} := c_{\text{n}} c_{\text{s}} - a_{\max} \left(1 + 2/c_{\text{n}}\right) - \bar{u}_{\max} d_{\max}$ *and* $\tilde{c}_{\text{FH}} := c_{\text{s}}^2 + 2 a_{\max}/c_{\text{n}}$.

Proof. The proof follows similar steps as these used to prove Theorem 9.5. The full proof is therefore omitted here, we only notice that, for the firing-rate-Hebbian dynamics, the Jacobian is partitioned into the following matrices:

$$\begin{aligned}
J_{\text{nn}} &= B_{\text{in}}[w] B_{\text{out}}^\top \left[\Phi'\left(B_{\text{in}}[w] B_{\text{out}}^\top \nu + u\right)\right] - c_{\text{n}} I_n, \\
J_{\text{ns}} &= B_{\text{in}}[B_{\text{out}}^\top \nu] \left[\Phi'\left(B_{\text{in}}[w] B_{\text{out}}^\top \nu + u\right)\right], \\
J_{\text{sn}} &= [h]\left([B_{\text{out}}^\top \Phi(\nu)] B_{\text{in}}^\top + [B_{\text{in}}^\top \Phi(\nu)] B_{\text{out}}^\top\right)[\Phi'(\nu)], \\
J_{\text{ss}} &= -c_{\text{s}} I_m.
\end{aligned}$$

Additionally, we compute the lower bounds on the contraction rate. To this purpose, consider the matrix

$$\tilde{J}_{\text{M-FH}} = \begin{bmatrix} d_{\max}(h_{\max} \phi_{\max}^2 + \bar{u}_{\max})/c_{\text{s}} - c_{\text{n}} & d_{\max} \phi_{\max}/c_{\text{n}} \\ 2 h_{\max} \phi_{\max} & -c_{\text{s}} \end{bmatrix}.$$

We have $p(\lambda) = \lambda^2 + \dfrac{1}{c_{\text{s}}} \left(\tilde{c}_{\text{FH}} + g_{\text{f}}\right) \lambda + g_{\text{f}}$. We observe that under condition (9.13) it is $g_{\text{f}} > 0$. We have $p(\lambda) = 0$ if and only if

$$\begin{aligned}
\lambda_1 &= -\frac{\tilde{c}_{\text{FH}} + g_{\text{f}} - \sqrt{(\tilde{c}_{\text{FH}} + g_{\text{f}})^2 - 4 g_{\text{f}} c_{\text{s}}^2}}{2 c_{\text{s}}}, \\
\lambda_2 &= -\frac{\tilde{c}_{\text{FH}} + g_{\text{f}} + \sqrt{(\tilde{c}_{\text{FH}} + g_{\text{f}})^2 - 4 g_{\text{f}} c_{\text{s}}^2}}{2 c_{\text{s}}}.
\end{aligned}$$

We observe that the determinant of $p(\lambda)$ is

$$\begin{aligned}\Delta &= \frac{1}{c_{\mathrm{s}}^2}\left(\left(c_{\mathrm{s}}^2 + g_{\mathrm{f}} + \frac{2}{c_{\mathrm{n}}}a_{\max}\right)^2 - 4g_{\mathrm{f}}c_{\mathrm{s}}^2\right)\\ &= \frac{1}{c_{\mathrm{s}}^2}\left(\left(g_{\mathrm{f}} - c_{\mathrm{s}}^2\right)^2 + \frac{4}{c_{\mathrm{n}}}a_{\max}\left(\frac{a_{\max}}{c_{\mathrm{n}}} + g_{\mathrm{f}} + c_{\mathrm{s}}^2\right)\right).\end{aligned}$$

Therefore, under condition (9.13) and being $a_{\max}, c_{\mathrm{n}}, c_{\mathrm{s}}$ non negative, it always results $\Delta > 0$, so that $\alpha(|J(x,w)|_{\mathrm{M}}) := \lambda_{\mathrm{FH}} = \lambda_1$. □

With the next result, we give a sufficient condition for the contractivity of the Hopfield-Oja model.

Theorem 9.7 (Strong infinitesimal contractivity of the Hopfield-Oja model)**.** *Consider the the coupled Hopfield-Oja system* (8.15) *and let Assuptions* (9.*A*1) – (9.*A*4) *hold. Further, assume that:*

$$c_{\mathrm{n}}c_{\mathrm{s}} > d_{\max}\left(3h_{\max}\phi_{\max}^2 + \bar{u}_{\max}\right) + 2\frac{c_{\mathrm{o}}}{c_{\mathrm{s}}}\phi_{\max}^2 d_{\max}\left(h_{\max}\phi_{\max}^2 + \bar{u}_{\max}\right). \tag{9.15}$$

Then, the dynamics (8.15) *is strongly infinitesimally contracting on* $\mathcal{X}\times\mathcal{W}$ *with respect to the norm* $\|\,[\|x\|_\infty, \|W\|_\infty]\,\|_{p,[\eta]}$*, for any* $p \in [1,\infty]$ *and where* η *is some positive vector. Moreover, the contraction rate is at least*

$$\lambda_{\mathrm{HO}} = -\frac{\tilde{c}_{\mathrm{HO}} + g_{\mathrm{o}} - \sqrt{\left(\tilde{c}_{\mathrm{HO}} + g_{\mathrm{o}}\right)^2 - 4g_{\mathrm{o}}c_{\mathrm{s}}^2}}{2c_{\mathrm{s}}},$$

where $\tilde{c}_{\mathrm{HO}} := c_{\mathrm{s}}^2 + 2b_{\max} + 2\phi^2 c_{\mathrm{o}}/c_{\mathrm{s}}\left(b_{\max} + d_{\max}\bar{u}_{\max}\right)$ *and* $g_{\mathrm{o}} := c_{\mathrm{n}}c_{\mathrm{s}} - 3d_{\max}h_{\max}\phi_{\max}^2 + d_{\max}\bar{u}_{\max} - 2\frac{c_{\mathrm{o}}}{c_{\mathrm{s}}}\phi_{\max}^2\left(d_{\max}h_{\max}\phi_{\max}^2 + d_{\max}\bar{u}_{\max}\right)$.

Proof. The full proof, which follows similar steps to the ones used to prove Theorem 9.5, is omitted here for brevity. We only note that, for the Hopfield-Oja dynamics, the Jacobian is partitioned into the following matrices:

$$\begin{aligned}J_{\mathrm{nn}} &= -c_{\mathrm{n}}I_n + B_{\mathrm{in}}[w]B_{\mathrm{out}}^\top[\Phi'(x)],\\ J_{\mathrm{ns}} &= B_{\mathrm{in}}[B_{\mathrm{out}}^\top\Phi(x)],\\ J_{\mathrm{sn}} &= [h]\left([B_{\mathrm{out}}^\top\Phi(x)]B_{\mathrm{in}}^\top + [B_{\mathrm{in}}^\top\Phi(x)]B_{\mathrm{out}}^\top\right)[\Phi'(x)] - 2c_{\mathrm{o}}[w][B_{\mathrm{in}}^\top\Phi(x)]B_{\mathrm{in}}^\top[\Phi'(x)],\\ J_{\mathrm{ss}} &= -c_{\mathrm{s}}I_m - c_{\mathrm{o}}[B_{\mathrm{in}}^\top\Phi(x)][B_{\mathrm{in}}^\top\Phi(x)].\end{aligned}$$

For completeness, we also compute the lower bounds on the contraction rate. To this purpose, consider the matrix

$$\tilde{J}_{\text{M-HO}} = \begin{bmatrix} d_{\max}(h_{\max}\phi_{\max}^2 + \bar{u}_{\max})/c_{\mathrm{s}} - c_{\mathrm{n}} & d_{\max}\phi_{\max} \\ 2\phi_{\max}(h_{\max} + c_{\mathrm{o}}(h_{\max}\phi_{\max}^2 + \bar{u}_{\max})/c_{\mathrm{s}}) & -c_{\mathrm{s}}\end{bmatrix}$$

and its characteristic polynomial $p(\lambda) = \lambda^2 + \left(\frac{\tilde{c}_{\text{HO}} + g_{\text{o}}}{c_{\text{s}}}\right)\lambda + g_{\text{o}}$. We have $p(\lambda) = 0$ if and only if

$$\lambda_1 = -\frac{\tilde{c}_{\text{HO}} + g_{\text{o}} - \sqrt{\left(\tilde{c}_{\text{HO}} + g_{\text{o}}\right)^2 - 4g_{\text{o}}c_{\text{s}}^2}}{2c_{\text{s}}},$$
$$\lambda_2 = -\frac{\tilde{c}_{\text{HO}} + g_{\text{o}} + \sqrt{\left(\tilde{c}_{\text{HO}} + g_{\text{o}}\right)^2 - 4g_{\text{o}}c_{\text{s}}^2}}{2c_{\text{s}}}.$$

The determinant of $p(\lambda)$ is

$$\begin{aligned}\Delta &= \frac{\left(c_{\text{s}}^2 + g_{\text{o}} + 2b_{\max} + 2\phi^2 c_{\text{o}}/c_{\text{s}}(b_{\max} + d_{\max}\bar{u}_{\max})\right)^2}{c_{\text{s}}^2} - 4g_{\text{o}} \\ &= \frac{(g_{\text{o}} - c_{\text{s}}^2)^2 + 4b_{\max}(b_{\max} + c_{\text{s}}^2 + g_{\text{o}})}{c_{\text{s}}^2} + \frac{4\phi^4 c_{\text{o}}^2/c_{\text{s}}^2(b_{\max} + d_{\max}\bar{u}_{\max})^2}{c_{\text{s}}^2} \\ &\quad + \frac{4\phi^2 c_{\text{o}}/c_{\text{s}}(b_{\max} + d_{\max}\bar{u}_{\max})\left(c_{\text{s}}^2 + g_{\text{o}} + 2b_{\max}\right)}{c_{\text{s}}^2}.\end{aligned}$$

Therefore, under condition (9.15) and being $b_{\max}$, c_{o}, and c_{s} non negative, it always results $\Delta > 0$, so that $\alpha(\tilde{J}_{\text{M-HO}}) := \lambda_{\text{HO}} = \lambda_1$. □

Finally, with the next result, we give a sufficient condition for the contractivity of the firing-rate-Oja model.

Theorem 9.8 (Strong infinitesimal contractivity of the firing-rate-Oja model)**.** *Consider the coupled firing-rate-Oja* (8.16) *and let Assumptions* (9.A1)*,* (9.A2) *and* (9.A4) *hold. Further, assume that:*

$$c_{\text{n}}c_{\text{s}} > d_{\max}h_{\max}\phi_{\max}^2\left(1 + \frac{2}{c_{\text{n}}}\right) + d_{\max}\bar{u}_{\max} + 2\frac{c_{\text{o}}}{c_{\text{s}}c_{\text{n}}}\phi_{\max}^2 d_{\max}\left(h_{\max}\phi_{\max}^2 + \bar{u}_{\max}\right). \quad (9.16)$$

Then, the dynamics (8.16) *is strongly infinitesimally contracting on $\mathcal{V} \times \mathcal{W}$ with respect to the norm $\| [\|\nu\|_\infty, \|W\|_\infty] \|_{p,[\eta]}$, for any $p \in [1, \infty]$ and where η is some positive vector. Moreover, the contraction rate is at least*

$$\lambda_{\text{FO}} = -\frac{\tilde{c}_{\text{FO}} + g_{\text{of}} - \sqrt{\left(\tilde{c}_{\text{FO}} + g_{\text{of}}\right)^2 - 4g_{\text{of}}c_{\text{s}}^2}}{2c_{\text{s}}},$$

where $a_{\max} := d_{\max}h_{\max}\phi_{\max}^2$, $\tilde{c}_{\text{FO}} := c_{\text{s}}^2 + 2a_{\max}/c_{\text{n}} + 2\phi^2\frac{c_{\text{o}}}{c_{\text{s}}c_{\text{n}}}\left(a_{\max} + d_{\max}\bar{u}_{\max}\right)$ and $g_{\text{of}} = c_{\text{n}}c_{\text{s}} - a_{\max}\left(1 + \frac{2}{c_{\text{n}}}\right) - d_{\max}\bar{u}_{\max} - 2\frac{c_{\text{o}}}{c_{\text{s}}c_{\text{n}}}\phi_{\max}^2\left(a_{\max} + d_{\max}\bar{u}_{\max}\right)$.

Proof. We omit the proof since it follows the same steps of Theorem 9.5. The main differences are the Jacobian of (8.16) and the bound on the contraction rate, that, for

completeness, we present here. The Jacobian is partitioned into the following matrices:

$$
\begin{aligned}
J_{\text{nn}} &= -c_{\text{n}} I_n + B_{\text{in}}[w] B_{\text{out}}^{\top} \left[\Phi'\left(B_{\text{in}}[w] B_{\text{out}}^{\top}\nu + u\right)\right], \\
J_{\text{ns}} &= B_{\text{in}}[B_{\text{out}}^{\top}\nu] \left[\Phi'\left(B_{\text{in}}[w] B_{\text{out}}^{\top}\nu + u\right)\right], \\
J_{\text{sn}} &= [h]\left([B_{\text{out}}^{\top}\Phi] B_{\text{in}}^{\top} + [B_{\text{in}}^{\top}\Phi] B_{\text{out}}^{\top}\right)[\Phi'] 2c_{\text{o}}[w][B_{\text{in}}^{\top}\Phi(x)] B_{\text{in}}^{\top}[\Phi'], \\
J_{\text{ss}} &= -c_{\text{s}} I_m - c_{\text{o}}[B_{\text{in}}^{\top}\Phi(x)][B_{\text{in}}^{\top}\Phi(x)].
\end{aligned}
$$

Additionally, the lower bound on the contractivity rate is given by the following standard reasoning. Given the matrix

$$
\tilde{J}_{\text{M-FO}} = \begin{bmatrix} \dfrac{d_{\max}(h_{\max}\phi_{\max}^2 + \bar{u}_{\max})}{c_{\text{s}}} - c_{\text{n}} & \dfrac{d_{\max}\phi_{\max}}{c_{\text{n}}} \\ 2\phi_{\max}\left(h_{\max} + \dfrac{c_{\text{o}}}{c_{\text{s}}}(h_{\max}\phi_{\max}^2 + \bar{u}_{\max})\right) & -c_{\text{s}} \end{bmatrix}
$$

and its characteristic polynomial $p(\lambda) = \lambda^2 + \left(\frac{\tilde{c}_{\text{FO}} + g_{\text{of}}}{c_{\text{s}}}\right)\lambda + g_{\text{of}}$, where for simplicity of notation we have defined $a_{\max} := d_{\max} h_{\max} \phi_{\max}^2$, $\tilde{c}_{\text{FO}} := c_{\text{s}}^2 + 2a_{\max}/c_{\text{n}} + 2\phi_{\max}^2 \frac{c_{\text{o}}}{c_{\text{s}} c_{\text{n}}}(a_{\max} + d_{\max}\bar{u}_{\max})$ and $g_{\text{of}} = c_{\text{n}} c_{\text{s}} - a_{\max}\left(1 + \frac{2}{c_{\text{n}}}\right) - d_{\max}\bar{u}_{\max} - 2\frac{c_{\text{o}}}{c_{\text{s}} c_{\text{n}}}\phi_{\max}^2 (a_{\max} + d_{\max}\bar{u}_{\max})$. We observe that under condition (9.16) it is $g_{\text{h}} > 0$. We have $p(\lambda) = 0$ if and only if

$$
\begin{aligned}
\lambda_1 &= -\frac{\tilde{c}_{\text{FO}} + g_{\text{of}} - \sqrt{\left(\tilde{c}_{\text{FO}} + g_{\text{of}}\right)^2 - 4 g_{\text{of}} c_{\text{s}}^2}}{2c_{\text{s}}}, \\
\lambda_2 &= -\frac{\tilde{c}_{\text{FO}} + g_{\text{of}} + \sqrt{\left(\tilde{c}_{\text{FO}} + g_{\text{of}}\right)^2 - 4 g_{\text{of}} c_{\text{s}}^2}}{2c_{\text{s}}}.
\end{aligned}
$$

It is

$$
\begin{aligned}
\Delta &= \frac{\left(c_{\text{s}}^2 + g_{\text{of}} + 2\frac{a_{\max}}{c_{\text{n}}} + 2\phi_{\max}^2 \frac{c_{\text{o}}}{c_{\text{s}} c_{\text{n}}}(a_{\max} + d_{\max}\bar{u}_{\max})\right)^2}{c_{\text{s}}^2} - 4g_{\text{of}} \\
&= \frac{(g_{\text{of}} - c_{\text{s}}^2)^2 + 4\frac{a_{\max}}{c_{\text{n}}}\left(\frac{a_{\max}}{c_{\text{n}}} + c_{\text{s}}^2 + g_{\text{of}}\right)}{c_{\text{s}}^2} + \frac{4\phi_{\max}^4 \left(\frac{c_{\text{o}}}{c_{\text{s}} c_{\text{n}}}\right)^2 (a_{\max} + d_{\max}\bar{u}_{\max})^2}{c_{\text{s}}^2} \\
&\quad + \frac{4\phi_{\max}^2 \frac{c_{\text{o}}}{c_{\text{s}} c_{\text{n}}}(a_{\max} + d_{\max}\bar{u}_{\max})\left(c_{\text{s}}^2 + g_{\text{of}} + 2\frac{a_{\max}}{c_{\text{n}}}\right)}{c_{\text{s}}^2}.
\end{aligned}
$$

Therefore, under condition (9.16) and being $b_{\max}$, c_{o}, and c_{s} non negative, it always results $\Delta > 0$, so that $\alpha(\tilde{J}_{\text{M-FO}}) := \lambda_{\text{FO}} = \lambda_1$. □

Finally, we close this section with the following observation. Comparing conditions (9.8), (9.13), (9.15) and (9.16), we can see that the contractivity test for the coupled Hopfield-Oja (8.15) and firing-rate-Oja (8.16) systems are more conservative than the

test for the coupled Hopfield-Hebbian (8.13) and firing-rate-Hebbian (8.14) systems. On the other hand, when $c_{\mathrm{n}} = 1$ the contractivity test for the Hopfield-Hebbian and the firing-rate-Hebbian models is the same, while when $c_n > 1$ (9.13) gives sharper contractivity condition with respect to (9.8). Vice versa when $c_n < 1$.

Remark 9.3.

- *Sparse connectivity enables the low-dimensional reformulations of the coupled neural-synaptic systems* (8.9) – (8.12) *as systems* (8.13) – (8.16)*. The contractivity conditions in* (9.8)*,* (9.13)*,* (9.15) *and* (9.16)*, are less conservative compared to what one could obtain if the analysis was applied directly to the original dynamics* (8.9) – (8.12)*.*
- *Throughout this section as in, e.g., [23, 79, 102, 59], we consider homogeneous decay rates. However, it is worth noting that our analysis can be generalized to heterogeneous decay rates. For example, let c_n^i be the decay rate for the i-th neuron so that the dynamics* (3.1) *reads $\dot{x}_i = -c_{\mathrm{n}}^i x_i + \sum_{j=1}^n W_{ij}\phi(x_j) + u_i$. Then the contractivity condition* (9.8) *becomes*

$$\big(\min_i c_{\mathrm{n}}^i\big)c_{\mathrm{s}} > 3d_{\max}h_{\max}\phi_{\max}^2 + d_{\max}\bar{u}_{\max}.$$

□

9.5 Invariance Properties of the Synaptic Dynamics

In this section, we explore invariance properties of the synaptic dynamics of our neural-synaptic models. These invariance results are important as they ensure that certain biological constraints are respected throughout the evolution of the system, thereby enhancing the biological plausibility of the models.

9.5.1 Dale's Principle

Biological neurons release either excitatory (E) or inhibitory (I) outgoing synapses, not both [143, 147]. This characteristic, known as *Dale's Principle*, imposes a strict constraint on the type of output a neuron can produce. Specifically, Dale's Principle implies that a single neuron cannot have a mixture of positive (excitatory) and negative (inhibitory) output synapses. Furthermore, the nature of these synapses is invariant over time, meaning that once a neuron is classified as excitatory or inhibitory, all of its outgoing synapses remain either non-negative or non-positive, respectively, for all time. Mathematically, this principle implies that the elements of the columns of the synaptic weight matrix $W(t)$ are either all non-negative or all non-positive at any time t.

We illustrate Dale's principle with a simple example of a network of five neurons in Figure 9.2. In the example, the network on the left satisfies the principle, as each neuron releases either excitatory or inhibitory outgoing synapses, but not both. In contrast, the network on the right violates Dale's Principle, as neurons 2 and 4 release both excitatory and inhibitory synapses.

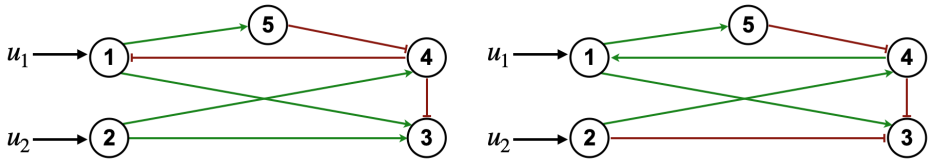

Figure 9.2: Left: Example of a network satisfying Dale's principle. Each neuron has either all positive (green) or all negative (red) output synapses. Right: Example of a network that violates Dale's Principle, as neurons 2 and 4 have both positive and negative output synapses.

9.5.2 Invariance Results for the Synaptic Dynamics: Dale's Principle

We now investigate if the models considered in this thesis satisfy Dale's Principle.

Lemma 9.9 (Dale's Principle)**.** *Consider the coupled neural-synaptic models* (8.9) – (8.12) *with external synaptic stimuli* $\bar{U} = 0$ *and let Assumptions* (9.A1)–(9.A3) *hold. Pick a neuron* $j \in \{1, \dots, n\}$*. If, for all* $i \in \{1, \dots, n\}$*:*

(i) $H_{ij} > 0$ *and* $W_{ij}(0) \geq 0$*, then* $W_{ij}(t) \geq 0$*,* $\forall t \geq 0$*,*

(ii) $H_{ij} < 0$ *and* $W_{ij}(0) \leq 0$*, then* $W_{ij}(t) \leq 0$*,* $\forall t \geq 0$*.*

Proof. We start by proving statement (i) for the coupled Hopfield-Oja model (8.11) with $\bar{U}_{ij} = 0$. We show the result by considering the synaptic dynamics

$$\dot{W}_{ij}(t) = H_{ij}\phi(y_i(t))\phi(y_j(t)) - (c_s + c_o\phi^2(y_i(t)))W_{ij}(t), \tag{9.17}$$

with $y_i(t)$ and $y_j(t)$ being exogenous inputs. Let $W_j := (W_{ij})_{i\in\{1,\dots,n\}} \in \mathbb{R}^n$ be the j-th column of W. We show that, if the assumptions in (i) are satisfied, then the positive orthant is forward invariant for the dynamics for W_j uniformly in $y_i(t)$ and $y_j(t)$.

To this aim, note that by assumptions when $W_{ij} = 0$, the right-hand side in (9.17) is non-negative. Hence, by Nagumo's Theorem 4.2, the positive orthant is forward invariant for (9.17). Moreover, since this property holds for all signals $y_i(t)$ and $y_j(t)$, this property also holds when $y_i(t) = x_i(t)$ and $y_j(t) = x_j(t)$. This gives the result for the coupled Hopfield-Oja (8.11) and firing-rate-Oja (8.12) models. Furthermore, the non-negativity condition for the right-hand side in (9.17) also holds when $c_o = 0$, and this, in turn, yields the result for coupled Hopfield-Hebbian (8.9) and firing-rate-Hebbian (8.10) models. The proof of statement (ii) follows similar reasoning and is omitted here for brevity. □

Remark 9.4. *A key assumption in Lemma 9.9 is that the models satisfy (9.A1), ensuring the activation function's non-negativity. It is worth noting that if the activation function acting on the pre-synaptic node* y_j *has an opposite sign with respect to the one acting on the post-synaptic node* y_i*, then not only Dale's principle is not satisfied, but neurons over time will change the outgoing synapses they release. That is, excitatory synapses become inhibitory and vice-versa.* □

9.5.3 Invariance Results for the Synaptic Dynamics: Symmetric Matrices

Finally, we investigate invariant results for symmetric synaptic matrices. We analyze this aspect as in the neuroscience literature this appears to be a key property for a number of well-known models, e.g., [22, 58, 24, 9]. Nevertheless, the assumption of symmetric weight matrices, which is often made to streamline the mathematical analysis, violates Dale's Principle. To investigate invariant results for symmetric synaptic matrices, we consider the dynamics (8.5) in vector form with $\bar{U} = 0$:

$$\dot{W}(t) = H \circ \Phi(y(t))\Phi(y(t))^\top - c_s W(t), \tag{9.18}$$

where $y(t)$ is an exogenous input. The following Lemma formalizes the fact that, if H is symmetric the system always converges to a symmetric synaptic matrix. Moreover, if $W(0)$ is symmetric, then $W(t) = W^\top(t)$, $\forall t \geq 0$.

Lemma 9.10. *[Invariance Results for the Symmetric Synaptic Matrices] Consider the coupled Hopfield-Hebbian (8.9) and firing-rate-Hebbian (8.10) models with external synaptic stimuli $\bar{U} = 0$, satisfying Assumptions (9.A1)–(9.A3). Assume that H is symmetric and let $W_S(t)$ and $W_A(t)$ be the symmetric and skew-symmetric components of $W(t)$, then:*

(i) if $W_A(0) = 0$, then $W_A(t) = 0$, $\forall t \geq 0$;

(ii) $\lim_{t\to\infty} W_A(t) = 0$.

Proof. The proof is inspired by [23, Appendix 8.1]. First, we write $W(t) = W_S(t) + W_A(t)$, $\forall t \geq 0$, so that equation (9.18) can be written as

$$\dot{W}_S + \dot{W}_A = (H \circ \Phi(y)\Phi(y)^\top - c_s W_S) - c_s W_A.$$

To prove statement (i) note that $W_A(0) = 0$ implies that the right end side in (9.18) is symmetric at time $t = 0$, thus $W_A(t) = 0$, $\forall t \geq 0$ and uniformly in $y(t)$. This leads to the desired result. Next, for statement (ii) it suffices to note that the dynamics for the skew-symmetric component of $W(t)$ are given by $\dot{W}_A(t) = -c_s W_A(t)$, whose solution is $W_A(t) = W_A(0)e^{-c_s t}$, $\forall t \geq 0$. The desired result then follows. □

Remark 9.5. *The previous results hold only when $c_o = 0$. In fact, if $c_o \neq 0$, in general, the right end side of (9.17) is not symmetric, and therefore Lemma 9.10 can't apply.* □

9.6 Numerical Example

We validate our theoretical results via a simple example and, for brevity, we present numerical results only for the Hopfield-Hebbian model (8.13). Inspired by one of the building blocks of the nematode C. elegans neural circuit studied in [146], we consider the simple network of Figure 9.3 with six neurons and six edges (four excitatory and two

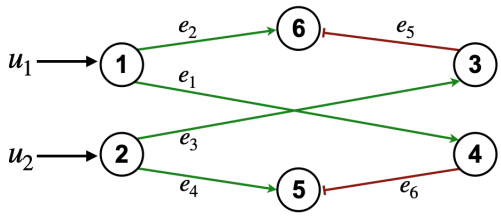

Figure 9.3: Coupled neural-synaptic model with six neurons i and six edges, e_i, $i = 1, \ldots, 6$, four excitatory (green) and two inhibitory (red). Only nodes 1 and 2 are subjected to the external stimuli u_1 and u_2, respectively. Colors online.

inhibitory). The C. elegans architecture can be schematically represented as a cascade of the blocks of the network in Figure 9.3.
The out- and in-incidence matrices for this network are:

$$B_{\text{in}} = \begin{bmatrix} 0 & 0 & 0 & 0 & 0 & 0 \\ 0 & 0 & 0 & 0 & 0 & 0 \\ 0 & 0 & 1 & 0 & 0 & 0 \\ 1 & 0 & 0 & 0 & 0 & 0 \\ 0 & 0 & 0 & 1 & 0 & 1 \\ 0 & 1 & 0 & 0 & 1 & 0 \end{bmatrix}, \; B_{\text{out}} = \begin{bmatrix} 1 & 1 & 0 & 0 & 0 & 0 \\ 0 & 0 & 1 & 1 & 0 & 0 \\ 0 & 0 & 0 & 0 & 1 & 0 \\ 0 & 0 & 0 & 0 & 0 & 1 \\ 0 & 0 & 0 & 0 & 0 & 0 \\ 0 & 0 & 0 & 0 & 0 & 0 \end{bmatrix}$$

In this case $d_{\max} = 2$ and we pick the elements of h in (8.13) from the interval $[-1, 1]$. These elements are selected so that e_i, $i \in \{1, \ldots, 4\}$, are excitatory, while e_5 and e_6 are inhibitory. For the neurons we set $\phi(x) = \frac{1}{1+e^{-x}}$ and hence $\phi_{\max} = 1$. In the network, only neurons 1 and 2 receive the external stimuli $u_1 = 20\sin(8t)$ and $u_2 = 15\cos(8t)$, respectively; also, the excitatory synaptic weights are subject to a constant stimulus $\bar{u} = 1.5$. In our experiments, we pick the initial conditions from the set $[-1, 1]$ and select the synaptic initial conditions so that Dale's Principle is satisfied. To numerically validate the results presented in Section 9.4 we set $c_n = 3.6$ and $c_s = 3.2$, so that condition (9.8) is satisfied, i.e., the Hopfield-Hebbian network is strongly infinitesimally contracting. The behavior of the network is illustrated in Figure 9.4. The contraction rate estimate given by (9.9) is $\lambda_{\text{HH}} = 0.54$. As expected, this estimate is more conservative than the empirical contraction rate of 4.10 obtained from numerical simulations. Moreover, a direct computation shows that $x_{\max} = 5.98$ and $w_{\max} = 0.78$, in accordance with Lemma 9.1. Also, the behavior in the figure is in accordance with Lemma 9.9: note indeed that the synaptic weights have always the same sign. We also note that, since our conditions guarantee the contractivity of the network, the Hopfield-Hebbian network becomes entrained by the periodic inputs u_1 and u_2 (see Figure 9.4).

Finally, to validate our results for RNNs, we introduce recurrent connections to the network in Figure 9.3, obtaining the network in Figure 9.5. Here, $d_{\max} = 2$ and we pick the elements of h in (8.13) from the interval $[-1, 1]$. These elements are selected so that e_5, e_6, and e_7 are inhibitory, while the other edges are excitatory. In the network, only neurons 1, 2, and 4 receive the external stimuli $u_1 = 5\tanh(t)$, $u_2 = 3\tanh(t)$,

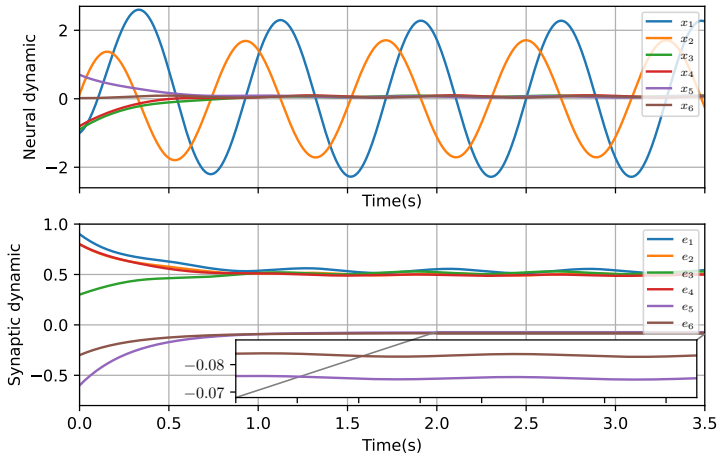

Figure 9.4: Simulation of the Hopfield-Hebbian model of Figure 9.3 exhibiting entrainment to periodic inputs typical of contracting systems. See Section 9.6 for the parameters.

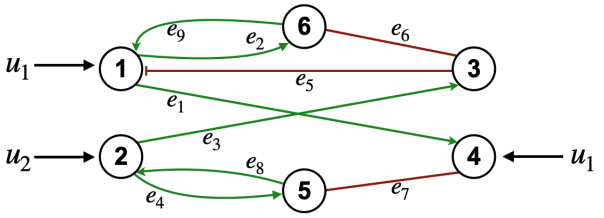

Figure 9.5: Coupled neural-synaptic model with six neurons i, $i = 1, \ldots, 6$, and nine edges, e_j, $j = 1, \ldots, 9$, six excitatory (green) and three inhibitory (red). Only nodes 1, 2, and 4 are subjected to the external stimuli u_1, u_2, and u_3, respectively. Colors online.

and $u_3 = 7 \tanh(t)$, respectively; also, the synaptic weights e_1 and e_4 are subject to a constant stimulus $\bar{u} = 1.5$, while e_2, e_3 and e_9 to $\bar{u} = 1$. In our experiments, we pick the initial conditions from the set $[-1, 1]$ and select the synaptic initial conditions so that Dale's Principle is satisfied. Also in this case, we set $c_n = 3.6$ and $c_s = 3.2$, so that condition (9.8) is satisfied. For this example, we perform an exploratory numerical study to investigate what happens when the network parameters are set so as to satisfy Theorem 9.5, but the activation functions are affected by the delay, say $\tau = 2s$ in our simulations. While it is well known that contraction is preserved through specific time-delayed communications [148], to the best of our knowledge this property has not been investigated for the types of dynamics considered here. The resulting behavior of the network, illustrated in Figure 9.6, shows that the delayed system appears to be still contracting. We leave the study of neural-synaptic networks with delays to future work.

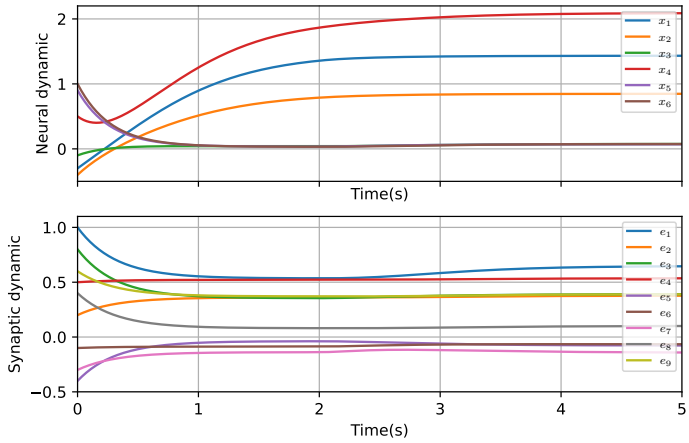

Figure 9.6: Simulation of the Hopfield-Hebbian model of Figure 9.5 with the activation functions affected by $2s$ of delay. Even with the delays the system appears to be still contracting. See Section 9.6 for the parameters.

9.7 Summary

In this chapter, we completed the analysis of Chapter 8 for the modeling and understanding of ANNs that more closely align with the principles governing natural NNs. Given the coupled neural-synaptic models combining RNNs with dynamical recurrent connections undergoing Hebbian learning rules, in this chapter we characterized key dynamical properties of such models, supporting some biologically realistic behaviors.

First, in Section 9.3 we established a key biologically-inspired forward invariance result for the trajectories of the system, showing bounded solutions for each model. This result mirrors the fact that biological neurons eventually saturate with high input values and that synaptic weights are bounded. Then in Section 9.4 we gave sufficient conditions for the non-Euclidean contractivity of the models. Importantly, each contractivity test we presented is based upon biologically meaningful quantities, i.e., neural and synaptic decay rate, maximum in-degree, and maximum synaptic strength. Specifically, we found that when the neural decay rate $c_{\mathrm{n}} > 1$ the model with the FNN has sharper contractivity conditions with respect to the one with the HNN. We then explored invariance properties of the synaptic dynamics in Section 9.5. Specifically, in Lemma 9.9 we showed that under suitable conditions the synaptic rules satisfy Dale's Principle. With this result, we enhanced the biological plausibility of our models. Additionally, in Theorem 9.10 we gave invariant results for symmetric synaptic matrices. Finally, to validate our theoretical results, we conducted a numerical example using a biologically inspired network. This example is based on a block of the C. elegans neural architecture.

The results of this chapter establish a theoretical framework for advancing ANNs that more closely align with biologically plausible principles, setting the stage for further developments in biologically inspired machine learning.

Part III

Contracting Dynamics for Convex Optimization

III.1 Introduction

Optimization problems are fundamental in science and engineering, with a wide range of applications spanning from control theory to computational neuroscience, as demonstrated in earlier parts of this thesis. Within the family of optimization problems, convex optimization stands out as a central tool across many domains.

Traditionally, optimization algorithms have been implemented as iterative procedures on digital devices, where the focus is on their numerical performance. However, a growing alternative approach for addressing possibly time-varying optimization problems is to synthesize continuous-time dynamical systems, akin to recurrent neural networks, which converge to equilibria that are also optimal solutions. As a result, significant efforts have been directed toward characterizing the stability and convergence rates of these systems, along with their robustness against uncertainty. Remarkably, strongly infinitesimally contracting systems exhibit these desirable properties such as convergence for time-invariant systems, tracking for time-varying systems, and robustness to noise.

Research questions: In the above context, several questions naturally arise:

- Can contractivity be used to obtain improved rate of convergence for canonical optimization problems?
- Can a contractivity-based approach be effectively applied to track solutions of continuous-time time-varying optimization problems?
- In many convex optimization problems, the associated dynamics are only weakly contracting. In which cases can we ensure convergence? And what is the convergence behavior for these cases?

III.2 Contracting Dynamics for Convex Optimization

In this final part of this thesis, motivated by the above questions, we explore the potential of a contractivity-based approach for convex optimization. Specifically, in Chapter 10, we consider four canonical time-invariant optimization problems, say them $P(x)$: unconstrained problems, monotone inclusions problems, linear equality-constrained problems, and composite minimization problems. For each of these problems, we provide a transcription to continuous-time dynamical systems, say it $F(x)$, and give conditions under which these dynamics are strongly infinitesimally contracting.

The goal is to use contracting dynamics whose equilibrium point corresponds to the optimal solution of the optimization problem. Informally, we can schematize this as:

$$x^\star = \arg\min P(x) \quad \Longleftrightarrow \quad x^\star \text{ eq. point of } \dot{x} = F(x).$$

For a static optimization problem, we know that for any input (or parameter) at each time instant strongly contracting dynamics admit a unique equilibrium. When

considering parametric and time-varying convex optimization, intuitively we can track the equilibrium trajectory by defining parametric and time-varying contracting dynamics.

Chapter 11 expands on these ideas. We present two results on equilibrium tracking for parameter-varying contracting dynamics, addressing scenarios where the rate of change of the parameter is known and unknown. Then, we introduce contracting continuous-time dynamical systems designed to track the optimal solutions of time-varying instances of monotone inclusions problems, linear equality-constrained problems, and composite minimization problems.

Finally, in Chapter 12 we extend our analysis beyond the case of strong convexity to examine convex (but not strongly convex) optimization problems with unique minimizers. We show that these problems lead to dynamics that are globally-weakly contracting in the state space and only locally-strongly contracting, such as the FCNs analyzed in Chapter 7. For such dynamics, we present a comprehensive analysis of their convergence behavior, showing that this is *linear-exponential*, in the sense that the distance between each solution and the equilibrium is upper-bounded by a function that first decreases linearly and then exponentially decays. This result extends the findings in Section 7.3, offering a refined convergence bound (we give more details on this in Chapter 12). In addition to convergence results, we also provide input-to-state stability conditions for these dynamics, further strengthening the robustness and applicability of the approach.

III.3 Overview

Studying optimization algorithms as continuous-time dynamical systems has been an active area of research since the seminal work of Arrow, Hurwicz, and Uzawa [120], with, e.g., [62] being one of the first works to design neural networks for LPs. Notable examples include Hopfield and Tank in dynamical neuroscience [121], Kennedy and Chua in analog circuit design [149], and Brockett in systems and control [150]. Recent advancements in, e.g., online and dynamic feedback optimization [151] and reservoir computing [152], have renewed the interest in continuous-time dynamics for optimization. A recent survey on studying optimization algorithms from a feedback control perspective is [153].

Asymptotic and exponential stability of dynamical systems solving convex optimization problems is a classical problem and has been studied in papers including [154, 155, 156, 157, 158] among many others. Compared to papers studying asymptotic and exponential stability, there are far fewer works studying the contractivity of dynamical systems solving optimization problems. A few exceptions include [105, 159] which analyze primal-dual dynamics and [160, 90] which study gradient flows on Riemannian manifolds. Additionally, optimization problems have been related to dynamical systems via proximal gradients, and the corresponding continuous-time proximal gradient dynamics are studied in, e.g., [51, 158, 52]. Exponential stability of continuous-time primal-dual dynamics with linear equality constraints with full row rank constraint matrices has been also studied in works including [156, 158, 161]. The exponential stability of such dynamics with not full rank constraints is established in [162, 163]. This result is extended in a contractivity framework in [164] using semicontraction theory, a branch of contractivity made by systems that are contracting only when restricted to a certain

subspace.

In the context of time-varying convex optimization, algorithms to track the optimal solution are designed based on Newton's method in discrete-time in [165, 166] and in continuous-time in [167]. Reviews of these results and theoretical extensions are given in [168] and [169]. These results have been applied to study the feedback interconnection of an LTI system and a dynamical system solving an optimization problem in [170]. Other examples of problems analyzed in a time-varying framework include works on distributed convex optimization with time-varying cost functions [171, 172, 173]. From a contraction theory perspective, both [105] and [159] provide tracking error bounds for continuous-time time-varying primal-dual dynamics.

Finally, the asymptotic behavior of weakly contracting dynamics is instead characterized in, e.g., [98] for monotone systems and in [36] for primal-dynamics with a locally stable equilibrium.

10 Contracting Dynamics for Canonical Convex Optimization Problems

In this chapter, we investigate whether a contractivity-based approach can effectively be applied to study optimization problems. To this end, we begin our analysis by providing a transcription of canonical convex optimization problems to continuous-time dynamical systems that are strongly infinitesimally contracting. These systems offer a robust framework for solving convex problems with guarantees of convergence to optimal solutions, laying the groundwork for robust, real-time solution tracking in dynamic optimization settings.

Some of the results in this chapter appeared in:

- A. Davydov, **V. Centorrino**, A. Gokhale, G. Russo, and F. Bullo. "Time-Varying Convex Optimization: A Contraction and Equilibrium Tracking Approach", conditionally accepted on *IEEE Transactions on Automatic Control*, June 2023, https://arxiv.org/abs/2305.15595.

Additionally, part of the results were presented at:

- Workshop "Variational Inequalities, Nash Equilibrium Problems and Applications". "On Contracting Dynamics for Convex Optimization", Oral Talk, Catania, July 11-12, 2024. Website: https://vinepa.dmi.unict.it/.

10.1 Introduction

Convex optimization plays a central role in many areas of applied mathematics, machine learning, control theory, and economics, offering a powerful framework for solving a broad class of problems. A paradigm that is becoming increasingly popular is that to synthesize continuous-time dynamical systems that converge to an equilibrium, which corresponds to the optimal solution of the optimization problem. A suitable tool to assess convergence and robustness is contraction theory, which has proven particularly useful for time-varying convex problems, as we explore in the next chapter.

Motivated by this, in this chapter, we consider canonical convex optimization problems, namely unconstrained problems, monotone inclusions problems, linear equality-constrained problems, and composite minimization problems. For each of these optimization problems, we provide a transcription to continuous-time dynamical systems and give conditions under which these dynamics are strongly infinitesimally contracting. In this way, we ensure global exponential convergence to the optimal solution, along with the other useful properties of contracting dynamics (we refer to Section 4.4 for a detailed list of these properties).

The chapter is organized as follows. In Section 10.2 we present a brief primer on convex optimization. Then we analyze the unconstrained optimization problem in Section 10.3, the monotone inclusion problem Section 10.3, the linear equality constrained optimization problems in Section 10.5, and the composite minimization problems in Section 10.6. Finally, in Section 10.7 we provide a summary table.

10.1.1 Contributions

We consider natural transcriptions into contracting dynamics for four canonical strongly convex optimization problems: unconstrained problems, monotone inclusions problems, linear equality-constrained problems, and composite minimization problems.

For (i) unconstrained problems and saddle dynamics, we review results known in the literature. For the remaining problems, we make specific contributions by introducing new or improved transcriptions of strongly contracting dynamics. Specifically, for (ii) monotone inclusion problems, we consider the *continuous-time forward-backward splitting dynamics*, a generalization of the projected dynamics studied in [174] and the proximal gradient dynamics studied in [51, 52]. We demonstrate that the continuous-time forward-backward splitting dynamics are contracting and provide improved rates of exponential convergence in certain special cases. For (iii) linear-equality constrained problems, we study the continuous-time primal-dual dynamics and prove their strong infinitesimal contractivity, providing the contractivity norm and explicit estimates of the rate of contraction. To the best of our knowledge, our rates are improved with respect to those presented in literature. Finally, for (iv) composite minimization, we adopt the proximal augmented Lagrangian approach from [158]. We show that the continuous-time primal-dual dynamics on the proximal augmented Lagrangian are contracting. This finding improves on the exponential convergence result from [158, Theorem 3] by allowing for a larger range of parameters, thus increasing the method's flexibility and applicability.

10.2 A Primer on Convex Optimization

In this section, we recall basic definitions and facts on convex optimization.

Convex optimization is a subfield of mathematical optimization that deals with problems where the objective function is convex, and the feasible region forms a convex set. We recall the following standard definitions.

Definition 10.1 (Convex set)**.** *A set $C \subseteq \mathbb{R}^n$ is* convex *if*

$$\alpha x_1 + (1-\alpha)x_2 \in C,$$

for all $x_1, x_2 \in C$ and for all $\alpha \in [0,1]$.

In words, a set is convex if any line segment connecting two points within the set remains entirely inside the set.

Definition 10.2 (Convex and strongly convex functions)**.** *Let $f\colon \mathbb{R}^n \to \mathbb{R}$ be a scalar function defined over a convex set $C \subseteq \mathbb{R}^n$. The function f is*

- convex *if* $\quad f(\alpha x_1 + (1-\alpha)x_2) \leq \alpha f(x_1) + (1-\alpha) f(x_2)$,
- strongly convex with parameter $m_f > 0$ *if*

$$f(\alpha x_1 + (1-\alpha)x_2) \leq \alpha f(x_1) + (1-\alpha) f(x_2) + \frac{1}{2} m_f \alpha (1-\alpha) \|x - y\|_2^2,$$

for all $x_1 \neq x_2 \in C$ and for all $\alpha \in [0,1]$. We refer to Figure 10.1 for an illustration of a convex (but not strongly convex) function and a strongly convex function.

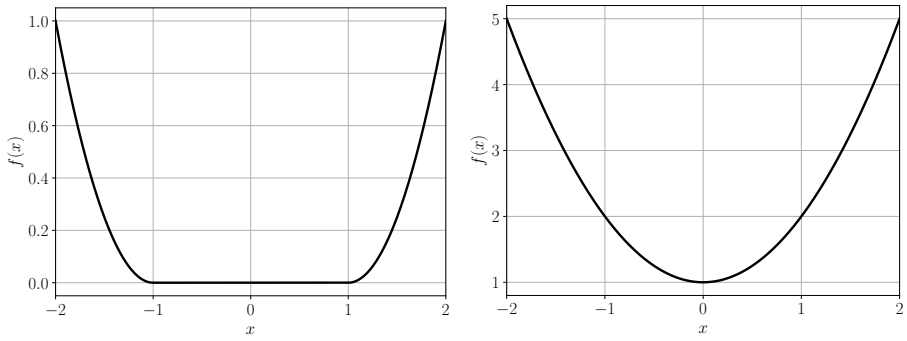

Figure 10.1: Left panel: Convex but not strongly convex function. Right panel: Strongly convex function.

Geometrically, a function is convex if the line segment between any two points on its graph lies above or on the graph. A key property of convex function that makes them particularly useful is the fact that any local minimum is a global minimum. Finally, we recall a characterization of convexity for twice-differentiable functions.

Lemma 10.1 (Second order characterization of convex function)**.** *Let $f\colon \mathbb{R}^n \to \mathbb{R}$ be a twice-differentiable function defined over a convex set $C \subseteq \mathbb{R}^n$. Then*

- *the function f is convex if and only if its Hessian matrix $\nabla^2 f(x) \succeq 0$ for all $x \in C$,*
- *the function f is strongly convex with parameter $m_f > 0$ if and only if its Hessian matrix $\nabla^2 f(x) \succeq m_f I_n$, for all $x \in C$.*

10.3 Unconstrained Optimization Problem

Let $f\colon \mathbb{R}^n \to \mathbb{R}^n$ be a convex and differentiable function. We are interested in solving the *unconstrained optimization problem*

$$\min_{x \in \mathbb{R}^n} f(x). \tag{10.1}$$

A common approach to solve problem (10.1) is through the *continuous-time gradient flow dynamics*, given by:

$$\dot{x} = -\nabla f(x) = \mathsf{F}_{\mathrm{GD}}. \tag{10.2}$$

In the following result, we give conditions under which the dynamics (10.2) is strongly infinitesimally contracting.

Lemma 10.2 (Contractivity of continuous-time gradient flow dynamics)**.** *Let $f\colon \mathbb{R}^n \to \mathbb{R}^n$ be continuously differentiable. Then*

(i) the map f is strongly convex with parameter $m_f > 0$ if and only if the gradient-flow dynamics (10.2) is strongly infinitesimally contracting with rate m_f with respect to the norm $\|\cdot\|_2$,

(ii) the map f is convex if and only if then the gradient-flow dynamics (10.2) is weakly contracting with respect to the norm $\|\cdot\|_2$.

Proof. The statements follows from Lemma 10.1 after noticing that $\mu_2\big(D\mathsf{F}_{\mathrm{GD}}\big) = \nabla^2 f(x)$. □

Remark 10.1.

(i) Statement (i) in Lemma 10.2 is also known as Kachurovskii's Theorem [175].

(ii) the result in Lemma 10.2 holds also when the function f is locally Lipschitz, by asking that the conditions are verified at every point where the function is differentiable.

□

10.4 Monotone Inclusion Problem

Let $\mathsf{F}\colon \mathbb{R}^n \to \mathbb{R}^n$ be monotone and $g\colon \mathbb{R}^n \to \overline{\mathbb{R}}$ be convex. We are interested in solving the *monotone inclusion problem*

$$\text{find } x^\star \in \mathbb{R}^n \text{ s.t.} \quad \mathbb{0}_n \in (\mathsf{F} + \partial g)(x^\star). \tag{10.3}$$

We make the following assumptions on the functions F and g.

Assumption 10.1. *The function $\mathsf{F}\colon \mathbb{R}^n \to \mathbb{R}^n$ is strongly monotone with parameter m_{F} and Lipschitz with constant L_{F}. The map $g\colon \mathbb{R}^n \to \overline{\mathbb{R}}$ is closed, convex and proper.*

Under Assumption 10.1, the monotone inclusion problem (10.3) has a unique solution due to strong monotonicity of F [176].

We begin with two examples of well-known problems that can be stated in terms of the monotone inclusion problem (10.3).

Example 10.1 (Convex minimization)**.** *Consider the convex optimization problem*

$$\min_{x\in\mathbb{R}^n} f(x) + g(x), \tag{10.4}$$

where $f\colon \mathbb{R}^n \to \mathbb{R}$ is strongly convex and continuously differentiable and $g\colon \mathbb{R}^n \to \overline{\mathbb{R}}$ is CCP. In this case, the unique point $x^\star \in \mathbb{R}^n$ that minimizes (10.4) also solves the inclusion problem (10.3) with $\mathsf{F} = \nabla f$.

Example 10.2 (Variational inequalities)**.** *Consider the* variational inequality

$$\textit{Find } x^\star \in \mathcal{C} \textit{ s.t.} \quad \mathsf{F}(x^\star)^\top (x - x^\star) \geq 0, \quad \forall x \in \mathcal{C}, \tag{10.5}$$

where $\mathcal{C}$ is a nonempty, convex, and closed set. We denote the problem (10.5) by $\mathrm{VI}(\mathsf{F}, \mathcal{C})$. It is known that $x^\star \in \mathcal{C}$ solves $\mathrm{VI}(\mathsf{F}, \mathcal{C})$ if and only if for all $\gamma > 0$, $x^\star$ is a fixed point of the map $\mathbb{P}_{\mathcal{C}} \circ (\mathsf{Id} - \gamma\mathsf{F})$, that is $x^\star = \mathbb{P}_{\mathcal{C}}(x^\star - \gamma\mathsf{F}(x^\star))$. In turn, this fixed-point condition is equivalent to asking $x^\star$ to solve the monotone inclusion problem (10.3) with $g = \iota_{\mathcal{C}}$ (see, e.g., [177, pp. 37]).

To solve the monotone inclusion problem (10.3), we consider the following *continuous-time forward-backward splitting dynamics* with parameter $\gamma > 0$:

$$\dot{x} = -x + \mathrm{prox}_{\gamma g}(x - \gamma\mathsf{F}(x)) =: \mathsf{F}^{\gamma}_{\mathrm{FB}}(x). \tag{10.6}$$

Remark 10.2.

(i) when $g = \iota_{\mathcal{C}}$ for some convex and closed set $\mathcal{C}$, then for any $\gamma > 0$, $\mathrm{prox}_{\gamma g} = \mathbb{P}_{\mathcal{C}}$, we are solving the $\mathrm{VI}(\mathsf{F}, \mathcal{C})$ (10.5) and the dynamics (10.6) are the projected dynamics *[174]*

$$\dot{x} = -x + \mathbb{P}_{\mathcal{C}}(x - \gamma\mathsf{F}(x)).$$

(ii) when $\mathsf{F} = \nabla f$ *for some continuously differentiable convex function* f*, we are solving the convex optimization problem* (10.4) *and the dynamics* (10.6) *corresponds to the* proximal gradient dynamics

$$\dot{x} = -x + \operatorname{prox}_{\gamma g}(x - \gamma \nabla f(x)).$$

□

First, we establish a result relating the equilibrium points of the dynamics (10.6) and the solutions of the inclusion problem (10.3).

Lemma 10.3 (Equilibria of (10.6))**.** *Consider the continuous-time forward-backward splitting dynamics* (10.6) *satisfying Assumption 10.1. Then for any* $\gamma > 0$*,* $\mathbb{0}_n \in (\mathsf{F} + \partial g)(x^\star)$ *if and only if* $x^\star \in \mathbb{R}^n$ *is an equilibrium point of the dynamics* (10.6)*.*

Proof. Note that equilibria of (10.6), $x^\star \in \mathbb{R}^n$, satisfy the fixed point equation

$$x^\star = \operatorname{prox}_{\gamma g}(x^\star - \gamma \mathsf{F}(x^\star)). \tag{10.7}$$

Moreover, it is known that fixed points of (10.7) also solve the monotone inclusion $\mathbb{0}_n \in (\mathsf{F} + \partial g)(x^\star)$ (see, e.g., [178, Proposition 26.1(iv)(a)]) noting that $\operatorname{prox}_{\gamma g}$ is the resolvent of ∂g with parameter γ. □

Remark 10.3. *Proposition 10.3 continues to hold under the assumption of monotone* F *[178, Propositon 26.1(iv)(a)].* □

Next, we give conditions on the parameter γ for which the dynamics (10.6) are strongly infinitesimally contracting.

Theorem 10.4 (Contractivity of continuous-time forward-backward splitting dynamics)**.** *Consider the dynamics* (10.6) *satisfying Assumption 10.1. Then*

(i) for every $\gamma \in]0, 2m_{\mathsf{F}}/L_{\mathsf{F}}^2[$*, the dynamics* (10.6) *are strongly infinitesimally contracting with respect to the norm* $\|\cdot\|_2$ *with rate* $1 - \sqrt{1 - 2\gamma m_{\mathsf{F}} + \gamma^2 L_{\mathsf{F}}^2}$*. Moreover, the contraction rate is optimized at* $\gamma^* = m_{\mathsf{F}}/L_{\mathsf{F}}^2$*.*

Additionally,

(ii) if $\mathsf{F} = \nabla f$ *for some strongly convex* $f \colon \mathbb{R}^n \to \mathbb{R}$*, for every* $\gamma \in]0, 2/L_{\mathsf{F}}[$*, the dynamics* (10.6) *are strongly infinitesimally contracting with respect to* $\|\cdot\|_2$ *with rate* $1 - \max\{|1 - \gamma m_{\mathsf{F}}|, |1 - \gamma L_{\mathsf{F}}|\}$*. Moreover, the contraction rate is optimized at* $\gamma^* = 2/(m_{\mathsf{F}} + L_{\mathsf{F}})$*;*

(iii) if $\mathsf{F}(x) = Ax + b$ *for all* $x \in \mathbb{R}^n$*, with* $A = A^\top \succ 0$*, then for every* $\gamma \in]1/\lambda_{\min}(A), +\infty[$*, the dynamics* (10.6) *are strongly infinitesimally contracting with respect to the norm* $\|\cdot\|_{(\gamma A - I_n)}$ *with rate* 1*.*

Proof. Regarding statement (i) note that, for every $\gamma > 0$, we have

- the map $\operatorname{prox}_{\gamma g}$ is nonexpansive with respect to the norm $\|\cdot\|_2$, being $g\colon \mathbb{R}^n \to \overline{\mathbb{R}}$ CCP (see, e.g., [178, Proposition 12.28]);
- the map $\mathsf{Id} - \gamma \mathsf{F}$ has Lipschitz constant upper bounded by $\sqrt{1 - 2\gamma m_{\mathsf{F}} + \gamma^2 L_{\mathsf{F}}^2}$ with respect to the norm $\|\cdot\|_2$ (see, e.g., [177, pp. 16]).

Now, since the Lipschitz constant of the composition of two maps is upper bounded by the product of the Lipschitz constants, we have

$$\begin{aligned}\operatorname{osL}(\mathsf{F}_{\mathrm{FB}}^{\gamma}) &= \operatorname{osL}(-\mathsf{Id} + \operatorname{prox}_{\gamma g}(\mathsf{Id} - \gamma \mathsf{F})) = -1 + \operatorname{osL}(\operatorname{prox}_{\gamma g} \circ (\mathsf{Id} - \gamma \mathsf{F})) \\ &\leq -1 + \mathsf{Lip}(\operatorname{prox}_{\gamma g})\, \mathsf{Lip}(\mathsf{Id} - \gamma \mathsf{F}) \\ &\leq -1 + \mathsf{Lip}(\mathsf{Id} - \gamma \mathsf{F}) \leq -1 + \sqrt{1 - 2\gamma m_{\mathsf{F}} + \gamma^2 L_{\mathsf{F}}^2},\end{aligned}$$

where in the first equality we used the translation property of osL and in the first inequality we used the upper bound $\operatorname{osL}(\mathsf{T}) \leq \mathsf{Lip}(\mathsf{T})$. Therefore, for $\gamma \in]0, 2m_{\mathsf{F}}/L_{\mathsf{F}}^2[$, we have $\operatorname{osL}(\mathsf{F}_{\mathrm{FB}}^{\gamma}) < 0$. Moreover, minimizing $\operatorname{osL}(\mathsf{F}_{\mathrm{FB}}^{\gamma})$ corresponds to minimizing $1 - 2\gamma m_{\mathsf{F}} + \gamma^2 L_{\mathsf{F}}^2$ as a function of $\gamma \in]0, 2m_{\mathsf{F}}/L_{\mathsf{F}}^2[$. This minimization occurs at $\gamma^\star = m_{\mathsf{F}}/L_{\mathsf{F}}^2$ and yields a one-sided Lipschitz estimate of $\operatorname{osL}(\mathsf{F}_{\mathrm{FB}}^{\gamma^\star}) \leq -1 + \sqrt{1 - m_{\mathsf{F}}^2/L_{\mathsf{F}}^2} < 0$. This concludes the proof of item (i). Statement (ii) follows the same argument as in item (i), after noticing that, for all $\gamma > 0$, $\mathsf{Lip}(\mathsf{Id} - \gamma \nabla f) \leq \max\{|1 - \gamma m_{\mathsf{F}}|, |1 - \gamma L_{\mathsf{F}}|\}$ (see, e.g., [177, pp. 15]). Moreover, the optimal choice of γ is $\gamma^\star = 2/(m_{\mathsf{F}} + L_{\mathsf{F}})$ and the corresponding bound on $\operatorname{osL}(\mathsf{F}_{\mathrm{FB}}^{\gamma^\star})$ is $-1 + (\kappa - 1)/(\kappa + 1)$, where $\kappa := L_{\mathsf{F}}/m_{\mathsf{F}} \geq 1$ (see, e.g., [177, pp. 15]).

Finally, to prove statement (iii), we compute

$$D\mathsf{F}_{\mathrm{FB}}^{\gamma}(x) = -I_n + D\operatorname{prox}_{\gamma g}(I_n - \gamma(Ax + b))(I_n - \gamma A)$$

for almost every $x \in \mathbb{R}^n$. Note that for all $x \in \mathbb{R}^n$ for which the Jacobian exists, there exists $G = G^\top \in \mathbb{R}^{n \times n}$ with $0 \preceq G \preceq I_n$ satisfying $D\operatorname{prox}_{\gamma g}(I_n - \gamma(Ax + b)) = G$ (see [53] for more details). Then, by the log-norm translation property, we have

$$\sup_x \mu(D\mathsf{F}_{\mathrm{FB}}^{\gamma}(x)) \leq -1 + \max_{0 \preceq G \preceq I_n} \mu(G(I_n - \gamma A)), \tag{10.8}$$

where the sup is over all x for which $D\mathsf{F}_{\mathrm{FB}}^{\gamma}(x)$ exists. Moreover, for $\gamma > 1/\lambda_{\min}(A)$, $\gamma A - I_n$ is positive definite and by Lemma 5.3 we have that $G(I_n - \gamma A)$ has all real eigenvalues and has the same number of positive, zero, and negative eigenvalues as $-G$ does, i.e., all eigenvalues are nonpositive. Then from Theorem 5.4, with the choice of norm $\|\cdot\|_{2,\gamma A - I_n}$, we find

$$\mu_{2,\gamma A - I_n}(G(I_n - \gamma A)) = \mu_{2,\gamma A - I_n}((-G)(\gamma A - I_n)) \leq 0,$$

where in the last equality we used the definition of ℓ_2 log-norm. Finally, since this equality holds for all symmetric G satisfying $0 \preceq G \preceq I_n$, by applying inequality (10.8) we have

$$\sup_{x \in \mathbb{R}^n} \mu_{2,\gamma A - I_n}(D\mathsf{F}_{\mathrm{FB}}^{\gamma}(x)) \leq -1.$$

□

Remark 10.4. *The rates of contraction in Theorem 10.4(i) and (ii) are consequences of the contraction rates of the discrete-time forward-backward splitting algorithm in monotone operator theory, see [177, pp. 25] and [178, Proposition 26.16]. Instead, Theorem 10.4(iii) is novel and provides an improved and sharp rate of contraction.* □

10.5 Linear Equality Constrained Optimization

Let $f\colon \mathbb{R}^n \to \mathbb{R}$ be convex, $A \in \mathbb{R}^{m\times n}$, and $b \in \mathbb{R}^m$. Consider the *linear equality-constrained problem*

$$\begin{aligned} \min_{x\in\mathbb{R}^n} \quad & f(x), \\ \text{s.t.} \quad & Ax = b. \end{aligned} \tag{10.9}$$

We make the following assumptions on the function f and the matrix A.

Assumption 10.2. *The function $f\colon \mathbb{R}^n \to \mathbb{R}$ is continuously differentiable, strongly convex and strongly smooth with parameters m_f and L_f, respectively. The matrix $A \in \mathbb{R}^{m\times n}$ satisfies $a_{\min} I_m \preceq AA^\top \preceq a_{\max} I_m$, for $a_{\min}, a_{\max} \in \mathbb{R}_{>0}$.*

Note that the linear equality-constrained problem (10.9) is a special case of the monotone inclusion problem (10.3) with $\mathsf{F} = \nabla f$ and $g = \iota_{\mathcal{C}}$, where $\mathcal{C} = \{z \in \mathbb{R}^n \mid Az = b\}$. In this case, we have that $\operatorname{prox}_{\alpha g} = \mathbb{P}_{\mathcal{C}}$ and $\mathbb{P}_{\mathcal{C}}(z) = z - A^\dagger(Az - b) = (I_n - A^\dagger A)z + A^\dagger b$, where $A^\dagger$ denotes the pseudoinverse of A. In this context, the forward-backward splitting dynamics (10.6) read

$$\dot{x} = -x + (I_n - A^\dagger A)(x - \gamma\nabla f(x)) + A^\dagger b. \tag{10.10}$$

The downside to using the dynamics (10.10) is the cost of computing $A^\dagger$. To remedy this issue, a common approach is to leverage duality and jointly solve primal and dual problems. In what follows, we take this approach and study contractivity of the corresponding primal-dual dynamics. To this purpose, consider the Lagrangian associated to problem (10.9), that is the map $L\colon \mathbb{R}^n \times \mathbb{R}^m \to \mathbb{R}$ given by

$$L(x, \lambda) = f(x) + \lambda^\top (Ax - b).$$

The *continuous-time primal-dual dynamics* (also called Arrow-Hurwicz-Uzawa flow [120]) are gradient descent of L in x and gradient ascent of L in λ, i.e.,

$$\begin{aligned} \dot{x} &= -\nabla_x L(x, \lambda) = -\nabla f(x) - A^\top \lambda, \\ \dot{\lambda} &= \nabla_\lambda L(x, \lambda) = Ax - b. \end{aligned} \tag{10.11}$$

We give a preliminary result on saddle matrices instrumental for our analysis.

Lemma 10.5 (Logarithmic norm of Hurwitz saddle matrices)**.** *Given $B = B^\top \in \mathbb{R}^{n\times n}$ and $A \in \mathbb{R}^{m\times n}$, with $m \leq n$, consider the* saddle matrix

$$\mathcal{B} = \begin{bmatrix} -B & -A^\top \\ A & 0 \end{bmatrix} \in \mathbb{R}^{(m+n)\times(m+n)}.$$

Then, for each matrix pair (B, A) satisfying $b_{\min} I_n \preceq B \preceq b_{\max} I_n$ and $a_{\min} I_m \preceq AA^\top \preceq a_{\max} I_m$, for $b_{\min}, b_{\max}, a_{\min}, a_{\max} \in \mathbb{R}_{>0}$, the following contractivity LMI holds:

$$\mathcal{B}^\top P + P\mathcal{B} \preceq -2cP \quad \iff \quad \mu_P(\mathcal{B}) \leq -c,$$

where

$$P = \begin{bmatrix} I_n & \alpha A^\top \\ \alpha A & I_m \end{bmatrix} \succ 0, \; \alpha = \frac{1}{2} \min\left\{ \frac{1}{b_{\max}}, \frac{b_{\min}}{a_{\max}} \right\}, \text{ and} \tag{10.12}$$

$$c = \frac{1}{2} \alpha a_{\min} = \frac{1}{4} \min\left\{ \frac{a_{\min}}{b_{\max}}, \frac{a_{\min}}{a_{\max}} b_{\min} \right\}. \tag{10.13}$$

Proof. We start by verifying that $P \succ 0$. Using the Schur complement of the $(2,2)$ entry, we need to verify that

$$I_n - \alpha^2 A^\top A \succ 0 \iff 1 - \alpha^2 a_{\max} > 0 \iff \alpha^2 < 1/a_{\max}.$$

The inequality $\alpha^2 < 1/a_{\max}$ follows from the tighter inequality $(2\alpha)^2 \leq \frac{1}{a_{\max}}$ which is proved as follows:

$$\begin{aligned} \min\left\{ \frac{1}{b_{\max}}, \frac{b_{\min}}{a_{\max}} \right\}^2 &\leq \min\left\{ \frac{1}{b_{\max}}, \frac{b_{\min}}{a_{\max}} \right\} \cdot \max\left\{ \frac{1}{b_{\max}}, \frac{b_{\min}}{a_{\max}} \right\} \\ &= \frac{1}{b_{\max}} \cdot \frac{b_{\min}}{a_{\max}} \leq \frac{1}{a_{\max}}. \end{aligned}$$

Next, we aim to show that $Q := -\mathcal{B}^\top P - P\mathcal{B} - 2cP \succeq 0$. After some bookkeeping, we compute

$$Q = \begin{bmatrix} 2B - 2\alpha A^\top A - 2cI_n & \alpha BA^\top - 2c\alpha A^\top \\ A + \alpha AB - A - 2c\alpha A & 2\alpha AA^\top - 2cI_m \end{bmatrix}.$$

The (2,2) block satisfies the lower bound

$$\begin{aligned} 2\alpha AA^\top - 2cI_m &= 2\big(\tfrac{1}{2}\alpha AA^\top - cI_m\big) + \alpha AA^\top \\ &\succeq 2\big(\tfrac{1}{2}\alpha a_{\min} - c\big) I_m + \alpha AA^\top = \alpha AA^\top \succ 0. \end{aligned}$$

Given this lower bound, we can factorize the resulting matrix as follows:

$$\begin{aligned} Q &= -\mathcal{B}^\top P - P\mathcal{B} - 2cP \\ &\succeq \begin{bmatrix} I_n & 0 \\ 0 & A \end{bmatrix} \begin{bmatrix} 2B - 2(\alpha A^\top A + cI_n) & \alpha B - 2c\alpha I_n \\ \alpha B - 2c\alpha I_n & \alpha I_n \end{bmatrix} \begin{bmatrix} I_n & 0 \\ 0 & A^\top \end{bmatrix}. \end{aligned}$$

Since $\alpha I_n \succ 0$, it now suffices to show that the Schur complement of the (2,2) block of $n \times n$ matrix is positive semidefinite. We proceed as follows:

$$\begin{aligned} &2B - 2(\alpha A^\top A + cI_n) - \alpha\big(B - 2cI_n\big)^2 \succeq 0 \\ &\iff 2B - \alpha B^2 + 4\alpha cB \succeq 2(\alpha A^\top A + cI_n) + 4\alpha c^2 I_n \\ &\impliedby 2B - \alpha B^2 \succeq 2(\alpha A^\top A + cI_n) \text{ and } 4\alpha cB \succeq 4\alpha c^2 I_n. \end{aligned}$$

To prove $2B - \alpha B^2 \succeq 2(\alpha A^\top A + cI_n)$, we upper bound the right hand side as follows:

$$2(\alpha A^\top A + cI_n) \overset{(10.12)}{\preceq} \alpha(2a_{\max} + a_{\min})I_n \overset{\alpha \leq \frac{1}{2} b_{\min}/a_{\max}}{\preceq} \frac{1}{2}\frac{b_{\min}}{a_{\max}}(2a_{\max} + a_{\min})I_n \preceq \frac{3}{2} b_{\min} I_n.$$

Next, since $\alpha \leq \frac{1}{2b_{\max}}$, we know $-\alpha b_{\max} \geq -\frac{1}{2}$. We then upper bound the left hand side as follows:

$$2B - \alpha B^2 \succeq 2B - \alpha b_{\max} B \succeq (2 - \tfrac{1}{2})B \succeq \tfrac{3}{2} b_{\min} I_n.$$

Finally, the inequality $4\alpha c B \succeq 4\alpha c^2 I_n$ follows from noting $c \leq \frac{1}{4}\frac{a_{\min}}{a_{\max}} b_{\min} < b_{\min}$. □

Finally, we give the main result of this section.

Theorem 10.6 (Contractivity of primal-dual dynamics)**.** *Consider the dynamics* (10.11) *satisfying Assumption 10.2. Then the continuous-time primal-dual dynamics* (10.11) *are strongly infinitesimally contracting with respect to* $\|\cdot\|_{2,P}$ *with rate* $c > 0$ *where*

$$P = \begin{bmatrix} I_n & \alpha A^\top \\ \alpha A & I_m \end{bmatrix} \succ 0, \ \alpha = \frac{1}{2}\min\left\{\frac{1}{L_f}, \frac{m_f}{a_{\max}}\right\}, \tag{10.14}$$

$$c = \frac{1}{2}\alpha a_{\min} = \frac{1}{4}\min\left\{\frac{a_{\min}}{L_f}, \frac{a_{\min}}{a_{\max}} m_f\right\}. \tag{10.15}$$

Proof. Since f is continuously differentiable, convex, and strongly smooth, it is almost everywhere twice differentiable so the Jacobian of the dynamics (10.11) exists almost everywhere and is given by $J_{\text{PD}}(z) := \begin{bmatrix} -\nabla^2 f(x) & -A^\top \\ A & 0 \end{bmatrix}$, where $z = (x, \lambda) \in \mathbb{R}^{n+m}$. To prove strong infinitesimal contractivity it suffices to show that for all z for which $J_{\text{PD}}(z)$ exists, the bound $\mu_{2,P}(J_{\text{PD}}(z)) \leq -c$ holds for P, c given in (10.14) and (10.15), respectively. The assumption of strong convexity and strong smoothness of f further imply $m_f I_n \preceq \nabla^2 f(x) \preceq L_f I_n$ for all x for which the Hessian exists. Moreover, it holds:

$$\sup_z \mu_{2,P}(J_{\text{PD}}(z)) \leq \max_{m_f I_n \preceq B \preceq L_f I_n} \mu_{2,P}\left(\begin{bmatrix} -B & -A^\top \\ A & 0 \end{bmatrix}\right),$$

where the sup is over all points for which $J_{\text{PD}}(z)$ exists. The result is then a consequence of Lemma 10.5. □

Remark 10.5. *Our method of proof in Lemma 10.5 follows the same method as was presented in [156, Lemma 2], but uses a sharper upper bounding to yield a sharper contraction rate of* $\frac{1}{4}\min\left\{\frac{a_{\min}}{L_f}, \frac{a_{\min}}{a_{\max}} m_f\right\}$ *compared to the estimate* $\frac{1}{8}\min\left\{\frac{a_{\min}}{L_f}, \frac{a_{\min}}{a_{\max}} m_f\right\}$ *in [156, Lemma 2].* □

10.6 Composite Minimization

Let $f\colon \mathbb{R}^n \to \mathbb{R}$ and $g\colon \mathbb{R}^m \to \overline{\mathbb{R}}$ be convex, and $A \in \mathbb{R}^{m\times n}$. We consider the *composite minimization problem* of the form

$$\min_{x\in\mathbb{R}^n} f(x) + g(Ax). \tag{10.16}$$

We make the following assumptions on the functions f, g, and the matrix A.

Assumption 10.3. *The function $f\colon \mathbb{R}^n \to \mathbb{R}$ is continuously differentiable, strongly convex, and strongly smooth with parameters m_f and L_f, respectively. The map $g\colon \mathbb{R}^m \to \overline{\mathbb{R}}$ is convex, closed and proper. Finally, the matrix $A \in \mathbb{R}^{m\times n}$ satisfies $a_{\min} I_m \preceq AA^\top \preceq a_{\max} I_m$, for $a_{\min}, a_{\max} \in \mathbb{R}_{>0}$.*

While problem (10.16) is a special case of (10.4), it may be computationally challenging to compute the proximal operator of $g \circ A$. Thus, we treat this problem separately, leveraging the approach proposed in [158] to solve it. We begin by noticing that, the optimization problem (10.16) is equivalent to

$$\begin{aligned} \min_{x\in\mathbb{R}^n, y\in\mathbb{R}^m} & f(x) + g(y), \\ \text{s.t.} \quad & Ax - y = \mathbb{0}_m. \end{aligned} \tag{10.17}$$

For $\gamma > 0$, consider the *augmented Lagrangian* associated to (10.17), that is the function $L_\gamma\colon \mathbb{R}^n \times \mathbb{R}^m \times \mathbb{R}^m \to \mathbb{R}$ defined by

$$L_\gamma(x, y, \lambda) = f(x) + g(y) + \lambda^\top (Ax - y) + \frac{1}{2\gamma}\|Ax - y\|_2^2,$$

and, by a slight abuse of notation, the *proximal augmented Lagrangian* associated to (10.17) is the function $L_\gamma\colon \mathbb{R}^n \times \mathbb{R}^m \to \mathbb{R}$ defined by

$$L_\gamma(x, \lambda) = f(x) + M_{\gamma g}(Ax + \gamma\lambda) - \frac{\gamma}{2}\|\lambda\|_2^2. \tag{10.18}$$

The proximal augmented Lagrangian corresponds to the augmented Lagrangian where the minimization over y has already explicitly been performed and the optimal value for y has been substituted (we refer to [158, Theorem 1] for more details). Moreover, minimizing (10.16) corresponds to finding saddle points of (10.18). To this end, the primal-dual flow corresponding to the proximal augmented Lagrangian is

$$\begin{aligned} \dot{x} &= -\nabla_x L_\gamma(x, \lambda) = -\nabla f(x) - A^\top \nabla M_{\gamma g}(Ax + \gamma\lambda), \\ \dot{\lambda} &= \nabla_\lambda L_\gamma(x, \lambda) = \gamma(-\lambda + \nabla M_{\gamma g}(Ax + \gamma\lambda)). \end{aligned} \tag{10.19}$$

To provide estimates on the contraction rate and the norm with respect to which the dynamics (10.19) are strongly infinitesimally contracting, we need to introduce a useful

nonlinear program. For $\varepsilon \in]0, 1/\sqrt{a_{\max}}[$, consider the nonlinear program

$$\max_{c\geq 0,\alpha\geq 0,\varkappa\geq 0} \quad c \tag{10.20a}$$

$$\text{s.t.} \quad \alpha \leq \min\Big\{\frac{1}{\sqrt{a_{\max}}} - \varepsilon, \frac{\gamma}{a_{\max}}\Big\}, \tag{10.20b}$$

$$\varkappa \geq \frac{2}{3}, \tag{10.20c}$$

$$c \leq \Big(\frac{3}{4} - \frac{1}{2\varkappa}\Big)\alpha a_{\min}, \tag{10.20d}$$

$$h(c, \alpha, \varkappa) \geq 0, \tag{10.20e}$$

with $h\colon \mathbb{R}_{\geq 0} \times \mathbb{R}_{\geq 0} \times \mathbb{R}_{\geq 0} \to \mathbb{R}$ given by

$$\begin{aligned} h(c, \alpha, \varkappa) =& 2m_f - \operatorname{ReLU}\Big(2\alpha - \frac{2}{\gamma}\Big)a_{\max} - 2c \\ &- \alpha\varkappa\frac{a_{\max}}{a_{\min}}\Big(\gamma^2\frac{a_{\max}}{a_{\min}} + (L_f + \frac{a_{\max}}{\gamma} + 2c)^2 + 2\gamma\frac{a_{\max}}{a_{\min}}(L_f + \frac{a_{\max}}{\gamma} + 2c)\Big). \end{aligned}$$

Theorem 10.7 (Contractivity of the dynamics (10.19))**.** *Consider the continuous-time primal-dual dynamics* (10.19) *satisfying Assumption 10.3 and let $\gamma > 0$ be arbitrary. Then the primal-dual dynamics* (10.19) *are strongly infinitesimally contracting with respect to $\|\cdot\|_{2,P}$ with rate $c^\star > 0$ where*

$$P = \begin{bmatrix} I_n & \alpha^\star A^\top \\ \alpha^\star A & I_m, \end{bmatrix} \tag{10.21}$$

and $\alpha^\star > 0, c^\star > 0$ are the arguments solving problem (10.20)*.*

Proof. Let $z = (x, \lambda) \in \mathbb{R}^{n+m}$ and let $\mathsf{F}\colon \mathbb{R}^{n+m} \to \mathbb{R}^{n+m}$ be the vector field (10.19) for $\dot{z} = \mathsf{F}(z)$. Let $y := Ax + \gamma\lambda$ and define $G(y) := \gamma\nabla^2 M_{\gamma g}(y)$ where it exists. The Jacobian of F is then

$$D\mathsf{F}(z) = \begin{bmatrix} -\nabla^2 f(x) - \frac{1}{\gamma}A^\top G(y)A & -A^\top G(y) \\ G(y)A & -\gamma(I_m - G(y)) \end{bmatrix},$$

which exists for almost every z. We then aim to show that $\mu_P(D\mathsf{F}(z)) \leq -c$, for almost every z. First, we note that for almost every z it holds

$$\sup_z \mu_P(D\mathsf{F}(z)) \leq \max_{\substack{0\preceq G\preceq I_m, \\ m_f I_n \preceq B \preceq L_f I_n}} \mu_P\left(\begin{bmatrix} -B - \frac{1}{\gamma}A^\top GA & -A^\top G \\ GA & \gamma(G - I_m) \end{bmatrix}\right).$$

The result is then a consequence of a generalization of [156, Lemma 4]. We refer to [53] for more details. □

Note that any triple $(c, \alpha, \varkappa) \in \mathbb{R}^3_{\geq 0}$ satisfying the constraints (10.20b)-(10.20e) provides a suboptimal contraction estimate, i.e., the dynamics (10.19) are strongly infinitesimally contracting with rate c (weakly contracting if $c = 0$) with respect to norm $\|\cdot\|_{2,P}$, where $P = \begin{bmatrix} I_n & \alpha A^\top \\ \alpha A & I_m \end{bmatrix}$.

10.7 Table of Contracting Dynamics

Let $f\colon \mathbb{R}^n \to \mathbb{R}$ be strongly convex and strongly smooth with parameters m_f and L_f, respectively. Let $g\colon \mathbb{R}^m \to \overline{\mathbb{R}}$ be a convex, closed, and proper function and $\mathcal{C}$ be a convex set. Finally, consider a matrix $A \in \mathbb{R}^{m\times n}$ satisfying $a_{\min} I_m \preceq AA^\top \preceq a_{\max} I_m$, for $a_{\min}, a_{\max} \in \mathbb{R}_{>0}$.

In the following, we provide a table summarizing the canonical optimization problems analyzed in this chapter and the corresponding transcription to continuous-time dynamical systems which are strongly contracting under the assumptions in Sections 10.3 – 10.6.

Convex Optimization Problem		**Contracting Dynamics**
Unconstrained:	$\min_{x\in\mathbb{R}^n} f(x)$	$\dot{x} = -\nabla f(x)$
Constrained:	$\min_{x\in\mathbb{R}^n} f(x),$ $x \in \mathcal{C}$	$\dot{x} = -x + \mathbb{P}_{\mathcal{C}}(x - \gamma f(x))$
Composite:	$\min_{x\in\mathbb{R}^n} f(x) + g(x)$	$\dot{x} = -x + \operatorname{prox}_{\gamma g}(x - \gamma\nabla f(x))$
Equality constraints:	$\min_{x\in\mathbb{R}^n} f(x),$ s.t. $Ax = b$	$\dot{x} = -\nabla f(x) - A^\top\lambda,$ $\dot{\lambda} = Ax - b$
Inequality constraints:	$\min_{x\in\mathbb{R}^n} f(x),$ s.t. $Ax \leq b$	$\dot{x} = -\nabla f(x) - A^\top \nabla M_{\gamma g}(Ax + \gamma\lambda),$ $\dot{\lambda} = \gamma(-\lambda + \nabla M_{\gamma g}(Ax + \gamma\lambda))$

Table 10.1: Table of canonical optimization problems and the corresponding transcription to contracting continuous-time dynamical systems. In the table, $f\colon \mathbb{R}^n \to \mathbb{R}$ is continuously differentiable, strongly convex and strongly smooth. The set $\mathcal{C}$ is convex. The map $g\colon \mathbb{R}^m \to \overline{\mathbb{R}}$ is convex, closed and proper. The matrix $A \in \mathbb{R}^{m\times n}$ satisfies $a_{\min} I_m \preceq AA^\top \preceq a_{\max} I_m$, for $a_{\min}, a_{\max} \in \mathbb{R}_{>0}$, and $b \in \mathbb{R}^m$. Finally, $\gamma > 0$ is a parameter.

10.8 Summary

In this chapter, we proposed a contractivity-based approach for solving strongly convex optimization problems. We considered natural transcriptions into contracting dynamics for four canonical convex optimization problems: unconstrained problems, monotone inclusions problems, linear equality-constrained problems, and composite minimization problems.

For the unconstrained problems and gradient dynamics, we reviewed results known in the literature. For the monotone inclusion problems, we considered the forward-

backward splitting dynamics and studied its contractivity in Theorem 10.4, providing improved rates of exponential convergence in certain cases. For the linear-equality constrained problems, we studied the contractivity properties of the primal-dual dynamics, providing explicit estimates of the rate of contraction in Theorem 10.6. Also, in this case, we provided improved rate with respect to those presented in the literature. For composite minimization, we considered the proximal augmented Lagrangian approach and gave conditions under which this is contracting in Theorem 10.7. This finding improves on previous exponential convergence results by allowing for a larger range of parameters, thus increasing the method's flexibility and applicability. We concluded with a summary table of the canonical optimization problems analyzed in the chapter and the corresponding strongly contracting dynamics.

The results of this chapter demonstrate the effectiveness of using contracting dynamics for static convex optimization, providing improved rates of exponential convergence in some cases. The advantages of strongly contracting systems are that these guarantee exponential stability, convergence, along with robustness features that make these dynamics particularly promising in a time-varying setting. In the next chapter, we expand on this framework, exploring a contractivity-based approach for time-varying convex optimization.

11 Contracting Dynamics for Time-Varying Convex Optimization

In the previous chapter, we introduced a contractivity-based approach for solving static convex optimization problems, demonstrating that for any given input or parameter at each moment, the strongly contracting dynamics yield a unique equilibrium that coincides with the optimization problem's minimizer. In this chapter, we expand on this approach, exploring a contractivity-based approach for time-varying convex optimization. These problems often arise in many real-world scenarios where conditions evolve continuously, and decision-making must adapt in real-time. To address these challenges, we examine contracting continuous-time dynamical systems designed to track the optimal solutions of the corresponding time-varying problems.

The results in this chapter appeared in the same paper and were presented at the same conferences as those in Chapter 10.

11.1 Introduction

Time-varying optimization problems are fundamental to modern applications, such as tracking moving targets, adapting in online learning, or following the trajectory of stochastic processes. Unlike static optimization, where the objective is fixed, time-varying problems require algorithms capable of continuously adjusting to changes and converging to an optimal solution at each time instant. In such problems, we aim for dynamical systems that not only converge to the unique optimal solution when the problem is time-invariant, but also converge to an explicitly-computable neighborhood of the optimal solution trajectory when the problem is time-varying. Beyond tracking optimal trajectories, a key desirable feature of optimization algorithms is robustness in the face of uncertainty. In many real-world scenarios, the exact value of the cost function or its gradients may not always be available in their true form; instead, they might be estimated with some error or delay. Thus, for practical use of an optimization algorithm, it is essential to ensure that this has these robustness features *built-in*. A powerful approach to achieve these goals is

through strongly infinitesimally contracting dynamical systems, which inherently ensure stability, convergence, and robustness against noise and time-delays. Motivated by this, we now present equilibrium tracking results for parameter-varying contracting dynamical systems. Building on the transcription of canonical convex optimization problems to continuous-time strongly infinitesimally contracting systems presented in Chapter 10, we show how contracting dynamics can be used to tackle time-varying instances of some canonical convex optimization problems.

The chapter is organized as follows. Section 11.2 presents the initial setup, defining the parameter-varying dynamical systems and their key properties. Next, in Section 11.3, we present our main results on equilibrium tracking for parameter-varying contracting dynamical systems, giving estimates of the tracking error for both unknown and known rates of parameter change. These results are then applied in Section 11.4 to establish tracking error bounds for contracting dynamics solving three canonical convex optimization problems. Finally, in Section 11.5, we validate the effectiveness of our approach through numerical simulations.

11.1.1 Contributions

We present two results on equilibrium tracking for parameter-varying contracting dynamics, addressing both scenarios where the rate of change of the parameter is known and unknown. For the first scenario, where the rate of change of the parameter is unknown, we prove a general theorem for parameter-dependent strongly infinitesimally contracting dynamics. Specifically, we prove that the tracking error between any solution trajectory and the equilibrium trajectory is uniformly upper-bounded and is asymptotically proportional to the rate of change of the parameter. For the scenario where the rate of change of the parameter is known, we propose an alternative dynamical system. This system augments the contracting dynamics in the first scenario with a feedforward term. This augmentation ensures that the tracking error is exponentially decaying to zero and does not require any Lipschitz condition on how the parameter appears in the dynamics.

We apply these results to contracting dynamics solving three canonical strongly convex optimization problems, as introduced in Chapter 10. Specifically, we focus on (i) monotone inclusions, (ii) linear equality-constrained problems, and (iii) composite minimization problems. For each of these problems, we provide estimates of the tracking error in time-varying convex optimization scenarios.

Finally, to validate our theoretical results, we present numerical experiments that showcase the tracking error bounds for time-varying equality and inequality-constrained minimization problems.

11.2 Parameter-Varying Contracting Dynamical Systems

Consider a *parameter-varying dynamical system*, that is a dynamical system that depends on a time-varying parameter, say it θ. Specifically, for a vector field $f\colon \mathbb{R}^n \times \mathbb{R}^d \to \mathbb{R}^n$, the system is described by

$$\dot{x}(t) = f(x(t), \theta(t)), \quad x(0) = x_0 \in \mathbb{R}^n, \tag{11.1}$$

where, for all $t \geq 0$, $x(t)$ and $\theta(t)$ take value in $\mathcal{X} \subseteq \mathbb{R}^n$ and $\Theta \subseteq \mathbb{R}^d$, respectively. In this chapter, we work under the following assumptions.

Assumption . *Assume there exist two norms $\|\cdot\|_{\mathcal{X}}, \|\cdot\|_{\Theta}$ on $\mathcal{X}$ and Θ, respectively, such that*

(11.A1) *there exists $c > 0$ such that for all θ, the map $x \mapsto f(x, \theta)$ is strongly infinitesimally contracting with respect to $\|\cdot\|_{\mathcal{X}}$ with rate c,*

(11.A2) *there exists $L_\theta \geq 0$ such that for all x, the map $\theta \mapsto f(x, \theta)$ is Lipschitz from $(\Theta, \|\cdot\|_{\Theta})$ to $(\mathcal{X}, \|\cdot\|_{\mathcal{X}})$ with constant L_θ.*

Note that Assumption (11.A1) implies that, for each $\theta \in \Theta$, there exists a unique *equilibrium solution* $x^\star_\theta \in \mathcal{X}$ such that $f(x^\star_\theta, \theta) = \mathbb{0}_n$. Given this, it is meaningful to define the following

Definition 11.1 (Equilibrium curve)**.** *Given $\theta \in \Theta$, consider the parameter-varying system (11.1) and let Assumption (11.A1) holds. We define* equilibrium curve *the map $x^\star\colon \Theta \to \mathcal{X}$ defined by $x^\star(\theta) = x^\star_\theta$.*

First, we give a result on the Lipschitzness of parametrized time-varying equilibrium trajectories and a bound on their time derivatives.

Lemma 11.1 (Lipschitzness of parametrized curves)**.** *Consider $\mathcal{X} \subseteq \mathbb{R}^n$ and $\Theta \subseteq \mathbb{R}^d$ with associated norms $\|\cdot\|_{\mathcal{X}}\colon \mathbb{R}^n \to \mathbb{R}_{\geq 0}$ and $\|\cdot\|_{\Theta}\colon \mathbb{R}^d \to \mathbb{R}_{\geq 0}$, respectively. Let $g\colon \Theta \to \mathcal{X}$ be Lipschitz with constant $\mathsf{Lip}(g)$. Then for every $a, b \in \mathbb{R}$ with $a < b$ and every continuously differentiable $\theta\colon]a, b[\to \Theta$,*

(i) the curve $x\colon]a, b[\to \mathcal{X}$ given by $x(t) = g(\theta(t))$ is locally Lipschitz;

(ii) $\|\dot{x}(t)\|_{\mathcal{X}} \leq \mathsf{Lip}(g)\|\dot{\theta}(t)\|_{\Theta}$, for almost every $t \in]a, b[$.

Proof. Statement (i) follows from the facts that continuously differentiable maps are locally Lipschitz and that a composition of Lipschitz maps is Lipschitz. Note that, in turn, this statement implies that $\dot{x}(t)$ exists almost everywhere by Rademacher's theorem

Next, to prove statement (ii), for all $t \in]a, b[$ for which $\dot{x}(t)$ exists, we compute

$$\begin{aligned}\|\dot{x}(t)\|_{\mathcal{X}} &= \Big\| \lim_{h\to 0^+} \frac{x(t+h)-x(t)}{h} \Big\|_{\mathcal{X}} = \lim_{h\to 0^+} \frac{1}{h}\|x(t+h)-x(t)\|_{\mathcal{X}} \\ &\leq \lim_{h\to 0^+} \frac{\mathsf{Lip}(g)}{h}\|\theta(t+h)-\theta(t)\|_{\Theta} \\ &= \mathsf{Lip}(g)\Big\| \lim_{h\to 0^+} \frac{\theta(t+h)-\theta(t)}{h} \Big\|_{\Theta} = \mathsf{Lip}(g)\|\dot{\theta}(t)\|_{\Theta},\end{aligned}$$

where we have used the continuity of $\|\cdot\|_{\mathcal{X}}$ and $\|\cdot\|_{\Theta}$ and the Lipschitzness of g. This concludes the proof. □

Next, we give a result on parametrized contracting systems.

Lemma 11.2 (Parametrized contractions)**.** *Consider the parameter-varying system* (11.1) *and let Assumptions* (11.A1) *and* (11.A2) *hold. Then the equilibrium curve* $x^\star \colon \Theta \to \mathcal{X}$ *is Lipschitz with constant* L_θ/c.

Proof. Given two constant inputs θ_1 and θ_2, let $x^\star(\theta_1)$ and $x^\star(\theta_2)$ be the two equilibrium solutions of (11.1), respectively. The assumptions of [42, Theorem 3.16] are satisfied with $c = -\operatorname{osL}_x(f)$ and $L_\theta = \mathsf{Lip}_\theta(f)$, and the ISS differential inequality [42, Equation 3.39] implies

$$0 \leq -c\|x^\star(\theta_1) - x^\star(\theta_2)\|_{\mathcal{X}} + L_\theta\|\theta_1 - \theta_2\|_\theta.$$

This concludes the proof. □

Given the previous results, we can give the following

Definition 11.2 (Time-varying equilibrium curve)**.** *Consider a continuously differentiable curve* $\theta \colon \mathbb{R}_{\geq 0} \to \Theta$ *and the parameter-varying system* (11.1) *satisfying Assumptions* (11.A1) *and* (11.A2)*. The* time-varying equilibrium curve *is the map* $t \mapsto x^\star(\theta(t))$.

Finally, we note that Lemma 11.1 implies that the time-varying equilibrium curve $x^\star(\theta(\cdot))$ is locally Lipschitz. Additionally, this curve satisfies the condition

$$f(x^\star(\theta(t)), \theta(t)) = \mathbb{0}_n, \qquad \text{for all } t \geq 0.$$

11.3 Equilibrium Tracking for Parameter-Varying Contracting Dynamical Systems

In this section, we derive tracking error bounds for parameter-varying contracting dynamical systems for both unknown and known rates of parameter change.

We begin by analyzing the case where the rate of parameter change is unknown. In the following theorem, we provide tracking error bounds between any trajectory of (11.1) and the time-varying equilibrium curve.

Theorem 11.3 (Equilibrium tracking for contracting dynamics)**.** *Let $\theta\colon \mathbb{R}_{\geq 0} \to \Theta$ be continuously differentiable and consider the parameter-varying system (11.1) satisfying Assumptions (11.A1) and (11.A2). Then the following statements hold for almost every $t \geq 0$:*

(i) the tracking error $\|x(t) - x^\star(\theta(t))\|_{\mathcal{X}}$ satisfies

$$D^+\|x(t) - x^\star(\theta(t))\|_{\mathcal{X}} \leq -c\|x(t) - x^\star(\theta(t))\|_{\mathcal{X}} + \frac{L_\theta}{c}\|\dot{\theta}(t)\|_\Theta.$$

(ii) the Grönwall inequality for Dini derivatives implies

$$\|x(t) - x^\star(\theta(t))\|_{\mathcal{X}} \leq \mathrm{e}^{-ct}\|x_0 - x^\star(\theta_0)\|_{\mathcal{X}} + \frac{L_\theta}{c}\int_0^t \mathrm{e}^{-c(t-\tau)}\|\dot{\theta}(t)\|_\Theta d\tau.$$

(iii) from any initial conditions $x_0 \in \mathbb{R}^n$, $\theta_0 \in \mathbb{R}^d$ and uniformly bounded $\|\dot{\theta}(t)\|_\Theta$, the following inequality holds

$$\limsup_{t\to\infty} \|x(t) - x^\star(\theta(t))\|_{\mathcal{X}} \leq \frac{L_\theta}{c^2}\limsup_{t\to\infty}\|\dot{\theta}(t)\|_\Theta. \tag{11.2}$$

Proof. Consider the dynamics

$$\dot{x}(t) = f(x(t), \theta(t)) + v(t) := T(x(t), \theta(t), v(t)), \tag{11.3}$$

where $T\colon \mathbb{R}^n \times \mathbb{R}^d \times \mathbb{R}^n \to \mathbb{R}^n$ and $v\colon \mathbb{R}_{\geq 0} \to \mathcal{X}$. Note that by assumption (11.A1), for fixed θ, v, the map $x \mapsto T(x, \theta, v)$ is strongly infinitesimally contracting with rate $c > 0$. Moreover, at fixed x, θ, the map $v \mapsto T(x, \theta, v)$ is Lipschitz on $(\mathcal{X}, \|\cdot\|_{\mathcal{X}})$ with constant $L_v = 1$. Next, consider the inputs $v_1(t) = \mathbb{0}_n$ and $v_2(t) = \dot{x}^\star(\theta(t))$ and note that $\dot{x}^\star(\theta(t)) = f(x^\star(\theta(t)), \theta(t)) + \dot{x}^\star(\theta(t))$, so that the curve $x^\star(\theta(\cdot))$ is a solution to system (11.3) with input $v_2(t)$ and initial condition $x^\star(\theta_0)$. Additionally, for any initial condition $x_0 \in \mathcal{X}$, the solution $x(t)$ to the dynamics (11.1) is a solution to the system (11.3) with input $v_1(t)$. By an application of the incremental ISS theorem for contracting dynamical systems [42, Theorem 3.15] to the trajectories $x(\cdot)$, and $x^\star(\theta(\cdot))$ arising from inputs $v_1(\cdot)$, and $v_2(\cdot)$, respectively, we get

$$\begin{aligned} D^+\|x(t) - x^\star(\theta(t))\|_{\mathcal{X}} &\leq -c\|x(t) - x^\star(\theta(t))\|_{\mathcal{X}} + \|\dot{x}^\star(\theta(t))\|_{\mathcal{X}} \\ &\leq -c\|x(t) - x^\star(\theta(t))\|_{\mathcal{X}} + \frac{L_\theta}{c}\|\dot{\theta}(t)\|_\Theta, \end{aligned}$$

where the last inequality follows from Lemma 11.1. This proves statement (i). Statement (ii) is a consequence of the Grönwall inequality. Finally, statement (iii) is a consequence of statement (ii). □

Remark 11.1. *A related result to Theorem 11.3 was proved in [105, Lemma 2], but with the tracking error bound depending on the knowledge of the rate of change of the equilibrium trajectory, which is unknown, in general. Instead, Theorem 11.3 provides a bound that depends purely on the rate of change of the parameter, which may be much easier to estimate.* □

Theorem 11.3 is a general result that establishes that one does not need to know $\dot{x}^\star(\theta(t))$ to obtain an estimate on the tracking error. However, if one knows the rate of change of the parameter, it stands to reason that some system should be able to track the equilibrium trajectory with eventually zero tracking error. To show this, we introduce a new dynamics that augment the contracting dynamics (11.1) with a feedforward term proportional to the rate of change of the parameter.

Specifically, consider a parameter-dependent vector field $f\colon \mathbb{R}^n \times \mathbb{R}^d \to \mathbb{R}^n$ continuously differentiable in both arguments, and let $\theta\colon \mathbb{R}_{\geq 0} \to \Theta \subseteq \mathbb{R}^d$ be continuously differentiable. Assume that the function f satisfies Assumption (11.A1). The *time-varying contracting dynamics with feedforward prediction* is defined by

$$\dot{x}(t) = f(x(t),\theta(t)) - (D_x f(x(t),\theta(t)))^{-1} D_\theta f(x(t),\theta(t))\dot{\theta}(t). \tag{11.4}$$

Remark 11.2. *Assumption (11.A1) implies that $D_x f(x,\theta)$ is invertible for all x,θ, which makes the dynamics (11.4) well-posed.* □

The following theorem shows that by considering the time-varying contracting dynamics with feedforward prediction we obtain exponential decay to zero tracking error.

Theorem 11.4 (Exact tracking with feedforward prediction)**.** *Given a parameter-dependent map $f\colon \mathbb{R}^n \times \mathbb{R}^d \to \mathbb{R}^n$ continuously differentiable in both arguments satisfying Assumption (11.A1), and a function $\theta\colon \mathbb{R}_{\geq 0} \to \Theta \subseteq \mathbb{R}^d$ continuously differentiable, consider the* time-varying contracting dynamics with feedforward prediction *(11.4). Then $\forall t \geq 0$,*

(i) the residual, $\|f(x(t),\theta(t))\|_{\mathcal{X}}$, satisfies

$$\|f(x(t),\theta(t))\|_{\mathcal{X}} \leq \mathrm{e}^{-ct}\|f(x(0),\theta(0))\|_{\mathcal{X}}. \tag{11.5}$$

(ii) the tracking error $\|x(t) - x^\star(\theta(t))\|_{\mathcal{X}}$ satisfies

$$\|x(t) - x^\star(\theta(t))\|_{\mathcal{X}} \leq \frac{1}{c}\mathrm{e}^{-ct}\|f(x(0),\theta(0))\|_{\mathcal{X}}. \tag{11.6}$$

Additionally, if f is Lipschitz in its first argument with constant L_x uniformly in θ, then

$$\|x(t) - x^\star(\theta(t))\|_{\mathcal{X}} \leq \frac{L_x}{c}\mathrm{e}^{-ct}\|x(0) - x^\star(\theta(0))\|_{\mathcal{X}}. \tag{11.7}$$

Proof. Given a trajectory $x(t)$ of (11.4), let $V(t) = \|f(x(t),\theta(t))\|_{\mathcal{X}}$. Then we compute, omitting dependencies of x and θ on time,

$$\begin{aligned}
D^+V(t) &= \limsup_{h\to 0^+} \frac{\|f(x(t+h),u(t+h))\|_{\mathcal{X}} - \|f(x(t),u(t))\|_{\mathcal{X}}}{h} \\
&\overset{(\star)}{=} \lim_{h\to 0^+} \frac{\|f(x,\theta) + h\frac{d}{dt}f(x,\theta)\|_{\mathcal{X}} - \|f(x,\theta)\|_{\mathcal{X}}}{h} \\
&\overset{(11.4)}{=} \lim_{h\to 0^+} \frac{\|f(x,\theta) + hD_x f(x,\theta)f(x,\theta)\|_{\mathcal{X}} - \|f(x,\theta)\|_{\mathcal{X}}}{h} \\
&\leq \|f(x,\theta)\|_{\mathcal{X}} \lim_{h\to 0^+} \frac{\|I_n + hD_x f(x,\theta)\|_{\mathcal{X}} - 1}{h} \\
&\leq \mu_{\mathcal{X}}(D_x f(x,\theta))V(t) \leq -cV(t),
\end{aligned}$$

where $\overset{(\star)}{=}$ is by a Taylor expansion of f in t and the equality $\overset{(11.4)}{=}$ holds since (11.4) implies that $\frac{d}{dt}f(x,\theta) = D_x f(x,\theta)\dot{x} + D_\theta f(x,\theta)\dot{\theta} = D_x f(x,\theta) f(x,\theta)$. The Grönwall inequality for Dini derivatives implies statement (i). Statement (ii) is a consequence of the fact that $\|f(x,\theta) - f(x^\star(\theta),\theta)\|_{\mathcal{X}} \geq c\|x - x^\star(\theta)\|_{\mathcal{X}}$ since $f(x^\star(\theta),\theta) = 0_n$ and for fixed θ, the map $x \mapsto f(x,\theta)$ is invertible and the inverse map is Lipschitz on $(\mathcal{X}, \|\cdot\|_{\mathcal{X}})$ with constant $1/c$ [42, Lemma 3.5]. □

Remark 11.3.

(i) A related treatment to Theorem 11.4 is proposed in [167], (see also the early reference [179]) where the authors study a continuous-time Newton method and show how to add a feedforward term to ensure zero tracking error in the Euclidean norm. In contrast, Theorem 11.4 is very general and applies to any contracting dynamics with respect to any norm and need not be limited to the solution of time-varying optimization problems.

(ii) Compared to Theorem 11.3, Theorem 11.4 does not require Assumption (11.A2) but does additionally require differentiability of f.

□

11.4 Parameter-Varying Contracting Dynamical Systems for Canonical Convex Optimization Problems

We now focus on three canonical strongly convex optimization problems from Chapter 10: monotone inclusions, linear equality-constrained problems, and composite minimization problems, each of which we assume to be time-varying. For these problems, we consider the natural transcriptions into contracting dynamics introduced in Chapter 10 and apply the result of the previous section to provide tracking error estimates.

11.4.1 Parameter-Varying Monotone Inclusion Problem

Let $\mathsf{F}\colon \mathbb{R}^n \times \Theta \to \mathbb{R}^n$ and $g\colon \mathbb{R}^n \times \Theta \to \overline{\mathbb{R}}$ and, for fixed $\theta \in \Theta$, denote by $\mathsf{F}_\theta\colon \mathbb{R}^n \to \mathbb{R}^n$ the map $\mathsf{F}(\cdot,\theta)$ and by $g_\theta\colon \mathbb{R}^n \to \overline{\mathbb{R}}$ the map $g(\cdot,\theta)$. We make the following assumptions on the functions F and g.

Assumption 11.2. *For each $\theta \in \Theta$, the function F_θ is Lipschitz with constant $\mathsf{Lip}_x(\mathsf{F})$ and strongly monotone with parameter m_{F}. The map g_θ is closed, convex, and proper. Additionally, at fixed $x \in \mathbb{R}^n$ the map $\theta \mapsto \mathsf{F}(x,\theta)$ is Lipschitz and, for every $\gamma > 0$ the map $\theta \mapsto \operatorname{prox}_{\gamma g_\theta}(x)$ is Lipschitz with constant $\mathsf{Lip}_\theta(\operatorname{prox}_{\gamma g})$.*

Consider the following *parameter-varying monotone inclusion problem*

$$\text{for } \theta \in \Theta, \text{ find } x^\star(\theta) \in \mathbb{R}^n \text{ s.t. } 0_n \in (\mathsf{F}_\theta + \partial g_\theta)(x^\star(\theta)), \tag{11.8}$$

To solve the monotone inclusion problem (11.8), we consider the corresponding *continuous-time parameter-varying forward-backward splitting dynamics* defined by

$$\dot{x} = -x + \operatorname{prox}_{\gamma g_\theta}(x - \gamma \mathsf{F}_\theta(x)) =: \mathsf{F}^\gamma_{\mathrm{MI}}(x, \theta), \tag{11.9}$$

where $\gamma > 0$ is a parameter.

For each $\theta \in \Theta$, Theorem 10.4 implies that, for suitable $\gamma > 0$, the dynamics (11.9) are strongly infinitesimally contracting. Therefore, problem (11.8) has a unique solution $x^\star(\theta)$. When $\theta \colon \mathbb{R}_{\geq 0} \to \Theta$ is a continuously differentiable curve, let $x^\star(\theta(\cdot))$ be the corresponding time-varying equilibrium curve. If the map $\theta \mapsto \mathsf{F}^\gamma_{\mathrm{MI}}(x, \theta)$ is Lipschitz, Theorem 11.3 ensures that trajectories of (11.9) track $x^\star(\theta(t))$ with a tracking error proportional to $\|\dot{\theta}(t)\|_\Theta$ after a transient. The following lemma formalizes this statement, providing a precise estimate of the tracking error.

Lemma 11.5 (Equilibrium tracking for (11.9))**.** *Consider the continuous-time parameter-varying forward-backward splitting dynamics* (11.9) *satisfying Assumption 11.2. Then*

(i) for fixed $x \in \mathbb{R}^n$, for any $\gamma > 0$ the map $\theta \mapsto \mathsf{F}^\gamma_{\mathrm{MI}}(x, \theta)$ is Lipschitz with constant

$$\operatorname{Lip}_\theta(\mathsf{F}^\gamma_{\mathrm{MI}}) \leq \operatorname{Lip}_\theta(\operatorname{prox}_{\gamma g}) + \gamma \operatorname{Lip}_\theta(\mathsf{F}).$$

Additionally, if the map $\theta \colon \mathbb{R}_{\geq 0} \to \Theta$ is continuously differentiable, then

(ii) for $\gamma \in \left]0, 2m_{\mathsf{F}} / \operatorname{Lip}^2_x(\mathsf{F})\right[$, any $x_0 \in \mathbb{R}^n$, and any trajectory $x(t)$ satisfying $\dot{x}(t) = \mathsf{F}^\gamma_{\mathrm{MI}}(x(t), \theta(t))$ with initial conditions $x(0) = x_0$ satisfies

$$\begin{aligned}\|x(t) - x^\star(\theta(t))\|_2 \leq \mathrm{e}^{-ct}\|x_0 - x^\star(\theta_0)\|_2 \\ + \frac{\operatorname{Lip}_\theta(\operatorname{prox}_{\gamma g}) + \gamma \operatorname{Lip}_\theta(\mathsf{F})}{c} \int_0^t \mathrm{e}^{-c(t-\tau)}\|\dot{\theta}(\tau)\| d\tau,\end{aligned}$$

where $c = 1 - \sqrt{1 - 2\gamma m_{\mathsf{F}} + \gamma^2 \operatorname{Lip}^2_x(\mathsf{F})}$.

Proof. To prove statement (i), let $\theta_1, \theta_2 \in \Theta$. For any $\gamma > 0$ we have

$$\begin{aligned}\|\mathsf{F}^\gamma_{\mathrm{MI}}(x, \theta_1) - \mathsf{F}^\gamma_{\mathrm{MI}}(x, \theta_2)\|_2 &= \|\operatorname{prox}_{\gamma g_{\theta_1}}(x - \gamma \mathsf{F}_{\theta_1}(x)) - \operatorname{prox}_{\gamma g_{\theta_2}}(x - \gamma \mathsf{F}_{\theta_2}(x))\|_2 \\ &\leq \|\operatorname{prox}_{\gamma g_{\theta_1}}(x - \gamma \mathsf{F}_{\theta_1}(x)) - \operatorname{prox}_{\gamma g_{\theta_2}}(x - \gamma \mathsf{F}_{\theta_1}(x))\|_2 \\ &\quad + \|\operatorname{prox}_{\gamma g_{\theta_2}}(x - \gamma \mathsf{F}_{\theta_1}(x)) - \operatorname{prox}_{\gamma g_{\theta_2}}(x - \gamma \mathsf{F}_{\theta_2}(x))\|_2 \\ &\leq \operatorname{Lip}_\theta(\operatorname{prox}_{\gamma g})\|\theta_1 - \theta_2\|_\Theta + \|x - \gamma \mathsf{F}_{\theta_1}(x) - x + \gamma \mathsf{F}_{\theta_2}(x)\|_2 \\ &\leq (\operatorname{Lip}_\theta(\operatorname{prox}_{\gamma g}) + \gamma \operatorname{Lip}_\theta(\mathsf{F}))\|\theta_1 - \theta_2\|_\Theta.\end{aligned}$$

Statement (ii) is a consequence of Theorem 10.4 for strong infinitesimal contractivity in x with rate $1 - \sqrt{1 - 2\gamma m_{\mathsf{F}} + \gamma^2 \operatorname{Lip}^2_x(\mathsf{F})}$ and statement (i) for Lipschitzness in θ. Theorem 11.3 then provides the bound. This concludes the proof. □

If, additionally, $\mathsf{F}^\gamma_{\mathrm{MI}}$ is differentiable in both arguments, one can design a feedforward term to attain zero tracking error leveraging Theorem 11.4.

11.4.2 Parameter-Varying Linear Equality Constrained Optimization

Let $f\colon \mathbb{R}^n \times \Theta \to \mathbb{R}$, $b\colon \Theta \to \mathbb{R}^m$, and $A \in \mathbb{R}^{m\times n}$ be full row rank. For fixed $\theta \in \Theta$ we denote by $f_\theta\colon \mathbb{R}^n \to$ the map $f(\cdot,\theta)$ and by $b_\theta \in \mathbb{R}^m$ the vector $b(\theta)$. We make the following assumptions.

Assumption 11.3. *For each $\theta \in \Theta$, the function f_θ is continuously differentiable, strongly convex and strongly smooth with parameters m_f and L_f, respectively. Additionally, at fixed $x \in \mathbb{R}^n$, the map $\theta \mapsto \nabla_x f(x,\theta)$ is Lipschitz with constant $\mathsf{Lip}_\theta(\nabla f)$. The map $\theta \mapsto b_\theta$ is Lipschitz with constant $\mathsf{Lip}_\theta(b)$. Finally, the matrix $A \in \mathbb{R}^{m\times n}$ satisfies $a_{\min} I_m \preceq AA^\top \preceq a_{\max} I_m$, for $a_{\min}, a_{\max} \in \mathbb{R}_{>0}$.*

Consider the *parameter-dependent equality-constrained minimization problem*:

$$\begin{aligned} \min_{x\in\mathbb{R}^n} \quad & f_\theta(x), \\ \text{s.t.} \quad & Ax = b_\theta. \end{aligned} \tag{11.10}$$

To solve this minimization problem, we consider the corresponding continuous-time *parameter-varying primal-dual dynamics* defined by

$$\begin{aligned} \dot{x} &= -\nabla f_\theta(x) - A^\top \lambda, \\ \dot{\lambda} &= Ax - b_\theta. \end{aligned} \tag{11.11}$$

By Theorem 10.6, for each $\theta \in \Theta$, the dynamics (11.11) is guaranteed to converge to the unique primal-dual pair solving problem (11.10). The following lemma shows that, under proper assumptions, the dynamics (11.11) track the time-varying equilibrium curve $x^\star(\theta(t)), \lambda^\star(\theta(t))$ with a tracking error proportional to $\|\dot\theta(t)\|$ after a transient.

Lemma 11.6 (Equilibrium tracking for (11.11))**.** *Consider the continuous-time parameter-varying forward-backward splitting dynamics (11.11) satisfying Assumption 11.3. Let $z = (x,\lambda) \in \mathbb{R}^{n+m}$, and let $f_{\text{PD}}\colon \mathbb{R}^{n+m} \times \Theta \to \mathbb{R}^{n+m}$ be the vector field defining $\dot z = f_{\text{PD}}(z,\theta)$ via the dynamics (11.11). Then*

(i) for fixed $z \in \mathbb{R}^{n+m}$, the map $\theta \mapsto f_{\text{PD}}(z,\theta)$ is Lipschitz with constant

$$\mathsf{Lip}_\theta(f_{\text{PD}}) \le \sqrt{\|P\|_2 \|P^{-1}\|_2 (\mathsf{Lip}_\theta(\nabla f)^2 + \mathsf{Lip}_\theta(b)^2)},$$

where the matrix P is defined in (10.14).

Additionally, if the map $\theta\colon \mathbb{R}_{\ge 0} \to \Theta$ is continuously differentiable, then

(ii) for any $x_0 \in \mathbb{R}^n, \lambda_0 \in \mathbb{R}^m$, and any trajectory $z = (x,\lambda) \in \mathbb{R}^{n+m}$ satisfying $\dot z(t) = f_{\text{PD}}(\theta(t), z(t))$ with initial condition $z_0 = (x_0,\lambda_0)$ further satisfies

$$\begin{aligned} \|z(t) - z^\star(\theta(t))\|_P &\le \mathrm{e}^{-ct} \|z_0(t) - z^\star(\theta_0(t))\|_P \\ &\quad + \frac{\sqrt{\|P\|_2 \|P^{-1}\|_2 (\mathsf{Lip}_\theta(\nabla f)^2 + \mathsf{Lip}_\theta(b)^2)}}{c} \int_0^t \mathrm{e}^{-c(t-\tau)} \|\dot\theta(\tau)\|_\Theta d\tau, \end{aligned}$$

where P is defined in (10.14) and $c > 0$ is defined in (10.15).

Proof. To prove statement (i), let $\theta, \varphi \in \Theta$. We compute

$$\begin{aligned}
\|f_{\mathrm{PD}}(\theta, z) - f_{\mathrm{PD}}(\varphi, z)\|_P^2 &= \left\| \begin{bmatrix} -\nabla f_\theta(x) - A^\top \lambda + \nabla f_\varphi(x) + A^\top \lambda \\ Ax - b_\theta - Ax + b_\varphi \end{bmatrix} \right\|_P^2 \\
&= \left\| \begin{bmatrix} \nabla f_\varphi(x) - \nabla f_\theta(x) \\ b_\varphi - b_\theta \end{bmatrix} \right\|_P^2 \\
&\leq \|P\|_2 \|P^{-1}\|_2 \left\| \begin{bmatrix} \nabla f_\varphi(x) - \nabla f_\theta(x) \\ b_\varphi - b_\theta \end{bmatrix} \right\|_2^2 \\
&= \|P\|_2 \|P^{-1}\|_2 (\|\nabla f_\theta(x) - \nabla f_\varphi(x)\|_2^2 + \|b_\theta - b_\varphi\|_2^2) \\
&\leq \|P\|_2 \|P^{-1}\|_2 (\mathsf{Lip}_\theta(\nabla f)^2 + \mathsf{Lip}_\theta(b)^2) \|\theta - \varphi\|_\Theta^2,
\end{aligned}$$

which implies the statement. Statement (ii) is a consequence of Theorem 10.6, which proves strong infinitesimal contractivity in z with rate c defined in Equation (10.15), and statement (i) for Lipschitzness in θ. Finally, Theorem 11.3 provides the bound. □

If, additionally, $\nabla_\theta f$ is differentiable in x and θ and b_θ is differentiable in θ, then we can design a feedforward term involving $\dot{\theta}$ leveraging Theorem 11.4 to attain zero tracking error.

Remark 11.4. *We have not let the matrix A depend on the parameter θ since the norm with respect to which the dynamics (10.11) are contracting depends on A. If A depends on θ, then the norm with respect to which the dynamics are contracting is also parameter-dependent and the results from Theorems 11.3 and 11.4 do not directly apply.* □

11.4.3 Parameter-Varying Composite Minimization

Let $f\colon \mathbb{R}^n \times \Theta \to \mathbb{R}$, $g\colon \mathbb{R}^m \times \Theta \to \overline{\mathbb{R}}$, and $A \in \mathbb{R}^{m \times n}$ be full row rank. For fixed $\theta \in \Theta$ we denote by $f_\theta\colon \mathbb{R}^n \to$ the map $f(\cdot, \theta)$ and by $g_\theta\colon \mathbb{R}^m \to \overline{\mathbb{R}}$ the map $g(\cdot, \theta)$. We make the following assumptions.

Assumption 11.4. *For each $\theta \in \Theta$, the function $f\colon \mathbb{R}^n \times \Theta \to \mathbb{R}$ is continuously differentiable, strongly convex and strongly smooth with parameters m_f and L_f, respectively, while the map g_θ is convex, closed and proper. Additionally, at fixed $x \in \mathbb{R}^n$, the map $\theta \mapsto \nabla_x f(x, \theta)$ is Lipschitz with constant $\mathsf{Lip}_\theta(\nabla f)$ and, for every $\gamma > 0$, the map $\theta \mapsto \mathrm{prox}_{\gamma g_\theta}(x)$ is Lipschitz with constant $\mathsf{Lip}_\theta(\mathrm{prox}_{\gamma g})$. Finally, the matrix $A \in \mathbb{R}^{m \times n}$ satisfies $a_{\min} I_m \preceq AA^\top \preceq a_{\max} I_m$, for $a_{\min}, a_{\max} \in \mathbb{R}_{>0}$.*

Consider the following *parameter-dependent composite minimization problem*

$$\min_{x \in \mathbb{R}^n} f_\theta(x) + g_\theta(Ax). \tag{11.12}$$

To solve this composite minimization problem we consider the primal-dual dynamics on the *parameter-varying proximal augmented Lagrangian* defined by

$$\begin{aligned}\dot{x} &= -\nabla f_\theta(x) - A^\top \nabla M_{\gamma g_\theta}(Ax + \gamma\lambda),\\ \dot{\lambda} &= \gamma(-\lambda + \nabla M_{\gamma g_\theta}(Ax + \gamma\lambda)).\end{aligned} \tag{11.13}$$

By Theorem 10.7, the dynamics (11.13) converge to the unique primal-dual pair solving the minimization problem (11.12). In what follows, we show that, under proper assumptions, the dynamics (11.13) track the time-varying equilibrium curve $x^\star(\theta(t)), \lambda^\star(\theta(t))$ with a tracking error proportional to $\|\dot{\theta}(t)\|$ after a transient.

Lemma 11.7 (Equilibrium tracking for (11.13))**.** *Consider the parameter-varying proximal augmented Lagrangian* (11.13) *satisfying Assumption 11.4. Let $z = (x, \lambda) \in \mathbb{R}^{n+m}$, and let $f_{\text{CM}} \colon \mathbb{R}^{n+m} \times \Theta \to \mathbb{R}^{n+m}$ be the vector field defining $\dot{z} = f_{\text{CM}}(z, \theta)$ via the dynamics* (11.13)*. Then*

(i) for fixed $z \in \mathbb{R}^{n+m}$, the map $\theta \mapsto f_{\text{CM}}(z, \theta)$ is Lipschitz with estimate

$$\mathsf{Lip}_\theta(f_{\text{CM}}) \leq \sqrt{\|P\|_2 \|P^{-1}\|_2 (\mathsf{Lip}_\theta(\nabla f)^2 + \left(\frac{a_{\max}}{\gamma^2} + 1\right) \mathsf{Lip}_\theta(\operatorname{prox}_{\gamma g})^2)} =: L_\theta,$$

where the matrix P is defined in (10.21)*.*

Additionally, if the map $\theta \colon \mathbb{R}_{\geq 0} \to \Theta$ is continuously differentiable, then

(ii) for any $x_0 \in \mathbb{R}^n, \lambda_0 \in \mathbb{R}^m$ and any trajectory $z = (x, \lambda) \in \mathbb{R}^{n+m}$ satisfying $\dot{z}(t) = f_{\text{CM}}(\theta(t), z(t))$ with initial condition $z_0 = (x_0, \lambda_0)$, satisfies

$$\|z(t) - z^\star(\theta(t))\|_P \leq \mathrm{e}^{-c^\star t} \|z_0(t) - z^\star(\theta_0(t))\|_P + \frac{L_\theta}{c^\star} \int_0^t \mathrm{e}^{-c^\star(t-\tau)} \|\dot{\theta}(\tau)\|_\Theta d\tau,$$

where P is defined in (10.21)*, $c^\star > 0$ is the optimal parameter solving* (10.20)*.*

Proof. The proof of statement (i) follows from analogous steps to the proof of 11.6(i) and using the equality $\nabla M_{\gamma g_\theta}(Ax+\gamma\lambda) = \frac{1}{\gamma}(Ax+\gamma\lambda - \operatorname{prox}_{\gamma g_\theta}(Ax+\gamma\lambda))$. Statement (ii) is a consequence of Theorem 11.3, which proves strong infinitesimal contractivity in z with rate $c^\star$, and statement (i) for Lipschitzness in θ with estimate L_θ. Finally, the bound follows from Theorem 11.3. □

Additionally, if f_{CM} is differentiable in both of its arguments, then we can leverage Theorem 11.4 to design a feedforward term involving $\dot{\theta}$ to attain zero tracking error.

Remark 11.5. *As in the case of linear equality-constrained minimization, the matrix A cannot depend on the parameter θ. For the same reason as before, the norm with respect to which the dynamics* (10.19) *are contracting depends on A.* □

11.5 Numerical Simulations

In this section, we report two numerical examples to validate the performance of the proposed dynamics. We present an application of Theorem 11.3 to a problem with equality constraints, which corresponds to Problem (11.10) and a case with inequality constraints, which corresponds to Problem (11.12).

11.5.1 Equality Constraints

Consider the following time-varying quadratic optimization problem with equality constraints

$$\begin{aligned} \min_{x\in\mathbb{R}^3} \quad & \frac{1}{2}\|x - r(t)\|_2^2, \\ \text{s.t.} \quad & x_1 + 2x_2 + x_3 = \sin(\omega t), \end{aligned} \tag{11.14}$$

where $\omega = 0.2$ and $r(t) = (\sin(\omega t), \cos(\omega t), 1)$. We can see that the minimization problem (11.14) is an instance of the parameter-dependent equality-constrained minimization problem (11.10) with $n = 3$ primal variables and $m = 1$ equality constraints by letting $\theta(t) = (\cos(\omega t), \sin(\omega t)) \in \Theta := \{z \in \mathbb{R}^2 \mid \|z\|_2 \leq 1\} \subset \mathbb{R}^2$. Letting $\|\cdot\|_\Theta = \|\cdot\|_2$, we can verify that the Lipschitz assumptions are verified for $f_{\theta(t)}(x) = \frac{1}{2}\|x - r(t)\|_2^2$ and $b_{\theta(t)} = \sin(\omega t)$. The corresponding primal-dual dynamics for problem (11.14) read

$$\begin{aligned} \dot{x}_1 &= -x_1 + \sin(\omega t) - \lambda, \\ \dot{x}_2 &= -x_2 + \cos(\omega t) - 2\lambda, \\ \dot{x}_3 &= -x_3 + 1 - \lambda, \\ \dot{\lambda} &= x_1 + 2x_2 + x_3 - \sin(\omega t). \end{aligned} \tag{11.15}$$

We simulate the dynamics (11.15) over the time interval $t \in [0, 50]$ with a forward Euler discretization with stepsize $\Delta t = 0.01$ and set the initial conditions $x(0) = \mathbb{0}_3, \lambda(0) = 0$. We plot the trajectories of the primal variables in dynamics along with the instantaneously optimal values $x^\star(\theta(t))$ in Figure 11.1.

We empirically observe how the trajectories of the dynamics track the instantaneously optimal values $x^\star(\theta(t))$ after a small transient.

11.5.2 Inequality Constraints

Consider the following time-varying quadratic optimization problem with inequality constraints

$$\begin{aligned} \min_{x\in\mathbb{R}^2} \quad & \frac{1}{2}\|x + r(t)\|_2^2, \\ \text{s.t.} \quad & -x_1 + x_2 \leq \cos(\omega t), \end{aligned} \tag{11.16}$$

where $\omega = 0.2$ and $r(t) = (\sin(\omega t), \cos(\omega t))$. We see that (11.16) is an instance of (11.13) with $g\colon \mathbb{R} \times \Theta \to \overline{\mathbb{R}}$ given by $g(z, \theta) = \iota_{\mathcal{C}_\theta}(z)$ where $\mathcal{C}_\theta = \{z \in \mathbb{R} \mid z \leq \theta_1\}$,

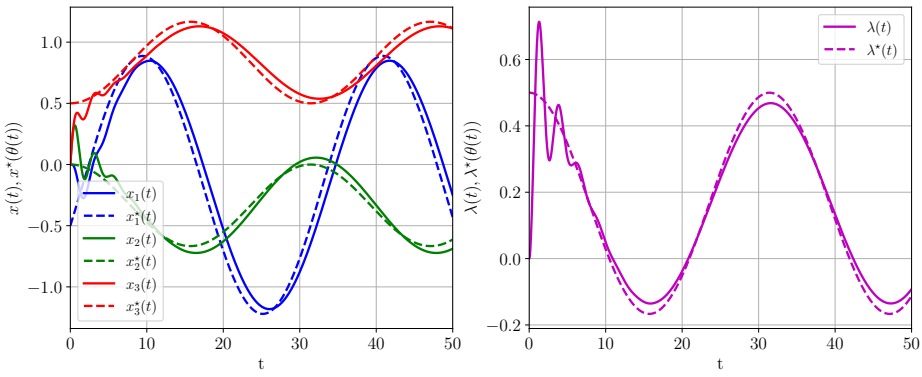

Figure 11.1: Plots of trajectories of the primal variables in dynamics (11.15) solving the equality-constrained minimization problem (11.14). Left panel: trajectories of the primal variables $x(t)$ as solid curves and trajectories of the instantaneously optimal primal variables $x^\star(\theta(t))$ as dashed curves. Right panel: trajectories of the dual variable $\lambda(t)$ as solid curve and trajectory of the instantaneously optimal dual variable $\lambda(\theta(t))$ as dashed curve.

$\theta(t) = (\cos(\omega t), \sin(\omega t)) \in \Theta := \{z \in \mathbb{R}^2 \mid \|z\|_2 \leq 1\}$, and $A = [-1, 1]$. Then for given $t, \theta(t), z$, we can verify that

$$\operatorname{prox}_{\gamma g_{\theta(t)}}(z) = \mathbb{P}_{\mathcal{C}_{\theta(t)}}(z) = \min\{z, \cos(\omega t)\}$$

and the corresponding Moreau envelope is

$$\nabla M_{\gamma g_{\theta(t)}}(z) = \frac{1}{\gamma}(z - \min\{z, \cos(\omega t)\}) = \frac{1}{\gamma}\operatorname{ReLU}(z - \cos(\omega(t))).$$

Thus, we can verify that the Lipschitz assumptions in θ hold. The corresponding primal-dual dynamics on the augmented Lagrangian for problem (11.16) then read

$$\begin{aligned}
\dot{x}_1 &= -x_1 - \sin(\omega t) + \frac{1}{\gamma}\operatorname{ReLU}(-x_1 + x_2 + \gamma\lambda - \cos(\omega t)),\\
\dot{x}_2 &= -x_2 - \cos(\omega t) - \frac{1}{\gamma}\operatorname{ReLU}(-x_1 + x_2 + \gamma\lambda - \cos(\omega t)),\\
\dot{\lambda} &= -\gamma\lambda + \operatorname{ReLU}(-x_1 + x_2 + \gamma\lambda - \cos(\omega t)).
\end{aligned}$$

We simulate the dynamics (11.17) with $\gamma = 10$ over the time interval $t \in [0, 50]$ with a forward Euler discretization with stepsize $\Delta t = 0.01$ and initial conditions $x(0) = \mathbb{0}_2, \lambda(0) = 0$. We plot the trajectories of the primal variables in dynamics along with the instantaneously optimal values $x^\star(\theta(t))$ in Figure 11.2.

We empirically observe how the trajectories of the dynamics track the instantaneously optimal values $x^\star(\theta(t))$ after a small transient.

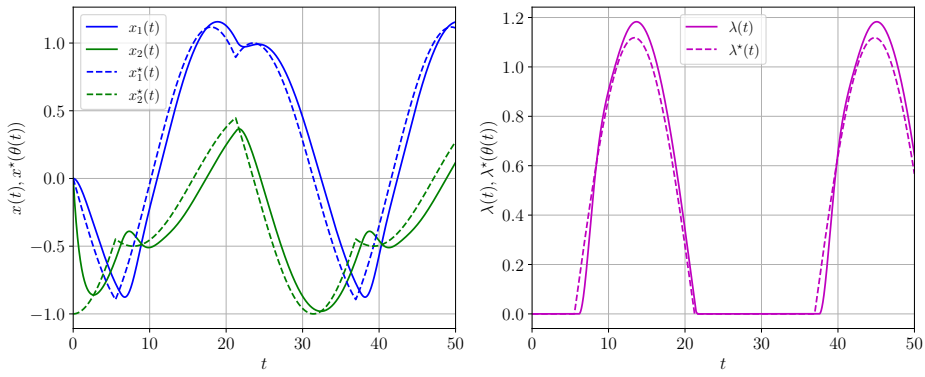

Figure 11.2: Plots of trajectories of the primal variables in dynamics (11.17) solving the inequality-constrained minimization problem (11.16). Left panel: trajectories of the primal variables $x(t)$ as solid curves and trajectories of the instantaneously optimal primal variables $x^\star(\theta(t))$ as dashed curves. Right panel: trajectories of the dual variable $\lambda(t)$ as solid curve and trajectory of the instantaneously optimal dual variable $\lambda(\theta(t))$ as dashed curve.

11.6 Summary

In this chapter, we proposed a contraction theory approach to the problem of tracking optimal trajectories in time-varying convex optimization problems. We presented two main results on equilibrium tracking for parameter-varying contracting dynamics, addressing both scenarios where the rate of change of the parameter is known and unknown. Specifically, in Theorem 11.3, we proved that the tracking error between any solution trajectory of a strongly infinitesimally contracting system and its equilibrium trajectory is upper bounded with an explicit estimate on the bound. This bound gives designers valuable insight into how they may accelerate their dynamics to achieve lower tracking errors. Specifically, we showed that the bound is asymptotically proportional to the rate of change of the parameter, confirming the intuitive result that the faster the system the bigger the tracking error. The applicability of these results has already been proved in other contexts. Specifically, [180] leveraged these findings to develop a computationally efficient barrier function-based contraction approach for safety verification. For the scenario where the rate of change of the parameter is known, in Theorem 11.4, we prove that by augmenting a strongly infinitesimally contracting system with a feedforward term we can ensure that the tracking error converges to zero exponentially quickly.

Then, we applied these results to convex optimization problems. By leveraging the contractivity results in Chapter 10, we applied Theorem 11.3 to provide explicit tracking error bounds. Specifically, we focused on monotone inclusions, linear equality-constrained problems, and composite minimization problems. We concluded the chapter with two numerical examples to validate the proposed bounds.

12 On Weakly Contracting Dynamics for Convex Optimization

In Chapters 10 and 11, we proposed a contractivity-based approach to effectively solve static and time-varying strongly-convex optimization problems. In this chapter, we extend our analysis beyond the case of strong convexity and focus on convex optimization problems with unique minimizers. As we will show, these problems lead to dynamics that are globally-weakly contracting in the state space and only locally-strongly contracting, such as the the firing rate competitive networks analyzed in Chapter 7. Our goal is to study and characterize the convergence behavior of these systems. The results presented in this chapter appeared in:

- **V. Centorrino**, A. Davydov, A. Gokhale, G. Russo, and F. Bullo. "On Weakly Contracting Dynamics for Convex Optimization". *IEEE Control Systems Letters*, vol. 8, pp. 1745-1750, June 2024. doi: 10.1109/LCSYS.2024.3414348.

Additionally, part of the results were presented at:

- Workshop "Variational Inequalities, Nash Equilibrium Problems and Applications". "On Contracting Dynamics for Convex Optimization", Oral Talk, Catania, July 11-12, 2024. Website: https://vinepa.dmi.unict.it/,
- **V. Centorrino**, A. Davydov, A. Gokhale, G. Russo, and F. Bullo. "On Weakly Contracting Dynamics for Convex Optimization", *63rd IEEE Conference on Decision and Control*, Milan, Italy, December 2024. Presented in the invited session "Contraction Theory in Systems and Control I".

12.1 Introduction

As established in previous chapters, one powerful way to analyze convex optimization problems is to synthesize continuous-time dynamical systems that *converge* to an equilibrium that is also the optimal solution to the problem. A suitable tool to assess the convergence of these dynamics is contraction theory. For optimization problems with strongly convex costs, the corresponding gradient dynamics, primal-dual dynamics (in the presence of constraints), or proximal gradient dynamics (for non-smooth costs) are strongly contracting, implying that trajectories exponentially converge to the equilibrium, which is also the optimal solution. In contrast, for optimization problems with only convex costs, the corresponding gradient, primal-dual, or proximal gradient dynamics are weakly contracting, and convergence depends on the existence of the minimizer. In this context, we now focus on convex optimization problems with a unique minimizer via continuous-time dynamical systems. These optimization problems lead to a class of continuous-time dynamical systems that are globally-weakly contracting in the state space and only locally-strongly contracting. We characterize the convergence behavior of such dynamics, showing that this is *linear-exponential*, and present local input-to-state stability (ISS) results.

The chapter is organized as follows. Section 12.2 presents the initial setup, formally defining the linear-exponential function and its properties. Then, we analyze the convergence properties of globally-weakly and locally-strongly contracting dynamics. Specifically, in Section 12.3 we analyze the case in which global and local contractivity are with respect to the same norm. The scenario of different norms is then analyzed in Section 12.4. Section 12.5 characterizes local ISS for input-dependent dynamics that are GW-LS-C. Finally, in Section 12.6, we illustrate the effectiveness of our results by applying them to a dynamical system solving the LP problem.

12.1.1 Contributions

We analyze the convergence behavior of the class of globally-weakly and locally-strongly contracting (GW-LS-C) dynamics, showing that this is *linear-exponential*, in the sense that the distance between each solution of the system and the equilibrium is upper bounded by a *linear-exponential function*, introduced in this chapter. Through a novel technical result, we characterize the evolution of certain dynamics with saturation in terms of the linear-exponential function. This result is then exploited for our convergence analysis, which is carried out considering two cases that require distinct mathematical approaches. First, we consider systems that are GW-LS-C with respect to the same norm. Then, we consider the case where the dynamics are GW-LS-C with respect to two different norms. Additionally, we characterize local ISS for input-dependent dynamics that are GW-LS-C with respect to the same norm. Finally, we show the effectiveness of our results by considering continuous-time dynamics tackling LPs and propose a general conjecture. The code to replicate our numerical example is given at `https://shorturl.at/vGNY1`.

12.2 Linear-Exponential Function

In this section, we define the *linear-exponential function*, which plays a pivotal role in bounding the convergence behavior of GW-LS-C systems.

Definition 12.1 (Linear-exponential function)**.** *Given a* linear decay rate $c_{\text{lin}} > 0$*, an* intercept $q > 0$*, an* exponential decay rate $c_{\text{exp}} > 0$*, and a* linear-exponential crossing time $t_{\text{cross}} < q/c_{\text{lin}}$*, the* linear-exponential function $\text{lin-exp}\colon \mathbb{R}_{\geq 0} \to \mathbb{R}_{\geq 0}$ *is defined by*

$$\text{lin-exp}(t) = \begin{cases} q - c_{\text{lin}} t & \text{if } t \leq t_{\text{cross}}, \\ \big(q - c_{\text{lin}} t_{\text{cross}}\big) \mathrm{e}^{-c_{\text{exp}}(t - t_{\text{cross}})} & \text{if } t > t_{\text{cross}}. \end{cases} \tag{12.1}$$

We write $\text{lin-exp}(t\ ;\ q, c_{\text{lin}}, c_{\text{exp}}, t_{\text{cross}})$ *when we want to highlight the parameters in* (12.1)*. See Figure 12.1 for an illustration of equation* (12.1) *for some parameters.*

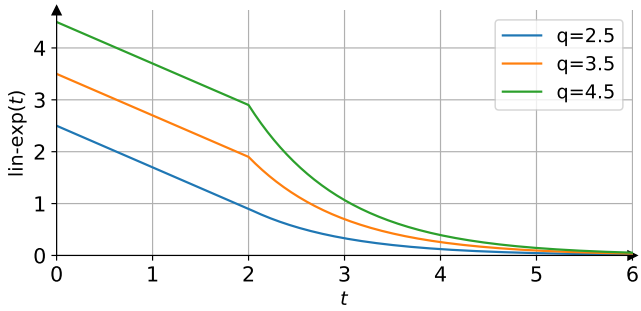

Figure 12.1: Plot of the linear-exponential function (12.1) with linear decay rate $c_{\text{lin}} = 0.8$, intercepts $q = \{2.5,\ 3.5,\ 4.5\}$, exponential decay rate $c_{\text{exp}} = 1$, and linear-exponential crossing time $t_{\text{cross}} = 2$.

The next result shows that the linear-exponential function is the solution of certain continuous-time dynamics with saturations.

Lemma 12.1 (Property of the linear-exponential function)**.** *Let* c_{exp} *and* d *be positive scalars. Consider the dynamics*

$$\dot{x}(t) = -c_{\text{exp}} \operatorname{sat}_d\big(x(t)\big), \quad x_0 = q > d. \tag{12.2}$$

Then, $x(t) = \text{lin-exp}(t\ ;\ q, c_{\text{lin}}, c_{\text{exp}}, t_{\text{cross}})$*, with* $c_{\text{lin}} = d c_{\text{exp}}$ *and* $t_{\text{cross}} := q c_{\text{lin}}^{-1} - c_{\text{exp}}^{-1}$*, is a solution of* (12.2)*.*

Proof. First, we note that being the right-hand side of the dynamics (12.2) locally Lipschitz continuous, the ODE (12.2) admits a unique continuous solution at least within a certain neighborhood of the initial condition. Using the definition of saturation function,

for all $t \in \mathbb{R}_{\geq 0}$ we can write the ODE (12.2) as

$$\dot{x}(t) = \begin{cases} dc_{\text{exp}} & \text{if } x(t) < -d, \\ -c_{\text{exp}} x(t) & \text{if } x(t) \in [-d, d], \\ -dc_{\text{exp}} & \text{if } x(t) > d, \end{cases} \tag{12.3}$$

which, in each interval $[t_0, t_1] \subseteq \mathbb{R}_{\geq 0}$ where the solution is continuous and does not change regime, has general solution

$$x(t) = \begin{cases} dc_{\text{exp}} t + x(t_0) & \text{if } x(t) < -d, \\ x(t_0) \mathrm{e}^{-c_{\text{exp}}(t - t_0)} & \text{if } x(t) \in [-d, d], \\ -dc_{\text{exp}} t + x(t_0) & \text{if } x(t) > d. \end{cases} \tag{12.4}$$

At time $t = 0$, we have $x_0 = q > d$. For continuity of the solution, there exists $t^\star$ such that $x(t) > d$, $\forall t \in [0, t^\star]$. Thus from equality (12.4) and being $x(t_0 = 0) = q$, it is $x(t) = -dc_{\text{exp}} t + q, \forall t \in [0, t^\star]$. Moreover being $x(t)$ decreasing, the time value $t^\star$ is finite and there exists a time, say it $\bar{t}$, such that $x(\bar{t}) = d$. Let $c_{\text{lin}} := dc_{\text{exp}}$, we have

$$x(\bar{t}) = d \iff -dc_{\text{exp}} \bar{t} + q = d \iff \bar{t} = q c_{\text{lin}}^{-1} - c_{\text{exp}}^{-1} := t_{\text{cross}}.$$

In summary, we have shown that the solution of (12.3) is $x(t) = q - c_{\text{lin}} t$ for all $t \in [0, t_{\text{cross}}]$ and is $x(t) = d$ at time t_{cross}. Thus, since $x(t_{\text{cross}}) = q - c_{\text{lin}} t_{\text{cross}}$, for all $t > t_{\text{cross}}$, from (12.4) we have $x(t) = \big(q - c_{\text{lin}} t_{\text{cross}}\big) \mathrm{e}^{-c_{\text{exp}}(t - t_{\text{cross}})}$. Specifically, $x(t) > 0$ for all $t > t_{\text{cross}}$, thus it can never be the case $x(t) < -d$. This concludes the proof. □

In the next sections, we focus on studying the convergence behavior of GW-LS-C dynamical systems of the form given by (4.1), where the function $f : \mathbb{R}_{\geq 0} \times \mathcal{C} \to \mathbb{R}^n$ is locally Lipschitz, and where $\mathcal{C} \subseteq \mathbb{R}^n$ is an open, convex, and f-invariant set. In what follows, we make the following assumptions.

Assumption . *There exist norms $\|\cdot\|_{\text{G}}, \|\cdot\|_{\text{L}}$ on $\mathbb{R}^n$ such that*

(12.A1) *f is weakly infinitesimally contracting on $\mathbb{R}^n$ with respect to $\|\cdot\|_{\text{G}}$,*
(12.A2) *f is c_{exp}-strongly infinitesimally contracting on a forward-invariant set $\mathcal{S}$ with respect to $\|\cdot\|_{\text{L}}$,*
(12.A3) *$x^\star \in \mathcal{S}$ is an equilibrium point, i.e., $f(t, x^\star) = \mathbb{0}_n$, for all $t \geq 0$.*

Remark 12.1. *Assumptions (12.A2), (12.A3) can be equivalently replaced by assuming the existence of a locally exponentially stable equilibrium.* □

In what follows, we first consider GW-LS-C systems with respect to the same norm and then GW-LS-C dynamics with respect to different norms. In both scenarios, we show that convergence is (globally) *linear-exponential*. That is, given a trajectory $x(t)$ of the dynamics, the distance $\|x(t) - x^\star\|_{\text{G}}$ is upper bounded by a linear-exponential function (12.1).

12.3 Convergence of Globally-Weakly and Locally-Strongly Contracting Dynamics with Respect to the Same Norm

We start by giving a bound on the upper right Dini derivative of the distance of any solution of the dynamical systems (4.1) with respect to the equilibrium $x^\star$.

Lemma 12.2 (Saturated error dynamics)**.** *Consider the dynamical system* (4.1) *and let Assumptions* (12.$A1$) – (12.$A3$) *hold with* $\|\cdot\|_{\mathrm{G}} = \|\cdot\|_{\mathrm{L}} := \|\cdot\|$. *Let* r *be the largest radius such that* $B\big(x^\star, r\big) \subseteq \mathcal{S}$. *Then, for every trajectory* $x(t)$ *starting from* $x_0 \notin \mathcal{S}$, *for almost every* $t \geq 0$, *we have*

$$D^+\|x(t) - x^\star\| \leq -c_{\exp}\,\mathrm{sat}_r(\|x(t) - x^\star\|). \tag{12.5}$$

Proof. Consider an arbitrary trajectory $x(t)$ starting from $x_0 \notin \mathcal{S}$ and a second trajectory equal to the equilibrium $x^\star$. Let μ be the log-norm associated to $\|\cdot\|$. For for almost every $t \geq 0$ it holds ([37, 38]):

$$D^+\|x(t) - x^\star\| \leq \int_0^1 \mu\Big(Df\big(t, x^\star + \alpha(x(t) - x^\star)\big)\Big)d\alpha \cdot \|x(t) - x^\star\| := RHS.$$

where $\alpha \in [0, 1]$, and $x^\star + \alpha(x(t) - x^\star)$ is the segment from $x^\star$ to $x(t)$.

For each $t \geq 0$, if $\|x(t) - x^\star\| \leq r$, then Assumption (12.$A2$) implies

$$RHS \leq \int_0^1 (-c_{\exp})d\alpha \cdot \|x(t) - x^\star\| = -c_{\exp}\|x(t) - x^\star\| = -c_{\exp}\,\mathrm{sat}_r\big(\|x(t) - x^\star\|\big),$$

where in the last equality we have used the definition of saturation function.
If $\|x(t) - x^\star\| \geq r$, define $\alpha^* = r/\|x(t) - x^\star\|$ and note that, for almost every $t \geq 0$, Assumptions (12.$A2$) and (12.$A1$) imply

$$\begin{aligned} \alpha \leq \alpha^* \quad &\Longrightarrow \quad \mu\big(Df(t, x^\star + \alpha(x(t) - x^\star))\big) \leq -c_{\exp}, \\ \alpha > \alpha^* \quad &\Longrightarrow \quad \mu\big(Df(t, x^\star + \alpha(x(t) - x^\star))\big) \leq 0. \end{aligned}$$

Therefore, for almost every $t \geq 0$, it holds

$$\begin{aligned} RHS &\leq \int_0^{\alpha^*} \mu\big(Df(t, x^\star + \alpha(x(t) - x^\star))\big)d\alpha \cdot \|x(t) - x^\star\| \\ &\quad + \int_{\alpha^*}^1 \mu\big(Df\big(t, x^\star + \alpha(x(t) - x^\star)\big)\big)d\alpha\Big) \cdot \|x(t) - x^\star\| \\ &\leq (-c_{\exp}\alpha^* + 0)\|x(t) - x^\star\| = -c_{\exp}r = -c_{\exp}\,\mathrm{sat}_r\big(\|x(t) - x^\star\|\big), \end{aligned} \tag{12.6}$$

where in the last equality we used the definition of saturation. Figure 12.2 provides an illustration of this result about the average of the log-norm. This concludes the proof. □

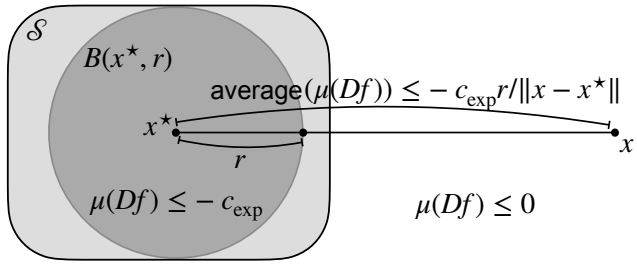

Figure 12.2: Illustration of the inequality (12.6) with $\|\cdot\| = \|\cdot\|_2$.

With this result in mind, we can now give our convergence result for GW-LS-C systems with respect to the same norm.

Theorem 12.3 (Linear-exponential convergence of GW-LS-C systems with respect to the same norm)**.** *Consider the dynamical system* (4.1) *and let Assumptions* (12.*A*1) – (12.*A*3) *hold with* $\|\cdot\|_{\text{G}} = \|\cdot\|_{\text{L}} := \|\cdot\|$. *Also, let* r *be the largest radius such that* $B\big(x^\star, r\big) \subseteq \mathcal{S}$. *For each trajectory* $x(t)$ *starting from* x_0*, it holds that*

(i) if $x_0 \in \mathcal{S}$*, then, for almost every* $t \geq 0$*,*

$$\|x(t) - x^\star\| \leq \mathrm{e}^{-c_{\text{exp}} t} \|x_0 - x^\star\|,$$

(ii) if $x_0 \notin \mathcal{S}$*, then, for almost every* $t \geq 0$*,*

$$\|x(t) - x^\star\| \leq \text{lin-exp}(t\ ;\ q, c_{\text{lin}}, c_{\text{exp}}, t_{\text{cross}}), \tag{12.7}$$

with

- *exponential decay rate* $c_{\text{exp}} > 0$*,*
- *linear decay rate* $c_{\text{lin}} = c_{\text{exp}}\, r$*,*
- *intercept* $q = \|x_0 - x^\star\|$*,*
- *linear-exponential crossing time* $t_{\text{cross}} = (q - r)/c_{\text{lin}}$.

Proof. Statement (i) follows from Assumption (12.*A*2). Item (ii) follows by using the Comparison Lemma 4.1 to upper bound the solution to the differential inequality (12.5). Additionally, the upper bound obeys precisely the initial value (12.2) in Lemma 12.1, for parameter values $d = r$, $c_{\text{lin}} = c_{\text{exp}} r$, $q = \|x_0 - x^\star\|$, and $t_{\text{cross}} = (q - r)/c_{\text{lin}}$. □

12.4 Convergence of Globally-Weakly and Locally-Strongly Contracting Dynamics with Respect to Different Norms

In this section, we extend the results from Section 7.3 by refining the convergence bound presented in Corollary 7.3. This improvement stems from a more accurate intercept and linear-exponential crossing time. Differently from the bound in inequality (7.13), the bound introduced here remains continuous at all times, and no jump can occur at t_{cross}.

We begin by formalizing the concept of the *ρ-contraction time*, where $0 < \rho < 1$ is the *contraction factor* introduced in Lemma 7.2. This concept plays a crucial role in quantifying the convergence behavior of the dynamics when different norms are applied globally and locally.

Definition 12.2 (ρ-contraction time)**.** *Let the dynamical system (4.1) be strongly infinitesimally contracting with respect to a norm $\|\cdot\|_\alpha$. Consider the* contraction factor *$0 < \rho < 1$, a norm $\|\cdot\|_\beta$, and a vector $x \in \mathbb{R}^n$.*

- *The* ρ-contraction time *is the time required for each trajectory starting in $B_\alpha(x, r)$, for some $r > 0$, to be inside $B_\alpha(x, \rho r)$,*
- *The* ρ-contraction time with respect to the norm $\|\cdot\|_\beta$ *is the time required for each trajectory starting in $B_\beta(x, r)$, for some $r > 0$, to be inside $B_\beta(x, \rho r)$.*

Remark 12.2. *It is implicit in Definition 12.2 that the ρ-contraction time for a specific trajectory depends on the initial condition and the center of the ball.* □

Lemma 12.4 (Contraction times with respect to distinct norms)**.** *Given $\|\cdot\|_\alpha$ and $\|\cdot\|_\beta$ norms on $\mathbb{R}^n$ with equivalence ratio $k_{\alpha,\beta}$, consider system (4.1) satisfying Assumptions (12.A2), (12.A3) with $\|\cdot\|_{\mathrm{L}} = \|\cdot\|_\alpha$. Then, for each contraction factor $0 < \rho < 1$,*

(i) the ρ-contraction time is $t_\rho = \ln(\rho^{-1})/c$,

(ii) the ρ-contraction time with respect to the norm $\|\cdot\|_\beta$ is $t_\rho^{\alpha,\beta} = \ln(k_{\alpha,\beta}\,\rho^{-1})/c$.

Proof. Consider a trajectory $x(t)$ of the dynamical system (4.1) such that $\|x_0\|_\alpha \le r$. To prove statement (i) we need to find the first time t_ρ such that $\|x(t_\rho) - x^\star\|_\alpha \le \rho r$. Clearly the worst-case time is achieved when $\|x_0 - x^\star\|_\alpha = r$. But c-strongly infinitesimal contractivity with respect to $\|\cdot\|_\alpha$ implies $\|x(t) - x^\star\|_\alpha \le \mathrm{e}^{-ct}\|x_0 - x^\star\|_\alpha$ and so t_ρ is determined by the equality $\mathrm{e}^{-ct_\rho} r = \rho r$, from which item (i) follows.

Regarding statement (ii), we need to find the first time $t_\rho^{\alpha,\beta}$ such that it holds the inequality $\|x(t_\rho) - x^\star\|_\beta \le \rho r$. We note that

$$
\begin{aligned}
x_0 \in B_\beta(x^\star, r) &\overset{(7.7),\ 2^{\text{nd}}\text{ inequality}}{\Longrightarrow} x_0 \in B_\alpha(x^\star, k_\alpha^\beta r),\\
x(t_\rho) \in B_\beta(x^\star, \rho r) &\overset{(7.7),\ 1^{\text{st}}\text{ inequality}}{\Longleftarrow} x(t_\rho) \in B_\alpha(x^\star, \rho r / k_\beta^\alpha).
\end{aligned}
$$

Thus, the contraction time from $B_\beta(x^\star, r)$ to $B_\beta(x^\star, \rho r)$ is upper bounded by the contraction time from $B_\alpha(x^\star, k_\alpha^\beta r)$ to $B_\alpha(x^\star, \rho r / k_\beta^\alpha)$. Therefore, the contraction factor with respect to the $\|\cdot\|_\alpha$ norm is $(\rho r / k_\beta^\alpha)/(k_\alpha^\beta r) = \rho / k_{\alpha,\beta}$. Statement (ii) then follows from statement (i). □

We can now give our convergence result for GW-LS-C systems with respect to the different norms.

Theorem 12.5 (Linear-exponential convergence of GW-LS-C systems)**.** *Let $\|\cdot\|_{\mathrm{L}}$ and $\|\cdot\|_{\mathrm{G}}$ be two norms on $\mathbb{R}^n$ with equivalence ratio $k_{\mathrm{L,G}}$. Consider system (4.1) satisfying Assumptions (12.A1) – (12.A3). Let r be the largest radius such that $B_{\mathrm{G}}(x^\star, r) \subseteq \mathcal{S}$. For each trajectory $x(t)$ starting from x_0, it holds that*

(i) if $x_0 \in \mathcal{S}$, then, for almost every $t \geq 0$,

$$\|x(t) - x^\star\|_{\mathrm{G}} \leq k_{\mathrm{L,G}} \mathrm{e}^{-c_{\exp} t} \|x_0 - x^\star\|_{\mathrm{G}}, \tag{12.8}$$

(ii) if $x_0 \notin \mathcal{S}$, then for any contractor factor *$0 < \rho < 1$ and, for almost every $t \geq 0$,*

$$\|x(t) - x^\star\|_{\mathrm{G}} \leq \text{lin-exp}(t\ ;\ q, c_{\text{lin}}, c_{\exp}, t_{\text{cross}}), \tag{12.9}$$

with

- *exponential decay rate* $c_{\exp} > 0$,
- *linear decay rate* $c_{\text{lin}} = c_{\exp} r(1-\rho) / \ln(k_{\mathrm{L,G}} \rho^{-1})$,
- *intercept* $q = \|x_0 - x^\star\|_{\mathrm{G}} + r(1-\rho) \dfrac{\ln(k_{\mathrm{L,G}})}{\ln(k_{\mathrm{L,G}} \rho^{-1})}$,
- *linear-exponential crossing time* $t_{\text{cross}} = \left\lceil \frac{\|x_0 - x^\star\|_{\mathrm{G}} - r}{(1-\rho) r} \right\rceil \ln(k_{\mathrm{L,G}} \rho^{-1}) / c_{\exp} + \ln(k_{\mathrm{L,G}}) / c_{\exp}$.

Proof. Consider a trajectory $x(t)$ starting from initial condition x_0. If $x_0 \in \mathcal{S}$, then statement (i) follows from Assumption (12.A2) and the equivalence of norms. Indeed, Assumption (12.A2) implies that for every $x_0 \in \mathcal{S}$ and for almost every $t \geq 0$, it holds

$$\|\phi_t(x_0) - x^\star\|_{\mathrm{L}} \leq \mathrm{e}^{-c_{\exp} t} \|x_0 - x^\star\|_{\mathrm{L}}.$$

Applying the equivalence of norms to the above inequality, we get

$$\|\phi_t(x_0) - x^\star\|_{\mathrm{G}} \leq k_{\mathrm{L,G}} \mathrm{e}^{-c_{\exp} t} \|x_0 - x^\star\|_{\mathrm{G}}. \tag{12.10}$$

If $x_0 \notin \mathcal{S}$, define the point $y_0 := x^\star + r \frac{x_0 - x^\star}{\|x_0 - x^\star\|_{\mathrm{G}}} \in \partial B_{\mathrm{G}}(x^\star, r)$[1]. The norm $\|y_0 - x^\star\|_{\mathrm{G}} = r$, therefore y_0 is a point on the boundary of $B_{\mathrm{G}}(x^\star, r)$. Moreover, the points $x^\star$, y_0, and x_0 lie on the same line segment, thus

$$\|x_0 - x^\star\|_{\mathrm{G}} = \|x_0 - y_0\|_{\mathrm{G}} + r. \tag{12.11}$$

[1] Note that $\partial B_{\mathrm{G}}(x^\star, r)$ means the boundary of $B_{\mathrm{G}}(x^\star, r)$.

By Lemma 12.4(ii) and because each trajectory originating in $B_{\mathrm{G}}(x^\star, r)$ remains in $\mathcal{S}$, the ρ-contraction with respect to $\|\cdot\|_{\mathrm{G}}$ for the $c_{\exp}$-strongly contracting map f is

$$t_\rho^{\mathrm{L,G}} = \frac{\ln(k_{\mathrm{L,G}}\rho^{-1})}{c_{\exp}}. \tag{12.12}$$

Then, for almost every $t \in [0, t_\rho^{\mathrm{L,G}}]$, we have

$$\begin{aligned}
\|\phi_t(x_0) - x^\star\|_{\mathrm{G}} &\le \|\phi_t(x_0) - \phi_t(y_0)\|_{\mathrm{G}} + \|\phi_t(y_0) - x^\star\|_{\mathrm{G}} && (12.13)\\
&\le \|x_0 - y_0\|_{\mathrm{G}} + k_{\mathrm{L,G}}\mathrm{e}^{-c_{\exp}t}\|y_0 - x^\star\|_{\mathrm{G}} && (12.14)\\
&\overset{(12.11)}{=} \|x_0 - x^\star\|_{\mathrm{G}} - \|x^\star - y_0\|_{\mathrm{G}} + k_{\mathrm{L,G}}\mathrm{e}^{-c_{\exp}t}r\\
&\overset{t=t_\rho^{\mathrm{L,G}}}{\le} \|x_0 - x^\star\|_{\mathrm{G}} - r(1 - k_{\mathrm{L,G}}\mathrm{e}^{-c_{\exp}t_\rho^{\mathrm{L,G}}})\\
&\overset{(12.12)}{=} \|x_0 - x^\star\|_{\mathrm{G}} - r(1-\rho), && (12.15)
\end{aligned}$$

where in (12.13) we added and subtracted $\phi_t(y_0)$ and applied the triangle inequality, while inequality (12.14) follows from Assumption (12.A1) and inequality (12.10). Now, equality (12.15) implies $\|\phi_{t_\rho^{\mathrm{L,G}}}(x_0) - x^\star\|_{\mathrm{G}} \le \|x_0 - x^\star\|_{\mathrm{G}} - r(1-\rho)$. If $\|x_0 - x^\star\|_{\mathrm{G}} - r(1-\rho) \le r$, then by Assumption (12.A2), for almost every in $t \ge t_\rho^{\mathrm{L,G}}$, we have

$$\|\phi_t(x_0) - x^\star\|_{\mathrm{G}} \le k_{\mathrm{L,G}}\mathrm{e}^{-c_{\exp}(t - t_\rho^{\mathrm{L,G}})}\big(\|x_0 - x^\star\|_{\mathrm{G}} - r(1-\rho)\big).$$

If $\|x_0 - x^\star\|_{\mathrm{G}} - r(1-\rho) > r$, we iterate the process. Specifically, let $x_\rho := \phi_{t_\rho^{\mathrm{L,G}}}(x_0)$, and define $y_\rho := x^\star + r\dfrac{x_\rho - x^\star}{\|x_\rho - x^\star\|_{\mathrm{G}}} \in \partial B_{\mathrm{G}}(x^\star, r)$. Consider the solution to $\dot{y} = f(t, y)$ with initial condition $y(t_\rho^{\mathrm{L,G}}) = y_\rho$ and note that $\phi_t(x_\rho) = \phi_{t+t_\rho^{\mathrm{L,G}}}(x_0)$. For almost every $t \in [t_\rho^{\mathrm{L,G}}, 2t_\rho^{\mathrm{L,G}}]$, we compute

$$\begin{aligned}
\|\phi_{t+t_\rho^{\mathrm{L,G}}}(x_0) - x^\star\|_{\mathrm{G}} &\le \|\phi_t(x_\rho) - \phi_t(y_\rho)\|_{\mathrm{G}} + \|\phi_t(y_\rho) - x^\star\|_{\mathrm{G}} && (12.16)\\
&\le \|x_\rho - y_\rho\|_{\mathrm{G}} + k_{\mathrm{L,G}}\mathrm{e}^{-c(t - t_\rho^{\mathrm{L,G}})}\|y_0 - x^\star\|_{\mathrm{G}} && (12.17)\\
&\overset{(12.11)}{=} \|x_\rho - x^\star\|_{\mathrm{G}} - \|x^\star - y_\rho\|_{\mathrm{G}} + k_{\mathrm{L,G}}\mathrm{e}^{-c(t - t_\rho^{\mathrm{L,G}})}r\\
&\le \|\phi_{t_\rho^{\mathrm{L,G}}}(x_0) - x^\star\|_{\mathrm{G}} - r(1 - k_{\mathrm{L,G}}\mathrm{e}^{-c(t - t_\rho^{\mathrm{L,G}})})\\
&\overset{(12.15)}{\le} \|x_0 - x^\star\|_{\mathrm{G}} - r(1-\rho) - r(1 - k_{\mathrm{L,G}}\mathrm{e}^{-c(t - t_\rho^{\mathrm{L,G}})})\\
&\overset{t=2t_\rho^{\mathrm{L,G}}}{\le} \|x_0 - x^\star\|_{\mathrm{G}} - 2r(1-\rho),
\end{aligned}$$

where in (12.16) we added and subtracted $\phi_t(y_0)$ and applied the triangle inequality, while (12.14) follows from Assumption (12.A1) and inequality (12.10). We now reason as done in $[0, t_\rho^{\mathrm{L,G}}]$. If $\|x_0 - x^\star\|_{\mathrm{G}} - 2r(1-\rho) \le r$, then Assumption (12.$A$2) implies

$$\|\phi_{t+t_\rho^{\mathrm{L,G}}}(x_0) - x^\star\|_{\mathrm{G}} \le k_{\mathrm{L,G}}\big(\|x_0 - x^\star\|_{\mathrm{G}} - 2r(1-\rho)\big)\mathrm{e}^{-c(t - 2t_\rho^{\mathrm{L,G}})}, \quad \forall t \ge 2t_\rho^{\mathrm{L,G}}.$$

If $\|x_0-x^\star\|_{\mathrm{G}}-2r(1-\rho)>r$, we proceed analogously until $\|x_0-x^\star\|_{\mathrm{G}}-Tr(1-\rho)\le r$. This inequality is verified after at most $T:=\left\lceil\frac{\|x_0-x^\star\|_{\mathrm{G}}-r}{(1-\rho)r}\right\rceil$ steps. Iterating the previous process, at step T, for almost every $t\in[(T-1)t_\rho^{\mathrm{L,G}},Tt_\rho^{\mathrm{L,G}}]$, we get

$$\begin{aligned}\|\phi_{t+(T-1)t_\rho^{\mathrm{L,G}}}(x_0)-x^\star\|_{\mathrm{G}}&\le\|x_0-x^\star\|_{\mathrm{G}}-(T-1)r(1-\rho)-r(1-k_{\mathrm{L,G}}\mathrm{e}^{-c(t-(T-1)t_\rho^{\mathrm{L,G}})}),\\ &\overset{t=kt_\rho^{\mathrm{L,G}}}{\le}\|x_0-x^\star\|_{\mathrm{G}}-Tr(1-\rho)\le r,\end{aligned}$$

where the last inequality follows from the definition of T. Local strong contractivity then implies

$$\|\phi_{t+Tt_\rho^{\mathrm{L,G}}}(x_0)-x^\star\|_{\mathrm{G}}\le k_{\mathrm{L,G}}\big(\|x_0-x^\star\|_{\mathrm{G}}-Tr(1-\rho)\big)\mathrm{e}^{-c(t-Tt_\rho^{\mathrm{L,G}})},\quad\text{for a.e. } t\ge Tt_\rho^{\mathrm{L,G}}.$$

The above reasoning together with Assumption (12.*A*1) implies that for almost every $t\in[it_\rho^{\mathrm{L,G}},(i+1)t_\rho^{\mathrm{L,G}}]$, $i\in\{0,\dots,T-1\}$, we have

$$\begin{aligned}\|\phi_{t+it_\rho^{\mathrm{L,G}}}(x_0)-x^\star\|_{\mathrm{G}}\le\min\Big\{&\|x_0-x^\star\|_{\mathrm{G}}-ir(1-\rho),\\ &\|x_0-x^\star\|_{\mathrm{G}}-ir(1-\rho)-r\big(1-k_{\mathrm{L,G}}\mathrm{e}^{-c(t-it_\rho^{\mathrm{L,G}})}\big)\Big\}.\end{aligned}\tag{12.18}$$

By partitioning the interval $[0,+\infty[$ as $[0,t_\rho^{\mathrm{L,G}}[\cup\dots\cup[(T-1)t_\rho^{\mathrm{L,G}},Tt_\rho^{\mathrm{L,G}}[\cup[Tt_\rho^{\mathrm{L,G}},+\infty[$ and summing up the above inequalities we obtain the bound:

$$\begin{aligned}\|\phi_t(x_0)-x^\star\|_{\mathrm{G}}\le\sum_{i=0}^{T-1}&\mathbf{1}_{\{it_\rho^{\mathrm{L,G}}\le t<(i+1)t_\rho^{\mathrm{L,G}}\}}(t)\cdot\\ &\min\Big\{\|x_0-x^\star\|_{\mathrm{G}}-ir(1-\rho),\|x_0-x^\star\|_{\mathrm{G}}-ir(1-\rho)\\ &\qquad-r\big(1-k_{\mathrm{L,G}}\mathrm{e}^{-c(t-it_\rho^{\mathrm{L,G}})}\big)\Big\}+\mathbf{1}_{\{t\ge Tt_\rho^{\mathrm{L,G}}\}}(t)\cdot\\ &\min\Big\{\|x_0-x^\star\|_{\mathrm{G}}-Tr(1-\rho),\\ &\quad k_{\mathrm{L,G}}\left(\|x_0-x^\star\|_{\mathrm{G}}-Tr(1-\rho)\right)\mathrm{e}^{-c(t-Tt_\rho^{\mathrm{L,G}})}\Big\}:=g_{\mathrm{B}}(t).\end{aligned}\tag{12.19}$$

Finally, statement (ii) follows by noticing that $g_{\mathrm{B}}(t)\le\text{lin-exp}(t\,;\,q,c_{\text{lin}},c_{\text{exp}},t_{\text{cross}})$, $t\ge0$, for $t_{\text{cross}}=T\ln(k_{\mathrm{L,G}}\rho^{-1})/c_{\text{exp}}+\ln(k_{\mathrm{L,G}})/c_{\text{exp}}$, $c_{\text{lin}}=r\,c_{\text{exp}}(1-\rho)/\ln(k_{\mathrm{L,G}}\rho^{-1})$, and $q=\|x_0-x^\star\|_{\mathrm{G}}+r(1-\rho)\dfrac{\ln(k_{\mathrm{L,G}})}{\ln(k_{\mathrm{L,G}}\rho^{-1})}$. This concludes the proof. □

Figure 12.3 illustrates the bound in (12.9) and the one in (7.13).

Remark 12.3.

(i) The bound in Theorem 12.5 generalizes the result for equal norms in Theorem 12.3. In fact, the factor $(1-\rho)/\ln(k_{\mathrm{L,G}}\rho^{-1})$ *is always less than 1 for* $k_{\mathrm{L,G}}>1$. *Moreover, when* $k_{\mathrm{L,G}}=1$ *it results* $\lim_{\rho\to1}(1-\rho)/\ln(k_{\mathrm{L,G}}\rho^{-1})=1$, *thereby exactly recovering the equal-norm result.*

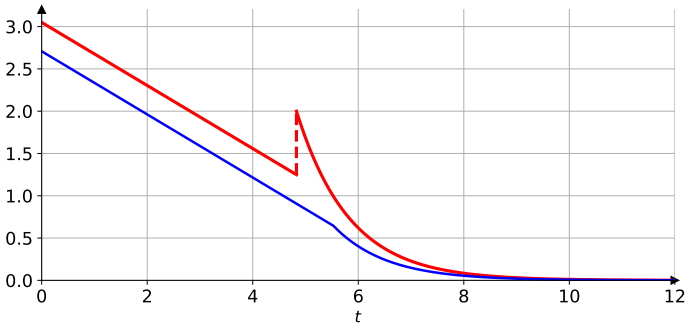

Figure 12.3: Linear-exponential bound in (12.9) (solid blue curve) and the decay bound in (7.13) (red curve) for $\|x_0 - x^\star\|_{\mathrm{G}} = 2.4$, $r = 1$, $c_{\mathrm{exp}} = 1$, $k_{L,G} = 2$, $\rho = 0.4$.

(ii) A consequence of Theorem 12.5 is that, jointly, Assumptions (12.A1), (12.A2), and (12.A3) preclude the existence of any other invariant sets besides $\mathcal{S}$, and the convergence towards the equilibrium is global.

(iii) Linear-exponential convergence is weaker than global exponential convergence, but stronger than global asymptotic convergence (e.g., we provide an explicit estimate of the time required to reach a neighborhood of the equilibrium).

□

With the following Lemma, we give the explicit expression for the optimal contraction factor ρ that maximizes the average linear decay rate c_{lin}.

Lemma 12.6 (Optimal contraction factor)**.** *Under the same assumptions and notations as in Theorem 12.5, for $k_{\mathrm{L,G}} > 1$ the contraction factor $\rho \in]0, 1[$ that maximize the average linear decay rate c_{lin} is*

$$\bar{\rho}(k_{\mathrm{L,G}}) = -\frac{1}{W_{-1}(-\mathrm{e}^{-1}k_{\mathrm{L,G}}^{-1})}, \tag{12.20}$$

where $W_{-1}(\cdot)$ is the branch of the Lambert function $W(\cdot)$ [2] satisfying $W(x) \leq -1$, for all $x \in [-1/\mathrm{e}, 0[$.

Proof. To maximize the linear decay rate c_{lin} we need to solve the optimization problem

$$\max_{0<\rho<1} \frac{1-\rho}{\ln(k_{\mathrm{L,G}}) - \ln(\rho)}. \tag{12.21}$$

We compute

$$\frac{d}{d\rho}\frac{1-\rho}{\ln(k_{\mathrm{L,G}}) - \ln(\rho)} = \frac{\rho\ln(\rho) - \rho\big(1+\ln(k_{\mathrm{L,G}})\big) + 1}{\rho\big(\ln(k_{\mathrm{L,G}}) - \ln(\rho)\big)^2} = 0,$$

[2] The Lambert function $W(\cdot)$ is a multivalued function defined by the branches of the converse relation of the function $f(x) = x\mathrm{e}^x$. See [181] for more details.

which holds if and only if

$$\rho \ln(\rho) - \rho\big(1 + \ln(k_{\mathrm{L,G}})\big) + 1 = 0. \tag{12.22}$$

Note that the equality (12.22) is a transcendental equation of the form $x \ln(x) + ax + b = 0$, whose solution is known to be the value $x = \frac{-b}{W_0(-b\mathrm{e}^a)}$ if $-b\mathrm{e}^a \geq 0$ and the two values $x = \frac{-b}{W_0(-b\mathrm{e}^a)}$ and $x = \frac{-b}{W_{-1}(-b\mathrm{e}^a)}$ if $-1/\mathrm{e} \leq -b\mathrm{e}^a < 0$, where $W_0(\cdot)$ is the branch satisfying $W(x) \geq -1$, and $W_{-1}(\cdot)$ is the branch satisfying $W(x) \leq -1$.

In our case it is $b = 1$ and $a = -(1 + \ln(k_{\mathrm{L,G}}))$, thus $-b\mathrm{e}^a = -\mathrm{e}^{-(1+\ln(k_{\mathrm{L,G}}))} \in]-\frac{1}{\mathrm{e}}, 0[$. Therefore, the solutions of the equality (12.22) are $\rho = -\frac{1}{W_0(-\mathrm{e}^{-1}k_{\mathrm{L,G}}^{-1})}$ and $\rho = -\frac{1}{W_{-1}(-\mathrm{e}^{-1}k_{\mathrm{L,G}}^{-1})}$. Being $0 < \rho < 1$, the only admissible solution is $\rho = -\frac{1}{W_{-1}(-\mathrm{e}^{-1}k_{\mathrm{L,G}}^{-1})}$, thus the thesis. □

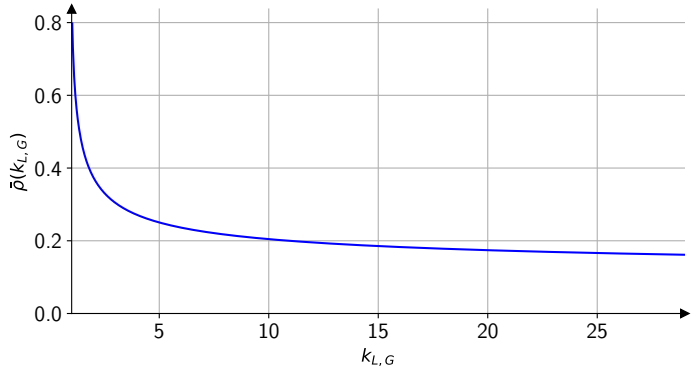

Figure 12.4: Plot of the optimal contraction factor $\bar{\rho}(k_{\mathrm{L,G}})$ given by equation (12.20).

12.5 Local Stability in the Presence of External Inputs

We now characterize local ISS for GW-LS-C systems with respect to the same norm. Specifically, we consider the input-dependent dynamics

$$\dot{x}(t) = f\big(t, x(t), u(t)\big). \tag{12.23}$$

where, $f\colon \mathbb{R}_{\geq 0} \times \mathcal{C} \times \mathcal{U} \to \mathbb{R}^n$, the map $x \mapsto f(t, x, u)$ is locally Lipschitz, for all t, u, with $\mathcal{C} \subseteq \mathbb{R}^n$ f-invariant, open and convex, and $\mathcal{U} \subset \mathbb{R}^m$. Given $\bar{u} \in \mathbb{R}^m$, we define the set of bounded inputs $\bar{\mathcal{U}} := \{u\colon \mathbb{R}_{\geq 0} \to \mathcal{U} \mid \|u(t)\|_{\mathcal{U}} \leq \bar{u}, \forall t \geq 0\}$. We make the following assumptions.

Assumption . *There exist norms $\|\cdot\|, \|\cdot\|_{\mathcal{U}}$ on $\mathcal{C}$ and $\mathcal{U}$, respectively, such that*

(12.A1') *for all t, u, the map $x \mapsto f(t,x,u)$ is weakly infinitesimally contracting on $\mathbb{R}^n$ w.r.t. $\|\cdot\|$,*
(12.A2') *for all t, x, the map $u \mapsto f(t,x,u)$ is Lipschitz with constant $L_u \geq 0$,*
(12.A3') *there exist a forward-invariant set $\mathcal{S}$ and $c_{\text{exp}} > 0$ such that, for all t, for each $u \in \bar{\mathcal{U}}$, the map $x \mapsto f(t,x,u(t))$ is c_{exp}-strongly infinitesimally contracting on $\mathcal{S}$ w.r.t. $\|\cdot\|$,*
(12.A4') *at $u(t) = \mathbb{0}_m$, for all t, there exists an equilibrium point $x^\star \in \mathcal{S}$.*

We begin by giving two technical lemmas, needed to prove the main result of this section.

Lemma 12.7 (Error dynamics for input-dependent systems)**.** *Consider the input-dependent dynamics (12.23) satisfying Assumption (12.A2'). Then any two solutions $x(t)$ and $y(t)$ with inputs $u_x, u_y \colon \mathbb{R}_{\geq 0} \to \mathbb{R}^m$, satisfy for almost every $t \geq 0$,*

$$D^+\|x(t)-y(t)\| \leq \int_0^1 \mu\Big(Df(y+\alpha(x-y),u_y)\Big)d\alpha\|x(t)-y(t)\|+L_u\|u_x(t)-u_y(t)\|_{\mathcal{U}}. \tag{12.24}$$

Proof. Let $x(t)$ and $y(t)$ be two trajectories of (12.23) with input signals u_x, u_y, respectively. Let $[\![\cdot,\cdot]\!]$ be a weak pairing compatible with $\|\cdot\|$. We compute

$$\|x(t)-y(t)\|D^+\|x(t)-y(t)\| = [\![f(t,x,u_x)-f(t,y,u_y), x-y]\!] \tag{12.25}$$
$$\leq [\![f(t,x,u_y)-f(t,y,u_y), x-y]\!] + \|f(t,x,u_x)-f(t,x,u_y)\|\|x-y\| \tag{12.26}$$
$$\leq [\![f(t,x,u_y)-f(t,y,u_y), x-y]\!] + L_u\|u_x-u_y\|_{\mathcal{U}}\|x-y\|, \tag{12.27}$$

where in (12.25) we used the curve norm derivative formula 2.7, in (12.26) we added and subtracted $f(t,x,u_y)$ and used the sub-additivity 2.7 and the Cauchy-Schwartz inequality 2.7, and in (12.27) we used Assumption (12.A2'). Next, by dividing both sides for $\|x(t)-y(t)\|$ we get

$$D^+\|x(t)-y(t)\| = \frac{[\![f(t,x,u_y)-f(t,y,u_y), x-y]\!]}{\|x-y\|^2}\|x-y\| + L_u\|u_x-u_y\|_{\mathcal{U}}. \tag{12.28}$$

By applying the mean-value Theorem 2.1 to (12.28), a.e., we get

$$D^+\|x(t)-y(t)\| \leq \frac{\left[\!\!\left[\int_0^1 Df(y+s(x-y),u_y)ds(x-y), x-y\right]\!\!\right]}{\|x-y\|}\frac{\|x-y\|}{\|x-y\|}+L_u\|u_x-u_y\|_{\mathcal{U}} \tag{12.29}$$
$$\leq \int_0^1 \frac{[\![Df(y+s(x-y),u_y)ds(x-y), x-y]\!]}{\|x-y\|^2}ds\|x-y\|+L_u\|u_x-u_y\|_{\mathcal{U}} \tag{12.30}$$

where in (12.29) we have used the weak pairing sub-additivity 2.7. Next, recall that Lumer's equality 2.7 implies, $\frac{[\![Az, z]\!]}{[\![z, z]\!]} \leq \mu(A)$ for every $A \in \mathbb{R}^{n\times n}$ and $z \neq \mathbb{0}_n$. By applying this equality to (12.30) (with $A = Df(y + s(x - y), u_y)$ and $z = x - y$) we get inequality (12.24). This concludes the proof. □

The next result gives a linear-exponential bound for the solution of dynamics with saturations and additive inputs.

Lemma 12.8 (Solution of dynamics with saturations and additive inputs)**.** *Let c_{exp} and d be positive scalars, and $u\colon \mathbb{R}_{\geq 0} \to \mathbb{R}^n$ satisfying $\|u(t)\|_\infty = u_{\max} < dc_{\text{exp}}$, for all t. Consider the dynamics*

$$\dot{x}(t) = -c_{\text{exp}}\,\text{sat}_d\big(x(t)\big) + u(t), \quad x_0 = q > d. \tag{12.31}$$

Then, a solution of (12.31) *satisfies*

$$x(t) \leq \text{lin-exp}(t\ ;\ q, c_{\text{lin}}, c_{\text{exp}}, t_{\text{cross}}) + \mathbf{1}_{[t_{\text{cross}},+\infty[}(t)(1 - \mathrm{e}^{-c_{\text{exp}}(t-t_{\text{cross}})})\frac{u_{\max}}{c_{\text{exp}}},$$

with $c_{\text{lin}} := dc_{\text{exp}} - u_{\max} > 0$ and $t_{\text{cross}} := \frac{q-d}{c_{\text{lin}}} > 0$.

Proof. Using the definition of saturation function, for all $t \in \mathbb{R}_{\geq 0}$ we can upper bound the ODE (12.31) as

$$\dot{x}(t) \leq \dot{y}(t) := \begin{cases} -dc_{\text{exp}} + u_{\max} & \text{if } y(t) > d, \\ -c_{\text{exp}}x(t) + u_{\max} & \text{if } y(t) \in [-d, d], \\ dc_{\text{exp}} + u_{\max} & \text{if } y(t) < -d, \end{cases} \tag{12.32}$$

which, in each interval $[t_0, t_1] \subseteq \mathbb{R}_{\geq 0}$ where the solution is continuous and does not change regime, has general solution

$$y(t) = \begin{cases} (-dc_{\text{exp}} + u_{\max})t + y(t_0) & \text{if } y(t) > d, \\ \Big(y(t_0) - \dfrac{\bar{u}}{c_{\text{exp}}}\Big)\mathrm{e}^{-c_{\text{exp}}(t-t_0)} + \dfrac{u_{\max}}{c_{\text{exp}}} & \text{if } y(t) \in [-d, d], \\ (dc_{\text{exp}} + u_{\max})t + y(t_0) & \text{if } y(t) < -d. \end{cases} \tag{12.33}$$

At time $t = 0$, we have $x_0 = q > d$. For continuity of the solution, there exists $t^\star$ such that $y(t) > d$ for all $t \in [0, t^\star]$. Thus from (12.33) and being $x(t_0 = 0) = q$, it is

$$y(t) = (-dc_{\text{exp}} + u_{\max})t + q,$$

for all $t \in [0, t^\star]$. Moreover being $u_{\max} < dc_{\text{exp}}$, the function $y(t)$ is decreasing, the time value $t^\star$ is finite and there exists a time, say it $\bar{t}$, such that $y(\bar{t}) = d$. Let $c_{\text{lin}} := dc_{\text{exp}} - u_{\max}$, we have

$$y(\bar{t}) = d \iff -c_{\text{lin}}\bar{t} + q = d \iff \bar{t} = \frac{q-d}{c_{\text{lin}}} := t_{\text{cross}}.$$

In summary, we have shown that $y(t) = q - c_{\text{lin}}t$, for all $t \in [0, t_{\text{cross}}]$, and $y(t) = d$ at time t_{cross}. Thus, from (12.33) and being $y(t_{\text{cross}}) = q - c_{\text{lin}}t_{\text{cross}}$, $\forall t > t_{\text{cross}}$ we have

$$y(t) = \big(q - c_{\text{lin}}t_{\text{cross}}\big)\mathrm{e}^{-c_{\text{exp}}(t-t_{\text{cross}})} + \big(1 - \mathrm{e}^{-c_{\text{exp}}(t-t_{\text{cross}})}\big)\frac{u_{\max}}{c_{\text{exp}}}.$$

Specifically, $y(t) > 0$ for all $t > t_{\text{cross}}$, thus it can never be $y(t) < -d$. This concludes the proof. □

We are now ready to state the main result of this section.

Theorem 12.9 (Local ISS for input-dependent GW-LS-C systems)**.** *Consider system* (12.23) *satisfying Assumptions* (12.A1') – (12.A4')*. Let r be the largest radius such that $B(x^\star, r) \subseteq \mathcal{S}$, $\bar{u} < rc_{\text{exp}}$, and $u_{\max} := \sup_{\tau\in[0,t]} \|u_x(\tau)\|_{\mathcal{U}} \leq \bar{u}$. For each trajectory $x(t)$ with input $u_x \in \bar{\mathcal{U}}$ starting from $x_0 \notin \mathcal{S}$, for almost every $t \geq 0$, we have:*

(i) $D^+\|x(t) - x^\star\| \leq -c_{\text{exp}}\,\text{sat}_r(\|x(t) - x^\star\|) + L_u\|u_x(t)\|_{\mathcal{U}}$,

(ii) $\|x(t) - x^\star\| \leq \text{lin-exp}(t\,;\, q, c_{\text{lin}}, c_{\text{exp}}, t_{\text{cross}}) + \mathbf{1}_{[t_{\text{cross}},+\infty[}(t)\dfrac{L_u}{c_{\text{exp}}}(1 - \mathrm{e}^{-c_{\text{exp}}t})u_{\max}$,

with

- *exponential decay rate* $c_{\text{exp}} > 0$,
- *intercept* $q = \|x_0 - x^\star\|$,
- *linear decay rate* $c_{\text{lin}} = rc_{\text{exp}} - u_{\max}$,
- *linear-exponential crossing time* $t_{\text{cross}} = (q - r)/c_{\text{lin}}$.

Proof. Consider an arbitrary trajectory $x(t)$ starting from $x_0 \notin \mathcal{S}$ with input u_x and a second trajectory equal to the equilibrium $x^\star$ with input $u = \mathbb{0}_m$. To prove statement (i), let μ be the log-norm associated to $\|\cdot\|$. By applying inequality (12.24) to those trajectories, for almost every $t \geq 0$, we have

$$D^+\|x(t) - x^\star\| \leq \int_0^1 \mu\Big(Df(x^\star + \alpha(x(t) - x^\star), 0)\Big)d\alpha\|x(t) - x^\star\| + L_u\|u_x\|_{\mathcal{U}}. \tag{12.34}$$

The proof follows by using similar reasoning as the one in the proof of Lemma 12.2. Statement (ii) follows by using the Comparison Lemma 4.1 and Lemma 12.8 to upper bound the solution to the differential inequality (i). □

12.6 Applications

We now demonstrate the effectiveness of the previous results by applying them to two dynamical systems: one minimizing the Huber loss, and the other addressing linear programming problems.

12.6.1 Huber Loss

Consider the convex minimization problem

$$\min_{x\in\mathbb{R}} h_\delta(x), \tag{12.35}$$

where $h_\delta\colon \mathbb{R}\to\mathbb{R}_{\geq 0}$ is the Huber loss [182] and is defined by

$$h_\delta(x) = \begin{cases} \frac{1}{2}x^2 & \text{if } |x|\leq \delta, \\ \delta\cdot\left(|x|-\frac{1}{2}\delta\right), & \text{if } |x|>\delta, \end{cases} \tag{12.36}$$

with $\delta\in\mathbb{R}_{\geq 0}$. The Huber loss is a function used in robust regression and represents a compromise between the ℓ_1 and ℓ_2 loss functions. Figure 12.5 illustrates the Huber loss (12.36) for different values of the parameter δ.

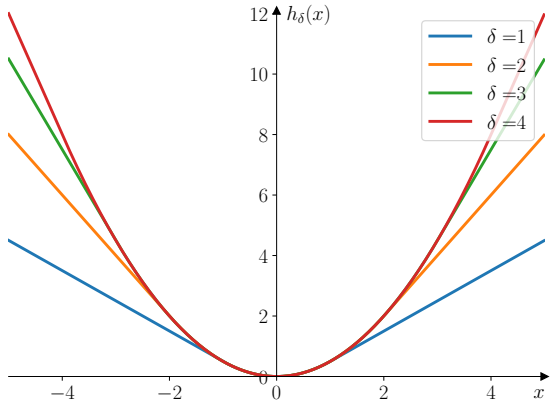

Figure 12.5: Huber Loss in equation 12.35 for $\delta = 1, 2, 3, 4$.

To solve (12.35), we consider the associated continuous-time *gradient flow dynamic*

$$\dot{x} = -\nabla h_\delta(x) = -\operatorname{sat}_\delta\big(x\big) = f_{\mathrm{H}}(x). \tag{12.37}$$

Given that the Huber loss is convex, the gradient dynamics (12.37) is weakly contracting, and not strongly contracting. The following theorem characterizes the convergence behavior of the gradient dynamics (12.37).

Theorem 12.10 (Contractivity of the Huber Loss function)**.** *Consider the gradient-flow dynamics* (12.37)*. Then*

(i) the dynamics (12.37) *is weakly contracting on* $\mathbb{R}$ *with respect to any norm;*

(ii) the dynamics (12.37) *is locally strongly contracting with respect to any norm in* $B(0,r)$*, for any* $0<r<\delta$ *with rate* $c=1$*.*

Proof. Statement (i) follows directly from Lemma 10.2, as the Huber loss is convex and the saturation function is locally Lipschitz.

To prove statement (ii), note that, by definition of saturation function, the equilibrium point of the gradient-flow dynamics (12.37) is $x^\star = 0$ and

$$f'_{\mathrm{H}}(x) = \begin{cases} 0 & if\ |x| > \delta, \\ -1 & if\ |x| < \delta. \end{cases}$$

Therefore, for any $0 < r < \delta$, we have $f'_{\mathrm{H}}(x) < -1$ for all $x \in B(0, r)$. This concludes the proof. □

Corollary 12.11 (Convergence of (12.37))**.** *Given $\delta > 0$, consider the gradient-flow dynamics (12.37). For each trajectory $x(t)$ starting from x_0, it holds that*

(i) if $x_0 < \delta$, then, for almost every $t \geq 0$,

$$x(t) \leq \mathrm{e}^{-t} x_0,$$

(ii) if $x_0 > \delta$, then, for almost every $t \geq 0$,

$$x(t) \leq \text{lin-exp}(t\ ;\ q, c_{\text{lin}}, c_{\text{exp}}, t_{\text{cross}}), \tag{12.38}$$

with exponential decay rate $c_{\text{exp}} = 1$, linear decay rate $c_{\text{lin}} = c_{\text{exp}}\,\delta$, intercept $q = x_0$, and linear-exponential crossing time $t_{\text{cross}} = (x_0 - \delta)/c_{\text{lin}}$.

Numerical Experiments

Consider the minimization problem (12.35) and the associated continuous-time gradient flow dynamics (12.37). We set $\delta = 2$ and simulate the dynamics (12.37) over the time interval $t \in [0, 11]$ starting from initial conditions $0.5, 3, 6, 9$, respectively. The simulation results show that each trajectory converges to the optimum $x^\star = 0$. Figure 12.6 illustrates the simulated trajectories of (12.37) and the corresponding bounds from Corollary 12.11. Depending on whether the initial condition x_0 is smaller or larger than the threshold $\delta = 2$, the convergence follows either an exponential decay or a linear-exponential decay, as predicted by Corollary 12.11.

12.6.2 Tackling Linear Programs

Given $c \in \mathbb{R}^n$, $A \in \mathbb{R}^{m \times n}$ and $b \in \mathbb{R}^m$, we consider the *linear program*:

$$\begin{aligned} \min_{x \in \mathbb{R}^n} \quad & c^\top x, \\ \text{s.t.} \quad & Ax \leq b, \end{aligned} \tag{12.39}$$

and its equivalent unconstrained formulation

$$\min_{x \in \mathbb{R}^n} c^\top x + \iota_{\mathcal{I}_b}(Ax), \tag{12.40}$$

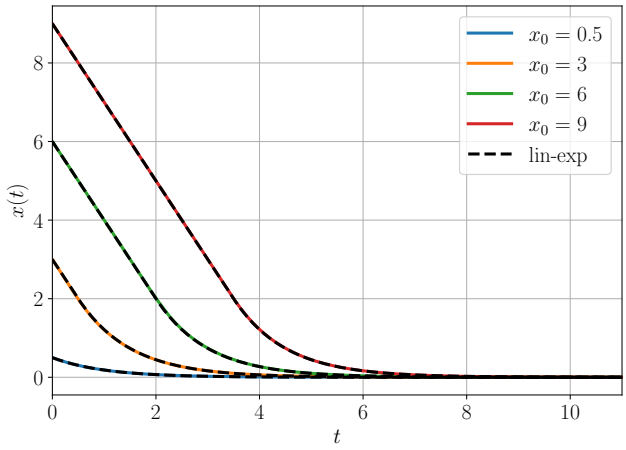

Figure 12.6: Plots of trajectories of the dynamics (12.37) starting from four different initial conditions. The figure shows the trajectories as solid curves and the corresponding linear-exponential bound from Corollary 12.11 as dashed curves. In agreement with Corollary 12.11 the convergence is linearly-exponentially bounded.

where $\mathcal{I}_b = \{y \in \mathbb{R}^m \mid y - b \leq \mathbb{0}_m\}$. We assume that (12.40) admits a unique equilibrium. Note that (12.40) is a particular composite minimization problem:

$$\min_{x \in \mathbb{R}^n} f(x) + g(Ax), \tag{12.41}$$

with $f(x) = c^\top x$ and $g(Ax) = \iota_{\mathcal{I}_b}(Ax)$. To solve (12.40), we leverage the proximal augmented Lagrangian approach proposed in [158] and consider the *proximal augmented Lagrangian*, $\tilde{L}_\gamma \colon \mathbb{R}^n \times \mathbb{R}^m \to \mathbb{R}$, defined by

$$\tilde{L}_\gamma(x, \lambda) = f(x) + M_{\gamma g}(Ax + \gamma\lambda) - \frac{\gamma}{2}\|\lambda\|_2^2, \tag{12.42}$$

where $\lambda \in \mathbb{R}^m$ is the Lagrange multiplier, $\gamma > 0$ is a parameter, and $M_{\gamma g}$ is Moreau envelope of g.

Remark 12.4. *For f continuously differentiable, convex, and with a Lipschitz continuous gradient, and g convex, closed and proper, solving the composite minimization problem* (12.41) *corresponds to finding saddle points of* (12.42)*, simultaneously updating the primal and dual variables [158, Theorem 2].* □

Next, consider the *continuous-time augmented primal-dual dynamics* associated to the proximal augmented Lagrangian of problem (12.40)

$$\begin{aligned}
\dot{x} &= -\nabla_x \tilde{L}_\gamma(x, \lambda) = -c - A^\top \nabla M_{\gamma \iota_{\mathcal{I}_b}}(Ax + \gamma\lambda) = -c - \frac{1}{\gamma} A^\top \operatorname{ReLU}\big(Ax + \gamma\lambda - b\big), \\
\dot{\lambda} &= \nabla_\lambda \tilde{L}_\gamma(x, \lambda) = -\gamma\lambda + \gamma \nabla M_{\gamma \iota_{\mathcal{I}_b}}(Ax + \gamma\lambda) = -\gamma\lambda + \operatorname{ReLU}\big(Ax + \gamma\lambda - b\big).
\end{aligned} \tag{12.43}$$

We let $F_{\text{LP}}\colon \mathbb{R}^{n+m} \to \mathbb{R}^{n+m}$ denote the vector field for (12.43).

Remark 12.5. *Equation* (12.43) *follows directly after noticing that for almost every* $y \in \mathbb{R}^m$ *it results*

$$\nabla M_{\gamma \iota_{\mathcal{I}}}(y) = \frac{1}{\gamma}\big(y - \mathbb{P}_{\iota_{\mathcal{I}}}(y)\big) = \frac{1}{\gamma}\big(y - \min\{y, b\}\big) = \frac{1}{\gamma}\,\mathrm{ReLU}\big(y - b\big).$$

□

The next result characterizes the convergence of (12.43).

Theorem 12.12 (Convergence of the linear program)**.** *Consider the dynamics* (12.43) *and let* $(x^\star, \lambda^\star) \in \mathbb{R}^{n+m}$ *be an equilibrium point. If* $DF_{\text{LP}}\big(x^\star, \lambda^\star\big)$ *is Hurwitz, then any solution of* (12.43) *linear-exponentially converges towards* $(x^\star, \lambda^\star)$.

Proof. To prove the statement we show that (12.43) satisfies the assumptions of Theorem 12.5. First, we prove that the system is globally-weakly contracting. To this purpose, let $z := (x, \lambda) \in \mathbb{R}^{n+m}$, $y := Ax + \gamma\lambda - b$ and define $G(y) := D\,\mathrm{ReLU}\big(y\big)$, for almost every $y \in \mathbb{R}^m$. The Jacobian of (12.43) is

$$DF_{\text{LP}}(z) = \begin{bmatrix} -\frac{1}{\gamma}A^\top G(y)A & -A^\top G(y) \\ G(y)A & -\gamma(I_m - G(y)) \end{bmatrix}.$$

Being $0 \preceq G(y) \preceq I_m$[3], a.e. $y \in \mathbb{R}^m$, we have

$$\sup_z \mu_2\big(DF_{\text{LP}}(z)\big) \leq \max_{0 \preceq G \preceq I_m} \mu_2\left(\begin{bmatrix} -\gamma^{-1}A^\top GA & -A^\top G \\ GA & \gamma\big(G - I_m\big) \end{bmatrix}\right),$$

By definition of μ_2, we have that

$$\begin{aligned}\mu_2\left(\begin{bmatrix} -\gamma^{-1}A^\top GA & -A^\top G \\ GA & \gamma\big(G - I_m\big) \end{bmatrix}\right) &= \lambda_{\max}\left(\begin{bmatrix} -\gamma^{-1}A^\top GA & 0 \\ 0 & \gamma\big(G - I_m\big) \end{bmatrix}\right) \\ &= \max\{\lambda_{\max}\big(-\gamma^{-1}A^\top GA\big), \lambda_{\max}\big(\gamma\big(G - I_m\big)\big)\} \leq 0.\end{aligned}$$

The last equality follows from the fact that $\lambda_{\max}\big(-\gamma^{-1}A^\top GA\big) = \lambda_{\max}\big(\gamma\big(G - I_m\big)\big) \leq 0$. In particular, the equality $\lambda_{\max}\big(-\gamma\big(G - I_m\big)\big) \leq 0$ follows directly from $0 \preceq G \preceq I_m$; while $\lambda_{\max}\big(-\gamma^{-1}A^\top GA\big) \leq 0$, follows noticing that $A^\top GA \succeq 0$[4]. This implies that (12.43) is weakly contracting on $\mathbb{R}^{n+m}$ with respect to $\|\cdot\|_2$. Thus (12.43) is weakly contracting on $\mathbb{R}^{n+m}$ with respect to $\|\cdot\|_2$.

Next, we prove that the system is locally-strongly contracting. To do so, we first note that for any equilibrium point $z^\star := (x^\star, \lambda^\star)$ of (12.43), both $D\,\mathrm{ReLU}(y^\star)$ and $DF_{\text{LP}}(z^\star)$ are differentiable in a neighborhood of $y^\star$ and $z^\star$, respectively. In fact, for each i, the KKT conditions ensures that either $(Ax^\star)_i - b_i = 0$ or $\lambda_i^\star = 0$. In turn, this implies that $y_i^\star = (Ax^\star)_i + \gamma\lambda_i^\star - b_i \neq 0$, for all i. Now, being by assumption $DF_{\text{LP}}(z^\star)$ Hurwitz,

[3] For every $\gamma > 0$, $0 \preceq \nabla^2 M_{\gamma g}(y) \preceq \frac{1}{\gamma} I_n$, a.e. $y \in \mathbb{R}^m$ [53, Lemma 18].

[4] $A^\top GA \succeq 0 \iff x^\top A^\top GAx \geq 0 \;\; \forall x \in \mathbb{R}^n \iff y^\top Gy \geq 0, \forall y \in \mathbb{R}^m \iff G \succeq 0$.

there exists Q invertible such that $\mu_{2,Q}(DF_{\text{LP}}(z^\star)) < 0$ [42, Corollary 2.33]. Let $\mathcal{K}$ be the set of differentiable points in a neighborhood of $z^\star$. Then, by the continuity property of the log-norm, there exists $B_{2,Q}\big(z^\star, p\big)$, with $p := \sup\{p > 0 \mid B_{2,Q}\big(z^\star, p\big) \subset \mathcal{K}\}$, where $DF_{\text{LP}}(z)$ exists and $\mu_{2,Q}(DF_{\text{LP}}(z)) < -c_{\text{exp}}$ for all $z \in B_{2,Q}\big(z^\star, p\big)$, for some $c_{\text{exp}} > 0$. Therefore (12.43) is strongly infinitesimally contracting with respect to $\|\cdot\|_{2,Q}$ in $B_{2,Q}\big(z^\star, p\big)$. This concludes the proof. □

A key hypothesis of Theorem 12.12 is that $DF_{\text{LP}}(x^\star, \lambda^\star)$ is Hurwitz. This hypothesis can only be verified by prior knowledge of the LP solution. This limitation motivates the following conjecture, which would relate stability of $DF_{\text{LP}}(x^\star, \lambda^\star)$ to matrix A and the KKT conditions.

Conjecture 1. *Let $(x^\star, \lambda^\star)$ be the equilibrium of (12.43). The LP (12.39) has a unique solution, $x^\star$, if and only if $DF_{\text{LP}}\big(x^\star, \lambda^\star\big)$ is Hurwitz.*

Numerical Experiments

Consider the following LP

$$\begin{aligned} \min_{x \in \mathbb{R}^3} \quad & x_1 + x_2 + x_3, \\ \text{s.t.} \quad & -1 \leq x_1 \leq 1, -1 \leq x_2 \leq 1, -1 \leq x_3 \leq 1. \end{aligned} \tag{12.44}$$

for which the unique optimal solution is $x^\star = (-1, -1, -1)$.

Next, consider the corresponding continuous-time augmented primal-dual dynamics:

$$\begin{aligned} \dot{x}_1 &= -1 - \frac{1}{\gamma}\Big(\text{ReLU}\left(x_1 + \gamma\lambda_1 - 1\right) - \text{ReLU}\left(-x_1 + \gamma\lambda_4 - 1\right)\Big), \\ \dot{x}_2 &= -1 - \frac{1}{\gamma}\Big(\text{ReLU}\left(x_2 + \gamma\lambda_2 - 1\right) - \text{ReLU}\left(-x_2 + \gamma\lambda_5 - 1\right)\Big), \\ \dot{x}_3 &= -1 - \frac{1}{\gamma}\Big(\text{ReLU}\left(x_3 + \gamma\lambda_3 - 1\right) - \text{ReLU}\left(-x_3 + \gamma\lambda_6 - 1\right)\Big), \\ \dot{\lambda}_1 &= -\gamma\lambda_1 + \text{ReLU}\left(x_1 + \gamma\lambda_1 - 1\right), \\ \dot{\lambda}_2 &= -\gamma\lambda_2 + \text{ReLU}\left(x_2 + \gamma\lambda_2 - 1\right), \\ \dot{\lambda}_3 &= -\gamma\lambda_3 + \text{ReLU}\left(x_3 + \gamma\lambda_3 - 1\right), \\ \dot{\lambda}_4 &= -\gamma\lambda_4 + \text{ReLU}\left(-x_1 + \gamma\lambda_4 - 1\right), \\ \dot{\lambda}_5 &= -\gamma\lambda_5 + \text{ReLU}\left(-x_2 + \gamma\lambda_5 - 1\right), \\ \dot{\lambda}_6 &= -\gamma\lambda_6 + \text{ReLU}\left(-x_3 + \gamma\lambda_6 - 1\right). \end{aligned} \tag{12.45}$$

We set $\gamma = 0.5$ and simulate the dynamics (12.45) over the time interval $t \in [0, 40]$ with a forward Euler discretization with step-size $\Delta t = 0.001$, starting from 150 initial conditions generated as follows: we first randomly generate an initial condition and then define the remaining 149 initial conditions by adding, to the first initial condition, random noise generated from a normal distribution with mean 0 and standard deviation 2. The simulation results show that each trajectory converges to $z^\star = (-1, -1, -1, 0, 0, 0, 1, 1, 1)$.

Next, we numerically found that $DF_{LP}(z^\star)$ is Hurwitz (in alignment with our conjecture). Figure 12.7 illustrates the mean and standard deviation of the log-norm of the ℓ_2 distance of the 150 simulated trajectories of (12.45) with respect to $z^\star$. In agreement with Theorem 12.12 the convergence is linearly-exponentially bounded.

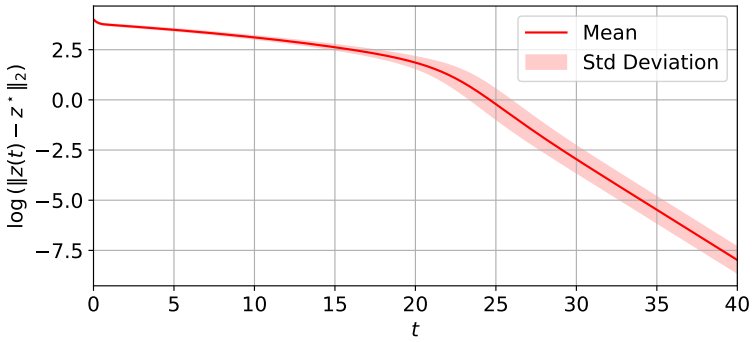

Figure 12.7: Mean (red curve) and standard deviation (shadow curve) of the log-norm of the Euclidean distance of 150 simulated trajectories of (12.45) with respect to the equilibrium point $z^\star$. In agreement with Theorem 12.12 the convergence is linearly-exponentially bounded.

12.7 Summary

In this chapter, we analyzed the convergence of globally-weakly and locally-strongly contracting dynamics, which naturally arise from convex optimization problems with a unique minimizer. First, in Lemma 12.1, we characterized the evolution of certain dynamics with saturation in terms of the linear-exponential function (12.1).

Then we studied the convergence behavior of GW-LS-C dynamics in two cases requiring distinct mathematical approaches. In the first case, for GW-LS-C systems with respect to the same norm, we applied Lemma 12.1 to establish linear-exponential convergence (Theorem 12.3). This means that the distance between each solution of the system and the equilibrium is upper bounded by a *linear-exponential function*. In the second case, for GW-LS-C dynamics with respect to two different norms, we also demonstrated linear-exponential convergence (see Theorem 12.5), extending the results from Section 7.3. Remarkably, linear-exponential convergence implies that convergence towards the equilibrium is global. Additionally, in Theorem 12.9, we characterized local ISS for input-dependent dynamics that are GW-LS-C with respect to the same norm. Finally, we illustrated our results on two applications: minimizing the Huber loss and solving LP problems. Our results motivated a conjecture relating the optimal solution of LPs to the local stability properties of the equilibrium of the resulting dynamics.

13 Conclusions and Future Work

> Life is a climb.
> But the view is great.
>
> *Miley Cyrus*

In this thesis, we proposed a normative framework for translating optimization problems into biologically plausible neural networks that are guaranteed to converge to equilibria corresponding to optimal solutions of the initial optimization problem. By leveraging contraction theory, we characterized stability and robustness of the proposed models, along with the other properties of contracting dynamics. We then used these models to solve static and time-varying convex optimization problems.

Our theoretical contributions began in Part I with the development of the mathematical tools needed for analyzing stability and convergence properties of continuous-time recurrent neural networks. Specifically, in Chapter 5 we provided sharp conditions for both strong and weak Euclidean contractivity of HNNs and FNNs with symmetric weights and possible non-smooth activation functions, together with a number of general algebraic results on matrix polytopes. With these findings, we proposed norms that are log-optimal for almost all synaptic matrices. In this sense our results are sharp – they are the best achievable within this framework. Remarkably, with our contractivity results, we filled a significant gap in the literature by enabling the use of RNNs with non-smooth activation functions, as most common activation functions such as ReLU and thresholding functions. Additionally, we addressed the weak contractivity case, thereby extending the applicability of our results to systems with invariance properties, as well as to RNNs designed to solve certain convex optimization problems.

We then proposed, in Chapters 6 and 7, a top/down normative framework to translate composite optimization problems into continuous-time firing rate neural networks. These results provided a biologically plausible explanation for how neural circuits solve sparse reconstruction and other composite optimization problems relevant to machine learning, compressed sensing, and signal processing applications. The framework we proposed is based upon the theory of proximal operators for composite optimization

and led to continuous-time firing rate neural networks that are therefore interpretable. Specifically, we proposed and analyzed the firing rate competitive network, FCN, and the positive firing rate competitive network, PFCN, to tackle sparse reconstruction and positive sparse reconstruction problems, respectively. Crucial for the PFCN is the fact that this is a positive system. To the best of our knowledge, the positive firing rate competitive network is the first RNN designed to tackle positive sparse reconstruction problems. We presented a detailed convergence analysis for our models, proving that convergence is linear-exponential. This, in turn, implies global convergence toward the equilibrium. We illustrated the effectiveness of our results via numerical examples where we proposed an FNN that solves certain quadratic optimization problems with box constraints. This application set the stage for further exploration of contracting FNNs for solving optimization problems.

Next, in Part II we investigated how to embed learning within our biologically plausible framework. To this purpose, we proposed embedding nonlinear Hebbian learning rules into the continuous-time RNN models analyzed in Part I. In this way, we allowed for dynamic synaptic weight updates mirroring biological processes more closely. Specifically, we studied four coupled neural-synaptic systems: the Hopfield-Hebbian model, the firing-rate-Hebbian model, the Hopfield-Oja model, and the firing-rate-Oja model. To capture the synaptic sparsity of neural circuits, for each model we derived a low dimensional formulation that allowed us to go from a system with $n \times n^2$ variables–n neurons and n^2 synaptic connections–to a system with $n \times m$ variables, where $m \ll n^2$ is the number of non zero elements of the synaptic connection matrix H. We then characterized the key dynamical properties of the models. First, we gave a biologically-inspired forward invariance result for the trajectories of the system, showing bounded solutions for each model. Then we provided sufficient conditions for the non-Euclidean contractivity of the models. Each contractivity test we presented is based upon biologically meaningful quantities, i.e., neural and synaptic decay rate, maximum in-degree, and maximum synaptic strength. Notably, we showed that under specific neural decay rates, the FNN model displayed sharper contractivity conditions compared to the HNN. Additionally, we proved that under suitable conditions the synaptic rules satisfy Dale's Principle, further enhancing the biological plausibility of our models. We illustrated the effectiveness of our results via numerical examples based on a block of the C. Elegans neural architecture.

In the final part, Part III, we explicitly considered optimization problems, using contracting continuous-time dynamical systems to address both static and time-varying convex optimization problems. We first applied contraction theory to time-invariant problems by considering four canonical time-invariant optimization problems. For each of these problems, we provided a transcription to continuous-time dynamical systems and gave conditions under which these dynamics are strongly infinitesimally contracting. We then extended this approach to the problem of tracking optimal trajectories in time-varying convex optimization problems. To this purpose, with our two main results, we proved (i) that the tracking error between any solution trajectory of a strongly infinitesimally contracting system and its equilibrium trajectory is upper bounded with an explicit estimate on the bound, (ii) that any strongly infinitesimally contracting system can be

augmented with a feedforward term to ensure that the tracking error converges to zero exponentially quickly. We established the strong infinitesimal contractivity of canonical dynamical systems solving optimization problems and applied our main results to provide explicit tracking error bounds. We validated these bounds in two numerical examples. With these results, we showed the potential of a contractivity-based approach for analyzing strongly convex optimization problems. Finally, we extended our analysis beyond the case of strong convexity and focused on convex (but not strongly convex) optimization problems with unique minimizers. This led to the analysis of globally weakly and locally strongly contracting dynamics. For such dynamics, we showed linear-exponential convergence to the equilibrium. Specifically, we demonstrated that linear-exponential behavior arises naturally in certain dynamics with saturations and used this result for our convergence analysis. Depending on the norms where the system is GW-LS-C, we considered two different scenarios that required two distinct mathematical approaches, yielding convergence bounds that are sharper than those provided in Part I.
Additionally, after giving a sufficient condition for local ISS, we illustrated our results on the continuous-time augmented primal-dual dynamics solving LPs. Our results motivated a conjecture relating the optimal solution of LPs to the local stability properties of the equilibrium of the resulting dynamics.

Overall, this thesis advances the understanding of how biologically plausible neural networks can solve sparse reconstruction and other optimization problems. Additionally, we showed the effectiveness of using contracting dynamics for static and time-varying convex optimization, highlighting their value for both theoretical exploration and practical applications. We believe that our work not only provides theoretical foundations but also provides practical tools for future research in both neuroscience and optimization.

13.1 Future Work

Several interesting research directions emerge from the findings of this thesis, each offering promising avenues for further exploration.

One key area for future research involves extending our results to design networks able to tackle sparse *coding* problems [71, 183], which involves learning features to reconstruct a given stimulus. We expect this will lead to the study of coupled neural-synaptic dynamics. Building on the approach developed in Part I, our goal is to derive together with the dynamics of neural activity, also learning rules for synaptic weights from the same objectives. While doing this from the composite optimization problems analyzed in this thesis remains an open and challenging question, a promising direction was introduced in [72] (see also [74, 14]). The proposed approach, based on a novel cost function called *similarity matching*, provides a biologically plausible neural network with Hebbian learning rules. Interestingly, from this objective function a number of dimensionality reduction problems [73, 15, 16], including sparse reconstructions, can be obtained. However, the proposed algorithm still lacks a formal theoretical proof of convergence, and we are currently working on bridging this gap.

Additionally, we aim to explore sparse reconstruction problems involving more general and non-convex sparsity-inducing cost functions [184]. This would broaden the

scope of our current results, potentially allowing us to tackle a wider range of tasks.

In terms of extending our contractivity analysis, future work will focus on broadening our current results to cover more general synaptic matrices, including arbitrary (non-symmetric) synaptic matrices and heterogeneous dissipation matrices. We propose preliminary conservative results in this direction in Appendix A. Further investigation into higher-order contractivity properties using the theory of k-contraction [93] and the analysis of the stochastic models [89] will also be of interest. In particular, stochastic models and systems with arbitrary synaptic matrices could yield new insights into both neuroscience and machine learning problems.

Moreover, motivated by the numerical findings reported in Figure 9.6, it would be interesting to investigate models with delays. This could allow to better understand the effects of temporal lags in neural dynamics and their potential implications for both theoretical models and real-world applications.

Additionally, we aim to prove Conjecture 1 introduced in Chapter 12 and extend our input-to-state stability (ISS) analysis to systems evaluated under different norms.

Least but not last, it is important to highlight that the potential applications of our results extend across a wide range of problems, particularly in the realm of complex systems and risk-related issues. In this direction, implementing the proposed dynamics to design efficient and robust algorithms would be a valuable next research direction. Testing these algorithms on real-world datasets will provide an additional application-oriented validation of the theoretical results developed in this thesis.

13.2 List of Publications

Journal Publications

- **V. Centorrino**, A. Davydov, A. Gokhale, G. Russo, and F. Bullo, "On Weakly Contracting Dynamics for Convex Optimization", *IEEE Control Systems Letters*, vol. 8, pp. 1745-1750, June 2024, doi: 10.1109/LCSYS.2024.3414348.

- **V. Centorrino**, A. Gokhale, A. Davydov, G. Russo, and F. Bullo, "Positive Competitive Networks for Sparse Reconstruction", *Neural Computation*, May, 36 (6): 1163–1197, 2024, doi: 10.1162/neco_a_01657.

- **V. Centorrino**, F. Bullo, and G. Russo, "Modelling and Contractivity of Neural-Synaptic networks with Hebbian learning", *Automatica*, 164:111636, 2024, doi: 10.1016/j.automatica.2024.111636.

- **V. Centorrino**, A. Gokhale, A. Davydov, G. Russo, and F. Bullo, "Euclidean Contractivity of Neural Networks with Symmetric Weights", IEEE Control Systems Letters, 7:1724-1729, 2023, doi: 10.1109/LCSYS.2023.3278250. Recipient of the *2024 IEEE Control Systems Letters Outstanding Paper Award*.

Conferences

- **V. Centorrino**, F. Bullo, G. Russo, "Contraction Analysis of Hopfield Neural Networks with Hebbian Learning", *2022 IEEE 61st Conference on Decision and Control*, Cancun, Mexico, pp. 622-627, 2022. doi: 10.1109/CDC51059.2022.9993009. Presented in the invited session "Brain Dynamics and Control".
- **V. Centorrino**, A. Davydov, A. Gokhale, G. Russo, and F. Bullo, "Euclidean Contractivity of Neural Networks with Symmetric Weights", *62nd IEEE Conference on Decision and Control*, Singapore, December 2023. Presented in the invited session "Contraction Theory for Analysis, Synchronization, and Regulation I".
- **V. Centorrino**, A. Davydov, A. Gokhale, G. Russo, and F. Bullo, "On Weakly Contracting Dynamics for Convex Optimization", *63rd IEEE Conference on Decision and Control*, Milan, Italy, December 2024. Presented in the invited session "Contraction Theory in Systems and Control I".

Workshops (Oral Talks)

- Workshop "Variational Inequalities, Nash Equilibrium Problems and Applications", "On Contracting Dynamics for Convex Optimization", Oral Talk, Catania, July 11-12, 2024. Website: https://vinepa.dmi.unict.it/.
- Workshop "Mathematics for Artificial Intelligence and Machine Learning", "Biologically Plausible Neural Networks for Sparse Reconstruction: a Normative Framework", Oral Talk, Milan, January 17-19, 2024. https://dec.unibocconi.eu/mathematics-artificial-intelligence-and-machine-learning.

Poster Presentation

- **V. Centorrino**, A. Gokhale, A. Davydov, G. Russo, and F. Bullo, "Contractivity of Symmetric Neural Networks for Non-negative Sparse Approximation", *CCS/Italy23 Conference*, Naples, October 9-11, 2023. Website: https://italy.cssociety.org/index.php/2023/05/23/ccs-italy-conference-2023/.

Preprints & Publications Under Review

- A. Davydov, **V. Centorrino**, A. Gokhale, G. Russo, and F. Bullo, "Time-Varying Convex Optimization: A Contraction and Equilibrium Tracking Approach", Conditionally accepted on *IEEE Transactions on Automatic Control*, June 2023, https://arxiv.org/abs/2305.15595.

Appendix A

Euclidean Contractivity of Firing Rate Neural Networks with Dissipation

In this appendix, we present additional and preliminary novel results on the contractivity of FNN with dissipation. These results are direct applications of recent findings in [185] and have not been published elsewhere yet.

While the contractivity results in Corollary 5.7 are sharp (in the sense that they are the best achievable), they are limited to dynamics with homogeneous dissipation and symmetric weight matrices. In this appendix, we address these limitations by providing conditions for the Euclidean contractivity of FNN with heterogeneous dissipation and general weight matrices. The drawback of this approach is that, as we will show, leads to conservative results. Consider the continuous-time FNN (3.2) with dissipation, i.e.,

$$\dot{\nu} = -D\nu + \Phi(W\nu + u), \tag{A.1}$$

where $D \in \mathbb{R}^{n\times n}$ is a positive diagonal matrix and the other terms are defined as in (3.2). We assume that the activation function is Lipschitz and slope restricted, that is Assumption 5.2 in Chapter 5, but we do not make any assumption on the matrix W.

To study the contractivity of the dynamics (A.1), we adopt a different approach compared to the methods used in Chapter 5. Specifically, we (i) reformulate the FNN (A.1) as a Lur'e system[1], and (ii) use the contractivity conditions recently developed in [185] to analyze the stability of the resulting system.

To begin with our analysis we note that we can rewrite the FNN (A.1) as a Lur'e

[1] A Lur'e system is a nonlinear system obtained by connecting a linear time-invariant (LTI) system with a time-varying nonlinear feedback control. The resulting closed-loop system is $\dot{x} = Ax + BF(t, Cx)$, where A, B, and C are matrices of the proper dimensions.

system. In fact, let us consider the Lur'e system

$$\begin{cases} \dot{\nu}(t) = -D\nu(t) + b(t), \\ y(t) = W\nu(t) + u(t) \end{cases}$$

with $b(t) = \Phi\big(t, y(t)\big)$. The resulting closed-loop system is $\dot{\nu}(t) = -D\nu(t) + \Phi(W\nu(t) + u(t))$, which corresponds exactly to the FNN in (A.1).

The following theorem is a rewriting of [185, Theorem 1] in the context of the FNN dynamics (A.1). This result provides sufficient conditions for the contractivity of a Lur'e system in a closed-loop form.

Theorem A.1 (Sufficient condition for contractivity)**.** *Consider the FNN* (A.1) *with Lipschitz and slope restricted in* $[0, 1]$ *activation function. Let* $P = P^\top \in \mathbb{R}^{n\times n}$ *be a positive definite matrix. The system* (A.1) *is strongly infinitesimally contracting with respect to the weighted Euclidean norm* $\|\cdot\|_{2,P}$ *with rate* $c > 0$ *if there exists* $\gamma \geq 0$ *such that the following LMI holds:*

$$\begin{bmatrix} 2cP - DP - PD & P + \gamma W^\top \\ P + \gamma W & -2\gamma I_n \end{bmatrix} \preceq 0 \iff \begin{bmatrix} DP + PD - 2cP & -P - \gamma W^\top \\ -P - \gamma W & 2\gamma I_n \end{bmatrix} \succeq 0. \tag{A.2}$$

Theorem A.1 implies that to study the contractivity of the FNN (A.1) we have to find a matrix $P = P^\top \succ 0$ and a scalar $\gamma \geq 0$ (and $c > 0$) such that the LMI (A.2) holds.

Next, we recall the following definition, needed for our analysis.

Definition A.1 (Lyapunov Diagonally Stability)**.** *A matrix* $A \in \mathbb{R}^{n\times n}$ *is* Lyapunov Diagonally Stable (LDS) *with rate* $\eta > 0$ *if there exists a diagonal* $P = [p]$, $p \in \mathbb{R}^n_{>0}$ *satisfying the LMI*

$$PA + A^\top P \prec 2\eta P. \tag{A.3}$$

Before proceeding with our analysis, we verify whether the LMI (A.2) holds for the results in Corollary 5.7, which we know implies contractivity of the FNN (A.1). For simplicity, we are gonna check it only for the case when $\alpha(W) < 0$.

Remark A.1 (Check if the LMI (A.2) holds for results in Corollary 5.7)**.** *Let* $D = I_n$ *and* $W = W^\top \in \mathbb{R}^{n\times n}$ *satisfying* $\alpha(W) < 0$*. Additionally, let* $P = (-W)^{1/2}$ *and* $c = 1$*. In this case, the LMI* (A.2) *reads: find* $\gamma \geq 0$ *such that*

$$\begin{bmatrix} 0_{n\times n} & -(-W)^{1/2} - \gamma W \\ -(-W)^{1/2} - \gamma W & 2\gamma I_n \end{bmatrix} \succeq 0. \tag{A.4}$$

For $\gamma \neq 0$*, since* $2\gamma I_n \succ 0$*, applying the Schur complement to the LMI* (A.4) *yields: the LMI* (A.4) *holds if and only if*

$$-\frac{1}{2\gamma}\Big((-W)^{1/2} + \gamma W\Big)^2 \succeq 0 \iff \Big((-W)^{1/2} + \gamma W\Big)^2 \preceq 0.$$

which leads to an absurd. Therefore, the LMI (A.2) does not hold in this case, even though we know the system is contracting. This discrepancy is likely due to the fact that the results in Corollary 5.7 are optimal, whereas the conditions in (A.2) are conservative.

Finally, we note also that if $W \neq I_n$ is diagonal, then the matrix $-D + W = -I_n + W \prec 0$ is Lyapunov Diagonally Stable (LDS) with respect to $P = (-W)^{1/2}$. In fact, we have

$$\begin{aligned}(-W)^{1/2}\big(-I_n + W\big) + \big(-I_n + W\big)^\top (-W)^{1/2} \\ &= (-W)^{1/2}\big(-I_n + W\big) + \big(-I_n + W\big)(-W)^{1/2} \\ &= -2(-W)^{1/2} + (-W)^{1/2}W + W(-W)^{1/2} \\ &= 2(W)^{1/2} - 2(W)^{1/2}W \\ &= 2(W)^{1/2}\Big(I_n - \Lambda\Big) \prec 0,\end{aligned}$$

where the last LMI follows from being $W \prec 0$ and $I_n - \Lambda \succ 0$. □

The next result characterizes the contractivity of the FNN (A.1).

Theorem A.2 (Contractivity of the FNN (A.1))**.** *Consider the FNN (A.1) with Lipschitz and slope restricted in $[0, 1]$ activation function. Assume that the matrix $-D+W \in \mathbb{R}^{n\times n}$ is LDS with rate η for some diagonal matrix $P \succ 0$. If*

$$\eta \geq \frac{1}{4}\frac{\lambda_{\max}\big(P\big)}{\lambda_{\min}\big(P\big)}\frac{\lambda_{\max}(W^\top W)}{\lambda_{\min}\big(D\big)}, \tag{A.5}$$

then the FNN (A.1) is strongly infinitesimally contracting with respect to $\|\cdot\|_{2,P}$.

Proof. To prove our result we apply Theorem A.1. Therefore we have to find $P = P^\top \succ 0$ and $\gamma \geq 0$ (and $c > 0$) such that the LMI (A.2) holds. We compute

$$\begin{aligned}\begin{bmatrix}-DP - PD + 2cP & P + \gamma W^\top \\ P + \gamma W & -2\gamma I_n\end{bmatrix} &= \begin{bmatrix}-2PD + 2cP & P + \gamma W^\top \\ P + \gamma W & -2\gamma I_n\end{bmatrix} \\ &= \begin{bmatrix}P & 0_{n\times n} \\ 0_{n\times n} & P\end{bmatrix}\begin{bmatrix}-2D + 2cI_n & I_n \\ I_n & 0_{n\times n}\end{bmatrix} \\ &\quad + \begin{bmatrix}0_{n\times n} & \gamma W^\top \\ \gamma W & -2\gamma I_n\end{bmatrix}.\end{aligned}$$

First, we show that $\gamma \neq 0$. In fact, for $\gamma = 0$ the LMI (A.2) becomes

$$\begin{bmatrix}P & 0_{n\times n} \\ 0_{n\times n} & P\end{bmatrix}\begin{bmatrix}2cI_n - 2D & I_n \\ I_n & 0_{n\times n}\end{bmatrix} \preceq 0.$$

The above LMI holds if and only if

$$\begin{bmatrix}2c - 2D & I_n \\ I_n & 0_{n\times n}\end{bmatrix} \preceq 0 \iff \begin{bmatrix}2(D - cI_n) & -I_n \\ -I_n & 0_{n\times n}\end{bmatrix} \succeq 0. \tag{A.6}$$

The Schur complement characterization implies that the LMI (A.6) holds if and only if

1. $D - cI_n \succ 0$,
2. $-(D - cI_n)^{-1} \succeq 0$,

which leads to an absurd. Therefore it has to be $\gamma \neq 0$.

Next, let $\gamma > 0$. By assumption there exists $P = [p]$, $p \in \mathbb{R}^n_{>0}$ such that

$$P(-D + W) + (-D + W^\top)P \preceq -2\eta P. \tag{A.7}$$

Consider the LMI (A.2) with P being the matrix satisfying (A.7). Our goal is to find $\gamma > 0$ (and $c > 0$) such that the following LMI holds

$$\begin{bmatrix} 2P(D - cI_n) & -(P + \gamma W^\top) \\ -(P + \gamma W) & 2\gamma I_n \end{bmatrix} \succeq 0. \tag{A.8}$$

Since $2\gamma I_n \succ 0$, we can apply the Schur complement characterization to the LMI (A.8): the LMI (A.8) holds if and only if

$$\begin{aligned}
&2P(D - cI_n) - (P + \gamma W^\top)\frac{1}{2\gamma}(P + \gamma W) \succeq 0 \iff \\
&2PD - \frac{1}{2\gamma}P^2 - \frac{1}{2}PW - \frac{1}{2}W^\top P - \frac{\gamma}{2}W^\top W \succeq 2cP \iff \\
&PD + \frac{1}{2}\Big(P(D - W) + (D - W)P\Big) - \frac{1}{2\gamma}P^2 - \frac{\gamma}{2}W^\top W \succeq 2cP \impliedby \\
&PD + \eta P - \frac{1}{2\gamma}P^2 - \frac{\gamma}{2}W^\top W \succeq 2cP.
\end{aligned} \tag{A.9}$$

Let $p_{\min} := \lambda_{\min}\big(P\big)$, $p_{\max} := \lambda_{\max}\big(P\big)$, and $d_{\min} := \lambda_{\min}\big(D\big)$. For proper $c > 0$ the LMI (A.9) follows if there exists $\gamma > 0$ such that

$$\begin{aligned}
PD \succeq \frac{1}{2\gamma}P^2 &\iff P\Big(D - \frac{1}{2\gamma}P\Big) \succeq 0 \iff D - \frac{1}{2\gamma}P \succeq 0 \\
&\iff D \succeq \frac{1}{2\gamma}P \iff d_{\min} \geq \frac{1}{2\gamma}p_{\max};
\end{aligned} \tag{A.10}$$

$$\begin{aligned}
\eta P \succeq \frac{\gamma}{2}W^\top W &\iff \eta p_{\min} \geq \frac{\gamma}{2}\lambda_{\max}\big(W^\top W\big) \\
&\iff \eta \geq \frac{\gamma}{2}\frac{\lambda_{\max}\big(W^\top W\big)}{p_{\min}}.
\end{aligned} \tag{A.11}$$

Now, note that inequalities (A.10) and (A.11) implies, respectively:

$$\gamma \geq \frac{1}{2}\frac{p_{\max}}{d_{\min}} \quad \text{and} \quad \gamma \leq \frac{2\eta p_{\min}}{\lambda_{\max}\big(W^\top W\big)}.$$

Such a γ exists if and only if

$$\begin{aligned}
\frac{1}{2}\frac{p_{\max}}{d_{\min}} \leq 2\eta\frac{p_{\min}}{\lambda_{\max}\big(W^\top W\big)} &\iff 2\eta\frac{p_{\min}}{\lambda_{\max}\big(W^\top W\big)} \geq \frac{1}{2}\frac{p_{\max}}{d_{\min}} \\
&\iff \eta \geq \frac{1}{4}\frac{p_{\max}}{p_{\min}}\frac{\lambda_{\max}(W^\top W)}{d_{\min}},
\end{aligned}$$

which is true by assumptions. Note that, for proper $c > 0$, the LMI (A.9) follows also if

$$\begin{aligned} PD \succeq \frac{\gamma}{2} W^\top W &\iff p_{\min} d_{\min} \geq \frac{\gamma}{2} \lambda_{\max}\left(W^\top W\right) \\ \eta P \succeq \frac{1}{2\gamma} P^2 &\iff \eta I_n \succeq \frac{1}{2\gamma} P \\ &\iff \eta \geq \frac{1}{2\gamma} p_{\max}. \end{aligned}$$

These bounds lead to the same condition on η. □

Remark A.2. *As intuitively shown by Remark (A.1), for a given diagonal matrix P, the LDS is not sufficient to guarantee the existence of a $\gamma \geq 0$ such that the LMI (A.2) holds. Instead, the value of η for which the LDS holds is crucial. In the following, we provide a simple numerical example showing that for the choice of diagonal P in Remark (A.1), the LDS with parameter $\eta > 0$ does not hold for η satisfying inequality (A.5). Let*

$$W = \begin{pmatrix} -9 & 0 & 0 \\ 0 & -4 & 0 \\ 0 & 0 & -1 \end{pmatrix} \quad \text{and} \quad P = (-W)^{1/2} = \begin{pmatrix} 3 & 0 & 0 \\ 0 & 2 & 0 \\ 0 & 0 & 1 \end{pmatrix} \tag{A.12}$$

We compute

$$P(-I_3 + W) + (-I_3 + W)P = \begin{pmatrix} -60 & 0 & 0 \\ 0 & -20 & 0 \\ 0 & 0 & -4 \end{pmatrix} \prec 0, \tag{A.13}$$

therefore the $-I_3 + W$ is LDS with respect to the diagonal matrix $(-W)^{1/2}$. Next, pick

$$\eta = \frac{1}{4} \frac{p_{\max}}{p_{\min}} \frac{\lambda_{\max}(W^\top W)}{d_{\min}} = \frac{1}{4} \frac{3}{1} \frac{81}{1} = \frac{243}{4}. \tag{A.14}$$

We have

$$P(-I + W) + (-I + W)P + 2\eta P = \begin{pmatrix} \frac{609}{2} & 0 & 0 \\ 0 & 223 & 0 \\ 0 & 0 & \frac{235}{2} \end{pmatrix},$$

which is positive definite. Therefore the "strong" LDS with parameter η satisfying inequality (A.5) does not hold and indeed, as proved in Remark (A.1), there not exists $\gamma \geq 0$ such that the LMI (A.2) holds. □

Bibliography

[1] P. Hagmann, L. Cammoun, X. Gigandet, R. Meuli, C. J. Honey, V. Wedeen, and O. Sporns, "Mapping the structural core of human cerebral cortex," *PLoS Biology*, vol. 6, no. 7, p. e159, 2008.

[2] D. O. Hebb, *The Organization of Behavior: A Neuropsychological Theory*. John Wiley & Sons, 1949.

[3] B. A. Olshausen and D. J. Field, "Sparse coding with an overcomplete basis set: A strategy employed by V1?" *Vision Research*, vol. 37, no. 23, pp. 3311–3325, 1997.

[4] F. Rosenblatt, "The perceptron: a probabilistic model for information storage and organization in the brain." *Psychological Review*, vol. 65, no. 6, p. 386, 1958.

[5] D. E. Rumelhart, G. E. Hinton, and R. J. Williams, "Learning representations by back-propagating errors," *Nature*, vol. 323, no. 6088, pp. 533–536, 1986.

[6] I. Goodfellow, Y. Bengio, and A. Courville, *Deep Learning*. MIT Press, 2016. [Online]. Available: http://www.deeplearningbook.org

[7] R. O'Reilly and Y. Munakata, *Computational Explorations in Cognitive Neuroscience Understanding the Mind by Simulating the Brain*. MIT Press, 2000.

[8] D. Krotov and J. J. Hopfield, "Unsupervised learning by competing hidden units," *Proceedings of the National Academy of Sciences*, vol. 116, p. 201820458, 03 2019.

[9] B. Scellier and Y. Bengio, "Equilibrium propagation: Bridging the gap between energy-based models and backpropagation," *Frontiers in Computational Neuroscience*, vol. 11, p. 24, 2017.

[10] V. Volodymyr, K. Kavukcuoglu, D. Silver, A. A. Rusu, J. Veness, M. G. Bellemare, A. Graves, M. Riedmiller, A. K. Fidjeland, G. Ostrovski *et al.*, "Human-level control through deep reinforcement learning," *Nature*, vol. 518, no. 7540, pp. 529–533, 2015.

[11] D. Silver, A. Huang, C. Maddison, A. Guez, L. Sifre *et al.*, "Mastering the game of go with deep neural networks and tree search," *Nature*, vol. 529, no. 7587, pp. 484–489, 2016.

[12] B. M. Lake, T. D. Ullman, J. B. Tenenbaum, and S. J. Gershman, "Building machines that learn and think like people," *Behavioral and Brain Sciences*, vol. 40, 2016.

[13] N. M. Gottschling, V. Antun, B. Adcock, and A. C. Hansen, "The troublesome kernel – on hallucinations, no free lunches and the accuracy-stability trade-off in inverse problems," 2024. [Online]. Available: https://arxiv.org/abs/2001.01258

[14] C. Pehlevan and D. B. Chklovskii, "Neuroscience-inspired online unsupervised learning algorithms: Artificial neural networks," *IEEE Signal Processing Magazine*, vol. 36, no. 6, pp. 88–96, 2019.

[15] C. Pehlevan, S. Mohan, and D. B. Chklovskii, "Blind nonnegative source separation using biological neural networks," *Neural Computation*, vol. 29, no. 11, pp. 2925–2954, 2017.

[16] D. Lipshutz, C. Pehlevan, and D. B. Chklovskii, "Biologically plausible single-layer networks for nonnegative independent component analysis," *Biological Cybernetics*, 2022.

[17] J. J. Hopfield and D. W. Tank, "Computing with neural circuits: A model," *Science*, vol. 233, no. 4764, pp. 625–633, 1986.

[18] M. M. Churchland, J. P. Cunningham, M. T. Kaufman, J. D. Foster, P. Nuyujukian, S. I. Ryu, and K. V. Shenoy, "Neural population dynamics during reaching," *Nature*, vol. 487, no. 7405, pp. 51–56, 2012.

[19] S. Saxena and J. P. Cunningham, "Towards the neural population doctrine," *Current Opinion in Neurobiology*, vol. 55, pp. 103–111, 2019.

[20] D. Sussillo, "Neural circuits as computational dynamical systems," *Current Opinion in Neurobiology*, vol. 25, pp. 156–163, 2014.

[21] S. Vyas, M. D. Golub, D. Sussillo, and K. V. Shenoy, "Computation through neural population dynamics," *Annual Review of Neuroscience*, vol. 43, no. 1, pp. 249–275, 2020.

[22] D. W. Dong and J. J. Hopfield, "Dynamic properties of neural networks with adapting synapses," *Network: Computation in Neural Systems*, vol. 3, no. 3, pp. 267–283, 1992.

[23] M. Galtier, O. Faugeras, and P. Bressloff, "Hebbian learning of recurrent connections: A geometrical perspective," *Neural Computation*, vol. 24, pp. 2346–83, 05 2012.

[24] L. Kozachkov, M. Lundqvist, J.-J. E. Slotine, and E. K. Miller, "Achieving stable dynamics in neural circuits," *PLoS Computational Biology*, vol. 16, no. 8, pp. 1–15, 2020.

[25] W. Lohmiller and J.-J. E. Slotine, "On contraction analysis for non-linear systems," *Automatica*, vol. 34, no. 6, pp. 683–696, 1998.

[26] G. Russo, M. Di Bernardo, and E. D. Sontag, "Global entrainment of transcriptional systems to periodic inputs," *PLoS Computational Biology*, vol. 6, no. 4, p. e1000739, 2010.

[27] A. Davydov, S. Jafarpour, and F. Bullo, "Non-Euclidean contraction theory for robust nonlinear stability," *IEEE Transactions on Automatic Control*, 2022.

[28] S. Xie, G. Russo, and R. H. Middleton, "Scalability in nonlinear network systems affected by delays and disturbances," *IEEE Transactions on Control of Network Systems*, vol. 8, no. 3, pp. 1128–1138, 2021.

[29] S. Jafarpour, A. Davydov, A. V. Proskurnikov, and F. Bullo, "Robust implicit networks via non-Euclidean contractions," in *Advances in Neural Information Processing Systems*, Dec. 2021. [Online]. Available: http://arxiv.org/abs/2106.03194

[30] D. S. Bassett and M. S. Gazzaniga, "Understanding complexity in the human brain," *Trends in Cognitive Sciences*, vol. 15, no. 5, pp. 200–209, 2011.

[31] C. Westlin, J. E. Theriault *et al.*, "Improving the study of brain-behavior relationships by revisiting basic assumptions," *Trends in Cognitive Sciences*, vol. 27, no. 3, pp. 246–257, 2023.

[32] A. Helmi, M. W. Fakhr, and A. F. Atiya, "Multi-step ahead time series forecasting via sparse coding and dictionary based techniques," *Applied Soft Computing*, vol. 69, pp. 464–474, 2018.

[33] Z. Yu, X. Zheng, F. Huang, W. Guo, L. Sun, and Z. Yu, "A framework based on sparse representation model for time series prediction in smart city," *Frontiers of Computer Science*, vol. 15, no. 1, pp. 1–13, 2021.

[34] H. Lyu, C. Strohmeier, G. Menz, and D. Needell, "COVID-19 time-series prediction by joint dictionary learning and online NMF," 2020. [Online]. Available: https://arxiv.org/abs/2004.09112

[35] N. Giamarelos, E. N. Zois, M. Papadimitrakis, M. Stogiannos, N.-A. I. Livanos, and A. Alexandridis, "Short-term electric load forecasting with sparse coding methods," *IEEE Access*, vol. 9, pp. 102 847–102 861, 2021.

[36] S. Jafarpour, P. Cisneros-Velarde, and F. Bullo, "Weak and semi-contraction for network systems and diffusively-coupled oscillators," *IEEE Transactions on Automatic Control*, vol. 67, no. 3, pp. 1285–1300, 2022.

[37] F. H. Clarke, *Optimization and Nonsmooth Analysis*. John Wiley & Sons, 1983.

[38] A. Davydov, A. V. Proskurnikov, and F. Bullo, "Non-Euclidean contraction analysis of continuous-time neural networks," *IEEE Transactions on Automatic Control*, Sep. 2024.

[39] G. Dahlquist, "Stability and error bounds in the numerical integration of ordinary differential equations," Ph.D. dissertation, (Reprinted in Trans. Royal Inst. of Technology, No. 130, Stockholm, Sweden, 1959), 1958.

[40] S. M. Lozinskii, "Error estimate for numerical integration of ordinary differential equations. I," *Izvestiya Vysshikh Uchebnykh Zavedenii. Matematika*, vol. 5, pp. 52–90, 1958, (in Russian). [Online]. Available: http://mi.mathnet.ru/eng/ivm2980

[41] W. A. Coppel, *Stability and Asymptotic Behavior of Differential Equations*. Heath, 1965.

[42] F. Bullo, *Contraction Theory for Dynamical Systems*, 1.2 ed. Kindle Direct Publishing, 2024. [Online]. Available: https://fbullo.github.io/ctds

[43] J. Stoer and C. Witzgall, "Transformations by diagonal matrices in a normed space," *Numerische Mathematik*, vol. 4, pp. 158–171, 1962.

[44] A. Davydov, A. V. Proskurnikov, and F. Bullo, "Non-Euclidean contractivity of recurrent neural networks," in *American Control Conference*, 2022.

[45] T. Ström, "On logarithmic norms," *SIAM Journal on Numerical Analysis*, vol. 12, no. 5, pp. 741–753, 1975.

[46] G. Russo, M. Di Bernardo, and E. D. Sontag, "A contraction approach to the hierarchical analysis and design of networked systems," *IEEE Transactions on Automatic Control*, vol. 58, no. 5, pp. 1328–1331, 2013.

[47] F. Bullo, *Lectures on Network Systems*, 1.6 ed. Kindle Direct Publishing, Jan. 2022. [Online]. Available: http://motion.me.ucsb.edu/book-lns

[48] P. L. Combettes and J. Pesquet, "Proximal splitting methods in signal processing," *Fixed-point Algorithms for Inverse Problems in Science and Engineering*, pp. 185–212, 2011.

[49] A. Beck, *First-Order Methods in Optimization*. SIAM, 2017.

[50] N. Parikh and S. Boyd, "Proximal algorithms," *Foundations and Trends in Optimization*, vol. 1, no. 3, pp. 127–239, 2014.

[51] B. Abbas and H. Attouch, "Dynamical systems and forward–backward algorithms associated with the sum of a convex subdifferential and a monotone cocoercive operator," *Optimization*, vol. 64, no. 10, pp. 2223–2252, 2015.

[52] S. Hassan-Moghaddam and M. R. Jovanović, "Proximal gradient flow and Douglas-Rachford splitting dynamics: Global exponential stability via integral quadratic constraints," *Automatica*, vol. 123, p. 109311, 2021.

[53] A. Davydov, V. Centorrino, A. Gokhale, G. Russo, and F. Bullo, "Contracting dynamics for time-varying convex optimization." [Online]. Available: https://arxiv.org/abs/2305.15595

[54] W. Gerstner, W. M. Kistler, R. Naud, and L. Paninski, *Neuronal Dynamics: From Single Neurons To Networks and Models of Cognition*. Cambridge University Press, 2014. [Online]. Available: https://neuronaldynamics.epfl.ch

[55] R. J. Douglas and K. A. Martin, "A functional microcircuit for cat visual cortex." *The Journal of physiology*, vol. 440, no. 1, pp. 735–769, 1991.

[56] C. V. V. Carl and H. Sompolinsky, "Chaos in neuronal networks with balanced excitatory and inhibitory activity," *Science*, vol. 274, no. 5293, pp. 1724–1726, 1996.

[57] H. R. Wilson and J. D. Cowan, "Excitatory and inhibitory interactions in localized populations of model neurons," *Biophysical Journal*, vol. 12, no. 1, pp. 1–24, 1972.

[58] J. J. Hopfield, "Neurons with graded response have collective computational properties like those of two-state neurons," *Proceedings of the National Academy of Sciences*, vol. 81, no. 10, pp. 3088–3092, 1984.

[59] K. D. Miller and F. Fumarola, "Mathematical equivalence of two common forms of firing rate models of neural networks," *Neural Computation*, vol. 24, no. 1, pp. 25–31, 2012.

[60] H. Hewamalage, C. Bergmeir, and K. Bandara, "Recurrent neural networks for time series forecasting: Current status and future directions," *International Journal of Forecasting*, vol. 37, no. 1, pp. 388–427, 2021.

[61] D. Sussillo and L. F. Abbott, "Generating coherent patterns of activity from chaotic neural networks," *Neuron*, vol. 63, no. 4, pp. 544–557, 2009.

[62] D. W. Tank and J. J. Hopfield, "Simple "neural" optimization networks: An A/D converter, signal decision circuit, and a linear programming circuit," *IEEE Transactions on Circuits and Systems*, vol. 33, no. 5, pp. 533–541, 1986.

[63] A. Bouzerdoum and T. R. Pattison, "Neural network for quadratic optimization with bound constraints," *IEEE Transactions on Neural Networks*, vol. 4, no. 2, pp. 293–304, 1993.

[64] C. J. Rozell, D. H. Johnson, R. G. Baraniuk, and B. A. Olshausen, "Sparse coding via thresholding and local competition in neural circuits," *Neural Computation*, vol. 20, no. 10, pp. 2526–2563, 2008.

[65] A. Yang, J. Xiong, M. Raginsky, and E. Rosenbaum, "Input-to-state stable neural ordinary differential equations with applications to transient modeling of circuits," in *Conference on Learning for Dynamics and Control*, vol. 168, 2022, pp. 663–675. [Online]. Available: https://proceedings.mlr.press/v168/yang22b.html

[66] E. Oja, "Simplified neuron model as a principal component analyzer," *Journal of Mathematical Biology*, vol. 15, no. 3, pp. 267–273, 1982.

[67] P. Földiák, "Forming sparse representations by local anti-Hebbian learning." *Biological Cybernetics*, vol. 64(2), pp. 165–70, 1990.

[68] W. Gerstner and W. Kistler, "Mathematical formulations of Hebbian learning," *Biological Cybernetics*, vol. 87, pp. 404–15, 2003.

[69] B. Siri, H. Berry, B. Cessac, B. Delord, and M. Quoy, "A mathematical analysis of the effects of Hebbian learning rules on the dynamics and structure of discrete-time random recurrent neural networks," *Neural Computation*, vol. 20, no. 12, pp. 2937–2966, 2008.

[70] V. Centorrino, F. Bullo, and G. Russo, "Modelling and contractivity of neural-synaptic networks with Hebbian learning," *Automatica*, vol. 164, p. 111636, 2024.

[71] C. S. N. Brito and W. Gerstner, "Nonlinear Hebbian learning as a unifying principle in receptive field formation," *PLoS Computational Biology*, vol. 12, no. 9, p. e1005070, 2016.

[72] T. Hu, C. Pehlevan, and D. B. Chklovskii, "A Hebbian/Anti-Hebbian network for online sparse dictionary learning derived from symmetric matrix factorization," in *2014 48th Asilomar Conference on Signals, Systems and Computers*. IEEE, 2014, pp. 613–619.

[73] C. Pehlevan and D. B. Chklovskii, "A Hebbian/Anti-Hebbian network derived from online non-negative matrix factorization can cluster and discover sparse features," in *2014 48th Asilomar Conference on Signals, Systems and Computers*. IEEE, 2014, pp. 769–775.

[74] C. Pehlevan, A. M. Sengupta, and D. B. Chklovskii, "Why do similarity matching objectives lead to Hebbian/anti-Hebbian networks?" *Neural Computation*, vol. 30, no. 1, pp. 84–124, 2017.

[75] T. Chen and S. I. Amari, "Stability of asymmetric Hopfield networks," *IEEE Transactions on Neural Networks*, vol. 12, no. 1, pp. 159–163, 2001.

[76] Y. Fang and T. G. Kincaid, "Stability analysis of dynamical neural networks," *IEEE Transactions on Neural Networks*, vol. 7, no. 4, pp. 996–1006, 1996.

[77] S. Haykin, *Neural Networks and Learning Machines*, 3rd ed. Prentice Hall, 2008.

[78] V. Centorrino, A. Gokhale, A. Davydov, G. Russo, and F. Bullo, "Euclidean contractivity of neural networks with symmetric weights," *IEEE Control Systems Letters*, vol. 7, pp. 1724–1729, 2023.

[79] W. Gerstner and W. Kistler, "Mathematical formulations of Hebbian learning," *Biological Cybernetics*, vol. 87, pp. 404–15, 2003.

[80] M. Di Bernardo, D. Liuzza, and G. Russo, "Contraction analysis for a class of nondifferentiable systems with applications to stability and network synchronization," *SIAM Journal on Control and Optimization*, vol. 52, no. 5, pp. 3203–3227, 2014.

[81] H. Tsukamoto, S.-J. Chung, and J.-J. E. Slotine, "Contraction theory for nonlinear stability analysis and learning-based control: A tutorial overview," *Annual Reviews in Control*, vol. 52, pp. 135–169, 2021.

[82] S. Banach, "Sur les opérations dans les ensembles abstraits et leur application aux équations intégrales," *Fundamenta Mathematicae*, vol. 3, no. 1, pp. 133–181, 1922.

[83] D. C. Lewis, "Metric properties of differential equations," *American Journal of Mathematics*, vol. 71, no. 2, pp. 294–312, 1949.

[84] B. P. Demidovič, "Dissipativity of a nonlinear system of differential equations," *Uspekhi Matematicheskikh Nauk*, vol. 16, no. 3(99), p. 216, 1961.

[85] N. N. Krasovskiĭ, *Stability of Motion. Applications of Lyapunov's Second Method to Differential Systems and Equations with Delay*. Stanford University Press, 1963, translation of the 1959 edition in Russian by J. L. Brenner.

[86] A. Pavlov, A. Pogromsky, N. Van de Wouw, and N. Nijmeijer, "Convergent dynamics, a tribute to Boris Pavlovich Demidovich," *Systems & Control Letters*, vol. 52, no. 3-4, pp. 257–261, 2004.

[87] W. Wang and J. J. Slotine, "On partial contraction analysis for coupled nonlinear oscillators," *Biological Cybernetics*, vol. 92, no. 1, pp. 38–53, 2005.

[88] Q. C. Pham and J.-J. E. Slotine, "Stable concurrent synchronization in dynamic system networks," *Neural Networks*, vol. 20, no. 1, pp. 62–77, 2007.

[89] Z. Aminzare, "Stochastic logarithmic Lipschitz constants: A tool to analyze contractivity of stochastic differential equations," *IEEE Control Systems Letters*, vol. 6, pp. 2311–2316, 2022.

[90] J. W. Simpson-Porco and F. Bullo, "Contraction theory on Riemannian manifolds," *Systems & Control Letters*, vol. 65, pp. 74–80, 2014.

[91] F. Forni and R. Sepulchre, "A differential Lyapunov framework for contraction analysis," *IEEE Transactions on Automatic Control*, vol. 59, no. 3, pp. 614–628, 2014.

[92] G. Russo and F. Wirth, "Matrix measures, stability and contraction theory for dynamical systems on time scales," *Discrete & Continuous Dynamical Systems - B*, 2021.

[93] C. Wu, I. Kanevskiy, and M. Margaliot, "k-contraction: Theory and applications," *Automatica*, vol. 136, p. 110048, 2022.

[94] M. A. Al-Radhawi and D. Angeli, "New approach to the stability of chemical reaction networks: Piecewise linear in rates Lyapunov functions," *IEEE Transactions on Automatic Control*, vol. 61, no. 1, pp. 76–89, 2016.

[95] H. Qiao, J. Peng, and Z.-B. Xu, "Nonlinear measures: A new approach to exponential stability analysis for Hopfield-type neural networks," *IEEE Transactions on Neural Networks*, vol. 12, no. 2, pp. 360–370, 2001.

[96] V. Centorrino, F. Bullo, and G. Russo, "Contraction analysis of Hopfield neural networks with Hebbian learning," in *IEEE Conf. on Decision and Control*, Cancún, México, Dec. 2022, pp. 622–627.

[97] G. Como, E. Lovisari, and K. Savla, "Throughput optimality and overload behavior of dynamical flow networks under monotone distributed routing," *IEEE Transactions on Control of Network Systems*, vol. 2, no. 1, pp. 57–67, 2015.

[98] S. Coogan, "A contractive approach to separable Lyapunov functions for monotone systems," *Automatica*, vol. 106, pp. 349–357, 2019.

[99] M. Picallo, S. Bolognani, and F. Dörfler, "Sensitivity conditioning: Beyond singular perturbation for control design on multiple time scales," *IEEE Transactions on Automatic Control*, vol. 68, no. 4, pp. 2309–2324, 2022.

[100] L. Cothren, F. Bullo, and E. Dall'Anese, "Online feedback optimization and singular perturbation via contraction theory," 2024. [Online]. Available: https://arxiv.org/abs/2310.07966

[101] M. Revay and I. Manchester, "Contracting implicit recurrent neural networks: Stable models with improved trainability," in *Conference on Learning for Dynamics and Control*, vol. 120, 2020, pp. 393–403. [Online]. Available: https://proceedings.mlr.press/v120/revay20a.html

[102] L. Kozachkov, M. Ennis, and J.-J. E. Slotine, "RNNs of RNNs: Recursive construction of stable assemblies of recurrent neural networks," in *Advances in Neural Information Processing Systems*, Dec. 2022.

[103] M. Zakwan, L. Xu, and G. Ferrari-Trecate, "Robust classification using contractive hamiltonian neural odes," *IEEE Control Systems Letters*, vol. 7, pp. 145–150, 2022.

[104] M. Revay, R. Wang, and I. R. Manchester, "Lipschitz bounded equilibrium networks," 2020. [Online]. Available: https://arxiv.org/abs/2010.01732

[105] H. D. Nguyen, T. L. Vu, K. Turitsyn, and J.-J. E. Slotine, "Contraction and robustness of continuous time primal-dual dynamics," *IEEE Control Systems Letters*, vol. 2, no. 4, pp. 755–760, 2018.

[106] V. Centorrino, A. Davydov, A. Gokhale, G. Russo, and F. Bullo, "On weakly contracting dynamics for convex optimization," *IEEE Control Systems Letters*, vol. 8, pp. 1745–1750, 2024.

[107] V. Centorrino, A. Gokhale, A. Davydov, G. Russo, and F. Bullo, "Positive competitive networks for sparse reconstruction," *Neural Computation*, vol. 36, no. 6, p. 1163–1197, 2024.

[108] E. D. Sontag, "Contractive systems with inputs," in *Perspectives in Mathematical System Theory, Control, and Signal Processing*, J. C. Willems, S. Hara, Y. Ohta, and H. Fujioka, Eds. Springer, 2010, pp. 217–228.

[109] Z. Aminzare and E. D. Sontag, "Synchronization of diffusively-connected nonlinear systems: Results based on contractions with respect to general norms," *IEEE Transactions on Network Science and Engineering*, vol. 1, no. 2, pp. 91–106, 2014.

[110] P. Giesl, S. Hafstein, and C. Kawan, "Review on contraction analysis and computation of contraction metrics," *Journal of Computational Dynamics*, vol. 10, no. 1, pp. 1–47, 2023.

[111] A. Davydov and F. Bullo, "Perspectives on contractivity in control, optimization, and learning," 2024. [Online]. Available: https://arxiv.org/abs/2404.11707

[112] H. K. Khalil, *Nonlinear Systems*, 3rd ed. Prentice Hall, 2002.

[113] M. Nagumo, "Über die Lage der Integralkurven gewöhnlicher Differentialgleichungen," *Proceedings of the Physico-Mathematical Society of Japan. 3rd Series*, vol. 24, pp. 551–559, 1942.

[114] F. Bullo, P. Cisneros-Velarde, A. Davydov, and S. Jafarpour, "From contraction theory to fixed point algorithms on Riemannian and non-Euclidean spaces," in *2021 60th IEEE Conference on Decision and Control (CDC)*, 2021, pp. 2923–2928.

[115] A. Davydov, S. Jafarpour, A. V. Proskurnikov, and F. Bullo, "Non-Euclidean monotone operator theory and applications," *Journal of Machine Learning Research*, vol. 25, no. 307, pp. 1–33, 2024. [Online]. Available: http://jmlr.org/papers/v25/23-0805.html

[116] D. H. Hubel and T. N. Wiesel, "Receptive fields and functional architecture of monkey striate cortex," *The Journal of Physiology*, vol. 195, no. 1, pp. 215–243, 1968.

[117] H. B. Barlow, "Single units and sensation: a neuron doctrine for perceptual psychology?" *Perception*, vol. 1, no. 4, pp. 371–394, 1972.

[118] D. J. Field, "Relations between the statistics of natural images and the response properties of cortical cells," *Journal of the Optical Society of America A*, vol. 4, no. 12, pp. 2379–2394, 1987.

[119] B. A. Olshausen and D. J. Field, "Sparse coding of sensory inputs," *Current Opinion in Neurobiology*, vol. 14, no. 4, pp. 481–487, 2004.

[120] K. J. Arrow, L. Hurwicz, and H. Uzawa, Eds., *Studies in Linear and Nonlinear Programming*. Stanford University Press, 1958.

[121] J. J. Hopfield and D. W. Tank, ""Neural" computation of decisions in optimization problems," *Biological Cybernetics*, vol. 52, no. 3, pp. 141–152, 1985.

[122] H. Zhang, Z. Wang, and D. Liu, "A comprehensive review of stability analysis of continuous-time recurrent neural networks," *IEEE Transactions on Neural Networks and Learning Systems*, vol. 25, no. 7, pp. 1229–1262, 2014.

[123] A. Balavoine, C. J. Rozell, and J. Romberg, "Global convergence of the locally competitive algorithm," in *2011 Digital Signal Processing and Signal Processing Education Meeting (DSP/SPE)*. IEEE, 2011, pp. 431–436.

[124] A. Balavoine, J. Romberg, and C. J. Rozell, "Convergence and rate analysis of neural networks for sparse approximation," *IEEE Transactions on Neural Networks and Learning Systems*, vol. 23, no. 9, pp. 1377–1389, 2012.

[125] A. Balavoine, C. J. Rozell, and J. Romberg, "Convergence of a neural network for sparse approximation using the nonsmooth Łojasiewicz inequality," in *International Joint Conference on Neural Networks*, 2013, pp. 1–8.

[126] A. S. Charles, P. Garrigues, and C. J. Rozell, "A common network architecture efficiently implements a variety of sparsity-based inference problems," *Neural Computation*, vol. 24, no. 12, pp. 3317–3339, 2012.

[127] A. Balavoine, C. J. Rozell, and J. Romberg, "Convergence speed of a dynamical system for sparse recovery," *IEEE Transactions on Signal Processing*, vol. 61, no. 17, pp. 4259–4269, 2013.

[128] M. Zhu and C. J. Rozell, "Visual nonclassical receptive field effects emerge from sparse coding in a dynamical system," *PLoS Computational Biology*, vol. 9, no. 8, p. e1003191, 2013.

[129] A. Balavoine, C. J. Rozell, and J. Romberg, "Discrete and continuous-time soft-thresholding for dynamic signal recovery," *IEEE Transactions on Signal Processing*, vol. 63, no. 12, pp. 3165–3176, 2015.

[130] J. J. Hopfield, "Neural networks and physical systems with emergent collective computational abilities," *Proceedings of the National Academy of Sciences*, vol. 79, no. 8, pp. 2554–2558, 1982.

[131] R. Laje and D. V. Buonomano, "Robust timing and motor patterns by taming chaos in recurrent neural networks," *Nature Neuroscience*, vol. 16, pp. 925–933, 2013.

[132] M. Revay, R. Wang, and I. R. Manchester, "A convex parameterization of robust recurrent neural networks," *IEEE Control Systems Letters*, vol. 5, no. 4, pp. 1363–1368, 2021.

[133] H. Wen, X. He, and T. Huang, "Sparse signal reconstruction via recurrent neural networks with hyperbolic tangent function," *Neural Networks*, vol. 153, pp. 1–12, 2022.

[134] M. Forti and A. Tesi, "New conditions for global stability of neural networks with application to linear and quadratic programming problems," *IEEE Transactions on Circuits and Systems I: Fundamental Theory and Applications*, vol. 42, no. 7, pp. 354–366, 1995.

[135] E. Nozari and J. Cortés, "Hierarchical selective recruitment in linear-threshold brain networks—part I: Single-layer dynamics and selective inhibition," *IEEE Transactions on Automatic Control*, vol. 66, no. 3, pp. 949–964, 2021.

[136] R. A. Horn and C. R. Johnson, *Matrix Analysis*, 2nd ed. Cambridge University Press, 2012.

[137] E. J. Candès and M. B. Wakin, "An introduction to compressive sampling," *IEEE Signal Processing Magazine*, vol. 25, no. 2, pp. 21–30, 2008.

[138] J. Wright, A. Y. Yang, A. Ganesh, S. S. Sastry, and Y. Ma, "Robust face recognition via sparse representation," *IEEE Transactions on Pattern Analysis & Machine Intelligence*, vol. 31, no. 2, pp. 210–227, 2008.

[139] M. Elad, M. A. T. Figueiredo, and Y. Ma, "On the role of sparse and redundant representations in image processing," *Proceedings of the IEEE*, vol. 98, no. 6, pp. 972–982, 2010.

[140] J. Wright and Y. Ma, *High-Dimensional Data Analysis with Low-Dimensional Models: Principles, Computation, and Applications*. Cambridge University Press, 2022.

[141] B. A. Olshausen and D. J. Field, "Natural image statistics and efficient coding," *Network: Computation in Neural Systems*, vol. 7, no. 2, pp. 333–339, 1996.

[142] E. J. Candès and T. Tao, "The Dantzig selector: Statistical estimation when p is much larger than n," *Quality Control and Applied Statistics*, vol. 54, no. 1, pp. 83–84, 2009.

[143] H. Dale, "Pharmacology and Nerve-Endings," *Proceedings of the Royal Society of Medicine*, vol. 28, no. 3, pp. 319–332, 1935.

[144] T. P. Lillicrap, D. Cownden, D. B. Tweed, and C. J. Akerman, "Random synaptic feedback weights support error backpropagation for deep learning," *Nature Communications*, vol. 7, no. 1, 2016.

[145] P. Lin, D. Oller, T. Seno *et al.*, "Outracing champion Gran Turismo drivers with deep reinforcement learning," *Nature*, vol. 602, no. 7896, pp. 223–228, 2022.

[146] N. Bhattasali, A. M. Zador, and T. Engel, "Neural circuit architectural priors for embodied control," *Advances in Neural Information Processing Systems*, vol. 35, pp. 12 744–12 759, 2022.

[147] J. C. Eccles, P. Fatt, and K. Koketsu, "Cholinergic and inhibitory synapses in a pathway from motor-axon collaterals to motoneurones," *The Journal of Physiology*, vol. 126, no. 3, p. 524, 1954.

[148] W. Wang and J.-J. E. Slotine, "Contraction analysis of time-delayed communications and group cooperation," *IEEE Transactions on Automatic Control*, vol. 51, no. 4, pp. 712–717, 2006.

[149] M. P. Kennedy and L. O. Chua, "Neural networks for nonlinear programming," *IEEE Transactions on Circuits and Systems*, vol. 35, no. 5, pp. 554–562, 1988.

[150] R. W. Brockett, "Dynamical systems that sort lists, diagonalize matrices, and solve linear programming problems," *Linear Algebra and its Applications*, vol. 146, pp. 79–91, 1991.

[151] G. Bianchin, J. Cortés, J. I. Poveda, and E. Dall'Anese, "Time-varying optimization of LTI systems via projected primal-dual gradient flows," *IEEE Transactions on Control of Network Systems*, vol. 9, no. 1, pp. 474–486, 2022.

[152] G. Tanaka, T. Yamane, J. B. Héroux, R. Nakane, N. Kanazawa, S. Takeda, H. Numata, D. Nakano, and A. Hirose, "Recent advances in physical reservoir computing: A review," *Neural Networks*, vol. 115, pp. 100–123, 2019.

[153] A. Hauswirth, Z. He, S. Bolognani, G. Hug, and F. Dörfler, "Optimization algorithms as robust feedback controllers," *Annual Reviews in Control*, vol. 57, p. 100941, 2024.

[154] J. Wang and N. Elia, "A control perspective for centralized and distributed convex optimization," in *IEEE Conf. on Decision and Control and European Control Conference*, Orlando, USA, 2011, pp. 3800–3805.

[155] A. Cherukuri, B. Gharesifard, and J. Cortes, "Saddle-point dynamics: Conditions for asymptotic stability of saddle points," *SIAM Journal on Control and Optimization*, vol. 55, no. 1, pp. 486–511, 2017.

[156] G. Qu and N. Li, "On the exponential stability of primal-dual gradient dynamics," *IEEE Control Systems Letters*, vol. 3, no. 1, pp. 43–48, 2019.

[157] J. Cortés and S. K. Niederländer, "Distributed coordination for nonsmooth convex optimization via saddle-point dynamics," *Journal of Nonlinear Science*, vol. 29, no. 4, pp. 1247–1272, 2019.

[158] N. K. Dhingra, S. Z. Khong, and M. R. Jovanović, "The proximal augmented Lagrangian method for nonsmooth composite optimization," *IEEE Transactions on Automatic Control*, vol. 64, no. 7, pp. 2861–2868, 2019.

[159] P. Cisneros-Velarde, S. Jafarpour, and F. Bullo, "Distributed and time-varying primal-dual dynamics via contraction analysis," *IEEE Transactions on Automatic Control*, vol. 67, no. 7, pp. 3560–3566, 2022.

[160] P. M. Wensing and J.-J. E. Slotine, "Beyond convexity — Contraction and global convergence of gradient descent," *PLoS One*, vol. 15, no. 8, pp. 1–29, 2020.

[161] D. Ding and M. R. Jovanović, "Global exponential stability of primal-dual gradient flow dynamics based on the proximal augmented lagrangian," in *2019 American Control Conference (ACC)*, 2019, pp. 3414–3419.

[162] I. K. Ozaslan and M. R. Jovanović, "On the global exponential stability of primal-dual dynamics for convex problems with linear equality constraints," in *2023 American Control Conference (ACC)*, 2023, pp. 210–215.

[163] ——, "Tight lower bounds on the convergence rate of primal-dual dynamics for equality constrained convex problems," in *2023 62nd IEEE Conference on Decision and Control (CDC)*, 2023, pp. 7312–7317.

[164] A. Gokhale, A. Davydov, and F. Bullo, "Contractivity of distributed optimization and nash seeking dynamics," *IEEE Control Systems Letters*, vol. 7, pp. 3896–3901, 2023.

[165] A. Simonetto, A. Mokhtari, A. Koppel, G. Leus, and A. Ribeiro, "A class of prediction-correction methods for time-varying convex optimization," *IEEE Transactions on Signal Processing*, vol. 64, no. 17, pp. 4576–4591, 2016.

[166] A. Simonetto and E. Dall'Anese, "Prediction-correction algorithms for time-varying constrained optimization," *IEEE Transactions on Signal Processing*, vol. 65, no. 20, pp. 5481–5494, 2017.

[167] M. Fazlyab, S. Paternain, V. M. Preciado, and A. Ribeiro, "Prediction-correction interior-point method for time-varying convex optimization," *IEEE Transactions on Automatic Control*, vol. 63, no. 7, pp. 1973–1986, 2018.

[168] E. Dall'Anese, A. Simonetto, S. Becker, and L. Madden, "Optimization and learning with information streams: Time-varying algorithms and applications," *IEEE Signal Processing Magazine*, vol. 37, no. 3, pp. 71–83, 2020.

[169] A. Simonetto, E. Dall'Anese, S. Paternain, G. Leus, and G. B. Giannakis, "Time-varying convex optimization: Time-structured algorithms and applications," *Proceedings of the IEEE*, vol. 108, no. 11, pp. 2032–2048, 2020.

[170] M. Colombino, E. Dall'Anese, and A. Bernstein, "Online optimization as a feedback controller: Stability and tracking," *IEEE Transactions on Control of Network Systems*, vol. 7, no. 1, pp. 422–432, 2020.

[171] S. Rahili and W. Ren, "Distributed continuous-time convex optimization with time-varying cost functions," *IEEE Transactions on Automatic Control*, vol. 62, no. 4, pp. 1590–1605, 2017.

[172] S. Sun, J. Xu, and W. Ren, "Distributed continuous-time algorithms for time-varying constrained convex optimization," *IEEE Transactions on Automatic Control*, vol. 68, no. 7, pp. 3931–3946, 2023.

[173] Y. Ding, H. Wang, and W. Ren, "Distributed continuous-time time-varying optimization for networked lagrangian systems with quadratic cost functions," *Automatica*, vol. 171, p. 111882, 2025.

[174] X.-B. Gao, "Exponential stability of globally projected dynamic systems," *IEEE Transactions on Neural Networks*, vol. 14, no. 2, pp. 426–431, 2003.

[175] I. R. Kachurovskii, "On monotone operators and convex functionals," vol. 15, no. 4, p. 213–215, 1960.

[176] E. K. Ryu and W. Yin, *Large-Scale Convex Optimization via Monotone Operators*. Cambridge University Press (to be published, 2022.

[177] E. Ryu and S. Boyd, "A primer on monotone operator methods," *Applied and Computational Mathematics*, vol. 15, pp. 3–43, 01 2016.

[178] H. H. Bauschke and P. L. Combettes, *Convex Analysis and Monotone Operator Theory in Hilbert Spaces*, 2nd ed. Springer, 2017.

[179] Y. Zhao and M. N. S. Swamy, "A novel technique for tracking time-varying minimum and its applications," in *Conference Proceedings. IEEE Canadian Conference on Electrical and Computer Engineering*, vol. 2. IEEE, 1998, pp. 910–913.

[180] Z. Marvi, F. Bullo, and A. G. Alleyne, "Control barrier proximal dynamics: A contraction theoretic approach for safety verification," *IEEE Control Systems Letters*, vol. 8, pp. 880–885, 2024.

[181] R. M. Corless, G. H. Gonnet, D. E. G. Hare, D. J. Jeffrey, and D. E. Knuth, "On the Lambert W function," *Advances in Computational Mathematics*, vol. 5, no. 1, pp. 329–359, 1996.

[182] P. J. Huber, "Robust estimation of a location parameter," *The Annals of Mathematical Statistics*, vol. 35, no. 1, pp. 73 – 101, 1964.

[183] P. O. Hoyer, "Modeling receptive fields with non-negative sparse coding," *Neurocomputing*, vol. 52, pp. 547–552, 2003.

[184] V. Cerone, S. M. Fosson, and D. Regruto, "Fast sparse optimization via adaptive shrinkage," in *IFAC World Congress 2023, Yokohama, Japan*, 2023.

[185] A. Davydov and F. Bullo, "Exponential stability of parametric optimization-based controllers via lur'e contractivity," *IEEE Control Systems Letters*, 2024.